**UNIVERSITY COLLEGE LONDON**

# Oxygen-sensing and mitochondrial control of cell function

**2013**

Thomas Paul Briston

Thesis submitted for the degree
of Doctor of Philosophy

# Declaration

I, Thomas Paul Briston confirm that the work presented in this thesis is my own. Where information has been derived from other sources, I confirm that this has been indicated in the thesis.

# Acknowledgements

**To my supervisor,** Margaret....

Thanks for the endless encouragement, positive attitude and mentorship.

*....I can't thank you enough....*

**To the members of the Ashcroft group present,** Afshan, Luke and Nick....

Thanks for the laughs, the never faulting support and most importantly the friendship.

*....I couldn't have done this without any of you....*

**To the members of the Ashcroft group past,** Evon, Oli and Tom C....

Thanks for sharing your experience and knowledge and for teaching me how to be a scientist.

*....it was a pleasure....*

**To the members of the Szabadkai/Duchen lab,** Gyuri, Ronan, Will and Zhi….

Sincere thanks for your time, sharing your expertise and equipment and for really introducing me to mitochondrial biology.

*….I am truly grateful….*

**To the British Heart Foundation,**

For funding this research, allowing me to follow scientific curiosity and for providing a stepping stone for my future career.

**Finally and most importantly to my family,** Mum, Dad and Jen.... Thanks for maintaining my sanity, unconditional love and giving me something to come home to.

*....I love you all....*

Grandad.... You took my education seriously; you encouraged me, taught me the importance of working hard and were a true inspiration.

*....for this and much more, I am eternally grateful....*

# Abstract

The cellular response to low oxygen tension (hypoxia) is orchestrated through an elegant pathway involving a number of molecular players and is well characterised in development, physiology and pathology. The hypoxia inducible factors (HIFs) comprise a family of transcription factors whose activity is responsible for mediating transcriptional responses to hypoxia and maintaining cellular oxygen homeostasis.

Of particular interest, is the relationship between the HIFs and mitochondria. Mitochondria consume oxygen and generate chemical energy in the form of adenosine triphosphate (ATP). Mitochondrial function and the electron transport chain are necessary for the stabilisation of HIF-α protein in response to hypoxia and the transactivation of HIF target genes. Conversely, mitochondrial adaptation to hypoxia is controlled through a number of HIF target genes. However, the molecular relationship between the HIFs and mitochondria and *vice versa* is still emerging.

Oxygen-dependent regulation of HIF-α protein stability is controlled by the prolyl hydroxylase domain (PHD) proteins. Using several approaches to stabilise and activate the HIFs, this thesis has explored the role of the oxygen-sensing machinery in regulating mitochondrial function. This work identifies altered subcellular localisation of the HIF-complex and PHD proteins. Additionally, manipulation of the oxygen-sensing pathway results in gross mitochondrial morphological and ultrastructural differences in addition to alterations in a number of mitochondrial parameters, including DNA maintenance, electron transport chain (ETC) protein expression, bioenergetics and autophagy.

Together these data identify a novel role for members of the oxygen-sensing machinery in mitochondrial function.

# Table of Contents

# List of Figures

## Chapter 1



## Chapter 2



## Chapter 3

## Chapter 4

## Chapter 5

## Chapter 6

# List of Tables

# Abbreviations

**ADM** Adrenomedullin

**ADP** Adenosine diphosphate

**AMP** Adenosine monophosphate

**ANF** Atrial natriuretic factor

**ANT** Adenine nucleotide translocase

**AOX** Alternative oxidase

**ARNT** Aryl hydrocarbon receptor nucleotide translocator

**ATG** Autophagy related gene

**ATP** Adenosine triphosphate

**BCL-2** B-cell lymphoma-2

**bHLH** Basic helix-loop-helix

**BNIP3** BCL2/adenovirus E1B 19kDa protein-interacting protein 3

**CCCP** Carbonyl cyanide m-chlorophenyl hydrazone

**CCRCC** Clear cell renal cell carcinoma

**ChIP** Chromatin immunoprecipitation

**CUL2** Cullin 2

**CVD** Cardiovascular disease

**DCF** Dihydrodichlorofluorescein

**DFO** Desferrioxamine

**DNA** Deoxyribonucleic acid

**DRP-1** Dynamin-related protein-1

**DRS** Disulphide relay system

**ECV** Elongin B/C-CUL2-VHL

**EGF** Epidermal growth factor

**EGFP** Enhanced green fluorescent protein

**EM** Electron microscopy

**EMSA** Electrophoretic mobility shift assay

**EPAS** Endothelial PAS domain protein

**EPO** Erythropoietin

**ETC** Electron transport chain

**FADH** Flavin adenine dinucleotide

**FH** Fumarate hydratase

**FIH** Factor inhibiting HIF

**FIS-1** Fission protein-1

**GFM1** Elongation factor G1

**GFP** Green fluorescent protein

**GLUT** Glucose transporter

**HBSS** Hanks balance salt solution

**HDAC** Histone deacetylase

**HIF** Hypoxia inducible factor

**HO-1** Haem oxygenase -1

**HRE** Hypoxic response element

**HSP** Heat shock protein

**Hx** Hypoxia

**IAA** Iodoacetic acid

**IGF** Insulin-like growth factor

**IMM** Inner mitochondrial membrane

**IMS** Intermembrane space

**IPAS** Inhibitory PAS domain protein

**KCN** Potassium cyanide

**LAMP** Lysosomal-associated membrane protein

**LDH** Lactate dehydrogenase

**MAPK** Mitogen activated protein kinase

**MCT** Mono carboxylate transporter

**MFF** Mitochondrial fission factor

**MFN** Mitofusin

**mPTP** Mitochondrial permeability transition pore

**mRNA** Messenger RNA

**MRP** Mitochondrial ribosomal protein

**MRRF1** Mitochondrial ribosomal release factor -1

**MRS** Magnetic resonance spectroscopy

**mTOR** Mammalian target of rapamycin

**MTS** Mitochondrial targeting sequence

**NADH** Nicotinamine adenine dinucleotide

**NHE** Sodium hydrogen antiporter

**NOS** Nitric oxide synthase

**NRF** Nuclear respiratory factor

**NSC** Non-silencing control

**Nx** Normoxia

**OCR** Oxygen consumption rate

**ODD** Oxygen-dependent degradation

**OMM** Outer mitochondrial membrane

**PARL** Presenilins-associated rhomboid-like protein

**PAS** Per-ARNT-Sim

**PD** Parkinson's disease

**PDGF** Platelet derived growth factor

**PDH** Pyruvate dehydrogenase

**PDK** Pyruvate dehydrogenase kinase

**PHB** Prohibitin

**PHD** Prolyl hydroxylase domain

**PI3K** Phosphatidylinositide 3-kinases

**PINK1** PTEN-induced putative kinase 1

**PKA** Protein kinase A

**PKB** Protein kinase B

**PKC** Protein kinase C

**PKM2** Pyruvate kinase M2

**PMF** Proton motive force

**POLG** Mitochondrial DNA polymerase gamma

**PPAR** Peroxisome proliferator activated receptor

**PTEN** Phosphatase and tensin homolog

**RBX-1** RING-box protein 1

**RLU** Relative luminescent unit

**ROS** Reactive oxygen species

**RTK** Receptor tyrosine kinase

**S.E.M** Standard error of the mean

**SDH** Succinate dehydrogenase

**shRNA** Small hairpin RNA

**siRNA** Small interfering RNA

**SOD** Superoxide dismutase

**SUMO** Small ubiquitin modifier

**TCA** Tri-carboxylic acid

**TFAM** Mitochondrial transcription factor A

**TGF** Transforming growth factor

**TIF** Translation initiation factor

**tRNA** Transfer RNA

**TUFM** Tu translation elongation factor

**UCP** Uncoupling protein

**VDAC1** Voltage-dependent anion channel 1

**VEGF** Vascular endothelial growth factor

**VHL** von Hippel Lindau

# Chapter 1: Introduction

## 1.1 The importance of oxygen

Understanding how cells sense and respond to changes in oxygen tension, particularly low oxygen (hypoxia), is important. This extends not only from the perspective of understanding physiology, development and adaptation to environmental change, but also pathophysiology of disease. Cancer, cardiovascular disease and stroke can all be characterised by an impairment of oxygen perfusion to tissue and cells**.** Without an adequate supply of oxygen, cells do not survive. Therefore it is essential that cells maintain an appropriate level of oxygenation to sustain viability. Cells have compensatory mechanisms by which they can adapt to changes in oxygen tension both rapidly and effectively. Atmospheric oxygen concentration varies depending on altitude and atmospheric pressure, however despite this and under ambient conditions, healthy cells in the same organ (e.g. kidney) *in vivo* may experience as little as 5% oxygen tension (Solaini et al., 2010).

Cells respond and adapt to hypoxia through the activation of multiple signalling pathways, which cooperate to minimise cellular injury and maintain survival. The capacity of cells to react and adapt to variations in oxygen relies on a family of transcription factors known as the hypoxia inducible factors (HIFs). The involvement of HIFs in hypoxia signalling, cancer, ischaemia and cardiovascular disease is well established with the HIFs playing a crucial role particularly in regulating metabolism, maintaining vascular supply and promoting cell survival (Shohet and Garcia, 2007, Ziello et al., 2007). Notably, small molecule activation of the HIFs has been proposed as a novel strategy in treating ischaemic injury. Conversely, inhibition of the HIF pathway is used as adjunct to traditional therapy in treating solid tumours (Harten et al., 2010). Therefore, much interest is focused on understanding the cellular mechanisms that regulate the HIFs and components of the oxygen-sensing machinery as a basis for exploiting the HIF pathway therapeutically.

## 1.2 The HIF pathway

The major physiological mechanism by which cells respond to hypoxic stress is through activation of the HIFs, which regulate the cell's transcriptional responses to hypoxia. The prototype of the family is hypoxia inducible factor-1 (HIF-1), which was first identified through analysis of a *cis*-acting sequence termed the hypoxic response element (HRE; 5'-

RCGTG-3') found within the 3'-enhancer of the *erythropoietin* (*EPO*) gene (Semenza and Wang, 1992). It was recognised that HIF-1 binding to this pentanucleotide HRE sequence increased *EPO* gene transcription and protein levels under hypoxic conditions (Semenza et al., 1991 , Semenza and Wang, 1992). These DNA sequences have since been found to be present in a broad range of genes in many cell types, thus providing a universal role in cellular oxygen-sensing (Maxwell et al., 1993, Webb et al., 2009). The identification of genes regulated either directly or indirectly by HIF-1 now extends to over one hundred and fifty (Mole et al., 2009), which are implicated in a plethora of physiological processes and regulatory networks. As such, the HIFs transcriptional activity maintains homeostatic responses to cellular variations in oxygen tension and permits the regulation of genes involved in cell survival, angiogenesis and metabolism (Wenger, 2002, Weidemann and Johnson, 2008).

### 1.2.1 *Structure and function of HIF-1*

HIF-1 is a heterodimeric DNA-binding protein complex, comprising of an oxygen-regulated HIF-1α subunit and constitutively expressed non-oxygen-regulated beta subunit (HIF-1β), a product of the *ARNT* gene (aryl hydrocarbon nuclear translocator; ARNT) (Wang and Semenza, 1995, Wang and Semenza, 1993). Both HIF-1α and HIF-1β messenger RNAs (mRNA) are constitutively transcribed and levels remain constant regardless of oxygen availability, as such HIF-1 is well placed to respond appropriately and rapidly to variations in oxygen concentration (Kallio et al., 1997). Both HIF-1 subunits are members of the basic helix-loop-helix (bHLH) PAS domain (Per/Arnt/Sim) containing family of transcription factors (Jiang et al., 1996a, Wang et al., 1995). The HIF-1α subunit translocates to the nucleus, where it dimerises with the HIF-1β/ARNT subunit via the bHLH and PAS domains (Figure 1.1) (Wang et al., 1995, Wang and Semenza, 1995, Semenza et al., 1997). Dimerisation of the alpha and beta subunits, instigates an alpha subunit conformational change (Kallio et al., 1997) and through the N- and C-terminal transactivation domains (N-TAD and C-TAD), recruits and interacts with its co-activators including p300/CBP (CREB; cAMP-response element binding protein) (Jiang et al., 1996a, Arany et al., 1996). The HIF-1 dimer along with its co-activators then binds via its basic region to DNA at the HRE consensus in either promoter or enhancer sites of target genes.

In addition to HIF-1α, various other family members have since been identified; HIF-2α (also known as EPAS-1; endothelial PAS domain protein-1) (Tian et al., 1997, Ema et al.,

1997) and HIF-3α (Gu et al., 1998), whose expression pattern is more restricted and function more enigmatic (Wenger, 2002)**.** Among the several identified splice variants of HIF-3α, the inhibitory PAS domain protein (IPAS) has been identified as an endogenous HIF antagonist having a dominant-negative effect on gene expression under hypoxic conditions, through lack of a transactivational domain (Bardos and Ashcroft, 2005, Makino et al., 2001, Makino et al., 2002). Bioinformatic analysis reveals HIF-1α and HIF-2α share 48% structural homology and HIF-3α exhibits high similarity in the bHLH and PAS domains but lacks the C-terminal transactivation domain (C-TAD) (Hara et al., 2001). HIF-2α is also stabilised in hypoxia and binds HIF-1β/ARNT to form the HIF-2 complex and regulates gene expression through the same mechanism as HIF-1 (Tian et al., 1997, Ema et al., 1997).

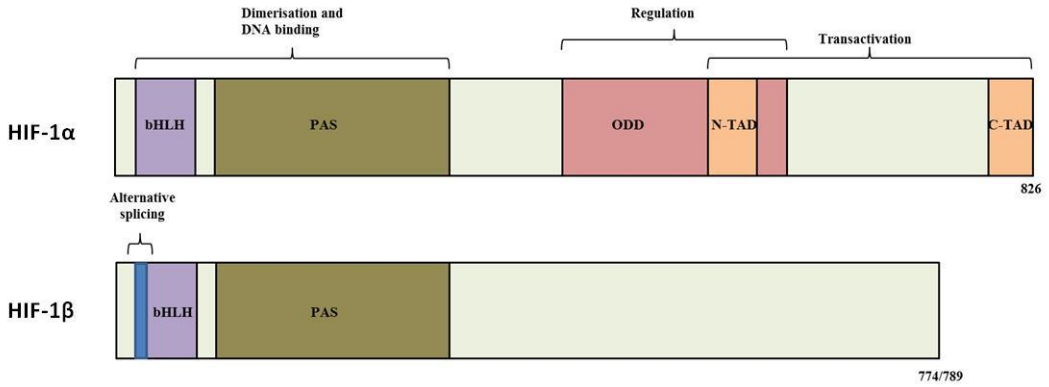


**Figure 1.1: Schematic representation of the HIF-1 protein.**

**The bHLH and PAS domains of hypoxia-inducible factor 1α (HIF-1α) are involved in dimerisation and DNA binding; the oxygen dependent degradation (ODD) domain is required for degradation via the proteasome; and the transactivation domains (N-TAD and C-TAD) are involved in regulating gene expression. Hydroxylation of proline residues 402 and 564 within the ODD domain mediates an interaction between HIF-1α and the von Hippel-Lindau tumour suppressor protein (pVHL). Hydroxylation of asparagine 803 in the C-TAD blocks the association between HIF-1α and transcriptional co-activator p300/CBP. bHLH = basic helix–loop-helix, PAS = Per-ARNT-Sim, ODD = oxygen dependent degradation, N-TAD = N-terminal transactivation, C-TAD = C-terminal transactivation. Adapted from (Poon et al., 2009).**

In response to hypoxia, the HIF-1 complex binds to genes involved in a number of distinct processes that each mediates cellular adaptation to the oxygen-limiting environment. Genes are activated that promote glycolysis (*enolase*), angiogenesis (*vascular endothelial*

*growth factor; VEGF* and *Flt-1/VEGFR1*), iron metabolism (*transferrin* and *transferrin receptor*), cellular proliferation and autophagy (*insulin-like growth factor-1; IGF*-1 and *BCL2/adenovirus E1B 19kDa protein-interacting protein 3; BNIP3*) among many others (Figure 1.2) (Semenza, 2003). The physiological role of HIF-2α will be discussed in chapter 6.

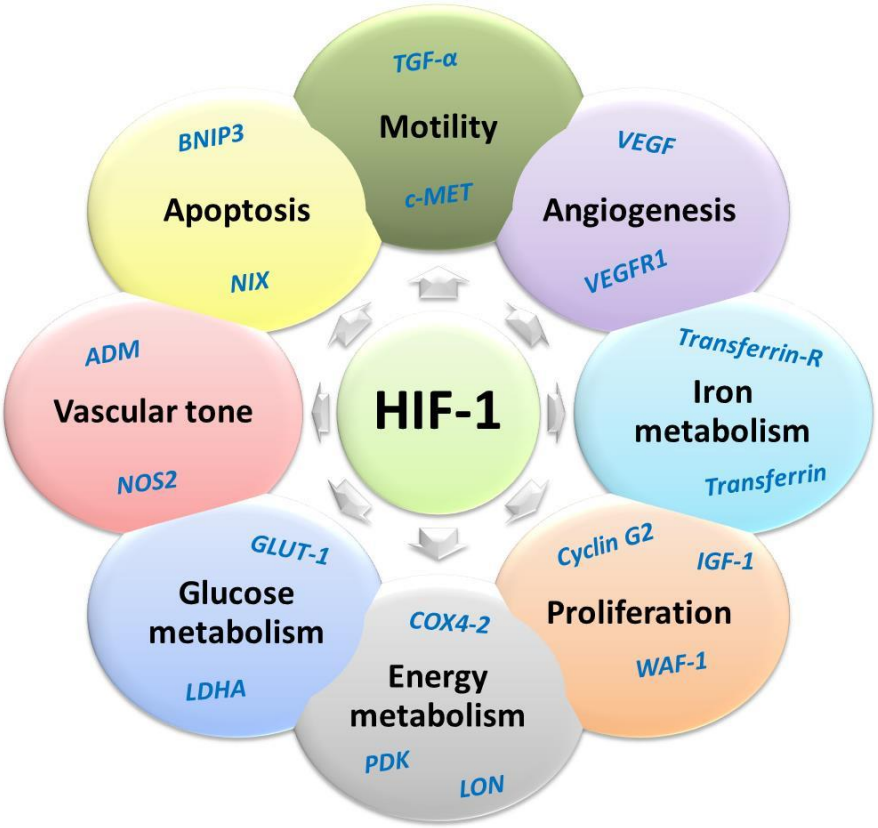


**Figure 1.2: Diagram showing processes regulated by HIF-1 transcriptional activity.**

**Activation of HIF-1 induces expression of genes involved in processes such as maintenance of vascular tone and proliferation among many others. This allows the cell to adapt to changes in local oxygen tension. TGF-α = transforming growth factor alpha, ADM = adrenomedullin, NOS2 = nitric oxide synthase 2, LDHA = lactate dehydrogenase A, COX4-2 = cytochrome c oxidase subunit 4-2, PDK = pyruvate dehydrogenase kinase. Adapted from (Semenza, 2003).**

Germline loss of *Hif-1α* and *Hif-2α* produce distinct phenotypes. Knock-out of *Hif-1α* in the mouse germline proves embryonically lethal in mid gestation at E9.5 and loss of *Hif-2α* can cause either embryonic or perinatal lethality, with some surviving to exhibit developmental abnormalities (Iyer et al., 1998, Tian et al., 1998, Peng et al., 2000, Scortegagna et al.,

2003). These distinct phenotypes suggests that although there are common sets of target genes and some degree of redundancy, significant differences in their behaviour exist and hence functional overlap is avoided (Hu et al., 2003, Loor and Schumacker, 2008). Observations reveal HIF-2α to have a specific contribution to yolk sac vascularisation (Peng et al., 2000), while HIF-1α is important for mesenchymal cell survival and consequently *Hif-1α*$^{-/-}$ mice die with cardiovascular malformations and open neural tube defects (Iyer et al., 1998). Tissue specific loss of HIF-1α has been associated with distinct phenotypes (Helton et al., 2005, Cramer and Johnson, 2003). For instance, neurone and myeloid lineage specific knock-out of *Hif-1α* leads to neuroprotection and decreased inflammatory and antimicrobial responses respectively (Helton et al., 2005, Cramer and Johnson, 2003).

### 1.2.2 *Oxygen-dependent regulation of HIF-1*

In adequately oxygenated cells, HIF-1α has an extremely short half-life ($t_{1/2}$~3-5 min). HIF-1α and HIF-2α (from here on referred to as HIF-α) are not regulated by oxygen directly, instead their stabilisation and transactivational capacity is tightly regulated and coordinated by a number of post-translational modifications, including the hydroxylation of proline and asparagine residues respectively, described below (Brahimi-Horn et al., 2005, Lee et al., 2004). HIF-1α protein stabilisation occurs under hypoxia, an event which affects the subunit's subcellular localisation and transcriptional potency (Lee et al., 2004). Contrary to this, protein levels of the HIF-1β subunit remain constant irrespective of oxygen availability, a phenomenon first demonstrated in HeLa and HepG2 cells and since found to be cell line independent (Kallio et al., 1997, Jiang et al., 1996a).

### 1.2.3 *Control of HIF-1α protein stabilisation by the PHD proteins and the ubiquitin-proteasome pathway*

The HIF-1α protein remains at low levels under normoxia as it undergoes a tightly regulated process of continuous synthesis and degradation. HIF-1α protein stabilisation can be observed in culture and physiologically from approximately 5% oxygen, through immunoblotting and analysis of target gene expression (Jiang et al., 1996b, Tormos and Chandel, 2010). The targeting of HIF-1α for degradation, under ambient oxygen, is achieved through hydroxylation of conserved proline residues, $Pro^{402}$ and $Pro^{564}$, which contain a common core motif in the oxygen dependent degradation (ODD, residues 401-603) domain of HIF-1α (Masson et al., 2001). This rapid degradation is mediated through recognition of the hydroxylated residues and subsequent ubiquitination of HIF-1α by an E3-ubiquitin

ligase complex, which polyubiquitinates HIF-1α and 'tags' it for proteolytic degradation through the ubiquitin-proteasome pathway (Salceda and Caro, 1997, Maxwell et al., 1999, Ohh et al., 2000, Jaakkola et al., 2001) (Figure 1.3).

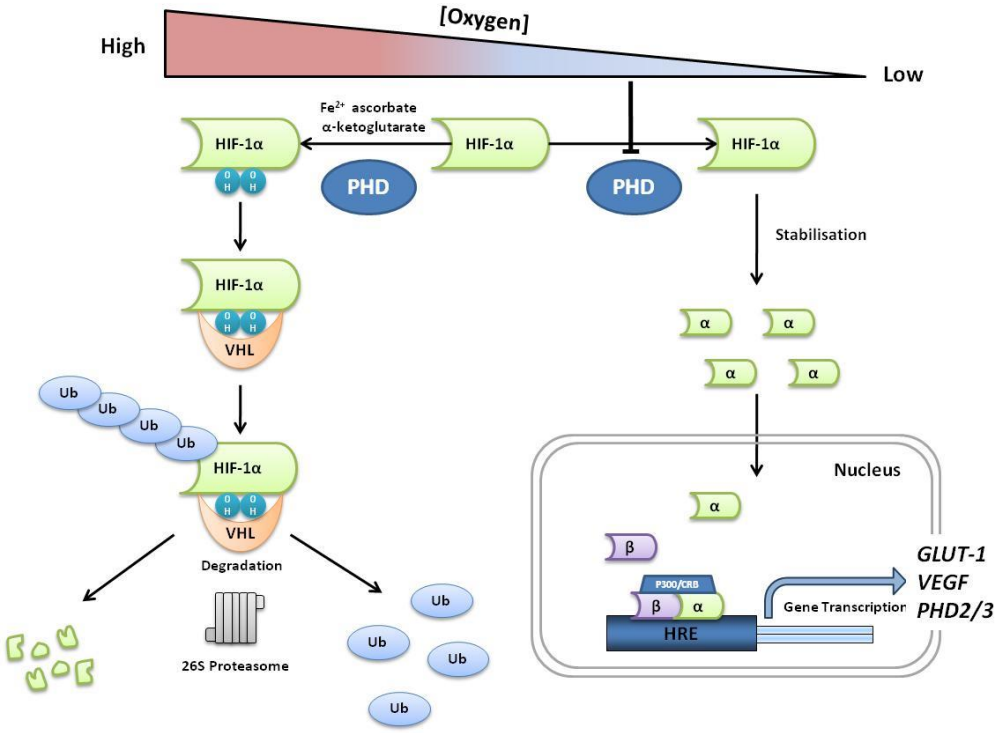


**Figure 1.3: Oxygen-dependent regulation of HIF-1α.**

**Under conditions of ambient oxygen, HIF-1α is hydroxylated on specific proline residues by the PHD proteins and degraded in a pVHL-dependent manner. When oxygen becomes limiting, failure to hydroxylate HIF-1α allows protein stabilisation and translocation to the nucleus, where it dimerises with HIF-1β and binds hypoxic response elements in target gene DNA. OH = hydroxyl group, Ub = ubiquitin, HRE = hypoxic response element, PHD = prolyl hydroxylase domain enzyme, VHL = von Hippel Lindau protein.**

The proline hydroxylation reaction is catalysed by the oxygen-sensing prolyl hydroxylase domain (PHD) enzymes. The PHDs are Krebs-cycle (tri-carboxylic acid (TCA) cycle) intermediate α-ketoglutarate (2-oxoglutarate)-dependent dioxygenases, requiring non-haem iron ($Fe^{2+}$) and ascorbate as co-factors (Wenger, 2002). The reaction utilises molecular oxygen and proceeds through the conversion of α-ketoglutarate into succinate with subsequent carbon dioxide release (Webb et al., 2009, McNeill et al., 2002, Lando et

al., 2002). Ascorbate maintains iron in its ferrous ($Fe^{2+}$) form, important for full enzymatic activity, therefore pharmacological chelators of iron, such as desferrioxamine (DFO) can be used to activate this pathway and stabilise HIF-α (Figure 1.4).

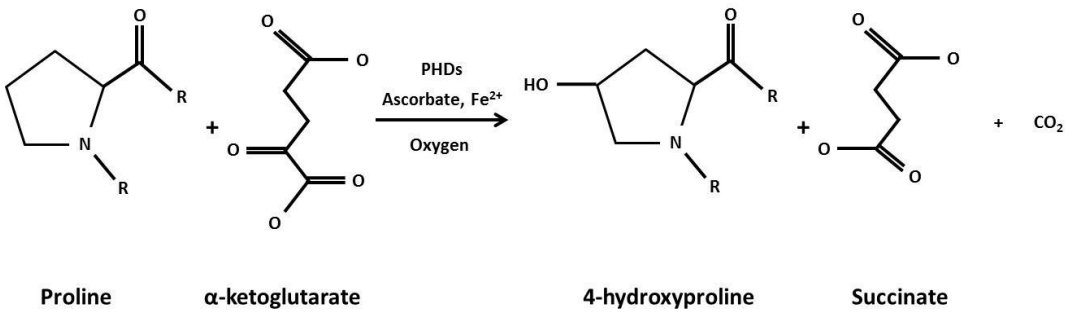


**Figure 1.4: PHD catalysed generation of 4-hydroxylproline.**
**Molecular oxygen, $Fe^{2+}$ and α-ketoglutarate are utilised to hydroxylate specific proline residues within the HIF-α ODD domain. Adapted from (Sen Banerjee et al., 2012).**

Three PHD isoforms have been described and well characterised; PHD1/HPH3/EGLN2, PHD2/HPH2/EGLN1 and PHD3/HPH1/EGLN3, of which PHD2 has the greatest affinity toward HIF-1α and is suggested to be the key rate-limiting enzyme relating to its stabilisation (Berra et al., 2003, Appelhoff et al., 2004). PHD2 has been shown to be the major oxygen-sensor responsible for the normoxic turnover of HIF-1α, as silencing alone through RNA interference is sufficient to mediate HIF-1α stabilisation (Berra et al., 2003). The recruitment of PHD2 is seemingly aided by $Leu^{574}$ residing on HIF-1α which promotes the efficient hydroxylation of $Pro^{564}$ (Kageyama et al., 2004). PHD3 primarily targets HIF-2α, while PHD1 demonstrates some selectivity for HIF-1α (Appelhoff et al., 2004). Recently a fourth hydroxylase, PHD4 has been identified in the membrane of the endoplasmic reticulum, with its catalytic site within the lumen (Oehme et al., 2002). PHD4 differs from those previously characterised, however it has also been shown to be capable of hydroxylating HIF-1α *in vitro*, yet questions remain over its role *in vivo* (Koivunen et al., 2007b, Oehme et al., 2002).

*PHD2* and *PHD3* are both HIF-1 target genes and mRNA expression is increased in response to hypoxia (Aprelikova et al., 2004). Increased PHD3 is thought to regulate the HIF response to prolonged hypoxia (Metzen et al., 2005, Pescador et al., 2005). The tissue expression

patterns of the enzyme family also differ (Lieb et al., 2002), as does their subcellular localisation (Metzen et al., 2003). PHD1 appears exclusively nuclear, PHD2 primarily cytosolic and PHD3 being localised to both nuclear and cytosolic compartments (Metzen et al., 2003). Studies in mice have demonstrated that knockout of *Phd2 in vivo* is embryonically lethal, with embryos displaying placental and cardiovascular defects (Takeda et al., 2006). However both *Phd1* and *Phd3* nulls are viable and appear normal (Takeda et al., 2006). In hypoxia, the Siah E3 ligase (Siah2) regulates the protein abundance of PHD1 and PHD3 after targeting for proteasomal degradation, therefore positively regulating hypoxic HIF-α stabilisation (Nakayama et al., 2004).

The PHD-dependent 4-hydroxyproline modification in ambient oxygen concentrations facilitates the recruitment and highly specific binding of the von Hippel-Lindau protein (pVHL) through its β-domain (Maxwell et al., 1999, Jaakkola et al., 2001, Ohh et al., 2000). pVHL encodes the protein product of the *VHL* gene and in co-operation with elongins B and C, cullin-2 and ring-box 1 (RBX-1) forms the ECV multi-protein E3-ligase complex. pVHL is analogous to an F-box protein and so is the principal component responsible for substrate recognition and recruitment to the ubiquitination machinery (Brahimi-Horn et al., 2005, Ohh et al., 2000). As a result the poly-ubiquitinated HIF-1α protein is then targeted for degradation by the 26S proteasome (Maxwell et al., 1999, Jaakkola et al., 2001).

pVHL is expressed ubiquitously throughout different tissues and has the ability to shuttle between the nucleus and cytoplasm enabling it to target HIF-1α for degradation in both cellular compartments (Berra et al., 2001). Mutation of either or both proline residues on HIF-1α abrogates the association between HIF-1α and pVHL and consequently allows partial or full HIF-1α stabilisation respectively, despite normal oxygen levels (Masson et al., 2001). The same holds true for loss of function *VHL* mutation, a phenotype associated with VHL disease and observed in clear cell renal cell carcinomas (CCRCC) (Maxwell et al., 1999, Kaelin, 2002).

### 1.2.4 *Control of HIF-1 transcription by FIH-1*

HIF-1α can be transactivationally controlled through the α-ketoglutarate and $Fe^{2+}$ dependent dioxygenase - factor inhibiting HIF-1 (FIH-1) (Mahon et al., 2001, Lando et al., 2002, McNeill et al., 2002). FIH-1 functions as a homodimer to inhibit the trans-acting co-activator p300/CBP binding HIF-1α. FIH-1 splits molecular oxygen to enzymatically hydroxylate the beta-carbon of asparagine 803 in the C-TAD of HIF-1α ($Asp^{851}$ in HIF-2α)

(Webb et al., 2009, Lancaster et al., 2004a, Lancaster et al., 2004b). Thus FIH-1 acts as a negative regulator of HIF-1 transcriptional activity (Mahon et al., 2001, Lando et al., 2002, McNeill et al., 2002). Expression of FIH-1 protein and mRNA are independent of oxygen concentration and the FIH-1 protein is primarily cytosolic as demonstrated by three dimensional 2-photon confocal fluorescence microscopy (Metzen et al., 2003). Asparagine hydroxylation disrupts hydrogen bonding between HIF-1α and its co-activators and prevents binding (Maxwell, 2005, Semenza, 2004). Hypoxia abrogates this interaction as oxygen, the major substrate for FIH-1 is decreased thereby allowing p300/CBP co-activator binding and transactivation of downstream HIF target genes (Mahon et al., 2001, Lando et al., 2002). The FIH-1-mediated hydroxylation reacts to variations in oxygen concentration over the physiological range. It is also worth noting that there are isoform and cell specific differences with regulatory control of the various HIF-α proteins by FIH-1. For example in mouse embryonic fibroblasts (MEFs), HIF-2α is not hydroxylated by FIH-1 (Park et al., 2003). Moreover, FIH-1 has been suggested to interact with pVHL, forming a ternary complex along with HIF-1α that will modulate protein stability and transcriptional activity (Mahon et al., 2001, Khan et al., 2011). Because of the inherent oxygen dependency of the hydroxylases, decreasing oxygen availability linearly reduces the enzymatic capacity of both the PHDs and FIH-1 and as substrate levels become limited enzymatic activity diminishes.

### 1.2.5 *Oxygen-independent regulation of HIF-α*

In addition to the oxygen dependency of HIF-α regulation, there are also oxygen-independent mechanisms that can govern HIF-α protein synthesis, stabilisation and transactivation. HIF-1α can undergo various distinct regulatory post-translational modifications. Examples include phosphorylation at threonine 706 by casein kinase 2 which inhibits FIH-1 binding (Lancaster et al., 2004b) and also by mitogen activated protein kinases (MAPKs) at serine 641 and serine 643 which promotes nuclear translocation and transactivation (Mylonis et al., 2006). *S*-nitrosylation at cysteine 800 has also been shown to affect HIF-1α transcriptional activation. However, whether this modification promotes or inhibits the interaction of HIF-α with co-activators and how it affects transactivation remains a matter of debate (Cho et al., 2007, Yasinska and Sumbayev, 2003). Conflicting reports also relate to the SUMOylation of HIF-1α, as conjugation has been shown to increase stabilisation (Bae et al., 2004) and more recently to decrease transcriptional activity (Berta et al., 2007).

Transition metals also play a role in regulating HIF-1α. These include regulation by cobalt and nickel which stabilise HIF-1α under normoxia, as does nitric oxide (NO) produced through inducible nitric oxide synthase (iNOS) (Chun et al., 2002, Huang et al., 1999). Growth factor-mediated activation of phosphoinositol-3-kinase (PI3K) and MAPK pathways are involved in promoting synthesis of HIF-1α protein, through either receptor tyrosine kinase (RTK), non-RTK or G-protein coupled receptors (Poon et al., 2009, Fukuda et al., 2002, Laughner et al., 2001). Under normoxic conditions HIF-1α can be induced by various growth factors including, insulin-like growth factor -1 and -2 (IGF-1 and IGF-2), epidermal growth factor (EGF), fibroblast growth factor-2 (FGF-2), transforming growth factor-β1 (TGF-β1) and platelet derived growth factor-β (PDGF-β) (Feldser et al., 1999, Richard et al., 2000, Wenger, 2002). An array of protein effectors have also been observed to be involved in regulating the stabilisation of HIF-1α, including the oxygen-independent degradation of HIF-α by hypoxia-associated factor (HAF) (Koh and Powis, 2009), positive regulation of HIF-α through mammalian target of rapamycin (mTOR) (Hudson et al., 2002) and the protein chaperone heat shock protein 90 (HSP90) (Minet et al., 1999).

Interestingly, a number of TCA cycle intermediates have been identified to inhibit the PHD proteins, thereby indirectly affecting HIF-1α stabilisation. Fumarate, succinate and oxaloacetate have been observed to inhibit all three of the PHD proteins and additionally citrate demonstrated to inhibit PHD3 and most effective at inhibiting FIH-1 (Koivunen et al., 2007a). These observations highlight an exciting link between mitochondrial function and PHD-mediated regulation of HIF. Finally, recent observations suggest that mitochondria themselves, as the primary consumers of oxygen, play an important role in oxygen sensing. Mitochondria are hypothesised to be involved in the hypoxic stabilisation of HIF-α, via the PHDs and various paradigms exist as to the mechanism. The importance of mitochondria to the HIF/hypoxia response and *vice versa* therefore remains a subject of intense current interest within the field.

## 1.3 Mitochondrial oxygen homeostasis in cells

The control of metabolic homeostasis in cells involves tightly regulated dynamic pathways, able to respond rapidly to changes in the environment, energy demand and bioenergetic substrate supply (Shohet and Garcia, 2007). Central mediators in this process are mitochondria, whose primary function is the provision of sufficient energy requirements.

Amazingly mitochondrial respiration is only compromised at environmental oxygen concentrations of less than 0.1% due to the extremely high affinity that cytochrome c oxidase has for molecular oxygen (Tello et al., 2011). In the heart, a highly metabolically active aerobic organ, to cope with demand, mitochondrial composition extends to ~25-35% of total cardiomyocyte volume (Pi et al., 2007). This energy is provided in the form of the co-enzyme adenosine triphosphate (ATP), which acts as the physiological currency of energy transduction and releases intrinsic energy through the hydrolysis of two phosphoanhydride bonds (Jeremy M Berg, 2002). *In vivo*, oxidative phosphorylation (OxPhos) provides the majority of ATP necessary for cellular function. However, depending on the cell type there is a different reliance on ATP produced by glycolysis. Mitochondria are often referred to as being the 'powerhouse of the cell'; that being said it is also extremely clear that the role of mitochondria extend beyond that of just vital ATP biosynthesis. Indeed mitochondria also participate in multiple regulatory signalling pathways stimulated in response to physiological stressors such as ischaemia, hypoxia and oxidative damage. Thus, they are considered integral in their role in processes such as, cell survival and apoptosis.

### 1.3.1 *Respiration, the electron transport chain and oxidative phosphorylation*

Oxidative metabolism (OxPhos) is a vital function of mitochondria under normal conditions, functioning to maintain adequate ATP to meet fluctuating cellular demand. Mitochondrial substrate utilisation for OxPhos is dependent on the cell type or tissue. Under normal physiological conditions, in the well oxygenated heart, beta-oxidation of fatty acids provides the primary carbon fuel source and undergoes a process of oxidation, hydration and cleavage to yield 90% of the acetyl coenzyme-A (acetyl co-A) to enter the TCA cycle (Jeremy M Berg, 2002, Neely and Morgan, 1974, Solaini and Harris, 2005, Jafri et al., 2001, Neely et al., 1972). In cells distinct from cardiomyocytes, it is the oxidation of glucose that produces the substrates which are delivered to the TCA cycle. Pyruvate is produced through enzyme-mediated, stepwise conversion from glucose and its ordered dehydrogenation. Pyruvate is then converted to the common precursor acetyl co-A by pyruvate dehydrogenase (PDH) in mitochondria, ultimately feeding the TCA cycle (Jafri et al., 2001).

The TCA cycle occurs in the matrix of mitochondria and links the glycolysis and fatty acid oxidation to OxPhos. The TCA cycle provides the reducing equivalents required to feed into

the electron transport chain (ETC), while producing various intermediates such as α-ketoglutarate, succinate, citrate and fumarate (Jafri et al., 2001), some of which regulate the HIF response as outlined above.

OxPhos is the process through which cells produce the majority of ATP. ATP is synthesised through the generation and coupling of a proton gradient across the inner mitochondrial membrane to phosphorylation of adenosine diphosphate (ADP) at the $F_1F_O$-ATPase (complex V) (Jafri et al., 2001). ATP synthesis is achieved through an intricate system of electron transfer through a series of acceptor cytochromes (complexes I-IV) (Semenza, 2007b). Reducing equivalents such as reduced nicotinamide adenine dinucleotide (NADH) and flavin adenine dinucleotide ($FADH_2$), products of the TCA cycle donate electrons to ETC complexes I and II respectively. The sequential transfer of electrons through to complex III, cytochrome c and finally to complex IV is coupled to proton flux across the mitochondrial inner membrane from the matrix into the intermembrane space (IMS) (Figure 1.5). At complex IV, oxygen is utilised as the final electron acceptor to produce water. Serial electron transfer and proton flux creates an electrochemical gradient of protons ($\Delta\mu H^+$) of approximately 200 mV across the mitochondrial inner membrane (Solaini and Harris, 2005). The electrochemical gradient (proton motive force) consists of a pH gradient between the matrix and the IMS cytosol (of -1 pH unit; -60 mV) and electrical potential/voltage gradient (of 140 mV) (negative inside) (Wheaton and Chandel, 2011, Brand and Nicholls, 2011). The electrochemical potential is used to drive ATP biosynthesis from ADP and phosphate via proton flow back down their gradient, through the membrane bound $F_1F_O$-ATPase. Alternatively, a small proportion of protons may leak back across the inner membrane into the matrix (Heineman and Balaban, 1990, von Ballmoos et al., 2009, Bruce Alberts, 2002). The process of oxidative metabolism is not 100% efficient despite generating 38 molecules of ATP per molecule of glucose (Taylor and Pouyssegur, 2007) and is estimated that 0.2-2% of the total oxygen consumption will be incompletely reduced and yield reactive oxygen species (ROS) (Solaini and Harris, 2005, Addabbo et al., 2009). At low levels, ROS by-products may play a physiological role in signal transduction and their detoxification via mitochondrial and cytosolic superoxide dismutases (SODs) is carefully balanced. Changes in levels of ROS or their neutralizing enzymes can have pathophysiological consequences, such as in ischaemia-reperfusion injury, a state during which cells and tissue experience lack of oxygen and nutrients as a result of infarct, while reperfusion results in a burst of ROS, causing further cellular damage.

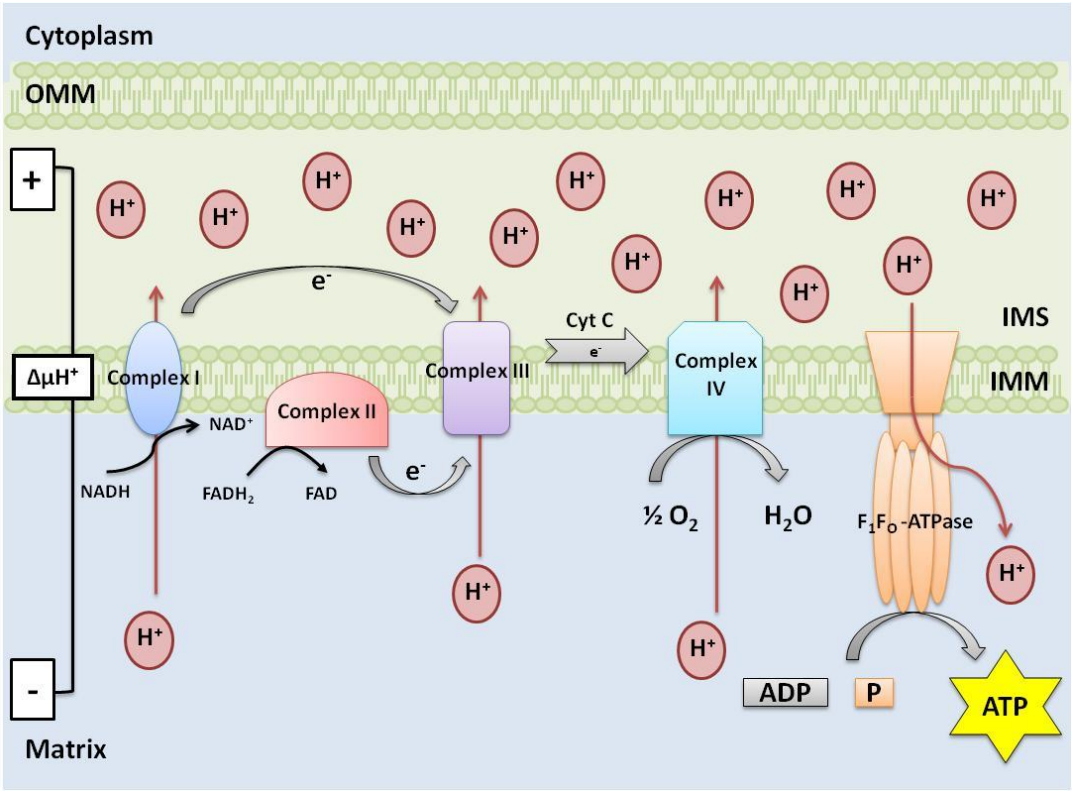


**Figure 1.5: Diagrammatic representation of proton and electron flow through the electron transport chain (ETC).**

**Electrons are passed along the ETC and using the free energy generated, protons ($H^+$) are moved against their concentration gradient from the matrix to the inter-membrane space (IMS) to generate an electrochemical gradient of protons ($\Delta\mu H^+$) across the inner mitochondrial membrane (IMM). Protons then flow back down their gradient through the $F_1F_O$-ATPase in a reaction coupled to the phosphorylation of ADP to ATP. OMM = outer mitochondrial membrane.**

### 1.3.2 *Mitochondria and oxygen-sensing*

The PHD proteins are inhibited by oxygen deprivation and were initially thought of as the sole regulators of HIF-α (defined this now above) stabilisation under low oxygen. However recent data points to the fact that mitochondria act as additional oxygen sensors *in vivo*, although the cellular mechanism for this remains to be understood. Over the last decade several groups have shown mitochondrial involvement in the process of oxygen-sensing and demonstrated that the regulation of HIF-α stabilisation under hypoxia and HIF-dependent gene transcription requires mitochondria (Agani et al., 2000, Chandel et al., 1998, Chandel et al., 2000, Guzy et al., 2005, Hagen et al., 2003, Lin et al., 2008, Mansfield et al., 2005, Emerling et al., 2005, Brunelle et al., 2005). However, under anoxia (0% $O_2$), oxygen deprivation and substrate limitation to the PHD proteins inhibits proline

hydroxylation of HIF-α and in this environment mitochondria are not required for the HIF/hypoxic response (Srinivas et al., 2001, Vaux et al., 2001). Currently two independent theories have been proposed through which mitochondria may participate in HIF-α stabilisation; (i) the generation of ROS from complex III mediates hypoxic HIF-α stabilisation and (ii) mitochondrial oxygen consumption and the redirection of oxygen away from the cytoplasm (and the PHD proteins) to mitochondria in hypoxia leads to HIF-1α stabilisation (Tormos and Chandel, 2010).

#### *1.3.2.1 HIF-α stabilisation in hypoxia requires a functional ETC*

Although debate continues as to the specific mechanism of mitochondrial involvement in HIF-α stabilisation, one observation is clear and has been re-produced across a number of laboratories; the stabilisation of HIF-α cannot occur in response to hypoxia without a functional ETC (Agani et al., 2000, Chua et al., 2010, Chandel et al., 2000, Chandel et al., 1998, Chandel and Schumacker, 1999, DeHaan et al., 2004, Schroedl et al., 2002, Agani et al., 2002). Early observations identified the necessity of a functional ETC for the stabilisation of HIF-1α and HIF-2α in hypoxia (1% oxygen) using pharmacological inhibitors such as 1-methyl-4-phenyl-1,2,3,6-tetrahydropyridine (MPTP) and rotenone (complex I inhibitors), myxothiazol and stigmatellin (complex III inhibitors). The use of genetic models and mitochondrial DNA deficient rho-zero cells ($\rho^0$ cells) confirmed these initial observations (Chandel et al., 1998, Guzy et al., 2005, Mansfield et al., 2005, Bell et al., 2007). $\rho^0$ cells are engineered through culture of parental cells with a low concentration of ethidium bromide over a number of weeks. Although mitochondrial DNA (mtDNA) only encodes 13 protein encoding genes, genetic ablation of these genes leads to the absence of components of complexes I, III, IV and V. Consequently, these cells lack the capacity to respire and despite containing petit mitochondria and a membrane potential, they rely solely on ATP generated from glycolysis alone to survive (Chandel and Schumacker, 1999). There is additional evidence demonstrating that HIF-1α stabilisation in $\rho^0$ cells in response to anoxia can occur despite the lack of a functional ETC (Srinivas et al., 2001, Vaux et al., 2001). Collectively, these observations suggest that mitochondria are important for HIF-1α stabilisation in hypoxia but not anoxia due to the inherent oxygen dependence of the PHD proteins. Notably, there may be biochemical and technical considerations regarding $\rho^0$ cell heterogeneity and generation that may affect how $\rho^0$ cells respond differently to hypoxia versus anoxia (Bell et al., 2005).

One early observation by Agani *et al* (Agani et al., 2000), noted that the neurotoxin and complex I inhibitor MPTP blocked HIF-1α induction in hypoxia and abrogated HIF-1 DNA binding capacity. MPTP produced an approximate 56% inhibition of complex I activity by 5 hours treatment in a neuroblastoma cell line. Additionally, MPTP intra-peritoneal injection in the striatum after hypoxic challenge produced a similar phenotype (Agani et al., 2000). Xenomitochondrial cybrids engineered using human $\rho^0$ cells fused with primate mitochondrial DNA and harbouring a 40% reduction in complex I activity, also prevented the hypoxic accumulation of HIF-1α. Interestingly, HIF-1α stabilisation was restored when indirectly supplying complex II with the substrate succinate, re-establishing electron flux to complex III. This suggests that even a mild reduction in complex I activity and oxygen consumption results in failure to stabilise HIF-1α in hypoxia (Agani et al., 2000).

Genetic approaches have been exploited to determine which elements of the ETC are necessary for the hypoxic stabilisation of HIF-1α (Guzy et al., 2005, Mansfield et al., 2005, Bell et al., 2007). These studies have identified that two components of the ETC are vital for the HIF/hypoxic response; complex III and cytochrome c. For example, using RNA interference (RNAi) toward the Rieske iron-sulphur protein and Q0 site of complex III (Guzy et al., 2005, Bell et al., 2007) or cytochrome c embryonic knockout mice (Mansfield et al., 2005), studies have demonstrated failure of HIF-1α stabilisation in hypoxia. Notably however, neither perturbation to the ETC affected stabilisation of HIF-1α in anoxia, possibly due to oxygen limiting effects on the PHDs (Bell et al., 2005, Appelhoff et al., 2004).

#### *1.3.2.2 Mitochondrially derived ROS and their role in stabilisation of HIF-1α in response to hypoxia*

ROS have been recognised as signalling molecules as well as being cytotoxic. Paradoxically ROS levels have been observed to increase in hypoxia, through an unknown mechanism (Chandel et al., 1998, Guzy et al., 2005, Duranteau et al., 1998). Specifically, cardiomyocytes have been shown to increase ROS production in hypoxia, by oxidation of the redox-sensitive fluorescent probe 2, 7-dichlorofluorescein (DCF), which was attenuated by antioxidants (Duranteau et al., 1998). Upon tissue reperfusion complexes I and III appear to be the primary sites for ROS generation (Duranteau et al., 1998). The pathophysiological significance of reoxygenation/reperfusion injury is clear (Solaini and Harris, 2005) and ROS production during hypoxia/ischaemia and at the restoration phase is a principal mediator of the pathology associated with this injury. Hence, it is important to decipher the role of

ROS as signalling molecules and their potential for oxidative damage, as is delineating the mechanism behind their generation and behaviour in each situation. Mitochondrial manganese or cytosolic copper/zinc superoxide dismutase's (Mn-SOD, Cu/Zn-SOD) catalyse the production of hydrogen peroxide ($H_2O_2$) from superoxide ($O_2^-$), which will either be converted to oxygen and water by catalase or under certain circumstances, react with transition metals or nitric oxide to form the highly reactive hydroxyl radical (·OH) or distinct reactive nitrogen species (RNS) respectively (Li and Jackson, 2002, Goswami et al., 2007). The absence of oxygen creates an environment whereby ETC complexes become and remain in their reduced state and allows for further superoxide production, an event compounded through the highly oxidative environment at reperfusion (Li and Jackson, 2002).

The first theory regarding a mechanism underlying mitochondrial involvement in HIF-1α hypoxic stabilisation concerns the necessity of mitochondrial ROS produced under hypoxia for HIF-1α protein stability. A small percentage of the oxygen utilised by mitochondria is incompletely reduced, yielding ROS even in the resting/quiescent state (Tormos and Chandel, 2010, Addabbo et al., 2009, St-Pierre et al., 2002). ROS produced by the mitochondrial ETC complex III are generated through the Q-cycle, whereby ubiquinone is reduced to ubiquinol (Tormos and Chandel, 2010) and have the capacity to diffuse into the mitochondrial matrix or mitochondrial IMS as the ubiquinol oxidation site which generates the superoxide is located adjacent to the IMS (Sun and Trumpower, 2003). In contrast, superoxides formed at complexes I and II are released into the matrix only (Muller et al., 2004, Tormos and Chandel, 2010). The increase in ROS in hypoxia has been proposed by a number of groups to mediate stabilisation and transcriptional activation of HIF-α (Brunelle et al., 2005, Agani et al., 2000, Chandel et al., 2000, Guzy et al., 2005, Mansfield et al., 2005, Poyton et al., 2009, Chandel et al., 1998). A proposed mechanism is that ROS oxidise the PHD protein substrate $Fe^{2+}$ to form $Fe^{3+}$, via Fenton chemistry. $Fe^{3+}$ cannot be utilised by the PHD proteins, decreasing their catalytic activity and enabling HIF-1α stabilisation (Guzy et al., 2005, Guzy and Schumacker, 2006, Gerald et al., 2004, Pan et al., 2007).

Chandel *et al* in 1998 were first to correlate hypoxia-induced gene transcription with mitochondrial ROS production (Chandel et al., 1998). Chandel *et al* observed an increase in DCF oxidation and fluorescence at decreasing oxygen levels and the attenuation of this effect using the glutathione peroxidise mimetic ebselen, which catalyses the conversion of

$H_2O_2$ to water. Chandel *et al* also demonstrated that mitochondria were required for the increase in ROS production during hypoxia using $\rho^0$ cells which are devoid of mitochondrial DNA and produced no ROS and DCF fluorescence in hypoxia. Chandel *et al* proposed that the ROS generated at complex III were necessary for the activation of HIF-1α in hypoxia. Additionally Chandel *et al* suggested that hypoxic ROS, produced in hypoxia, promoted HIF-1α DNA binding and HIF-1 target gene expression - an event abolished by the addition of the antioxidants ebselen and thiol reductive agent pyrrolidine dithiocarbamate (PDTC) (Chandel et al., 1998). The same group demonstrated two years later that ROS generated by the mitochondria were not just necessary but sufficient to stabilise HIF-1α protein through the observation that exogenous $H_2O_2$ stabilised HIF-1α in normoxia (Chandel et al., 2000).

Schroedl *et al* (Schroedl et al., 2002) confirmed using $\rho^0$ cells, the necessity of a functional ETC for the hypoxic stabilisation of HIF-1α and demonstrated that anoxic stabilisation of HIF-1α occurs in a mitochondrially-independent manner. Schroedl *et al* proposed that prolyl hydroxylases are not the single primary oxygen sensor and suggested a role for activation of mitochondrial-dependent ROS-mediated intracellular signalling pathways. Using a ROS-sensitive dye, Schroedl *et al* demonstrated that hypoxia, but not anoxia, increases mitochondrial ROS generation and using a HRE-driven luciferase reporter showed that transcriptional activation of HIF-1 was inhibited in $\rho^0$ cells. The same group also observed the abolition of hypoxic (1.5% $O_2$) but not anoxic stabilisation of HIF-1α, using the complex I inhibitor rotenone, which proximally blocks electron transfer through to complex III. Using the complex II substrate methyl-succinate, bypassing complex I and restoring electron flow even in the presence of rotenone, reversed this complex I mediated block on HIF-1α stabilisation by rotenone (Schroedl et al., 2002). These data from $\rho^0$ cells and rotenone mediated complex I inhibition were later replicated by Guzy *et al* in 2005 (Guzy et al., 2005). Furthermore, Guzy *et al*, used RNA interference (RNAi) methods and a novel redox-sensitive fluorescence resonance energy transfer (FRET) protein sensor and over-expression of antioxidants to assess the contribution of mitochondrial-dependent oxidant signalling and determined that again a functional ETC and complex III ROS generation is necessary for hypoxic HIF-1α protein stabilisation (Guzy et al., 2005). Moreover Guzy *et al* observed involvement of the Rieske-iron sulphur protein, which regulates electron flux through complex III and effects free radical generation and demonstrated that lack of this component prevented hypoxic mitochondrial ROS generation and HIF-1α stabilisation. Guzy

*et al* deduced that $H_2O_2$, not superoxide, is the responsible ROS mediating HIF-1α stabilisation in hypoxia (Guzy et al., 2005).

More recently, genetic approaches have been used to navigate around the contention surrounding pharmacological ETC disruption and variability in the production and prolonged culture of $\rho^0$ cells (Mansfield et al., 2005, Brunelle et al., 2005). Mansfield *et al* (Mansfield et al., 2005) demonstrated the importance of cytochrome c for the HIF/hypoxic response, after targeted mutagenesis of the *cytochrome c* gene (Li et al., 2000) in murine embryonic cells. Mansfield *et al* observed that subsequent stable re-expression of mutant cytochrome c protein, which prevents oxidation of cytochrome c1 and maintains the Rieske iron-sulphur protein in a reduced state, prevented the HIF/hypoxic response but not anoxic HIF-1α stabilisation (Mansfield et al., 2005). Brunelle *et al*, used siRNA to knockdown the Rieske iron-sulphur protein resulting in loss of Q-cycle initiation, formation of ubisemiquinone radical and subsequent ROS generation. Brunelle *et al* confirmed that observed by Mansfield *et al* (Mansfield et al., 2005) and the resultant in failure of hypoxic, but not anoxic HIF-1α stabilisation (Brunelle et al., 2005). In the same study, Brunelle *et al* (Brunelle et al., 2005) used fibroblasts with *SURF-1* mutation, derived from patients with Leigh's syndrome. *SURF-1* encodes a protein involved in the assembly of cytochrome c oxidase and produces a phenotype of impaired OxPhos but residual electron transport. *SURF-1* null fibroblasts are still capable of stabilising HIF-1α in hypoxia. In addition to this the authors also provided evidence demonstrating that Chinese hamster ovary cells, with over 90% complex I deficiency are able to stabilise HIF-1α in hypoxia. Brunelle *et al* confirmed that hydrogen peroxide and not superoxide, is the species responsible for the effects on HIF-1α, by demonstrating that over-expression of catalase and glutathione peroxidise, but not superoxide dismutase 1 (SOD1) or SOD2 could prevent the hypoxia-induced stabilisation of HIF-1α. Brunelle *et al* concluded that electron transport, but not the consumption of oxygen or OxPhos, is necessary for hypoxic stabilisation of HIF-1α, due to the production of ROS. Brunelle *et al* suggested that OxPhos and generation of intracellular oxygen gradients are dispensable and not responsible for the regulation of hypoxic stabilisation of HIF-1α (Brunelle et al., 2005).

Cytochrome b is a subunit component of complex III. Bell *et al* (Bell et al., 2007) re-expressed a mutant form of this protein into $\rho^0$ cells to create mutant cybrids which are unable to consume oxygen and however generate ROS. Bell *et al* observed that these

cybrids were still able stabilise HIF-α in hypoxia, adding further evidence to the hypothesis that mitochondrial ROS, derived from complex III are required for the hypoxic stabilisation of HIF-1α (Bell et al., 2007).

The studies described above link hypoxia signalling with mitochondrial ROS production and their cytosolic diffusion. These observations demonstrate a role for mitochondria in oxygen sensing in hypoxia, through as yet an unknown mechanism, but potentially one which is dependent on PHD proteins. Until anoxic (0% $O_2$) conditions, when the PHDs are completely inactivated, HIF-α hydroxylation is completely inhibited, blocking subsequent degradation and thereby enabling a HIF-α response (Guzy et al., 2005). Because of the inherent difficulties in measuring ROS and the variable data in ROS measurements between laboratories, questions still remain as to their mitochondrial production in hypoxia, which species of ROS is responsible and the mechanism by which they act to stabilise HIF-1α. Nevertheless, enough evidence exists to suggest the ROS regulation of HIF-1α is most definitely evident.

Finally, data also suggest an essential role for mitochondrial-derived ROS in the non-hypoxic stabilisation of HIF-1α in response to the vasoactive hormone angiotensin II (Ang II) in vascular smooth muscle cells (Patten et al., 2010, Richard et al., 2000). Ang II has demonstrated effects on HIF-1α, such as increased stabilisation, activation and gene transcription, which all require mitochondrial ROS generated at complex III as an signalling intermediary (Patten et al., 2010). Interestingly these findings by Pattern *et al* (Patten et al., 2010, Richard et al., 2000) link hormone-mediated signalling, ROS and HIF. Other growth factors, such as IGF-1 have also been linked to redox chemistry and ROS-dependent receptor activation (Vardatsikos et al., 2009) and it would be of interest to determine whether any inherent ROS-dependency is necessary for IGF-1 mediated HIF-α induction.

#### *1.3.2.3 Mitochondrial oxygen consumption and stabilisation of HIF-1α in hypoxia*

The mitochondrial ETC consumes the majority of cellular oxygen and therefore it is conceivable the ETC plays a critical role in oxygen sensing. An alternative ROS-independent model has been proposed to explain why a functional ETC is required for HIF-1α stabilisation in hypoxia (Hagen et al., 2003, Taylor, 2008). This model is based on the premise that actively respiring cells will consume oxygen and hence have a lower intracellular oxygen concentration than those treated with respiratory inhibitors. The "oxygen re-distribution model" hypothesises that mitochondria control intracellular oxygen

availability in hypoxia, through alterations in oxygen consumption at cytochrome c oxidase and this may be responsible for HIF-1α protein stabilisation, independent of ROS generation at complex III (Hagen et al., 2003, Chua et al., 2010, Doege et al., 2005) with a similar conclusion with HIF-2α (Brown and Nurse, 2008). Through the generation of an intracellular oxygen gradient in hypoxia, the oxygen concentration at mitochondria will be higher in order to maintain a degree of electron transport, while the oxygen concentration will be lower in the cytoplasm (Figure 1.6). The latter would inhibit the PHD proteins and promote stabilisation of HIF-1α. Therefore, at 1% oxygen, ETC inhibitor-treated cells would have an intracellular oxygen concentration at or around 1%, sufficient to allow the PHDs to functionally hydroxylate HIF-1α. In untreated cells the rate of hydroxylation will decrease as the ETC consumes oxygen and continue until oxygen is depleted. To summarise, a decrease in the rate of mitochondrial oxygen consumption and electron transport when the ETC is blocked by inhibitors results in an increase in cytoplasmic oxygen concentration and PHD re-activation, through a re-distribution of intracellular oxygen.

Hagen *et al* championed the "oxygen re-distribution model" as an alternative idea to the ROS-dependent model for HIF-α stabilisation, based on the observation that antioxidants did not reverse the inhibition of hypoxia-dependent HIF-1α stabilisation by myxothiazol and antioxidants failed to prevent HIF-1α stabilisation in hypoxia (Hagen et al., 2003). Through this work and previous observations (Mateo et al., 2003), Hagen *et al* proposed that re-distributed oxygen is a consequence of competitive binding of nitric oxide (NO). Hagen *et al* used nitric oxide donors to cytochrome c oxidase and ETC inhibition as a means to an increase non-respiratory oxygen and demonstrate inhibition of HIF-1α stabilisation at 3% oxygen as a result of PHD mediated prolyl hydroxylation and increased proteasomal degradation (Hagen et al., 2003).

The use of the $F_1F_O$-ATPase inhibitor oligomycin has also been observed to decrease HIF-1α protein in hypoxia, however not in response to PHD inhibitors DFO or dimethyloxalylglycine (DMOG) or in cells treated under anoxic conditions (Gong and Agani, 2005). Oligomycin decreases mitochondrial oxygen consumption, increases mitochondrial membrane potential and increases mitochondrial ROS. However, despite an increase in ROS induced after oligomycin treatment, HIF-1α fails to be stabilised in hypoxia (Gong and Agani, 2005). Collectively, these findings suggest that the mitochondrial ETC is necessary for the hypoxic stabilisation of HIF-1α, independent of ROS generation and instead as a result of

mitochondrial oxygen consumption indirectly modulating PHD function (Gong and Agani, 2005).

Chua and colleagues contributed the most striking observation to date to confirm the ROS-independent mechanism for mitochondrially mediated HIF-1α stabilisation in hypoxia. Chua *et al* demonstrated that by bypassing complex III, HIF-1α can still be stabilised in hypoxia (Chua et al., 2010). Chua *et al* observed no significant increase in ROS generation using dihydroethidium, after exposure of cells to hypoxia (1% $O_2$) and no reduction in response to ETC inhibitors, indicating no role for mitochondrial ROS in HIF-1α stabilisation in hypoxia. Chua *et al* continued to demonstrate that, in spite of using myxothiazol to inhibit complex III and superoxide production, that the artificial electron donor to cytochrome c and complex IV, N,N,N',N'-tetramethyl-p-phenylenediamine (TMPD) could rescue the myxothiazol-induced block on HIF-1α stabilisation. Hence, the restoration of oxygen consumption at complex IV is sufficient to stabilise HIF-1α in hypoxia and the inhibitory effects on HIF-α stabilisation after myxothiazol treatment alone, are potentially due to the consequential reduction in oxygen utilisation/consumption. Additionally, bypassing complex III and complex IV altogether using alternative oxidase (AOX) to accept electrons from co-enzyme Q and directly reduce oxygen to water, allowed maintenance of oxygen consumption and avoidance of complex III-dependent ROS production. Using AOX, HIF-1α was also observed to be stabilised under hypoxia, suggesting complex III and ROS are not involved. Finally, Chua *et al* demonstrated using an *in vitro* hydroxylation assay that exogenous hydrogen peroxide does not inhibit PHD protein activity directly (Chua et al., 2010).

The mechanism underlying both the ROS-dependent and oxygen re-distribution models is one involving the PHD proteins, although the precise role of the PHD proteins has yet to be demonstrated. It is likely that the role of mitochondria in the hypoxic stabilisation of HIF-α in hypoxia will involve elements of both these models. It is highly likely that in fact, mitochondrial ROS generation and oxygen re-distribution occurs during hypoxia and may allow for fine tuning of the HIF response.

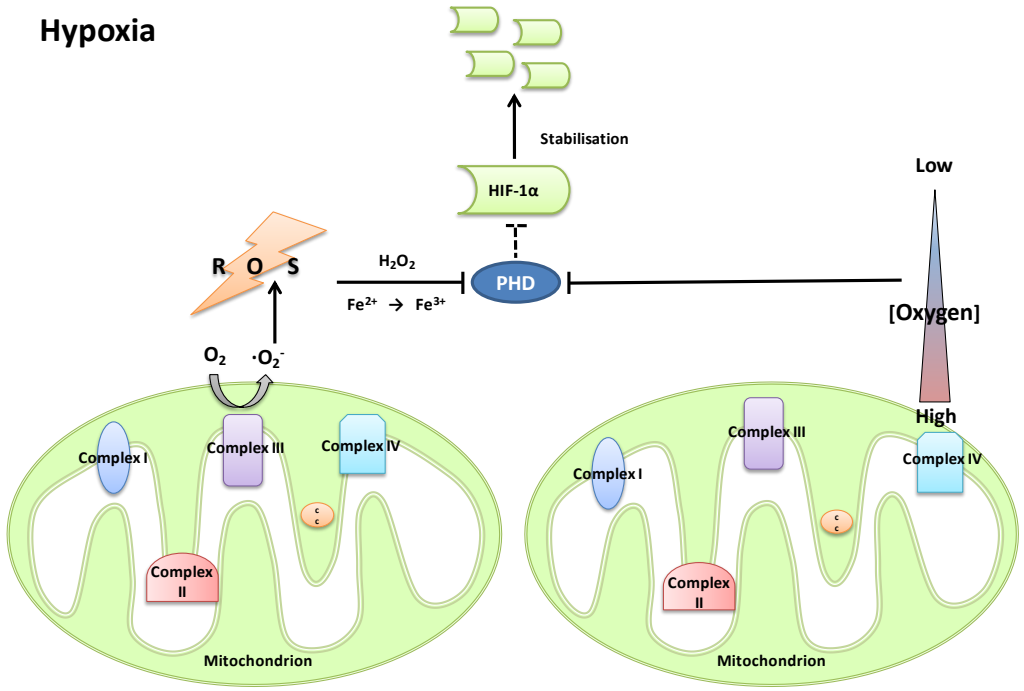


**Figure 1.6: Diagram showing alternative models for mitochondrial involvement in the hypoxic stabilisation of HIF-1α.**

**The ROS-dependent (left) and oxygen re-distribution (right) are two alternate models described for the role of mitochondria in the stabilisation of HIF-α in hypoxia. Mitochondria, shown in green, in hypoxia provide a source of ROS from complex III (left) or alternatively as the primary consumers of oxygen, create an oxygen gradient within cell (right). Both models are proposed to mediate the inhibition of PHD activity, stabilising HIF-α protein in hypoxia.**

### *1.3.2.4 Regulation of HIF-1α through interaction with the mitochondrial import machinery*

Ultrastructural analysis of mitochondria reveals that they consist of two aqueous compartments, the matrix and the IMS, separated by an inner membrane. Recently, a conserved mechanism for mitochondrial IMS protein import and biogenesis has been discovered, central to which is the mitochondrial protein Mia40, identified in yeast as essential for viability and import of small translocase of the inner membrane (Tim) proteins (Naoe et al., 2004, Chacinska et al., 2004).

The human homologue of Mia40 was described as being soluble in the IMS and not tethered through an N-terminal sequence as in lower eukaryotes (Hofmann et al., 2005) as well as being the principal mechanism of import for a wide range of mitochondrial IMS

proteins (Koehler and Tienson, 2009). Subsequently our group has identified the human coiled-coil helix coiled-coil helix domain 4 (CHCHD4) mitochondrial protein family (Yang et al., 2012). The human CHCHD4 gene encodes two alternatively spliced isoforms (CHCHD4.1 and CHCHD4.2), which are differentially expressed across human tissues. CHCHD4.1 is identical to human MIA40 and contains structurally and functionally essential conserved cysteines, within the conserved CHCH domain. We have shown that CHCHD4 (MIA40) regulates cellular oxygen consumption rate and ATP synthesis and that CHCHD4 (MIA40) is essential for regulating HIF-1α stabilisation in response to hypoxia. CHCHD4 (MIA40) knockdown blocks HIF-1α induction and transcriptional activity, decreases oxygen consumption rate and ATP biosynthesis in normoxia and inhibits tumour growth and angiogenesis *in vivo*. The converse also holds true, where over-expression of CHCHD4 (MIA40) can enhance HIF-1α stabilisation in hypoxia, correlates with increased tumour progression and decreased survival (Yang et al., 2012).

Most proteins present in the IMS are small (<20 kDa) and contain conserved cysteine residues arranged in either twin C-$X_3$-C or twin C-$X_9$-C domains particularly important for the formation of disulphide bonds and ultimately their import and mitochondrial trapping through the disulphide relay system (DRS) and the CHCHD4 (MIA40) machinery. CHCHD4/MIA40 is ubiquitously expressed and contains six essential cysteine residues involved in disulphide bond formation, four structural (C-$X_9$-C) and two (CPC motif) involved in electron shuttling after direct interaction and oxidation of mitochondrially imported proteins after translocation through the translocase of the outer mitochondrial membrane (TOMM) complex**.** IMS protein import does not require ATP or an inner membrane potential, unlike those targeted to the inner membrane or matrix (Tokatlidis, 2005). IMS proteins are imported in their reduced state through the TOMM complex and interact with Mia40 through a transient disulphide bond between the first cysteine residue in the substrate and the N-terminal cysteine in the CPC motif of Mia40 (Koehler and Tienson, 2009). Mia40 is redox sensitive and can be present in two different oxidation states, capable only of forming transient disulphide bonds with its substrates in its fully oxidised form. It is the role of the FAD-linked sulfhydryl oxidase Erv1 to re-oxidise Mia40 through transfer of electrons (Mesecke et al., 2005, Bien et al., 2010), which are then passed to either oxygen or cytochrome c (Dabir et al., 2007). Electrons passed via a redox reaction through a physical interaction between Erv1 and cytochrome c continue down the

respiratory chain, allowing re-oxidation of Erv1 and preventing the formation of toxic hydrogen peroxide (Figure 1.7) (Bihlmaier et al., 2007, Allen et al., 2005).

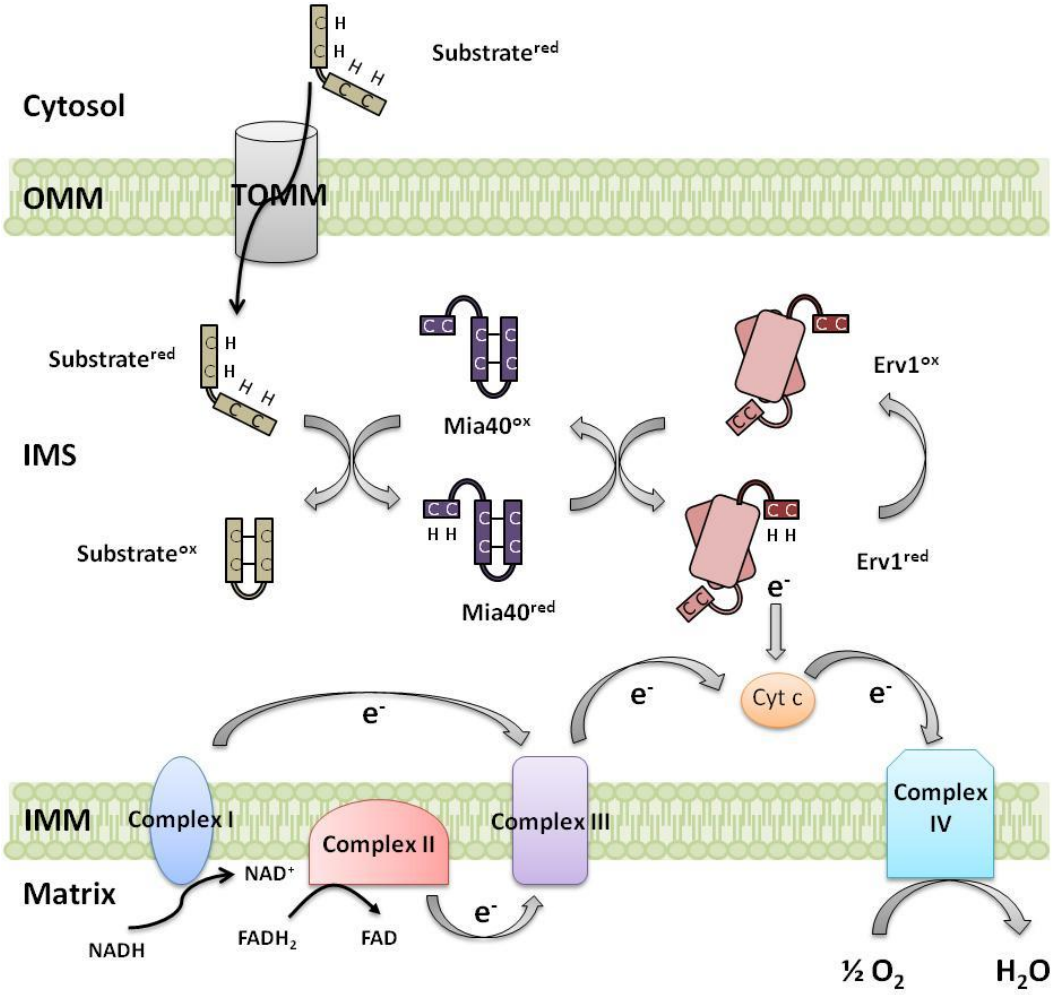


**Figure 1.7: Mitochondrial protein import through the disulphide relay system (DRS).**

**Diagram depicting protein import into the mitochondrial intermembrane space (IMS). Import substrates enter the mitochondrial IMS through the translocase of the outer mitochondrial membrane (TOMM) where they interact with oxidised Mia40. The substrate then becomes oxidised, folded and trapped in the IMS. Reduced Mia40 is re-oxidised through the donating an electron to Erv1 and subsequently to cytochrome c and the ETC. ox = oxidised, red = reduced.**

### 1.3.3 *Mitochondria and the HIFs*

Mitochondria and the HIFs exist in a reciprocal relationship. It has not only been observed that mitochondrial respiration plays a role in regulating HIF-α stabilisation and activity but

HIF activation also regulates mitochondrial metabolism. HIF is well documented to play a major role in the cellular metabolic adaptation to hypoxia (Figure 1.8). This regulation is indirect and mediated through increased expression of HIF-specific target genes. For example, expressed on cell surface membranes, the glucose transporter GLUT-1 is up-regulated in hypoxia through a HIF-dependent mechanism (Ebert et al., 1995). HIF-dependent induction of GLUT-1 was initially observed in HepG2 cells, over 12 hours hypoxia and is responsible for facilitating and regulating the transport glucose across the plasma membranes, increasing glycolytic substrate supply and flux under low oxygen tension (Ebert et al., 1995).

Substrate supply to the mitochondrial ETC is one of the limiting factors in respiratory rate. Acetyl co-A enters the Krebs cycle, after its conversion from pyruvate a reaction catalysed by pyruvate dehydrogenase (PDH). In hypoxia, the HIF targets pyruvate dehydrogenase kinase-1 (PDK-1) and PDK-3 in melanoma are up-regulated and drive pyruvate away from the mitochondria by phosphorylating and inactivating PDH, decreasing the supply of reducing equivalents to the ETC and suppressing respiration, ATP production and preventing hypoxia-induced oxidative damage (Kluza et al., 2012, Papandreou et al., 2006, Kim et al., 2006). Papandreou *et al* observed an increased sensitivity to the cytotoxin tirapazamine and cell death with loss of HIF-dependent PDK-1 expression. Papandreou *et al* therefore suggested, as a potential therapeutic strategy the combination of HIF-1 inhibitors, in order to force tumour cells to become more hypoxic, by inhibition of negative regulation of mitochondrial metabolism and hypoxic cytotoxics agents (Papandreou et al., 2006).

Hypoxic promotion of glycolysis functions in concert with the HIF-1α-dependent induction of lactate dehydrogenase A (LDHA), an enzyme that converts the pyruvate to lactate. Increased lactate contributes to a fall in intracellular pH, compensated for by HIF-dependent expression of the sodium/hydrogen exchanger-1 (NHE-1) and monocarboxylate transporter-4 (MCT-4) (Shimoda et al., 2006, Ullah et al., 2006), and further decreases pyruvate available to enter the TCA cycle (Firth et al., 1995).

HIF-dependent expression of *PKM2* encoding pyruvate kinase-M2, an isoform of pyruvate kinase expressed in the embryo and in cancer cells further limits substrate supply to the mitochondria in hypoxia. PKM2 functions in the terminal phase of glycolysis to convert phospho*enol*pyruvate (PEP) to pyruvate, which in turn enters the TCA cycle (Luo and

Semenza, 2011). Luo *et al* recently uncovered a HRE within the *PKM2* gene and observed HIF-1α to up-regulate its expression in hypoxia, a trait observed in cancer cells as a mechanism to increase aerobic glycolysis or the Warburg effect. Interestingly, PKM2 was observed to physically bind HIF-1α and HIF-2α and function as a transcriptional co-activator and augment transactivation of target genes and the shift from oxidative to glycolytic metabolism, functioning to promote HIF-dependent aerobic glycolysis (Luo and Semenza, 2011, Luo et al., 2011).

HIF-dependent cellular adaptation to hypoxia also directly regulates the ETC and OxPhos machinery. Fukuda *et al* (Fukuda et al., 2007), observed that under ambient oxygen, the predominant isoform of subunit 4 of cytochrome c oxidase is COX4-1. However, hypoxia increases mRNA transcription and protein expression of the more efficient COX4-2 isoform, (i.e. higher affinity for oxygen) in the liver and lungs of mice, in a HIF-dependent fashion. This increased expression works in tandem with HIF-mediated COX4-1 isoform degradation through up-regulated mitochondrial protease LON. Fukuda *et al* hypothesised that the COX4 subunit switch, from COX4-1 in normoxia to COX4-2 in hypoxia is a homeostatic response to maintain flow of electrons to complex IV and the reduction of oxygen to water to limit premature electron reduction earlier in the ETC and the formation of superoxide radicals, protecting the hypoxic cells from oxidant stress (Fukuda et al., 2007).

Tello *et al* (Tello et al., 2011), observed HIF-1α-dependent hypoxic induction of NADH dehydrogenase (ubiquinone) 1 alpha sub-complex, 4-like 2 (NDUFA4L2), a protein which down-regulates complex I activity, limiting mitochondrial oxygen consumption, mitochondrial membrane potential and ROS generation under hypoxia (Tello et al., 2011). Questions remain as to the precise role of NDUFA4L2 in hypoxic adaptation but it has been hypothesised to act in concert with PDK isoforms to limit substrate supply to the ETC through effects on complex I activity. Parallel decrease in NADH dehydrogenase (ubiquinone) 1 alpha sub-complex, 4 (NDUFA4) protein in hypoxia also may suggest that as observed with complex IV in hypoxia (Fukuda et al., 2007), there is the potential for a subunit switch (Tello et al., 2011). The role and position of NDUFA4L2 protein in complex I has not yet been fully elucidated.

Stabilisation and activation of HIF-1α has been shown to induce the transcription of microRNA-210 (miR-210) (Kulshreshtha et al., 2007). MicroRNAs (miRNAs) are small non-coding RNA oligonucleotides that bind to and facilitate cleavage of messenger RNA

preventing their respective translation and have surfaced as central regulators of gene expression (Bartel, 2004). miR-210 has been demonstrated to be up-regulated in hypoxia in a HIF-1 (but not HIF-2) dependent manner (Camps et al., 2008, Kulshreshtha et al., 2007) and negatively regulates mitochondrial metabolism in hypoxia through repression of iron-sulphur cluster assembly proteins -1 and -2 (ISCU-1/2) translation in human pulmonary artery endothelial cells (Chan et al., 2009). ISCU proteins are involved in the biogenesis and assembly of iron-sulphur clusters, prosthetic groups involved in electron transport and redox reactions. Iron sulphur cluster incorporation into proteins allows participation in numerous cellular processes and importantly identified to affect complexes I and IV of the mitochondrial ETC and the TCA cycle enzyme aconitase (Chan et al., 2009). Here, miR-210 directed translational repression of ISCU1/2 mediated a metabolic shift toward glycolysis, down-regulating mitochondrial function in hypoxia and promoting the Pasteur effect (Chan et al., 2009).

Finally, on a more macro scale, HIFs have been observed to affect mitochondrial biogenesis and turnover as an adaptive mechanism to hypoxia. The HIF-1α dependent expression of *MXI-1* negatively regulates c-MYC transcriptional activity in *VHL*-deficient renal cells by competing with c-MYC for binding to MAX. The c-MYC-MAX heterodimer is necessary for c-MYC-dependent gene transcription. Therefore the c-MYC induced expression of peroxisome proliferator activated receptor gamma (PPARγ) co-activator-1β (PGC-1β) is reduced under hypoxia, affecting mitochondrial biogenesis and negatively regulating mitochondrial mass, mitochondrial DNA content and cellular oxygen consumption rates (Zhang, 2007). A similar phenotype is observed through the HIF-1α dependent up-regulation of BNIP3. *BNIP3* gene transcription in prolonged hypoxia (48 hours) results in increased protein levels and displacement of the BH3-only protein, B-cell lymphoma-2 (BCL-2) binding beclin, freeing beclin and promoting autophagy and mitochondrial turnover, again preventing ROS-mediated damage and cell death in hypoxia (Zhang et al., 2008).

It is clear there is a central role for the HIFs in regulating mitochondrial metabolism and adaptation in response to hypoxia. Metabolic adaptations are not just observed physiologically, but also pathophysiologically, for example solid tumours have large hypoxic regions towards their core and consequent HIF-α activation in this location will promote adaptive tumour cell survival.

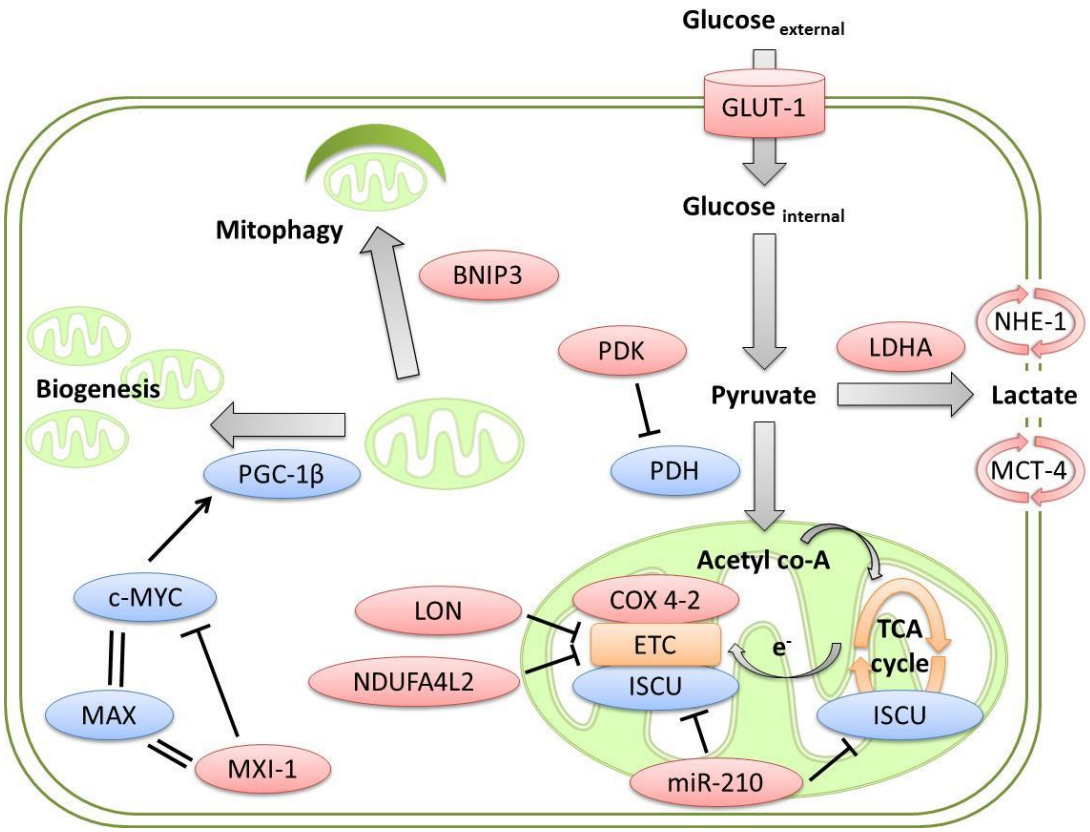


**Figure 1.8: HIF-1 regulates metabolic responses to hypoxia.**

**HIF-1 target genes, shown in red are involved in regulating glycolysis, mitochondrial biogenesis and oxidative metabolism through up-regulation of genes involved in glucose uptake, mitochondrial autophagy and the diversion of metabolic substrates. (For full description of proteins, see abbreviation list).**

## 1.4 Mitochondrial dysfunction in disease

### 1.4.1 *Mitochondria and cardiovascular disease*

The cardiovascular system is responsible for the delivery of oxygen and metabolic nutrients to tissues and principally mediates body and cell homeostasis. The heart is one of the most metabolically active organs and in most circumstances periods without oxygen and vital nutrients can be particularly detrimental and result in various pathologies (Shohet and Garcia, 2007). Ischaemic cardiovascular disease is characterised by disruption in the proper functioning and regulation of cardiac metabolism due to the body's inability to meet the hearts substantial metabolic demand, through the oxygen supply to the cardiac tissue being compromised. The cause of this, stems from either coronary artery occlusion or

increased myocardial oxygen requirements both resulting in reduced myocardial perfusion, localised tissue injury and ultimately in a heterogeneous group of pathological conditions (Shohet and Garcia, 2007). The severity of the resulting injury will be dependent on duration, intensity of the insult, and myocardial tolerance (Jafri et al., 2001).

In situations of myocardial ischaemia, diminished perfusion to the myocardium permits metabolic demand to outstrip supply and causes localised hypoxia. The interruption of the molecular oxygen supply causes OxPhos to slow, energy stores diminish and the quantity of reducing equivalents increase. The myocardium has a large bioenergetic demand, a high rate of ATP consumption and limited tolerance to perturbations in ATP supply (Heineman and Balaban, 1990). Cellular oxygen consumption falls when oxygen levels tend toward hypoxia (1-3% oxygen) and so in hypoxic or anoxic hearts as an adaptive response, metabolism switches from oxidation of fatty acids to a potentially 10-20% acceleration in glycolysis (Neely and Morgan, 1974). Under these situations electron flux through the respiratory chain decreases and consequently so does ATP biosynthesis, additionally in ischaemia this situation is accompanied by an build-up in lactate and cytosolic acidification (Solaini and Harris, 2005). Mitochondrial membrane potential will decrease during periods of ischaemia and the $F_1F_O$-ATPase reverses direction and instead of driving ATP synthesis will hydrolyse ATP and in an effort to maintain membrane potential (Leyssens et al., 1996). The outcome is a time-dependent loss of cellular integrity due to the amalgamation of ATP depletion, disruption of intracellular calcium signalling, mitochondrial permeability transition pore (mPTP) opening, ROS generation and failure of cellular repair mechanisms (Reviewed in (Cadenas et al., 2010, Levraut et al., 2003a)).

Activation of the glycolytic pathway alone is insufficient to satisfy the requirements of the demanding heart. In cardiac tissue the build-up of adenosine monophosphate (AMP) and phosphate will in turn inhibit the hearts contractile machinery and lactic acid, the by-product of anaerobic respiration, will in turn, cause extracellular pH to decrease (Halestrap et al., 2007, Jafri et al., 2001). Clinically, the first-line treatment for myocardial ischaemia is to re-establish blood flow, as irreversible necrotic ischaemic damage occurs within 20 minutes of occlusion (Downey et al., 2007). However, this is associated with its own problems such as enzyme and free radical release, and morphological changes, indicative of reperfusion injury (Halestrap et al., 2007).

Re-supplying the ischaemic myocardium with oxygen paradoxically results in more damage and this triggers a sequence of events leading to activation of cell death pathways, a phenomenon known as ischaemia-reperfusion (I/R) injury (Braunwald and Kloner, 1985). I/R injury is evident in a variety of clinical settings including in those individuals undergoing coronary artery bypass graft (CABG) surgery, patients who have survived cardiac arrest and those receiving thrombolysis or percutaneous coronary intervention (PCI) for an acute myocardial infarction (Hausenloy and Yellon, 2007).

In both mild and severe ischaemia, the heart is forced to adapt metabolically. As cells switch to aerobic respiration, the reperfusion post-ischaemia causes necrotic and apoptotic cell death, thought to be mediated by activation of FAS-ligand dependent cell death pathways, a rise in intracellular calcium and mitochondrial dysfunction (Taylor and Pouyssegur, 2007, Cadenas et al., 2010). Additionally, the cytotoxic ROS generated from mitochondria in combination with ROS generated elsewhere that is released during myocardial ischaemia and during reperfusion have detrimental consequences on the heart and particularly mitochondria (Levraut et al., 2003b, Di Lisa and Bernardi, 2006, Misra et al., 2009, Cadenas et al., 2010). It has been shown that oxidative stress during simulated ischaemia primes cardiomyocytes for cell death during reperfusion (Robin et al., 2007) and highlights the physiological importance of ROS homeostasis in the heart (Shohet and Garcia, 2007).

Increased oxidative stress is commonly associated with cardiovascular disease (CVD) risk and pathology, highlighting the importance of mitochondrially derived species. Oxidative stress correlates with a number of cardiovascular risk factors including hypercholesterolemia and oxidised low density lipoprotein, being observed *in vitro* to increase mitochondrial oxidant production and reduce membrane potential and free cholesterol to promote cytochrome c release and apoptosis (Ballinger, 2005). As mediators and targets of oxidative damage, mitochondria have also been implicated in the increased risk of diabetes associated with CVD (Ballinger, 2005). Interestingly, many disease causing mitochondrial DNA mutations have been associated with cardiac disease, particularly cardiomyopathy, which has been linked with mutations that affect mitochondrial protein synthesis (Ballinger, 2005).

HIF-α *in vivo* has been shown to be stabilised and activated in oxygen-deprived myocardium and after myocardial infarction (Lee et al., 2000). HIF-α is up-regulated in

response to chronic ischaemia (Lee et al., 2000) and *HIF-1α* mRNA levels and expression of its target gene *VEGF* were both increased after coronary artery occlusion (Lee et al., 2000).

### 1.4.2 *Mitochondria and neurodegenerative disease*

Parkinson's disease (PD) is a progressive neurodegenerative disorder, associated with postural instability, rigidity, tremor and bradykinesia with approximately only 5-10% of affected individuals having identified genetic causes, known as familial PD with the rest classified as idiopathic (Deas et al., 2011b). Quality control mechanisms exist in the cell to eliminate aged, damaged or dysfunctional mitochondria. Quality control mechanisms also allow the cell to prevent build up toxic reactive species, avoid activation of cell death pathways and rid itself of unnecessary metabolic burden (Vives-Bauza and Przedborski, 2011). Autophagy is an adaptive process by which the cell non-selectively degrades and recycles cytosolic components (He and Klionsky, 2009). The formation and elongation of an isolation membrane encapsulates and fuses, trapping cytosolic components forming a double membrane vesicle, known as the autophagosome (Mizushima, 2007). Mitophagy is the process of selective mitochondrial autophagy, a term coined by Lemasters in 2005 and has been observed be dysregulated in neurones in the substantia nigra in familial PD (Lemasters, 2005). Mitophagy uses the autophagic machinery to degrade mitochondria, however relies on specialised machinery to ensure mitochondrial targeting and specificity (Vives-Bauza and Przedborski, 2011).

Autophagy under basal conditions proceeds at a very low rate and is regulated by a large number of autophagy-related gene (ATG) proteins, which are recruited upon autophagic induction and are highly conserved between yeast and mammalian cells (He and Klionsky, 2009). Autophagosomes fuse with endosomes to form an intermediate known as an amphisome before fusing with the lysosome and creating the autophagolysosome. The content of the autophagosome are then degraded by the acid proteases within the lysosomal compartment and amino acids are recycled (Ravikumar et al., 2010).

Microtubule-associated protein 1 light chain 3 (LC3), is the only identified protein component of the inner autophagosome membrane. LC3 is synthesised as a pre-cursor and immediately cleaved in the cytoplasm at its C-terminus and forming LC3-I. It is then covalently bound to phosphatidylethanolamine by the concerted efforts of ATG7 and ATG3 to form LC3-II, which allows its targeting to both sides of the autophagosome membrane and thought to be necessary for the expansion and final fusion of the autophagosome (He

and Klionsky, 2009, Ravikumar et al., 2010). Autophagosomes then fuse with endosomes and finally the lysosome, involving lysosomal-associated membrane protein-2 (LAMP-2) and RAB7. The contents of the autophagosome are degraded by the acid proteases and released back into the cytosol to be re-used in bio-synthetic pathways (He and Klionsky, 2009).

Although the vast majority of PD occurs spontaneously, in approximately 5-10% of affected individuals there is a genetic link (Deas et al., 2011b). Heritable mutations in the 6 identified *PARK* genes are associated with dominant and recessive forms of the disease and result in loss of dopaminergic neurones in the substantia nigra and accumulation of cytoplasmic Lewy Bodies in the remaining neurones (Deas et al., 2011b). *PARK6* encodes the PTEN (phosphatase and tensin homologue)-induced putative kinase-1 (PINK1), a mitochondrially localised serine/threonine kinase, with kinase activity necessary for the translocation of parkin (encoded by *PARK2*) to the mitochondrial outer membrane (Vives-Bauza, 2010).

Mutations in PARK2 and PARK6, encoding parkin and PINK1 respectively are associated with recessive early onset PD. PINK1 and parkin were hypothesised to cooperate in the same pathway through the phenotypes of the respective knockouts in *Drosophila melanogaster* resulting in a similar phenotype (Park, 2006, Clark, 2006). *PINK1* knockout phenotype could be rescued by over-expression of parkin, however PINK1 over-expression failed to rescue *parkin* deficiency, suggesting parkin functions downstream of PINK1 (Clark, 2006, Park, 2006). The physical interaction of these proteins is still a matter of debate and the mechanism by which PINK1 recruits parkin to depolarised mitochondria remains unknown (de Vries and Przedborski, 2013).

Parkin is a cytosolic E3-ubiquitin ligase and associates with mitochondria that have stabilised PINK1 associated with their outer membrane. Parkin was first observed by Narendra *et al* in 2008 (Narendra et al., 2008) to translocate to mitochondria and promote their autophagic degradation after mitochondrial uncoupling and dissipation of the mitochondrial inner membrane potential using carbonyl cyanide m-chlorophenyl hydrazone (CCCP) (Narendra et al., 2008). Parkin translocation causes LC3B-II association of mitochondria and their turnover using the autophagic pathway (Narendra et al., 2008, Kawajiri, 2010).

Parkin translocation after depolarisation of the mitochondrial inner membrane was demonstrated to be PINK-1 dependent. PINK1 accumulates rapidly in pharmacologically depolarised mitochondria, using CCCP or combination of antimycin A and oligomycin, full length PINK1 can be observed in the mitochondrial fraction and this promotes the PINK1-parkin dependent peri-nuclear trafficking of mitochondria (Vives-Bauza, 2010). The voltage-dependent cleavage of PINK1 is inhibited by loss of membrane potential and its mitochondrial accumulation is independent of parkin expression however sufficient and necessary for parkin recruitment and mitophagy (Narendra, 2010). Presenilin-associated rhomboid-like protein (PARL) is the membrane potential sensitive component that is localised to the mitochondrial inner membrane and processes PINK1 under conditions where the membrane remains polarised and the PINK1 fragment is degraded by the proteasome. Loss of the mitochondrial proton gradient inhibits PARL activity and allows full-length PINK1 to accumulate and recruit parkin (Imai, 2012). Interestingly NIX has also been observed to increase parkin recruitment to mitochondria and induce parkin-mediated mitochondrial autophagy (Ding, 2010).

There are a number of mechanisms through which PINK1 and parkin may affect mitophagy. PINK1 and parkin have been observed to regulate mitochondrial size, through effects on fusion and fission machinery, promote peri-nuclear re-distribution of mitochondria toward the increased density of autophagosomes and lysosomes or directly recruit the autophagic machinery to the mitochondria. Disruption of these processes will lead to alteration in mitochondrial quality control and build-up of dysfunctional mitochondria and cellular damage and degeneration associated with neurones in the substantia nigra in PD (for review see (de Vries and Przedborski, 2013)).

Disease causing mutations in the *PARK2* gene are deficient in mitophagy, however mutants display distinct phenotypes determined by their capacity to ubiquitinate target proteins, which promotes final clearance, however dispensable for the peri-nuclear re-distribution of parkin-associated mitochondria (Lee et al., 2010b). E3-ligase activity deficient parkin mutants maintain their ability to associate with mitochondria and form peri-nuclear aggresomes however are defective in final clearance, unlike those with mutations in the ubiquitin-like domain, in which parkin fails to be recruited to mitochondria (Lee et al., 2010b).

Parkin has been observed to ubiquitinate several mitochondrial proteins that are associated with the outer mitochondria membrane such as voltage dependent anion channel-1 (VDAC1) and mitofusins -1 and -2 (MFN-1 and MFN-2) (Geisler, 2010, Gegg, 2010). The parkin-mediated degradation of MFNs promotes mitochondrial fragmentation prior to mitophagy, an event believed to inhibit the re-fusion of damaged mitochondria, ensure their removal and avoid their re-complementation with healthy mitochondria. Parkin-mediated ubiquitination of mitochondrial outer membrane proteins promotes the recruitment of key regulatory components of the mitophagic response. The polyubiquitinated proteins that line the outer mitochondrial membrane are recognised and bound by the adaptor molecules p62/sequestosome-1 and histone deacetylase-6 (HDAC6) (Figure 1.9) (Lee et al., 2010b, Pankiv, 2007, Lee et al., 2010a).

The protein p62 facilitates the association of the ubiquitinated mitochondria with the autophagosome membrane through direct binding to LC3 (Pankiv, 2007) and HDAC6 controls the fusion of the autophagosome and lysosome (Lee et al., 2010a). Narendra *et al* demonstrated that p62 is required for parkin-induced mitochondrial clustering but not necessary for mitophagy to occur (Narendra et al., 2010). In contrast to earlier observations, Narendra *et al* also demonstrated VDAC1, is dispensable for both the clustering of mitochondria and mitophagic turnover (Narendra et al., 2010, Geisler, 2010). Recently Sarraf *et al* have published a large proteomic study on the depolarisation-dependent parkin ubiquitylome (Sarraf et al., 2013). Investigations into mitochondrial depolarisation-dependent parkin ubiquitination has paved the way to better understand the diverse range of parkin substrates, its role in mitophagy and undoubtedly other cellular processes.

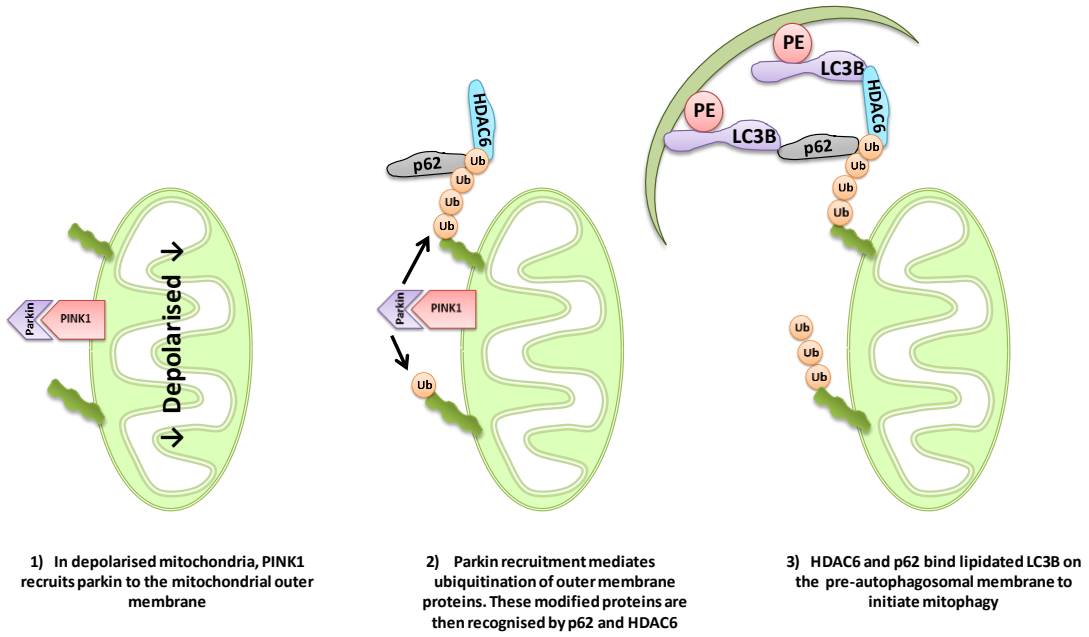


**Figure 1.9: Mechanism of PINK1 and parkin mediated mitophagy.**

**Mitochondrial depolarisation stabilises PINK1 and recruits parkin to the outer mitochondrial membrane. Parkin ubiquitinates target proteins and facilitates mitochondrial recognition by adaptor proteins HDAC6 and p62. Adaptor proteins then bind LC3B on the autophagosomal membrane and mitochondria are subsequently degraded through the classical autophagic pathway. Adapted from (Vives-Bauza and Przedborski, 2011).**

Interestingly, parkin has been identified not only to promote mitophagy *in vivo*, but also to induce the selective turnover of mitochondrial respiratory chain proteins in *Drosophila melanogaster* (Vincow et al., 2013). Using *parkin* knockout flies, Vincow *et al* demonstrated that loss of parkin *in vivo* prolongs mitochondrial protein half-life. Surprisingly 40 proteins demonstrated greater dependence on parkin for their turnover than on ATG7, which acts downstream, of parkin in the mitophagic pathway. This suggests a parkin-dependent ATG7-independent process mediating mitochondrial protein turnover. Within these 40 proteins, subunits of the ETC where over-represented and components of all five complexes identified, with most being membrane bound. Identification of parkin sensitive proteins suggests a wider role for parkin in the selective turnover of respiratory chain proteins which, for example in *PARK2* mutants could contribute to the mis-folding of ETC complexes observed in parkin mutant flies and perhaps in PD (Vincow et al., 2013).

### 1.4.3 *Mitochondria and cancer*

In 1956 Otto Warburg described the metabolic profile of cancer cells, that despite the abundance of oxygen, cancer cells will utilise glucose and glycolysis as their predominant source of energy (Warburg, 1956). Aerobic glycolysis became known as the Warburg effect. Despite Warburg's observation and contrary to what one might think, mitochondrial function is essential for the survival of cancer cells and depletion of their mitochondrial DNA reduces tumourigenicity and proliferation (Cavalli et al., 1997), highlighting the importance of mitochondrial function, outside their role of generating ATP.

As discussed, the HIFs have a well-recognised involvement in regulating mitochondrial metabolism and function in cancer. Through target gene transactivation, HIF stabilisation increases glucose uptake, up-regulates a number of glycolytic proteins and promotes lactate production. HIF additionally down-regulates mitochondrial oxidative metabolism and HIF is therefore well placed to promote tumour cell adaptation and survival and to support the classical Warburg effect (Semenza, 2007a). Mutations in mitochondrial enzymes fumarate hydratase (FH) and succinate dehydrogenase (SDH) also contribute to HIF-α stabilisation and to the tumourigenic profile of the HIFs. Mutations in these TCA cycle genes, causes excess fumarate and succinate respectively, which have been demonstrated to inhibit the PHD proteins and promote the stabilisation of HIF-α (Cardaci and Ciriolo, 2012, Koivunen et al., 2007a). These mutations support the expression of classical HIF target genes such as *VEGF*, involved in promoting angiogenesis, *IGF-1* which promotes cell survival and *plasminogen activator inhibitor-1* (*PAI-1*), which promotes metastasis (Poon et al., 2009). Thus targeting HIF, although challenging, is an alternative therapeutic strategy in cancer (Poon et al., 2009).

An interesting and distinct area of cancer biology is the role of mitochondria in determining the metastatic potential of cancer cells, which accounts for approximately 90% of cancer associated deaths. Through the production of trans-mitochondrial cybrids, whereby endogenous mitochondria DNA from a poorly metastatic cell line was replaced with that of a highly metastatic one and *vice versa*, Ishikawa *et al* demonstrated that the recipient cell acquired the metastatic potential of the donor (Ishikawa et al., 2008). Mitochondrial DNA from the highly metastatic cells contained a mutation in the *ND6* gene, encoding NADH dehydrogenase subunit 6, leading to complex I dysfunction and ROS generation. Increases in HIF-1α and VEGF protein expression were also demonstrated (Ishikawa et al., 2008).

Treatment of cells containing mitochondrial DNA from highly metastatic cells with ROS-scavengers repressed their metastatic potential, identifying a role of oxidant stress in the promotion of the metastatic phenotype (Ishikawa et al., 2008). In line with the anti-oxidant evidence, mice that expressed a mitochondrially targeted catalase were crossed those that developed metastatic breast cancer and demonstrated reduced metastatic burden compared to mice without mitochondrial catalase. This catalase-mediated metastatic suppression again suggested a role for mitochondrial ROS in promoting cancer metastasis (Goh et al., 2011). Mitochondrial DNA mutations in cancer cells have also been demonstrated to promote resistance to autophagy as a mechanism to increase metastatic potential (Kulawiec et al., 2009).

Loss of caveolin-1 in stromal fibroblasts, has led to a new paradigm of a two-compartment tumour metabolism model, termed "the reverse Warburg effect" or stromal-epithelial metabolic coupling (Wallace, 2012, Martinez-Outschoorn et al., 2010a, Martinez-Outschoorn et al., 2010b, Sotgia et al., 2012). $H_2O_2$ has been observed to be secreted from cancer cells into the adjacent heterogeneous mass of cells. $H_2O_2$-dependent loss of caveolin-1 from the stromal fibroblasts promotes their mitophagy. This reduces mitochondrial mass of these cells and promotes glycolysis. In stromal cells, mitochondrial dysfunction and promotion of the 'Warburg effect' or aerobic glycolysis leads to the excretion of lactate and ketones and their subsequent uptake by epithelial tumour cells. Lactate and ketones fuel cancer cell mitochondrial energy production and mitochondrial generation of precursors of cellular biogenesis and anabolic growth (Wallace, 2012, Martinez-Outschoorn et al., 2010a, Martinez-Outschoorn et al., 2010b, Sotgia et al., 2012). Interestingly, secondary tumours from metastatic breast cancer in the brain have dramatically increased oxidative metabolism compared to the tumour from which they originated. Cells from secondary tumours also exhibit up-regulation of genes involved in the pentose phosphate pathway and glutathione system, which reduces ROS. This increase in oxidative metabolism provides the metastatic cancer cell with resistance towards therapy as well as a proliferative and survival advantage (Chen et al., 2007). Metastatic breast cancer cells display oxidative metabolism and stain positively for TOMM20 and COX-IV. Conversely tumour adjacent fibroblasts stain positively for MCT-4 (glycolytic marker), demonstrating that two-compartments exist side-by-side in a primary tumour and its metastases (Sotgia et al., 2012).

Mitochondrial dynamics have also been shown to regulate cancer cell metabolism. Up-regulation and activation of the mitochondrial fission protein dynamin related protein -1 (DRP-1) and fragmented mitochondria have been observed in an invasive breast carcinoma cell line and their lymph node metastases. Silencing of DRP-1 and over-expression of MFN-1 reduces mitochondrial fission, promotes elongation and leads to reduced cancer cell invasion (Zhao et al., 2012). Lamellipodia are necessary for chemo-attractant-induced breast cancer invasion and metastasis. Increases in mitochondrial fusion or decreases in fission inhibits lamellipodia formation, whereas increases in mitochondrial fragmentation promotes the formation of lamellipodia (Zhao et al., 2012).

A number of mitochondrially metabolically targeted treatments are currently under investigation, including small molecule BH3-domain mimetics, which promote apoptosis in cancer cells, mitochondrially targeted heat shock protein 90 (HSP90) inhibitors, use of lipophilic molecules to take advantage of the hyperpolarised mitochondrial inner membrane potential of cancer cells as well as mitochondrially targeted catalase as discussed (Bhandary et al., 2012).

## 1.5 Conclusions

The relationship between HIF and mitochondria is clearly a well explored aspect of HIF biology. Important and intimate links exist between mitochondria, key organelles which consume oxygen and the cellular pathways through which low oxygen is sensed and relayed.

Drug discovery approaches aimed toward manipulating the HIF pathway hold the promise of clinical benefit and much interest exists in targeting the pathway for the purpose of treating defined pathologies. Activation of the HIF pathway may provide cardioprotection for those at risk of cardiovascular and ischaemic disease and conversely inhibition of HIF activity in solid cancers would reduce tumour cell survival and disease progression in response to conventional treatment.

How mitochondria interface with the HIF oxygen-sensing machinery is of great interest. The possibility that HIF and/or other components of the oxygen-sensing pathway perform yet unidentified novel mitochondrial functions that may result in cell survival/homeostasis are being explored in our lab and in other labs across the field.

# Chapter 2: Materials and methods

## 2.1 Tissue culture and protein analysis

### 2.1.1 *Antibodies and Reagents*

For all antibodies and reagents used please see table 1 and table 2.

### 2.1.2 *Cell culture*

Murine atrial HL-1 cardiomyocytes, described previously (Claycomb et al., 1998, White et al., 2004) were maintained in Claycomb medium (Sigma/SAFC biosciences) and supplemented with 2mM L-glutamine, 100U/ml penicillin, 100µg/ml streptomycin (all purchased from Gibco/Life Technologies), 100µM norepinephrine in 30mM L-ascorbic acid (both Sigma) and 10% fetal calf serum (FCS; Harian). Cells were subcultured at confluence in a split ratio of 1:3. Culture flasks (Falcon) were pre-coated with a solution of 0.02% (w/v) gelatin (Sigma) containing 1µg/ml fibronectin (Sigma).

HCT116 containing wild type p53 (designated HCT116 $^{+/+}$) described previously (Bunz et al., 1998), HeLa (Health Protection Agency) and pVHL positive and negative 786O cells, described previously (Iliopoulos et al., 1995) were maintained in Dulbecco Modified Eagle Medium (DMEM; Invitrogen), supplemented with 10% FCS, 2mM L-glutamine, 100U/ml penicillin and 100µg/ml streptomycin. Stable pools of RCC10 cells described previously (Bond et al., 2011), were maintained in DMEM selection media containing 0.5µM G418 (Sigma) in addition to supplements listed above. At confluence, cells were split in ratios between 1:10 – 1:20. All cells were maintained at standard cell culture conditions (37 °C, 5% $CO_2$ and 95% relative humidity).

Normoxia (Nx) or ambient oxygen refers to incubation at 37°C in (21%) oxygen and 5% carbon dioxide. For hypoxic (Hx) treatment, cells were placed in a Ruskinn *in vivo* 1000 hypoxic workstation at 1% $O_2$, 5% $CO_2$, and 94% $N_2$ at 37°C for the desired time, as stated.

### 2.1.3 *Cell Lysis*

Following treatment, samples were washed in ice-cold phosphate buffered saline (PBS) and harvested in 1% NP40 lysis buffer (100mM Tris pH 8, 100mM NaCl, 1% (v/v) NP40, 10% (v/v) glycerol, 0.5mM EDTA, supplemented with 10mM glycerophosphate, 1mM sodium fluoride, 1mM sodium orthovanadate and 100x EDTA-free protease inhibitor cocktail (Thermo Scientific).

### 2.1.4 *SDS-PAGE and western blotting*

Protein concentration in the cell lysate was measured using the Biorad DC protein assay (Biorad) according to manufacturer's instructions and 30-60µg of protein was made to volume with 2x sample buffer (125mM Tris pH 6.8, 4% sodium dodecyl sulphate (SDS), 0.01% (v/v) bromophenol blue, 10% (v/v) β-mercaptoethanol, 10% (v/v) glycerol). Proteins were separated using 7.5%, 10% or 12.5% SDS-polyacrylamide gel electrophoresis (SDS-PAGE) and subsequently transferred electrophoretically to a polyvinylidene fluoride (PVDF) membrane (Millipore) over night at 4°C at 30V or for 5 hours at 0.5A at 4°C. Membranes were then blocked for one hour at room temperature in 5% (w/v)-skimmed milk-Tris-buffered saline (140mM NaCl, 200mM Tris base, pH 7.4) - 0.1% (v/v) tween-20 (TBS-T). Membranes were incubated in primary antibody overnight at 4°C, before being washed for 5x 5 minutes in TBS-T and incubated with HRP-conjugated secondary antibody (Amersham or Dako) for one hour at room temperature. Membranes were washed again in TBS-T for 5x 5 minutes and bands were visualised using enhanced chemiluminescence solution (ECL) or ECL plus solution and hyperfilm-ECL (Amersham).

### 2.1.5 *Growth factor-mediated induction of HIF-1α protein*

HL-1 cardiomyocytes were plated at a density of $2.5x10^6$ in 6 well plates and incubated for 24 hours in Claycomb media at 37 °C and 5% $CO_2$. The media was aspirated and then was replaced with serum-free DMEM and returned to the incubator for 40 hours. Serum free media was replenished and IGF-1 (100ng/ml) was added to each well. Cells were harvested in ice cold 1% NP40 lysis buffer at specific time points.

## 2.2 Cell manipulation

### 2.2.1 *Plasmid preparation*

Enhanced green-fluorescent protein (EGFP) plasmids in pcDNA-3 for each of the PHD protein were provided by Prof. Patrick Maxwell (University of Cambridge, UK) and described previously (Metzen et al., 2003). Targeted ATP Luciferase constructs in pcDNAI, described previously (Jouaville et al., 1999), were provided by Dr. Gyuri Szabadkai (University College London, UK). Constructs were transformed into competent cells (BL21-GOLD (DE3), Agilent technologies) using a heat shock method described in the manufacturer's instructions. Purified DNA was prepared by Maxi-prep (Qiagen) as

manufacturer's instructions. Plasmid DNA was quantified using a Nanodrop 8000 UV-Vis spectrophotometer (Thermo Scientific).

### 2.2.2 *Transient transfection of plasmid DNA*

Cells at 70-80% confluence in 10cm tissue culture plates were transfected either using Lipofectamine 2000 (Invitrogen) as per manufacturer's instructions (2µg DNA:4µl Lipofectamine in one chamber of 6-well plate) or using the calcium phosphate method. Briefly, calcium phosphate-DNA complexes were prepared as follows for a 10cm plate: 10µg DNA was diluted in water to a total volume of 440µl. 500ul of 2x Hanks Balanced Salt Solution (HBSS; 280mM NaCl, 10mM KCl, 1.5mM $Na_2HPO_4$-$7H_2O$, 12mM dextrose, 50mM HEPES pH 6.8) was added to the DNA solution. 60 µL of 2M $CaCl_2$ was added drop wise to a final volume of 1ml. The mix was incubated at room temperature for 10-20 minutes to allow the complexes to form. The precipitate was re-suspended by gentle pipetting and added drop wise over the cell monolayer and returned to the incubator overnight for 16 hours. The precipitate was washed and replaced with fresh complete media and cells were allowed to recover for 24 hours at 37 °C.

### 2.2.3 *siRNA duplexes and transient transfection*

Custom made siRNA to human HIF-1α (5'-TACGTTGTGAGTGGTATTATT-3') and HIF-2α (5'-CCCGGATAGACTTATTGCCAA-3') were purchased from Dharmacon and used at a final concentration of 20nM. A non-silencing control siRNA duplex (5'-AATTCTCCGAACGTGTCACGT-3') was obtained from Qiagen and published previously (Carroll and Ashcroft, 2006, Carroll and Ashcroft, 2008). Transient transfection with siRNA duplexes were performed using HiPerfect™ (Qiagen) or Lipofectamine 2000 transfection reagent according to manufacturer's instructions. Protein knockdown was confirmed by western blotting and mRNA by real-time quantitative polymerase chain reaction (RT-qPCR).

### 2.2.4 *RNA isolation and complementary DNA synthesis*

Total RNA was extracted from cells using RNeasy mini kit with DNase digestion (Qiagen) as manufacturer's instructions and quantified using the Nanodrop 8000 spectrophotometer. 1µg of total RNA was used for first strand synthesis using the qScript First-Strand cDNA synthesis system (Quanta Biosciences) in a total volume of 20µl. Complementary DNA (cDNA) was synthesised using the G-Storm thermocycler with the following cycling parameters:

1) 25°C for 5 minutes
2) 42°C for 30 minutes
3) 85°C for 5 minutes
4) Hold at 4°C

cDNA was diluted to 600µl with RNase and DNase free dd$H_2O$ and used for RT-qPCR analysis.

### 2.2.5 *Real-time quantitative polymerase chain reaction (RT-qPCR)*

Forward and reverse primers were diluted to 2.5µM and used at a final concentration of 0.5µM in 25µl volume. 7.5µl diluted complementary DNA (cDNA) and 12.5µl 2x Mesa Blue SYBR green mix (Eurogentec) was used per reaction. Duplicate reactions were performed and average values obtained and used in analysis. Primer sequences can be found in table 3.

The PCR reaction was performed using a DNA Engine Opticon 2 (MJ Research) with the following cycling parameters:

1) 95°C for 5 minutes
2) 94°C for 20 seconds
3) 60°C for 25 seconds
4) 72°C for 50 seconds
5) Steps 2-4 were repeated 39 times

Data was analysed using the comparative cycle threshold (Ct) method. The Ct values were obtained during the exponential phase of the fluorescence logarithmic curve. Values from technical replicates were averaged and analysed using the equation below and as published (Schmittgen and Livak, 2008):

$$Relative\ expression\ (fold\ change) = 2^{-\Delta\Delta Ct}$$

$$2^{-\Delta\Delta Ct} = [(Ct\ gene\ of\ interest - Ct\ internal\ control)\ \boldsymbol{sample\ A} - (Ct\ gene\ of\ interest - Ct\ internal\ control)\ \boldsymbol{sample\ B}]$$

### 2.2.6 *Agarose gel electrophoresis*

PCR products were run on a 1.5% agarose gel in TAE buffer (40mM Tris-acetate, 1mM EDTA) plus ethidium bromide at 90V until completion and visualised using a BioDoc-It imaging system (UVP).

## 2.3 Mitochondrial and metabolic assays

### 2.3.1 *Mitochondrial isolation from cells*

After treatment, cells from confluent 15 cm plates were trypsinised and washed once in PBS before fractionation. Mitochondria were isolated using a mitochondrial isolation kit for cultured cells (Thermo Scientific). The non-mechanical, reagent-based method was used according to the manufacturer's instructions. Mitochondria were lysed in 1% NP40 lysis buffer and stored at -20°C until processing. Fractionated proteins were assessed by SDS-PAGE and western blotting.

Alternatively, mitochondria were isolated by differential centrifugation. Briefly, after treatment, cells from confluent 15 cm plates were trypsinised and washed once in PBS. Cells were re-suspended in homogenisation buffer A (250mM mannitol, 0.5mM 2-[4-(2-hydroxyethyl)piperazin-1-yl]ethanesulfonic acid (HEPES) pH 7.4 and 0.5mM ethylene glycol-bis(2-aminoethylether)-*N*,*N*,*N'*,*N'*-tetraacetic acid (EGTA); all obtained from Sigma, plus 100x EDTA-free protease inhibitor cocktail). Cells were homogenised with a glass-on-glass Dounce homogeniser using 100 strokes of a tight fitting pestle. A small volume of the total cell homogenate was removed and stored (load fraction). The homogenate was centrifuged at 900g for 10 minutes to pellet nuclei and intact cells, the supernatant containing mitochondria was removed and this step was repeated and supernatant again removed. Mitochondria were sedimented after centrifugation at 9000g for 10 minutes. The supernatant was removed and stored (cytosolic fraction). The crude mitochondrial pellet was washed in homogenisation buffer A and centrifuged at 9000g for 10 minutes. The pellet was lysed in 1% NP40 lysis (mitochondria fraction). All steps were performed on ice and centrifugation was performed at 4°C.

### 2.3.2 *Mitochondrial isolation from tissue*

Mitochondria were isolated from mouse livers, using differential centrifugation. Livers were collected from healthy mice, minced and washed in mitochondrial isolation buffer A

(250mM mannitol, 0.5mM HEPES pH 7.4 and 0.5mM EGTA, plus 100x EDTA-free protease inhibitor cocktail). Tissue was then homogenised using a Dounce homogeniser using 2ml of buffer A per gram of tissue (20 strokes loose, 20 strokes tight). A small sample of the resulting homogenate was removed and stored (homogenate). The remaining homogenate was centrifuged at 800g for 10 minutes to pellet nuclei and the supernatant was removed. This step was repeated on the supernatant. The post nuclear supernatant was then spun at 10,300g for 10 minutes to pellet mitochondria and a small volume of supernatant removed (post mitochondrial supernatant). The pellet was re-suspended and spin repeated to wash the pellet. Mitochondria were re-suspended in 1ml of buffer A and a small volume removed (crude mitochondria). Purified mitochondrial fraction was obtained after layering crude mitochondrial samples on a 30% (v/v) Percoll™ gradient in solution B (225mM mannitol, 5mM EGTA, 25mM HEPES pH 7.4 plus 100x protease inhibitor cocktail) and spinning at 95,000g for 40 minutes. Fractions were collected, washed in solution A and spun at 6,300g for 10 minutes, re-suspended in a solution A and stored at -20°C.

### 2.3.3 *Total cellular ATP assay*

Cells were either seeded in 96 wells plates in either DMEM containing glucose or galactose (both at 4.5g/l) for 24 hours prior to drug treatment or re-suspended to a constant cell concentration before addition of the reagent. Cell-Titre Glo reagent (Promega) was added and assay performed as outlined in the manufacturer's instructions. Samples were quantified using a Tropix TR717 microplate luminometer.

### 2.3.4 *Measurement of oxygen consumption and of extracellular acidification rate*

The oxygen consumption rate (OCR) and extracellular acidification (ECAR) rate was measured using the XF24 Bioanalyser (Seahorse Bioscience). Briefly, cells were seeded in complete media at densities between 15,000-20,000 for HL-1 and 45,000 for HCT116 cells in the Seahorse V7 cell culture plate the night before the assay using a 2 step seeding protocol. Prior to the assay, cells were washed twice and media changed to un-buffered basal DMEM, without sodium bicarbonate and phenol red (Sigma). This was supplemented with 4.5 g/l glucose or galactose, 4mM L-glutamine and 1mM pyruvate at pH 7.4 and placed into a non-$CO_2$ incubator. The dissolved oxygen in the media was measured and OCR and extracellular acidification rate calculated. Mix-wait-measure cycles were optimised to 3, 0.5, 3 minutes for HL-1 cells and 3, 2, 2 minutes respectively for HCT116 cells. Drug concentrations optimised to 0.5 µg/ml oligomycin, 1µM FCCP and 2µg/ml antimycin A for

HL-1 cells and 0.5 µg/ml oligomycin, 1.5µM FCCP and 2µg/ml antimycin A for HCT116 cells. Measurements were normalised to protein using the sulforhodamine B (SRB) assay.

The Seahorse XF24 extracellular flux analyser allows measurement of cellular oxygen consumption over time, in a multiwall plate based format. The XF24 analyser utilises fluorescent sensors to measure extracellular fluxes of oxygen. The fluorescent sensors form part of a bio-cartridge that during the assay lowers to approximately 200µm above the cell monolayer and creates a 7µl microchamber in which the change in oxygen concentration is measured over time (measure cycle). The bio-cartridge is then elevated and media allowed to equilibrate (mix and wait cycles), before the next reading (Ferrick et al., 2008).

### 2.3.5 *Sulforhodamine B (SRB) assay for analysis of cellular protein content*

Cells were fixed by removing media and adding ice cold 10% trichloroacetic acid for 30 minutes at 4°C before being washed 5 times with tap water and left to dry. To each well 100µL of 0.4% SRB/1% acetic acid solution was added and left for 10 minutes. Wells were then washed 5 time with 1% acetic acid and again left to dry as before. SRB was solubilised by adding 100µl of 10mM Tris buffer followed by gentle shaking for 10 minutes. The absorbance was read at 570nm using a Magellan plate reader.

### 2.3.6 *Polarography*

Cellular oxygen consumption rates were obtained using the Oxygraph 2K (O2K; Oroboros Instruments). Cells were trypsinised and re-suspended in 3-6ml of HEPES-buffered DMEM or for analysis of permeabilised cells re-suspended in mitochondrial respiration media (0.5mM EGTA, 3mM $MgCl_2.6H_2O$, 60mM k-lactobionate, 20mM taurine, 10mM $KH_2PO_4$, 20mM HEPES, 110mM sucrose, 1g/l (w/v) essentially fatty acid free bovine serum albumin (BSA) (all obtained from Sigma) and counted twice. Cells were added (2.2ml) to each chamber, plungers were replaced and cells incubated at 37°C under constant stirring. Cells were allowed to reach routine baseline respiration before the addition of the first compound. 2µg/ml oligomycin, 0.5µM increments FCCP, 0.5µM rotenone and 2.5µM antimycin A were injected in sequence and the OCR calculated.

### 2.3.7 *Real-time compartmental ATP Luciferase Assay*

HCT116 cells were plated at 400,000 per chamber of a 6-well plate and transfected with each plasmid encoding luciferase targeted to the mitochondria or a non-targeted plasmid (cytosolic) using Lipofectamine 2000 as described above. Cells were transfected for 6-8

hours; the complexes were then washed off, replaced with fresh complete media and incubated overnight at 37 °C. Cells were then trypsinised and re-plated in DMEM containing either glucose or galactose (both at 4.5g/l) at a density of 60,000 cells per well in white 96 well plates coated with 0.1% gelatine (Gibco) to aid adherence and left overnight. Immediately before the assay, the media was replaced with 200µl HEPES buffered phenol red free DMEM plus 10uM D-luciferin sodium salt (Sigma). Cells were placed in a temperature controlled Fluostar plate reader (BMG Labtech) at 37 °C and luminescence was read at one to two minutes intervals. Drugs were diluted in PBS plus 10µM D-luciferin and added in a 20µl volume at points indicated through an automated injection system.

### 2.3.8 *Metabolomics*

Cells were plated and treated in T175 flasks. Media was removed and stored at -80°C. Cells were washed in ice cold 0.9% saline and 6ml of ice cold methanol was added. Cells were incubated on ice for 10 minutes, after which they were scraped into a 50ml falcon tube and 6ml ice cold chloroform added. Tubes were vortexed vigorously for 30 seconds before 6ml of ice cold de-ionised water was added to each tube and again vortexed vigorously for 30 sec. Samples were centrifuged at ~10000rpm for 20 minutes for phase separation. The final chlorform: methanol: water ratio was 1:1:1 (v/v/v). The upper methanol-water phase contained the water-soluble cellular metabolites, the middle phase contained the protein pellet and the bottom chloroform phase contained the cellular lipids. After separation of the phases, the protein pellets were kept for protein concentration determination. The upper methanol-water phase was treated with Chelex 100 (~1mg/1ml) to remove divalent ions and centrifuged to remove Chelex, retaining the clear supernatants. The clear supernatents were lyophilized and dried samples stored at -20$^{o}$C. The bottom chloroform phase was transferred into glass tubes and left in a fume hood overnight. The dried samples were again stored at -20$^{o}$C minimum. Metabolite analysis was performed by Dr. Yuen-Li Chung (The Institute of Cancer Research, Sutton, UK).

### 2.3.9 *Flow cytometric analysis of mitochondrial membrane potential*

Following treatment or 24hrs after plating, cells were collected by trypsinisation and pelleted by centrifugation (1500rpm for 3 minutes), approximately 1x10$^{6}$ cells/ml were re-suspended in HEPES buffered DMEM plus 0.2nM 3,3'-Dihexyloxacarbocyanine Iodide (DIOC6(3); Sigma) and allowed to equilibrate for at least 30 minutes before analysis. Cells

were analysed using a CyAn ADP analyser (Beckman Coulter) and data analysed using the SUMMIT 4.3 software.

### 2.3.10 *Flow cytometric analysis of mitochondrial mass*

Cells were collected as above (2.3.9) and approximately $1x10^6$ cells/ml were re-suspended in HEPES buffered DMEM plus 100nM mitoview green (Biotium) for 30 minutes. The mitochondrial uptake of mitoview green is independent of mitochondrial inner membrane potential and fluoresces only after partitioning into the mitochondria. Cells were then pelleted and re-suspended in HEPES buffered DMEM. Cells were processed using a CyAn ADP analyser (Beckman Coulter) and data analysed using the SUMMIT 4.3 software.

### 2.3.11 *Determination of mitochondrial DNA copy number*

Total DNA was isolated from cell pellets using QIAamp DNA blood mini kit (Qiagen). The amount of mitochondrial DNA relative to nuclear genomic DNA was determined by quantitative real-time PCR using primers for *ND1* (mitochondrial) and *beta-2-microglobulin* (*ß2M*; nuclear). Primer sequences used are listed in table 3. Estimation of the number of copies of the mitochondrial genome relative to nuclear genome was based on the threshold cycle (Ct) using the following equation and as described previously (Venegas and Halberg, 2012):

$$\text{Mitochondrial copy number} = 2x2^{[\text{Ct}(\beta 2M)-\text{Ct}(ND1)]}$$

The PCR reaction was performed with the same cycling parameters as described in 2.2.5.

## 2.4 Microscopy

### 2.4.1 *Principles of fluorescence and fluorescence microscopy*

Fluorescence is a property of molecules, characterised by the rapid emission of light after the absorption of shorter wavelength light, with the difference between these two wavelengths known as 'Stokes shift'. Molecules that exhibit fluorescent properties are known as fluorophores and through filtering out only the wavelength of light used to excite the fluorophore, it is possible to observe molecules that are fluorescent.

After a fluorophore in its 'ground' or 'resting' state absorbs light energy, it becomes energetically 'excited', due to changes it the molecule's electronic, vibrational and

rotational state. The release of this energy through fluorescence emission is the principal mechanism by which these molecules return to their 'ground' state (Lichtman and Conchello, 2005). The fluorescent properties of chemicals, genetically encoded probes and the intrinsic fluorescence of organic substances have been widely exploited in the field of cell biology to study numerous parameters, including protein localisation, cell function and ion signalling.

### 2.4.2 *The epi-fluorescent microscope*

Mercury or xenon arc lamps are traditionally used to illuminate fluorescent samples, and differ in their wavelength coverage and intensity. A dichroic mirror is required to separate the light use to excite the fluorophore from the light which is emitted. A dichroic mirror is designed to reflect the shorter wavelength of light originating from the light source towards the sample, while light of a longer wavelength emitted from the sample passes through the dichroic mirror, and ultimately reaches a detector. The microscope's objective lens images, magnifies and also acts as a condenser to illuminate the specimen. Dichroic mirrors are used in combination with an excitation filter, to ensure only light of a specific wavelength reached the sample, and an emission long pass filter, to ensure only transmitted light above a certain wavelength reaches the detector. The excitation filter, dichroic mirror and emission filter are held in a structure known as the filter cube which can be easily changed depending on the properties of the fluorophore to be imaged (Figure 2.1). Alternatively a filter wheel can be used to rapidly switch between different excitation and emission filter; this approach uses the same more sophisticated dichroic mirror (Paddock, 2005, Lichtman and Conchello, 2005).

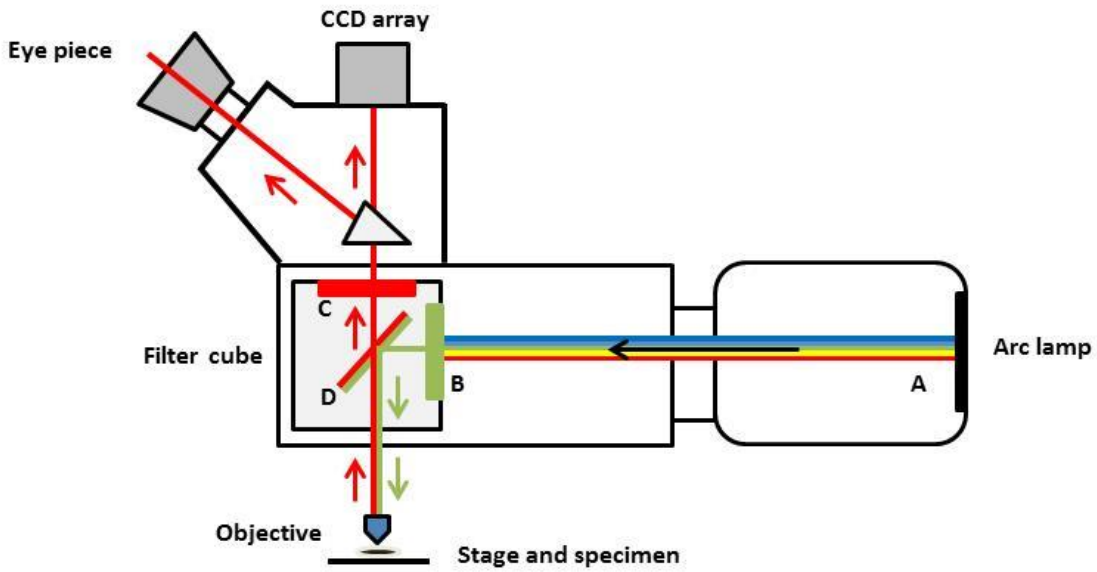


**Figure 2.1: Diagrammatic representation of an epi-fluorescent microscope system.**

**White light (A) emitted from the arc lamp is filtered by the excitation filter (B) such that only light of a specific wavelength reaches the dichroic mirror (D). Specific wavelength light is reflected toward the objective and focussed onto the sample. Emitted light from the sample collected by the objective, transmitted through the dichroic mirror and travels through the emission filter (C) and directed towards the camera or eye piece. Arrows indicate direction of light wave. Adapted from (Lichtman and Conchello, 2005).**

### 2.4.3 *Optical sectioning microscopy: Confocal imaging*

Confocal microscopy is a technique capable of optical sectioning, such that light from outside the focal plane is removed, and the user is able to acquire images of thin sections of specimens. Optical sectioning allows for improved contrast, resolution and the generation of three-dimensional reconstructions. Confocal microscopy produces optical sections through point by point laser scanning and illumination of the specimen in sequence until all regions in a field are sampled. A laser beam is focussed in the sample and at the same time a spatial pin hole, present in front of the detector removes unwanted fluorescence emission from above and below the focal plane, allowing imaging of discrete structures within an intact biological specimen. The objective lens is used to focus light to a single point and also return light from the sample collected after it has passed through the spatial pinhole, present at a optically conjugate plane to the in-focus plane (Paddock, 2005, Conchello and Lichtman, 2005) (Figure 2.2).

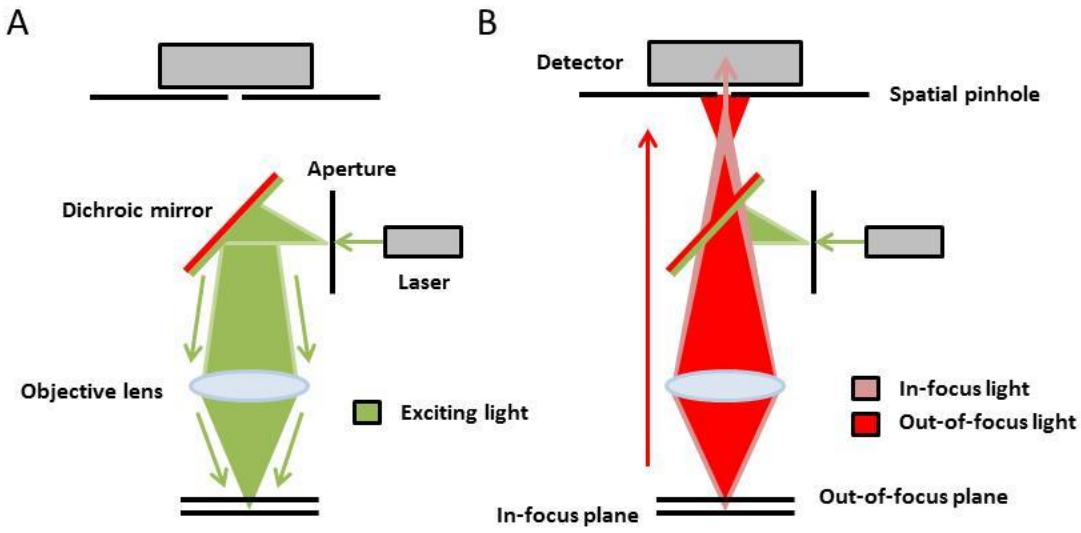


**Figure 2.2: Diagrammatic representation of the path of fluorescent light in optical sectioning microscopy.**

**(A) Light from the laser reflects off the dichroic mirror and is focussed onto the sample, illuminating the fluorophore. (B) Light of higher wavelength emitted from the sample is transmitted through the dichroic mirror. Only light originating from the in-focus plane is focussed on to the image plane where the spatial pinhole is located, such that light from the out-of-focus plane fails to reach the detector. Arrows indicate direction of light wave. Adapted from http://www.bioimaging.dk/index.php?id=71 (last accessed Nov 2013).**

### 2.4.4 *Immunofluorescence microscopy*

Cells were plated on glass coverslips (ø 13 mm, VWR) and allowed to adhere overnight. After treatment, cells were washed twice with PBS and fixed using 4% paraformaldehyde in PBS for 15 minutes. Cells were then washed twice with PBS and permeabilised for 10 minutes using 0.5% Triton X in PBS before being blocked with IFF (1% BSA, 1% FCS in PBS) for 1 hour. Coverslips were incubated with primary antibody for 1 hour at room temperature or overnight at 4°C before being washed and incubated with fluorophore conjugated secondary (Alexa Fluor 564 and 488; Invitrogen) antibody for 1 hour. Coverslips were again washed twice with PBS and incubated in 1µg/ml DAPI solution (Biotium) for 10 minutes, washed and then mounted using Fluoromount G (Southern Biotech). Images were acquired using a Nikon Eclipse E600 Upright microscope with a 40x objective and captured using a QIClick digital CCD camera (QImaging) and Image Pro Plus software (Media Cybernetics).

### 2.4.5 *Fluorescent live-cell imaging of mitochondrial membrane potential*

For 24-48 hours prior to assay, cells were seeded into 12 or 24 wells plates in complete DMEM. Before the assay cells were loaded with 50nM tetramethylrhodamine methyl ester (TMRM; Sigma) in imaging buffer (basal DMEM supplemented with 4.5 g/l glucose, 4mM L-glutamine, 1mM pyruvate, 10% FCS, 5mM HEPES) and allowed to equilibrate for 45-60 minutes. Baseline measurements were taken over 30 minutes, after which compounds were added. Three fields of view were selected from each well and each condition imaged in duplicate using an Optiscan II motorised stage system (Prior Scientific). Samples were illuminated using a Lumen 200 Pro metal halide lamp (Prior Scientific) and imaged using an IX71 inverted microscope (Olympus) equipped with an Orca $R^2$ C10600 digital CDD camera (Hamamatsu Photonics).

Image sequences were analysed using Image Pro Plus (Media Cybernetics), using 3 independent areas of interest per field of view and calculating the change in fluorescence intensity over time, with background subtraction.

### 2.4.6 *Confocal live-cell imaging*

Cells were seeded on to glass coverslips (ø 22mm, VWR) and stained with 1nM Hoechst and 50nM TMRM to visualise the nucleus and mitochondria respectively. Hoechst was excited at 405nm and emitted fluorescence (peak 465nm) collected using 435-485 band pass filter. TMRM was excited at 543nm and emitted fluorescence (peak 573nm) collected using a 560nm long pass filter. Mitoview green (Biotium) was used for mitochondrial imaging at a concentration of 100nM. EGFP and mitoview green were excited at 488nm and emitted fluorescence captured using a 505-530 band pass filter. Images were acquired with a Zeiss 510 META confocal laser scanning microscope using a 63× oil objective.

### 2.4.7 *Electron microscopy*

Cells were seeded on to glass coverslips (ø 13 mm, VWR), and fixed with 2% paraformaldehyde and 1.5% glutaraldehyde in 0.1M cacodylate buffer. Samples were post fixed with 1% osmium tetraoxide and 1.5% potassium ferrocyanine in 0.1M cacodylate buffer. Samples were dehydrated in a graded ethanol-water series, cleared in propylene oxide and infiltrated with agar-100 resin. Ultra-thin sections were cut and collected on 300-mesh grids and stained with lead citrate. Samples were viewed in a Joel 1010 transition electron microscope and images were recorded using a Gatan Orius CDD camera. Preparation and imaging of cells was undertaken by Mark Turmaine, UCL. Mitochondrial

length was analysed using ImageJ measure feature, calibrated to the scale bar of each image. Analysis of up to 15-20 mitochondria from 10 cells was performed. Statistical significance was calculated using an unpaired t-test.

**Table 1: Antibodies, protein apparent molecular weight (kDa), source and supplier.**

| Antibody | Apparent Molecular Weight | Clone | Company |
|---|---|---|---|
| **AKT1** | 60 | Mouse monoclonal | Cell Signalling (#2967) |
| **Anti-GFP** | 27(+) | Mouse monoclonal | Clontech or Roche |
| **ATG3** | 40 | Rabbit polyclonal | Cell signalling (#3415) |
| **ATG5** | 55 | Rabbit polyclonal | Cell Signalling (#8540) |
| **ATG7** | 78 | Rabbit polyclonal | Cell Signalling (#8558) |
| **ATP5B** | 52 | Mouse monoclonal | Abcam (ab14730) |
| **Beclin** | 60 | Rabbit polyclonal | Cell Signalling #3495 |
| **COX-IV** | 17 | Mouse monoclonal | Abcam (ab14744) |
| **DRP-1** | 78-82 | Rabbit polyclonal | Cell Signalling (#5391S) |
| **FIS-1** | 15 | Rabbit polyclonal | Sigma (HP017430) |
| **GLUT-1** | 45-55 | Rabbit polyclonal | Alpha Diagnostics (GT12-A) |
| **HIF-1α (OH-Pro$^{564}$)** | 120 | Rabbit polyclonal | Cell Signalling (#D43B5) |
| **HIF-1β/ARNT1** | 95 | Mouse monoclonal | BD Pharmagen (611079) |
| **HIF-2α** | 96 | Mouse monoclonal | Abcam (Ab199) |
| **HSP60** | 60 | Rabbit polyclonal | Cell Signalling (#4870) |
| **HIF-1α (human)** | 120 | Mouse monoclonal | BD Biosciences (610959) |
| **HIF-1α (Mouse)** | 120 | Rabbit polyclonal | Novus (100-449) |
| **Lamin B** | 67 | Goat Polyclonal | Santa Cruz (sc-6216) |
| **LC3B** | 14, 16 | Rabbit polyclonal | Cell signalling (#3868) |
| **MFN-1** | 84 | Rabbit polyclonal | Abcam (ab104274) |
| **MFN-2** | 86 | Rabbit polyclonal | Sigma (HPA030554) |
| **mtCO-2** | 19 | Mouse monoclonal | Abcam (ab110258) |
| **OPA-1** | 86-92 | Rabbit polyclonal | Sigma (HPA036926) |

| **Table continued:** | | | |
|---|---|---|---|
| **p62** | 62 | Rabbit polyclonal | Cell Signalling (#8025S) |
| **p-AKT (Ser$^{473}$)** | 60 | Rabbit polyclonal | Cell Signalling (#2971) |
| **Parkin** | 52 | Mouse monoclonal | Abcam (ab77924) |
| **p-DRP-1 (Ser$^{616}$)** | 78-82 | Rabbit polyclonal | Cell Signalling (#3455S) |
| **p-DRP-1 (Ser$^{637}$)** | 78-82 | Rabbit polyclonal | Cell Signalling (#4867S) |
| **PHB1** | 32 | Rabbit polyclonal | Cell Signalling (#2426) |
| **PHD1** | 40-45 | Rabbit polyclonal | Novus (100-310) |
| **PHD2** | 43-46 | Rabbit polyclonal | Novus (100-137) |
| **PHD3** | 27 | Rabbit polyclonal | Novus (100-303) |
| **pVHL** | 19, 30 | Mouse monoclonal | BD Pharmagen (Ig32; 556347) |
| **SDHA** | 70 | Rabbit polyclonal | Cell Signalling (#5839) |
| **VDAC1** | 31 | Rabbit polyclonal | Abcam (ab15895) |
| **α-tubulin** | 50 | Mouse monoclonal | Sigma (T6199) |
| **β-actin** | 42 | Mouse monoclonal | Abcam (Ab6276) |
| **Secondary anti-goat HRP conjugate** | - | Sheep | Dako |
| **Secondary anti-mouse HRP conjugate** | - | Sheep | Amersham |
| **Secondary anti-rabbit HRP conjugate** | - | Donkey | Amersham |
| **Alexa Fluor 488 goat anti-rabbit IgG** | - | Goat | Invitrogen (A-11034) |
| **Alexa Fluor 568 goat anti-mouse IgG** | - | Goat | Invitrogen (A-11031) |

**Table 2: Reagents, working concentrations and supplier. A.D = assay dependent**

| Reagent | Supplier | Assay Conc. |
|---|---|---|
| **Antimycin A** | Sigma | 2µM |
| **Carbonyl cyanide-p-trifluoromethoxyphenylhydrazone (FCCP)** | Sigma | A.D |
| **Chloroquine** | Sigma | 10µM |
| **Dimethyloxalylglycine (DMOG)** | Frontier Scientific | 1mM |
| **DMSO** | Sigma | A.D |
| **Insulin-like growth factor-1 (IGF-1)** | Sigma | 100ng/ml |
| **Iodoacetic acid (IAA)** | Sigma | 1mM |
| **MG132** | Calbiochem | 10µM |
| **Oligomycin** | Sigma | A.D |
| **PHD-I (400084) ($C_{21}H_{16}ClN_3O$)** | EMD Millipore | 5µM |
| **Rotenone** | Sigma | 1mM |

**Table 3: Forward and reverse primer sequences used for RT-qPCR and mitochondrial DNA copy number analysis.**

| Gene | Forward Primer | Reverse Primer |
|---|---|---|
| ***β-actin*** | CCCAGAGCAAGAGAGG | GTCCAGACGCAGGATG |
| ***COX-IV*** | GAGCAATTTCCACCTCTGT | CAGGAGGCCTTCTCCTTCTC |
| ***Cytochrome b*** | TATCCGCCATCCCATACATT | GGTGATTCCTAGGGGGTTGT |
| ***EGLN3*** | GATGCTGAAGAAAGGGC | CTGGCAAAGAGAGTATCTG |
| ***GFM1*** | TCACAGACAAAGCCAACAGC | TGGTCTCTCGAAAGGCAACT |
| ***GLUT-1*** | TGGCATGGCGGGTTGT | CCAGGGTAGCTGCTCCAGC |
| ***HIF-1α*** | CCAGTTACGTTCCTTCGATCAGT | TTTGAGGACTTGCGCTTTCA |
| ***HIF-2α/EPAS*** | AAGCCTTGGAGGGTTTCATTG | TGCTGATGTTTTCTGACAGAAA |
| ***LC3B*** | AGCAGCATCCAACCAAAATG | CTGGGAGGCATAGACCATGT |
| ***MRPL15*** | GATCCTGCCAAATTTCCTGA | ATCTGCCTTGGATCCTTCCT |
| ***MRPL20*** | GAACATGAGGACCCTCTGGA | CCGCTAGGACTTTCCTGTTG |
| ***MRPL3*** | CCAAGGATGGTCAAAAGCAT | CAGACAGGGTTGCCATTTTT |
| ***MRPL30*** | CAAGGACTTCCAGCAGAGGA | TCATGTGCTTTCTGCTCCAC |
| ***MRPL32*** | GATGGCAGCTCCCAAAAATA | CCCCTTCTTGCTTCCCTATC |
| ***MRPS16*** | GAGAGACTGCGAAGGAAACG | GGGCAACTCAGGATACTCCA |
| ***MRPS35*** | ACCCCAGAGCACGAGTAGTA | CCTCCTTAAAGGGCACCTATCTG |
| ***MRRF1*** | CCAGGGGAACACTCAGACAT | GTCCCTTGGCAACATCAAGT |
| ***mtCO-2*** | TTCATGATCACGCCCTCATA | TAAAGGATGCGTAGGGATGG |
| ***TIF2*** | AATGTTGGGCAAAAGTACGC | ACTTCTCACGGGCTTTCTGA |
| ***ND6*** | AGGTAGGATTGGTGCTGTGG | CCAATAGGATCCTCCCGAAT |
| ***NRF-1*** | GCAGCCGCTCTGAGAACTTCA | TCGTAAGAGGTGTCCTCGGG |
| ***NRF-2 (GABPa)*** | CACACTTCTAGTCGCGGGAG | CAAAGGATCAGTCCCACTC |
| ***p62*** | GTGGTAGGAACCCGCTACAA | GAGAAGCCCTCAGACAGGTG |
| ***Parkin*** | AACCGGTACCAGCAGTATGC | TTCGCAGGTGACTTTCCTCT |

| **Table continued:** | | |
|---|---|---|
| ***PEO-1*** | ACAGGATCGCAGCTCAAGAC | CTGCTTCCTGGCTTGCTTTG |
| ***PGC-1α*** | TGATGACAGCGAAGATGA | AGAAGAACAAGAAGGAGACA |
| ***PGC-1β*** | ACACTGACTACGATTCCAA | TCTGAGGTATTGAGGTATTCC |
| ***POLG*** | GGAGGAGTTCCTGCTCACTG | GAGGCAGCTTGAAAAACCA |
| ***SDHA*** | GGACAACTGGAGGTGGCATT | TTTTCTAGCTCGACCACGGC |
| ***TFAM*** | CCGAGGTGGTTTTTCATCTGT | ACGCTGGGCAATTCTTCTAA |
| ***TUFM*** | ATTGGCACCGGTCTAGTCAC | CTTAAACGCAAGGGAAGCTG |
| ***UCP2*** | TGCTGAGCTGGTGACCTATG | GGGCATGAACCCTTTGTAGA |
| ***UCP3*** | AGCCTCACTACCCGGATTTT | CGTCCATAGTCCCGCTGTAT |
| ***β2M*** **(copy number)** | TCCTCTCCCGCTCTGCACCC | GGCGGGCCACCAAGGAGAAC |
| ***ND1*** **(copy number)** | GCCCCAACGTTGTAGGCCCC | AGCTAAGGTCGGGGCGGTGA |

# Chapter 3: Inhibition of PHD-mediated oxygen-sensing and its effects on HIF-α localisation and mitochondrial function

## 3.1 Introduction

In light of the ever increasing wealth of literature referencing the complex and intimate regulatory relationship between mitochondria and HIF-1α, it is clear that much is still to be delineated (Briston et al., 2011, Yang et al., 2012, Fukuda et al., 2007, Zhang et al., 2008, Rane et al., 2009). The most recent link lies in the control of HIF-1α hypoxic stabilisation by the mitochondrial DRS protein CHCHD4/MIA40, connecting mitochondrial IMS protein import, redox state and electron transfer to the HIF/hypoxic response (Yang et al., 2012). Furthermore unpublished data from our group, suggests that HIF-1α protein interacts with CHCHD4/MIA40 and the HIF-1α:CHCHD4/MIA40 complex associates with mitochondria.

Indeed we have shown that HIF-1α is associated with mitochondria isolated from cells and tissues (Briston et al., 2011). Therefore, HIF-1α joins the list of well-characterised transcription factors that have recently been observed to localise to and perform non-transcriptional roles within mitochondria. For example, Gough *et al*, observed that the promotion of cellular transformation by the H-RAS oncogene by signal transducer and activator of transcription 3 (STAT3) is dependent on serine phosphorylation taking place in mitochondria (Gough et al., 2009). In addition to STAT3, other transcription factors have been observed to be associated with/localise to mitochondria, including, the glucocorticoid receptor (and other members of the nuclear hormone superfamily; peroxisome proliferator activated receptor γ (PPARγ), thyroid, retinoid X (RXR) and oestrogen receptors), p53, nuclear factor kappa-light-chain-enhancer of activated B cells (NF-κB), cyclic-AMP response element binding protein (CREB) and activator protein-1 (AP-1) (Marchenko et al., 2000, Psarra et al., 2005, Leigh-Brown et al., 2010, Psarra and Sekeris, 2009).

Questions remain unanswered as to the mitochondrial role of many of these transcription factors. Given their defined function in regulating the transcription of nuclear genes, the binding of these proteins to distinct regions of the mitochondrial genome is of prime interest. Regions have been identified in mitochondrial DNA that correspond to consensus sites of nuclear binding elements and the idea of mitochondrially localised nuclear transcription factors regulating mitochondrial gene expression have been proposed (Leigh-Brown et al., 2010).

In addition to our previous work in tumour cells (Briston et al., 2011), validation of the HIF-1α-mitochondria association in a non-tumour cell line is important, as is linking this novel relationship to a second disease phenotype. HIF has a well-defined role in cardiovascular

biology, demonstrating involvement in development, physiology, cardioprotection and pathology. As such, there has been much interest and investment in targeting and inhibiting the PHD proteins to promote HIF-α stabilisation and transcriptional activity for the treatment of cardiovascular disease. In cardiovascular disease, this extends to the treatment of atherosclerosis, ventricular remodelling, ischaemia/reperfusion injury and myocardial infarction (Sen Banerjee et al., 2012). Whether both short-term and/or acute induction of HIF-1α through inhibition of the PHD proteins can mediate cellular protection is yet to be established. The possibility that HIF-1α protein induced during brief periods of PHD inhibition or hypoxia, or in response to immediate exposure to PHD inhibition or hypoxia may provide a non-transcriptional role for HIF-1α is particularly interesting. With knowledge that HIF-1α co-localises with mitochondrial CHCHD4/MIA40, confirmation of HIF-1α mitochondrial localisation and investigation into the role of mitochondrial HIF-1α protein may provide novel insights into the regulation of mitochondrial function and metabolism.

## 3.2 Hypothesis

Activation of the oxygen-sensing pathway alters mitochondrial function and cellular metabolism.

## 3.3 Aims

1. To explore how inhibition of the PHD proteins affect HIF-1α subcellular localisation.

2. To determine the effects of PHD protein inhibition on mitochondrial function.

3. To correlate whether any effects on mitochondrial function are dependent on the stabilisation of HIF-1α and its subcellular localisation.

## 3.4 Characterisation of the HIF response in HL-1 cardiomyocytes

### 3.4.1 *HIF-1α protein is stabilised in response to hypoxia*

HL-1 cardiomyocytes are an immortalised cardiac atrial muscle cell line derived from the AT-1 mouse (Delcarpio et al., 1991), in which expression of simian virus 40 (SV40) large T-antigen is expressed under the control of the atrial natriuretic factor (ANF) promoter (Claycomb et al., 1998). These cells are currently the only published cardiomyocyte cell line that can spontaneously contract, maintain a differentiated phenotype and can be passaged serially in culture (White et al., 2004). Thus HL-1 cells provide a useful tissue culture model for assessing cardiac cell biology.

Previous studies have observed that HL-1 cells exhibit stabilisation of HIF-1α and increased transcription and expression of downstream HIF-1 target genes in response to hypoxia (Nguyen and Claycomb, 1999, Cormier-Regard et al., 1998). To confirm previous studies, HL-1 cells were exposed to periods of normoxia and hypoxia and HIF-α protein observed. Figure 3.1 demonstrates HIF-1α protein induction in response to hypoxia (1% $O_2$) over 24 hours. Glucose transporter-1 (GLUT-1) is a well-recognised HIF-1α transcriptional target (Zelzer et al., 1998, Ebert et al., 1995). As anticipated, GLUT-1 protein, as anticipated was found to be up-regulated at 24 hours in response to hypoxia, confirming a HIF-1 transcriptional effect (Figure 3.1). By 24 hours a decrease in HIF-1α protein levels was observed; a characterised behaviour of the HIF-1α protein described previously (Holmquist-Mengelbier, 2006).

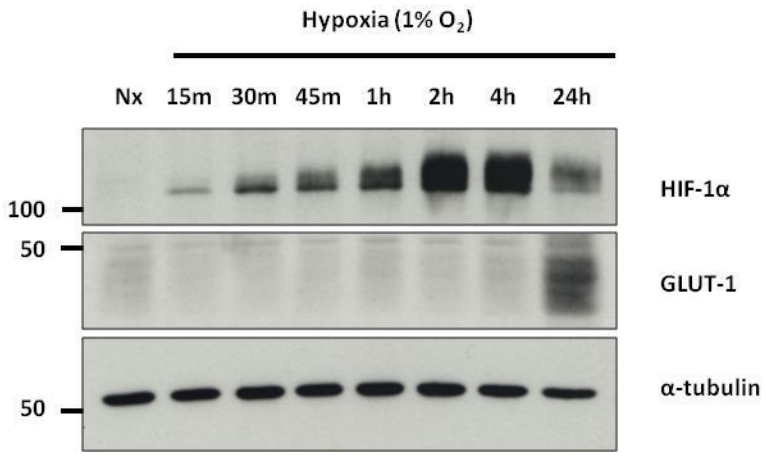


**Figure 3.1: HIF-1α protein is induced in response to hypoxia in HL-1 cardiomyocytes.**

**Western blot shows HIF-1α protein induction in response to normoxia (Nx) or hypoxia (1% oxygen) over a 24 hour time course (minutes (m) and hours (h)). GLUT-1 protein induction is shown as a HIF-1 transcriptional target and α-tubulin was used as a load control.**

### 3.4.2 *HIF-1α protein is stabilised in response to DMOG treatment*

Dimethyloxalylglycine (DMOG) is a well-characterised competitive inhibitor of α-ketoglutarate dependent dioxygenases, such as the PHD proteins and has been shown to induce proteins which correlate well with those whose expression changes in hypoxia (Elvidge et al., 2006). In order to determine the HIF-1α response in normoxia after PHD inhibition, 1mM DMOG was added to the culture media and cells harvested over a time course of 24 hours. SDS-PAGE and western blot analysis illustrates HIF-1α protein stabilisation can be observed after 1 hour and is fully stabilised at 4 hours of DMOG treatment (Figure 3.2). PHD3 is a HIF-1 target gene and induced in hypoxia (Aprelikova et al., 2004). A correlative increase in PHD3 protein expression is observed by 4 hours (Figure 3.2), indicating that HIF-1 is transcriptionally active by 4 hours DMOG treatment in HL-1 cells.

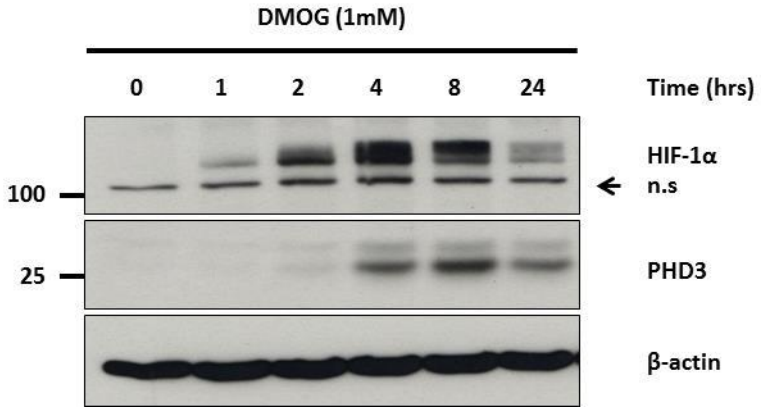


**Figure 3.2: HIF-1α protein is induced in response to DMOG treatment of HL-1 cardiomyocytes.**

**Western blot shows HIF-1α protein induction in response to 1mM DMOG over a 24 hour time course (hrs). PHD3 protein induction is shown as a HIF-1 transcriptional target and β-actin was used as a load control. n.s = non-specific band.**

### 3.4.3 *HIF-1α protein is induced in response to growth factor-mediated stimulation*

Growth factors have been previously demonstrated to induce HIF-α protein synthesis through phosphoinositide 3-kinase (PI3K) - protein kinase B (PKB/AKT) and mitogen activated protein kinase (MAPK) - dependent mechanisms in multiple cell types (Fukuda et al., 2002, Alam et al., 2009, Carroll and Ashcroft, 2006, Laughner et al., 2001). To explore whether growth factors can mediate an increase in HIF-1α protein in HL-1 cardiomyocytes, cells were serum starved for 40 hours before the addition of 100ng/ml insulin-like growth factor-1 (IGF-1). Samples were harvested over time and HIF-1α protein expression detected using SDS-PAGE and western blotting. Analysis revealed that HIF-1α protein was induced by 2 hours of IGF-1 stimulation (Figure 3.3). An increase in the ratio of phosphorylated AKT (p-AKT) at $Ser^{473}$ to total AKT demonstrates that the PI3K pathway was active under these conditions.

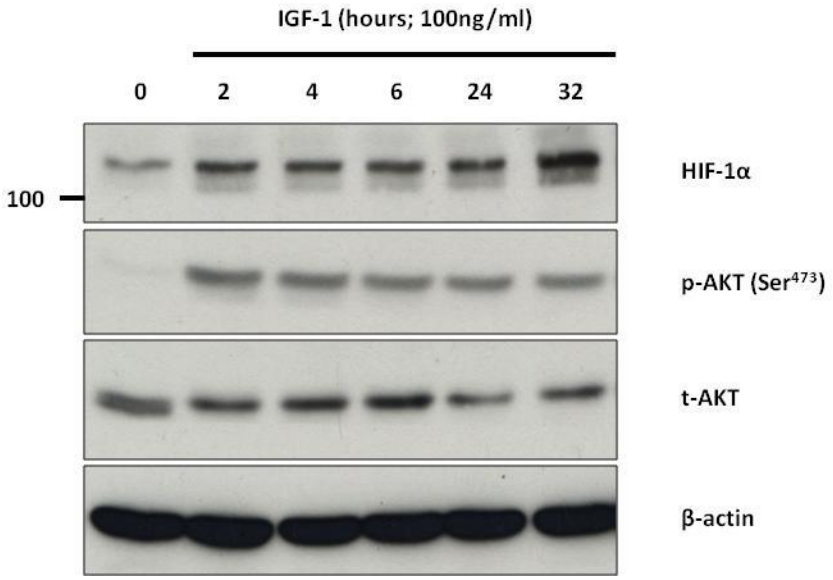


**Figure 3.3: HIF-1α protein is induced in response to IGF-1 treatment of HL-1 cardiomyocytes.**

**Western blot shows HIF-1α protein induction in response to of IGF-1 (100ng/ml) over time (0-32 hours). Phosphorylated AKT protein (p-AKT Ser$^{473}$) is shown as a positive control for activation of PI3K/AKT signalling. Total AKT (t-AKT) protein and α-tubulin were used as load controls.**

## 3.5 HIF-1α protein association with mitochondria

### 3.5.1 *HIF-1α protein associates with mitochondria in response to hypoxia and DMOG*

As discussed, there is a well-established, complex relationship between the HIF-1 pathway and mitochondria; whereby HIF-1, via transcriptional responses has been observed to modulate mitochondrial function. Conversely, mitochondrial function and electron transport is necessary for the hypoxic stabilisation of HIF-1α (Fukuda et al., 2007, Zhang et al., 2008, Chandel et al., 1998, Agani et al., 2000, Chua et al., 2010). Recent work from our laboratory has demonstrated that HIF-1α associates with mitochondria rapidly after stabilisation in response to PHD inhibition or hypoxia in tumour cell lines (Briston et al., 2011). These findings suggest a transcriptional-independent role for HIF-1α protein. To extend these studies and investigate whether HIF-1α also associates with mitochondria in HL-1 cardiomyocytes, cells were exposed to normoxia or hypoxia (1% $O_2$) to stabilise HIF-α over time. Subcellular fractionation was performed and samples were subject to SDS-PAGE and analysed by western blot. HIF-1α protein induction was observed in both cytosolic and

mitochondrial fractions in response to hypoxia (Figure 3.4). These data are consistent with our previous studies in tumour cells (Briston et al., 2011) and a previous report using cardiomyocytes (Rane et al., 2009). Lamin B, α-tubulin and cytochrome c oxidase subunit IV (COX-IV) proteins were used as markers for nuclear, cytosolic and mitochondrial compartments respectively, to show appropriate fractionation.

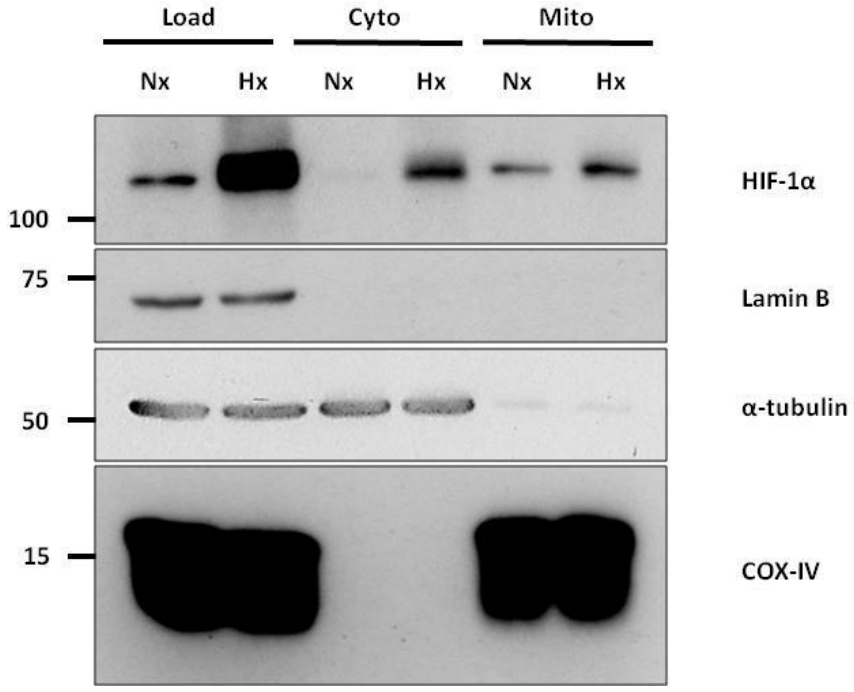


**Figure 3.4: HIF-1α protein associates with mitochondria in response to hypoxia in HL-1 cardiomyocytes.**

**Subcellular fractionation analysis of HL-1 cells after exposure to normoxia (Nx, 21% O2) or hypoxia (Hx, 1% O2) for 4 hours. Western blot shows HIF-1α protein induction in response to hypoxia (Hx) in total (Load), cytosolic (Cyto) and mitochondrial fractions (Mito). Lamin B, α-tubulin and COX-IV proteins were used as specific markers for the nuclear, cytosolic and mitochondrial fractions respectively.**

To confirm the effects on HIF-1α mitochondrial association observed in hypoxia, and investigate the time course and kinetics of the association, DMOG was used to inhibit the PHD proteins and stabilise HIF-1α protein in normoxia. Cells were treated with 1mM DMOG to stabilise HIF-α protein over a time course of 4 hours. Subcellular fractionation was performed and samples subject to SDS-PAGE and western blot analysis. HIF-1α protein

induction was observed by 2 hours of DMOG treatment (Load) and correlates with an increase in HIF-1α protein present in the mitochondrial fraction (Mito) (Figure 3.5). These data are consistent with observations in hypoxia (Figure 3.4) and our previous findings in tumour cells (Briston et al., 2011). Interestingly, HIF-1β protein was also detected in mitochondrial fractions. Lamin B, α-tubulin and voltage dependent anion channel-1 (VDAC1) were used as markers for nuclear, cytosolic and mitochondrial fractions respectively, to assess the efficiency of subcellular fractionation.

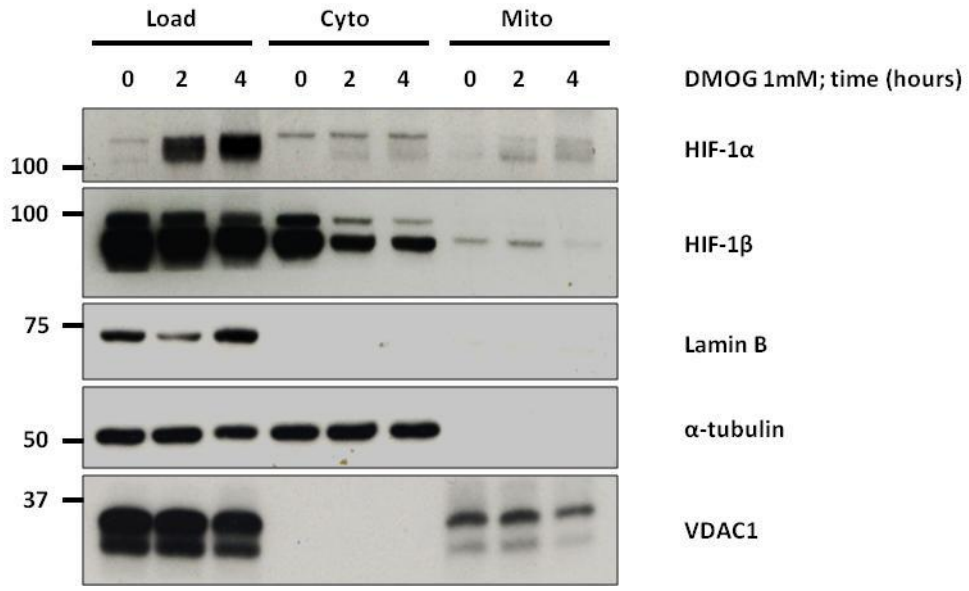


**Figure 3.5: HIF-1α associates with mitochondria in response to DMOG.**

**Subcellular fractionation analysis of HL-1 cells after DMOG (1mM) treatment over a time course of 0 to 4 hours. Western blot shows HIF-1α protein induction in response to DMOG in total (Load), cytosol (Cyto) and mitochondrial fractions (Mito). HIF-1β protein is detected in both cytosolic and mitochondrial fractions. Lamin B, α-tubulin and VDAC1 proteins were used as specific markers for the nuclear, cytosolic and mitochondrial fractions respectively.**

### 3.5.2 *HIF-1α protein is detected in purified mouse liver mitochondrial fractions*

HIF-1α protein appears to associate with mitochondria when oxygen is low or the PHD proteins are inhibited (Figure 3.4 and Figure 3.5). In order to elucidate whether the association of HIF-1α protein with mitochondria was evident *in vivo* and under normal physiological conditions, mitochondria were isolated from mouse liver tissue and subject to

Percoll™ gradient separation. Fractions were collected corresponding to the tissue homogenate (H), purified mitochondria (PM), crude mitochondria (CM) and post-mitochondrial supernatant (PMSN; including cytosolic components, microsomes and lysosomes). Samples were subject to SDS-PAGE and western blotting. Crude mitochondria (CM) were those pelleted and collected after differential centrifugation and purified mitochondria (PM) those mitochondria isolated after ultracentrifugation and separation on a Percoll™ gradient. Mouse HL-1 cells were used as a positive control for HIF-1α protein stabilisation having been incubated in hypoxia for 20 hours. Figure 3.6A demonstrates the presence of an enriched diffuse band in the PM fraction, that may potentially correspond to modified forms of HIF-1α protein. As discussed, HIF-1α is highly post-translationally modified and although the banding pattern in the PM fraction does not match the control HL-1 cells, these results raise the possibility that a distinct species of the HIF-1α protein is associated with mitochondria *in vivo*. There is enrichment of the mitochondrial protein COX-IV in the PM fraction, and absence of both nuclear and cytosolic markers lamin B and α-tubulin respectively, suggesting efficient subcellular fractionation.

In addition to HIF-1α protein, constitutively expressed HIF-1β protein can also be observed in mitochondrial fractions from HL-1 cells treated with DMOG (Figure 3.5). Interestingly, in cells treated with DMOG, after 2 hours incubation there appears to be a decrease in cytosolic localisation of HIF-1β protein (Figure 3.5). To confirm that HIF-1β is associated with mitochondria, the localisation of HIF-1β protein was assessed in mitochondria isolated from mouse liver and purified using Percoll™ gradient separation. Tissue homogenate (H), pure mitochondria (PM), crude mitochondria (CM) and post-mitochondrial supernatant (PMSN) were run in parallel as described previously. Figure 3.6B demonstrates HIF-1β protein was readily detected in the total tissue homogenate (H) and also in the PM fraction. Both the 87kDa and 84kDa protein isoforms of HIF-1β were observed in the PM fraction (Figure 3.6B). These findings pave the way for further investigation into the role of the HIF-1 complex with mitochondria and elucidation of its physiological relevance/importance in this context.

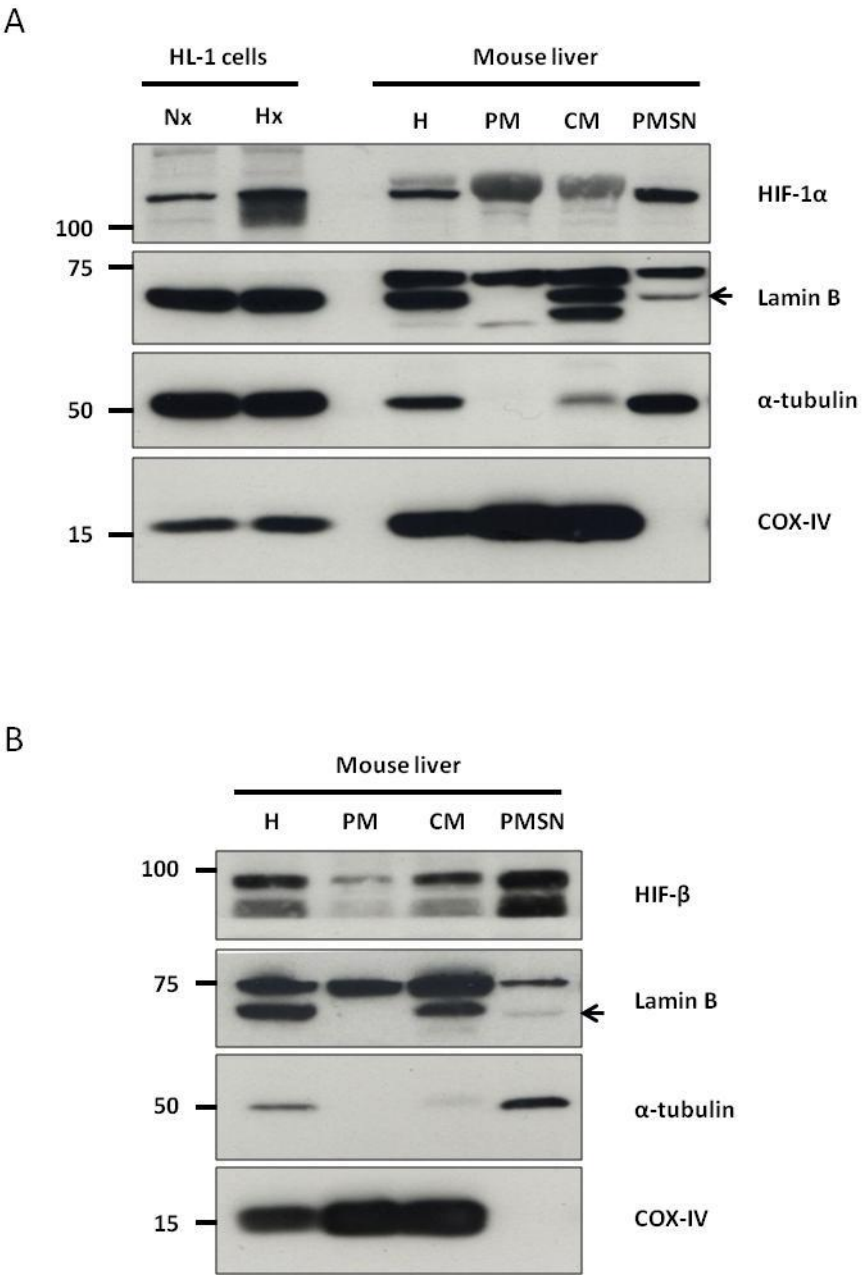


**Figure 3.6: HIF-1α and HIF-1β proteins are detected in mitochondrial fractions isolated from mouse liver.**

**(A) Western blot shows HIF-1α protein in mouse liver subcellular fractions (H = homogenate, PM = purified mitochondria, CM = crude mitochondria, PMSN = post mitochondrial supernatant). Normoxic (Nx) and hypoxic (Hx) HL-1 cell lysates were used as controls for HIF-1α protein. (B) Western blot shows HIF-1β protein in mouse liver subcellular fractions as indicated in A. Lamin B, α-tubulin and COX-IV proteins were used as markers for the nucleus, cytosol and mitochondria respectively.**

### 3.5.3 *Hydroxylated HIF-1α protein is detected in mitochondrial fractions*

As discussed in the introduction, HIF-1α is highly post-translationally modified. Proline hydroxylation by the PHD proteins is the best characterised modification of HIF-1α to date (Jaakkola et al., 2001). Hydroxylation of HIF-1α maintains the protein at low levels under normal oxygen conditions and provides a mechanism for the cell to react quickly to changes in oxygen tension. The turnover of the alpha subunit is mediated through proteolytic degradation by the proteasome (Maxwell et al., 1999). In humans, HIF-1α is hydroxylated on two proline residues, at positions 402 and 564 by the PHD proteins and it is this hydroxylation which serves as the targeting signal for ubiquitination and proteasomal degradation (Jaakkola et al., 2001). Using MG132, a selective inhibitor of the proteolytic activity of the proteasome, HIF-1α degradation is blocked, while PHD-mediated hydroxylation is unaffected (Figure 3.7). Thus MG132 causes accumulation of hydroxylated HIF-α protein that can be detected by western blot using a HIF-1α-hydroxyproline specific antibody, targeted toward $Pro^{564}$ (Figure 3.7; lane 2). The simultaneous addition of the PHD inhibitor DMOG causes a reduction of the band corresponding to the HIF-1α hydroxylated species (Figure 3.7; lane 3) confirming the specificity of the antibody and the expected effect of DMOG on inhibiting PHD activity.

Having previously observed a diffuse protein banding pattern for the mitochondrially associated HIF-1α protein in cells (Figure 3.5) and an interesting protein banding pattern in liver (Figure 3.6A), the possibility that mitochondrial associated HIF-1α protein is hydroxylated, was tested. After subcellular fractionation and mitochondrial isolation, samples were exposed to SDS-PAGE and western blotting. Analysis revealed the presence of the hydroxylated species at position 564 ($Pro^{564}$) on HIF-1α in mitochondrial fractions, in those samples treated with MG132 (Figure 3.7). Lamin B, α-tubulin and VDAC1 proteins were used as markers for nuclear, cytosolic and mitochondrial compartments respectively to demonstrate appropriate fractionation. These data suggest that hydroxylated HIF-1α protein is recruited to mitochondria, or most intriguingly, that HIF-1α protein is modified at the mitochondrial interface and/or within mitochondria. The possibility that HIF-1α protein is modified at the mitochondrial interface and/or within mitochondria would presumably rely on the PHD proteins sharing its mitochondrial association.

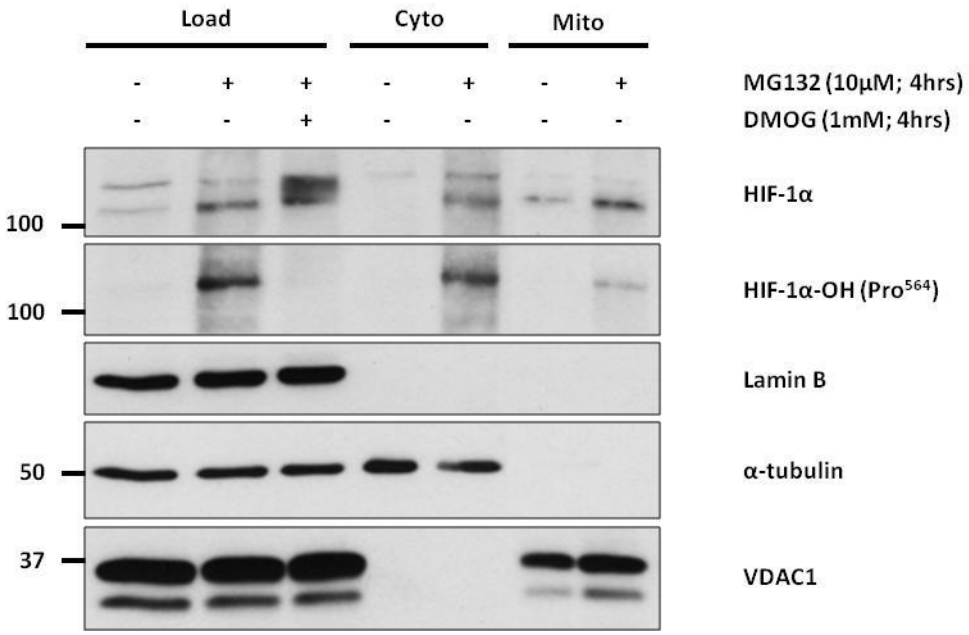


**Figure 3.7: Hydroxylated HIF-1α is detected in mitochondrial fractions after proteasomal inhibition.**

**Subcellular fractionation of HL-1 cells after treatment for 4 hours with MG132 (10μM), either alone or in combination with DMOG (1mM). Western blot shows the accumulation of hydroxylated HIF-1α (Pro$^{564}$) in response to MG132 treatment and clear reduction after PHD inhibition by DMOG. A band corresponding to the hydroxylated species of HIF-1α protein is present in the mitochondrial fraction. Lamin B, α-tubulin and VDAC1 were used organelle controls for the nucleus, cytosol and mitochondria respectively. Load = total cell homogenate, Cyto = cytosolic fraction, Mito = mitochondrial fraction.**

## 3.6 Prolyl hydroxylase domain (PHD) protein association with mitochondria

### 3.6.1 *PHD protein over-expression and analysis of subcellular localisation using EGFP-tagged constructs*

Having established that hydroxylated HIF-1α protein is detected in mitochondrial fractions, the subcellular localisation of the PHD proteins was investigated. The subcellular localisation of the exogenously expressed PHD proteins has previously been established using EGFP (enhanced green fluorescent protein)-tagged constructs (Metzen et al., 2003). Metzen *et al* demonstrated nuclear localisation of PHD1, cytoplasmic localisation for PHD2 and PHD3 was observed in both nuclear and cytoplasmic compartments (Metzen et al., 2003). Additionally and independently, it has been observed that the PHD3 orthologue in

rat, SM-20 is mitochondrial and contains a mitochondrial targeting sequence, that is absent in human PHD3 (Lipscomb et al., 2001). PHD2 has been described to co-localise with the adapter protein FKBP38 in mitochondria and ER (Barth et al., 2009), and PHD2 and PHD3 have been observed to localise to mitochondria in rat hepatocytes (Khan et al., 2006).

The subcellular localisation of PHD proteins was assessed after transient over-expression of EGFP-tagged PHD constructs in HeLa cells (Figure 3.8). Co-staining with Hoechst 33342 and TMRM was used to identify nuclei and mitochondria respectively (Figure 3.8A-C). Tetramethylrhodamine methyl ester (TMRM) accumulates in areas of negative potential based on its charge and is a well characterised tool to study mitochondrial membrane potential (Brand and Nicholls, 2011). The results obtained are in agreement with those described by Metzen *et al* in that PHD1 protein was predominantly nuclear, PHD2 protein was cytoplasmic and PHD3 protein was both nuclear and cytoplasmic (Figure 3.8A-C) (Metzen et al., 2003). There was little or no enrichment of any EGFP-PHD protein associated with mitochondria, however a small amount of EGFP-PHD2 and EGFP-PHD3 protein co-localised with the TMRM signal. Cells imaged were then harvested in lysis buffer and samples assessed by western blotting to confirm respective PHD protein expression (Figure 3.8D).

A

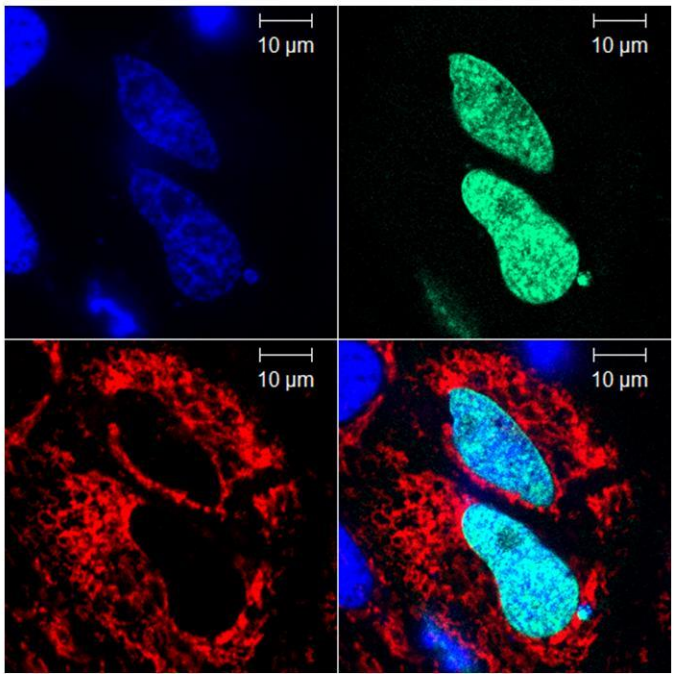
10 µm
10 µm
10 µm
10 µm
DAPI
EGFP-PHD1
TMRM
Merge

B

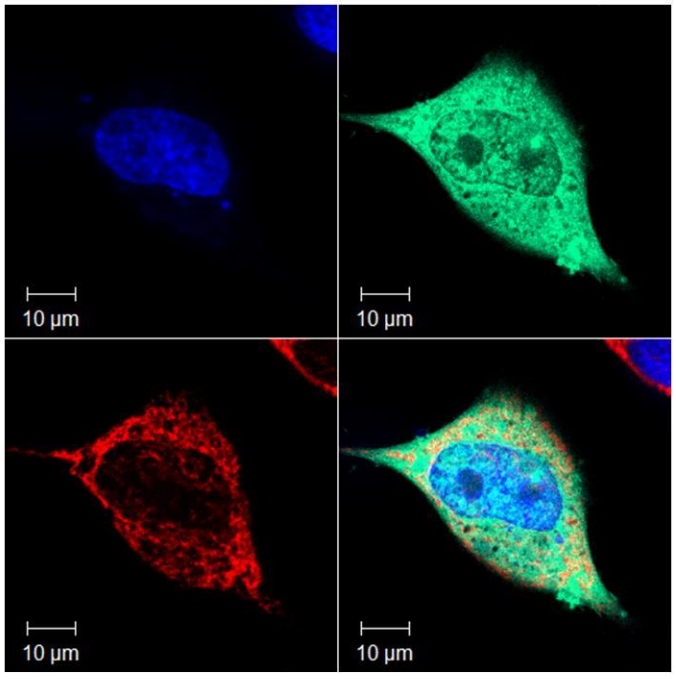
10 µm
10 µm
10 µm
10 µm
DAPI
EGFP-PHD2
TMRM
Merge

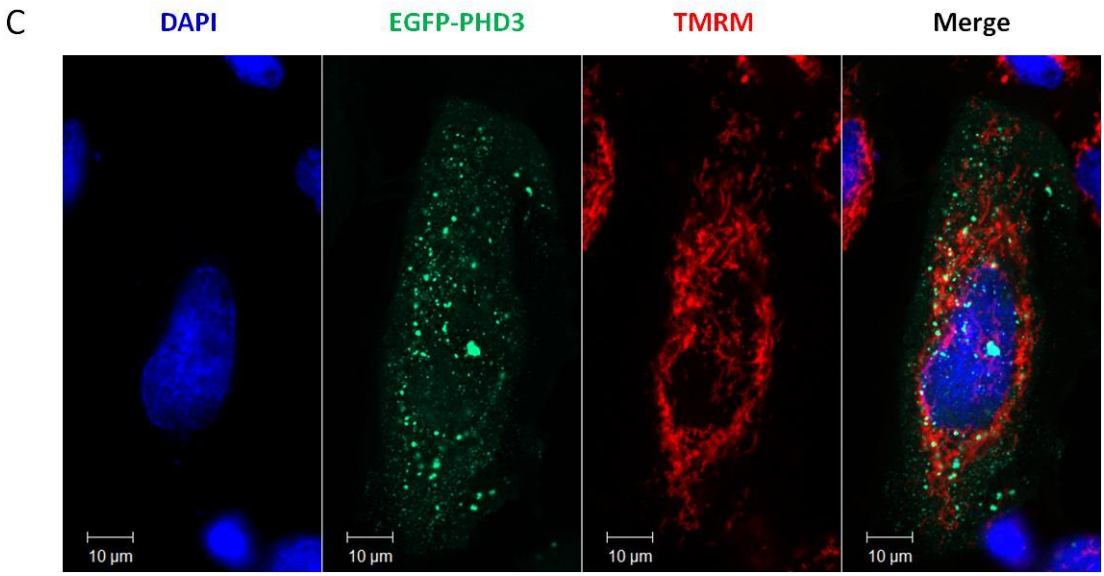
C
DAPI
EGFP-PHD3
TMRM
Merge
10 µm
10 µm
10 µm
10 µm

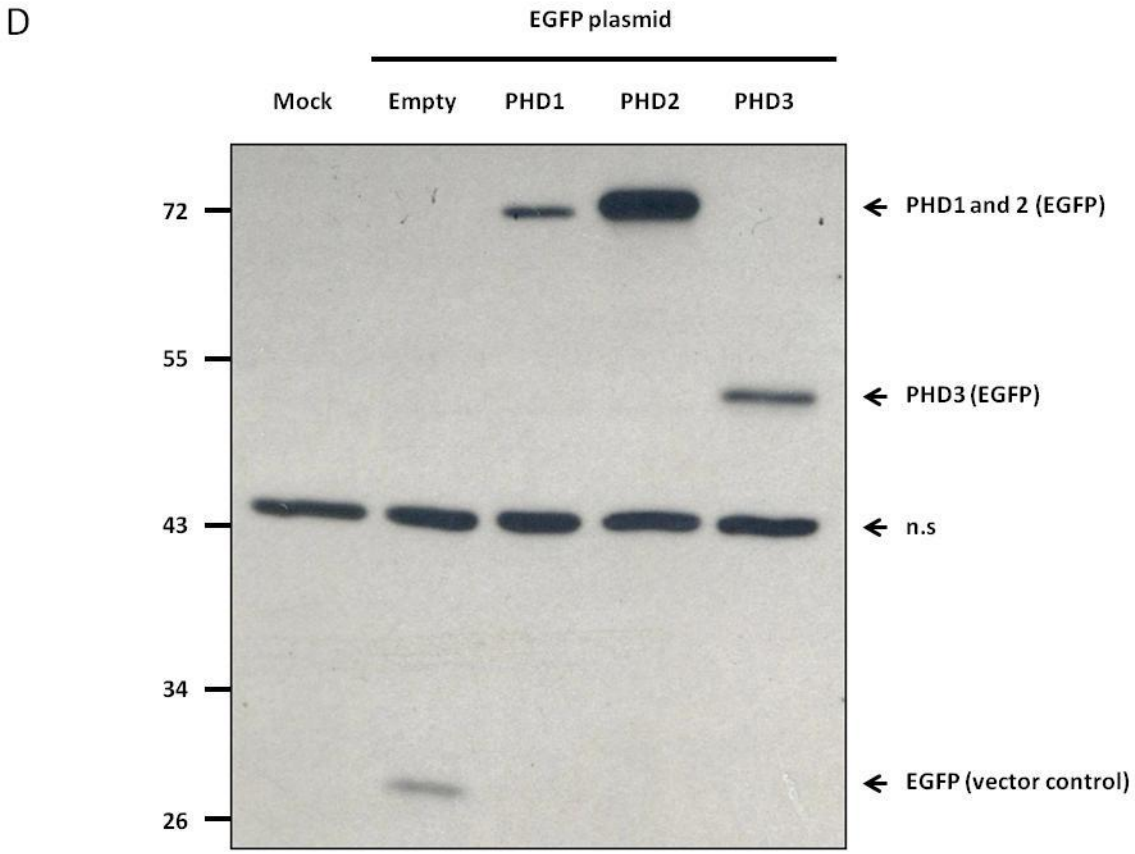
D
EGFP plasmid
Mock
Empty
PHD1
PHD2
PHD3
72
55
43
34
26
PHD1 and 2 (EGFP)
PHD3 (EGFP)
n.s
EGFP (vector control)

**Figure 3.8: Subcellular localisation and expression of EGFP-tagged PHD proteins.**

**(A-C) Confocal live-cell imaging of HeLa cells transiently transfected with EGFP-tagged PHD proteins. Cells were transfected on coverslips and localisation of the EGFP constructs analysed. (A) EGFP-PHD1 localises exclusively to the nucleus. (B) EGFP-PHD2 is diffusely localised throughout the cytoplasm. (C) EGFP-PHD3 is localised in aggregates and diffusely expressed throughout the cytoplasm. TMRM (50nM) was used to identify mitochondria (red) and Hoechst 33342 (1nM) used to stain the nucleus (blue). Images were acquired with a Zeiss 510 META confocal laser scanning microscope using a 63× oil objective. (D) Western blot analysis of samples from A-C, probed with an anti-GFP antibody to confirm molecular weights of over-expressed EGFP-PHD proteins. The protein band running at 43-45kDa is non-specific (n.s).**

### 3.6.2 *Localisation of PHD proteins in mouse liver mitochondria*

To further investigate the subcellular localisation of the PHD proteins, mitochondrial fractions were collected from mouse liver tissue and purified using a Percoll™ gradient as described above (Figure 3.6). Proteins were separated by SDS-PAGE and analysed by western blot. Tissue homogenate (H), pure mitochondria (PM), crude mitochondria (CM) and post-mitochondrial supernatant (PMSN) were run in parallel. Both PHD2 and PHD3 proteins are HIF-1α targets and are robustly induced in hypoxia (Figure 3.9; lanes 1 vs. 2) and given that the localisation of PHD1 protein is clearly nuclear (Figure 3.8), only PHD2 and PHD3 were assessed in the liver mitochondrial fractions. HL-1 normoxic (Nx) and hypoxic (Hx) samples were analysed to provide a positive control for PHD2 and PHD3 protein bands (Figure 3.9). PHD3 in mouse has an approximate molecular weight of approximately 27kDa (UniProt; Q91UZ4). Unfortunately, the PHD3 antibody used here detected several bands, however a hypoxia inducible protein band was observed that appeared distinct from the non-specific (n.s) bands and was also detected in the mitochondria enriched fractions (Figure 3.9; PM and CM; lanes 4 and 5). Additionally, there was an increase in protein expression of PHD2 observed in the HL-1 cardiomyocytes after 20 hours of exposure to hypoxia (Figure 3.9; Nx vs. Hx; lanes 1 vs. lane 2). PHD2 protein corresponding to an identical molecular weight was also detected in mitochondrial fractions of the mouse liver tissue (Figure 3.9; PM and CM; lanes 4 and 5). These results suggest the exciting possibility that the association of PHD2 and PHD3 proteins with mitochondria may be linked to the presence of the hydroxylated HIF-1α species observed in mitochondrial fractions described above (Figure 3.7).

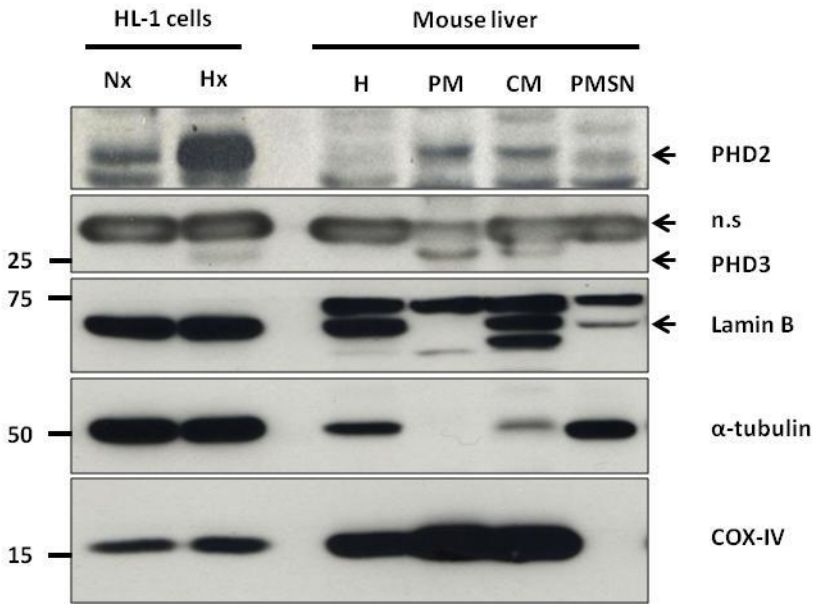


**Figure 3.9: PHD2 and PHD3 proteins are detected in mitochondrial fractions isolated from mouse liver tissue.**

**Western blot analysis of fractions obtained after subcellular fractionation of mouse liver. Tissue was homogenised and subject to differential centrifugation and subsequent Percoll™ gradient separation. Fractions obtained were separated by SDS-PAGE with protein equally loaded across lanes. PHD2 and PHD3 proteins induced in HL-1 cells in response to hypoxia, were also detected in purified mitochondria samples (indicated by the arrows). H = homogenate, PM = purified mitochondria, CM = crude mitochondria, PMSN = post mitochondrial supernatant. n.s = non-specific.**

## 3.7 Characterisation of DMOG-mediated HIF-1α dependent and independent regulation of mitochondrial processes

### 3.7.1 *Effects of DMOG treatment on cellular oxygen consumption rate*

There is interest around the potential use and development of PHD inhibitors as therapeutics, particularly in cardiovascular disease (Harten et al., 2010). Investigations into the activation of the HIF pathway through PHD protein inhibition generally extends to between 8-24 hours treatment (Sridharan et al., 2007, Sridharan et al., 2008, Elvidge et al., 2006). Previous studies have not investigated the effects of HIF-1α stabilisation after PHD protein inhibition on mitochondrial function within the first minutes to hours of exposure to treatment. Classically enzymes will catalyse their respective reactions at a rate dependent on the relative amounts of substrate, co-factors and catalysts, hence in the

presence of adequate ascorbate, α-ketoglutarate and oxygen, the PHD proteins will rapidly hydroxylate HIF-α. Substrate or co-factor limitation will have immediate consequences on the rate of the reaction and the result of this inhibition will immediately be paralleled by an increase in HIF-α protein abundance as a function of the regulatory system.

HIF-1α protein stabilisation was detected in mitochondrial fractions by 2 hours in culture after DMOG treatment (Figure 3.5). To determine the effect of the acute activation (0-4 hours) of the oxygen-sensing machinery on mitochondrial function it was first necessary to validate the concentration of DMOG necessary to fully inhibit the PHD proteins in HCT116 colon carcinoma cells. The hydroxylation of the HIF-α subunits by the PHD proteins is necessary for the subsequent degradation by the proteasome (Jaakkola et al., 2001). As described, MG132 is a selective inhibitor of the proteolytic activity of the proteasome. MG132 treatment therefore causes accumulation of the hydroxylated species of HIF-α subunit as shown above (Figure 3.7). To validate the concentration at which DMOG fully inhibits these enzymes, cells were incubated overnight for 20 hours with the inhibitor and for the final 4 hours in the presence or absence of 10μM MG132 (Figure 3.10A). The disappearance of the hydroxylated species of HIF-1α at 1mM DMOG in the presence of MG132 confirmed the inhibition of the PHD proteins (Figure 3.10A). A concentration of 1mM DMOG gave maximal HIF-1α stabilisation and is consistent with previous studies (Jin et al., 2012). Therefore 1mM was the concentration of DMOG used in functional studies.

In order to understand the consequences of activation of the oxygen-sensing pathway on mitochondrial function, it is necessary to evaluate the kinetics of the HIF-1α response to PHD inhibition using DMOG. Importantly, exposure of HCT116 cells to increasing durations of 1mM DMOG showed that HIF-1α protein stabilisation could be observed by 30 minutes treatment, suggesting rapid inhibition of the PHD proteins with DMOG (Figure 3.10B). Of particular interest, is the possibility that HIF-1α protein stabilisation within minutes of PHD inhibition has effects on mitochondrial function. To date, no other study has evaluated the immediate effects of the HIF response on mitochondrial parameters.

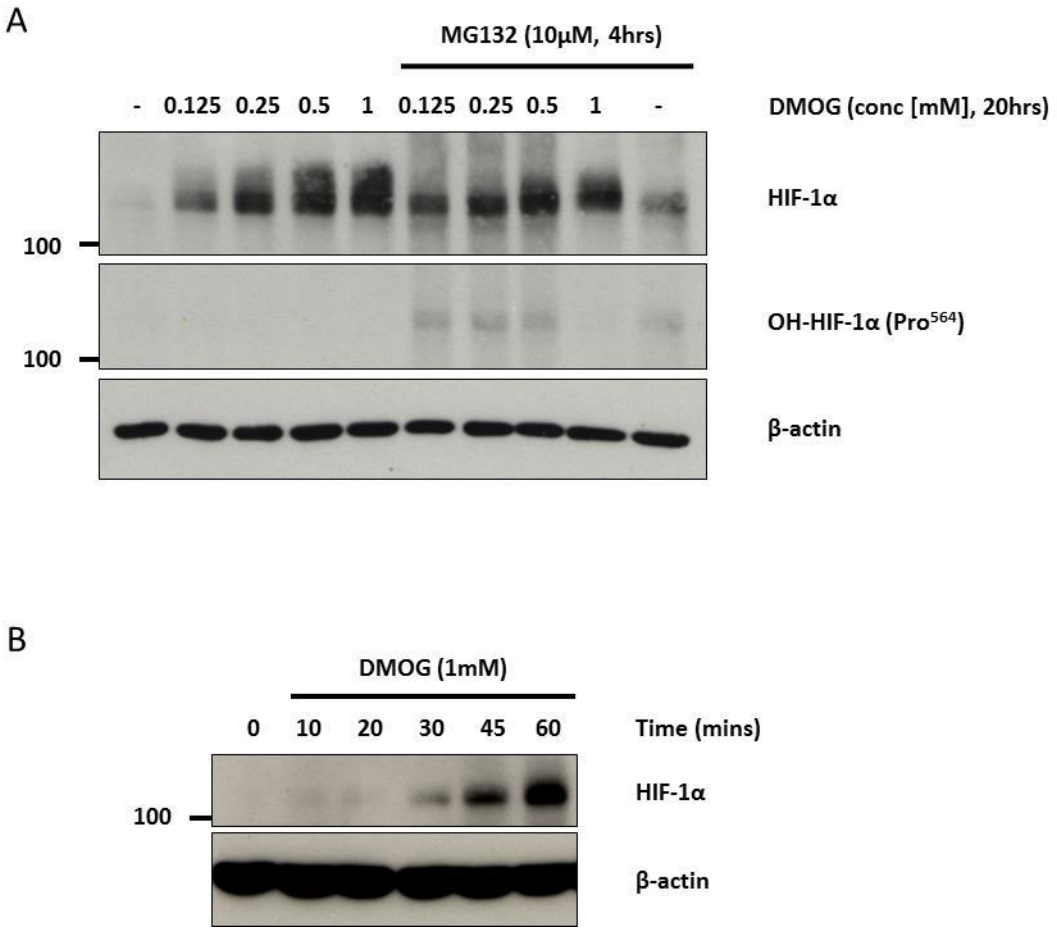


**Figure 3.10: Concentration and time-dependent inhibition of PHD proteins by DMOG.**

**(A) Western blot analysis of HCT116 cells treated over a concentration titration of DMOG (20 hours) in the presence and absence of the proteasome inhibitor MG132 (10μM) for the final 4 hours. Inhibition of the proteasome by MG132 prevents the degradation of the hydroxylated species of HIF-1α, and DMOG blocks the hydroxylation of HIF-1α. (B) Western blot analysis of HCT116 cells treated over a time course of 1 hour with 1mM DMOG. DMOG treatment induces HIF-1α protein expression between 20 and 30 minutes. β-actin is used as a load control for both experiments.**

To investigate the consequences of PHD protein inhibition, HIF-1α stabilisation and mitochondrial association on mitochondrial function, cellular oxygen consumption rate (OCR) was measured. DMOG was used to inhibit the PHD proteins and stabilise HIF-1α protein, and cellular OCR was measured using the Seahorse XF24 bio-analyser. OCR is primarily a measure of mitochondrial respiration and can be used as a measure of mitochondrial functionality. The Seahorse XF24 bioanalyser, uses fluorescent optics to measure dissolved oxygen present in the buffer and has been used to probe various

aspects of mitochondrial respiration, metabolism and dysfunction in response to chemicals, drugs and genotypes (Gohil et al., 2010, Beeson et al., 2010, Nadanaciva et al., 2012). The Seahorse platform has also been utilised for more novel and inventive approaches (Guo et al., 2012). Through protocol manipulation, exploitation of the mechanism of measurement and control of gas, it has been possible to induce cell ischaemia and use the Seahorse platform as a high-throughput means by which cardioprotective agents can be screened and investigated (Guo et al., 2012).

Basal OCR in HCT116 cells was measured for at least 4 cycles (of approximately 7 minutes) before the injection of 1mM DMOG or vehicle (DMSO, 1:2000). After addition, OCR was monitored for approximately 30 minutes and the average change in OCR, as a percentage of baseline compared between control and treated wells. HIF-1α has previously been observed as stabilised within this time period (Figure 3.10). The addition of DMOG significantly reduced OCR by approximately 30% compared to vehicle after 30 minutes of treatment (Figure 3.11). The addition of DMOG also had significant effects on maximal respiratory capacity, measured after the addition of the mitochondrial inner membrane protonophore, FCCP (Figure 3.11B), although using the Seahorse XF24 bioanalyser this effect was quite variable. There was no significant effect observed on the amount of oxygen consumed that was coupled to ATP synthesis between vehicle and DMOG treated cells (Leak respiration; OCR after the addition of $F_1F_O$-ATPase inhibitor, oligomycin). A representative trace is shown in figure 3.11B. These data suggest that DMOG is having effects on mitochondrial respiration within 30 minutes of treatment.

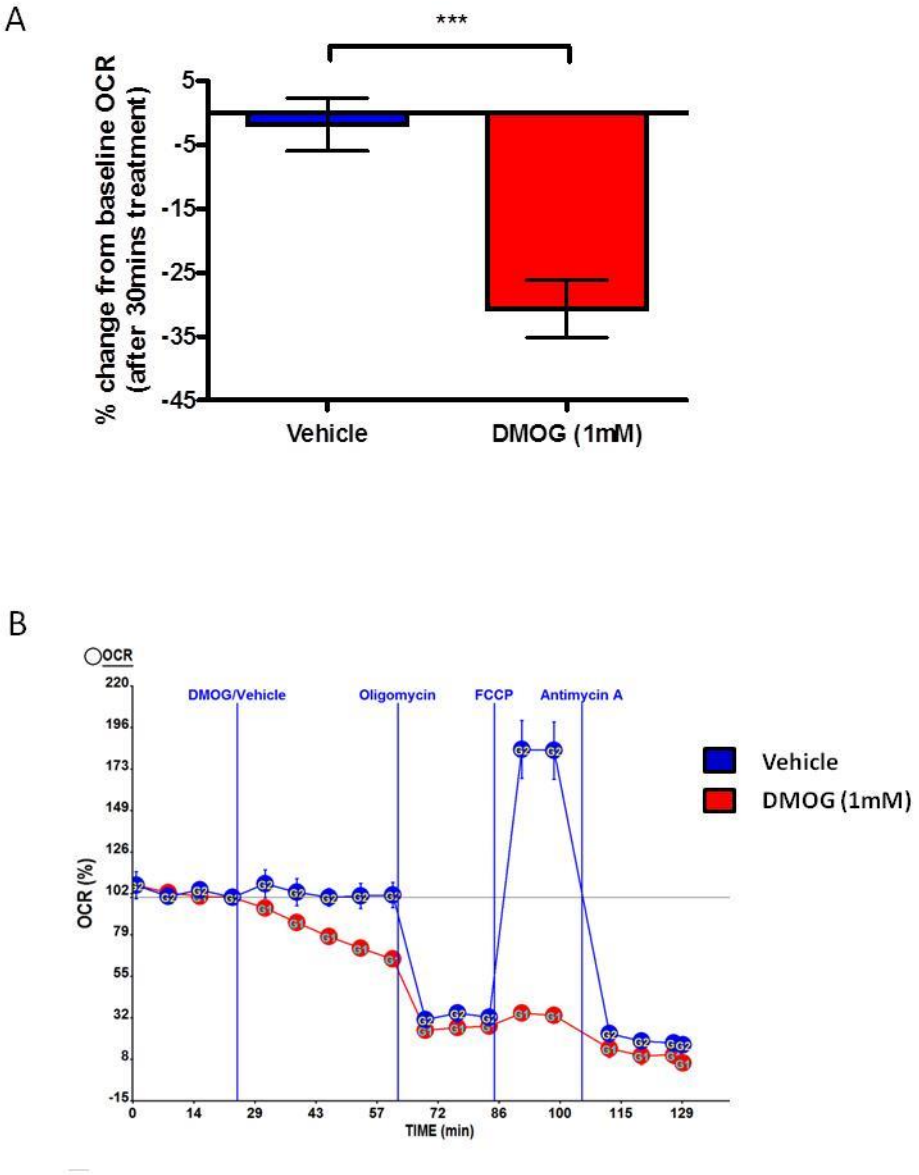


**Figure 3.11: DMOG reduces cellular OCR in HCT116 cells.**

**(A) HCT116 cells were either treated with vehicle (blue) or DMOG (1mM, red) and OCR was analysed over time using the Seahorse XF24 bioanalyser. Values are mean +/- S.E.M (n=4). Data was analysed using paired, two-tailed t-test (*** p<0.001). (B) Representative trace from the Seahorse XF24 bioanalyser demonstrating the addition of DMOG (1mM, red) or vehicle (blue) after four mix-wait-measure cycles. OCR reduced immediately upon treatment, decreasing further with time. Oligomycin (0.5µg/ml), FCCP (1.5µM) and antimycin A (2µM) were injected as indicated. Data was collected using a mix-wait-measure cycle of 3-2-2 after optimisation experiments. All changed from here on to n=**

### 3.7.2 *Effects of prolyl hydroxylase inhibition on cellular ATP*

There are a number of mechanisms through which the cell can synthesise energy in the form of ATP. The two main pathways for cellular ATP generation are OxPhos and glycolysis. A proportion of the cells consumed oxygen is coupled to ADP phosphorylation and ATP synthesis at the $F_1F_O$-ATPase. ATP coupled respiration can be experimentally measured by following oxygen consumption in the presence and absence of the $F_1F_O$-ATPase inhibitor oligomycin. Cancer cells are highly glycolytic (Warburg effect; (Warburg, 1956)), generating the majority of their ATP through glycolysis alone. In tissue culture, cells also generate much of their ATP from glycolysis due to the excess of glucose in the media and the negligible consequences of lactate production and acidification *in vitro* (Figure 3.12A). However cells can be forced to undergo oxidative metabolism by substituting glucose for galactose in the culture media. Under these conditions cells utilise pyruvate and glutamine to generate ATP through OxPhos (Figure 3.12B). This is known as the Leloir pathway, the metabolic pathway for the catabolism of galactose. D-galactose is modified to a series of intermediates through sequential enzyme catalysed reactions, involving galactokinase, galactose-1-phosphate uridylyltransferase and UDP-galactose-4-epimerase to produce glucose-1-phosphate and subsequently glucose-6-phosphate (G-6-P) that feeds the canonical glycolytic pathway (Frey, 1996). The rates of these reaction are slower than the conversion of glucose to G-6-P, forcing cells to compensate by promoting mitochondrial respiration (Weinberg et al., 2010).

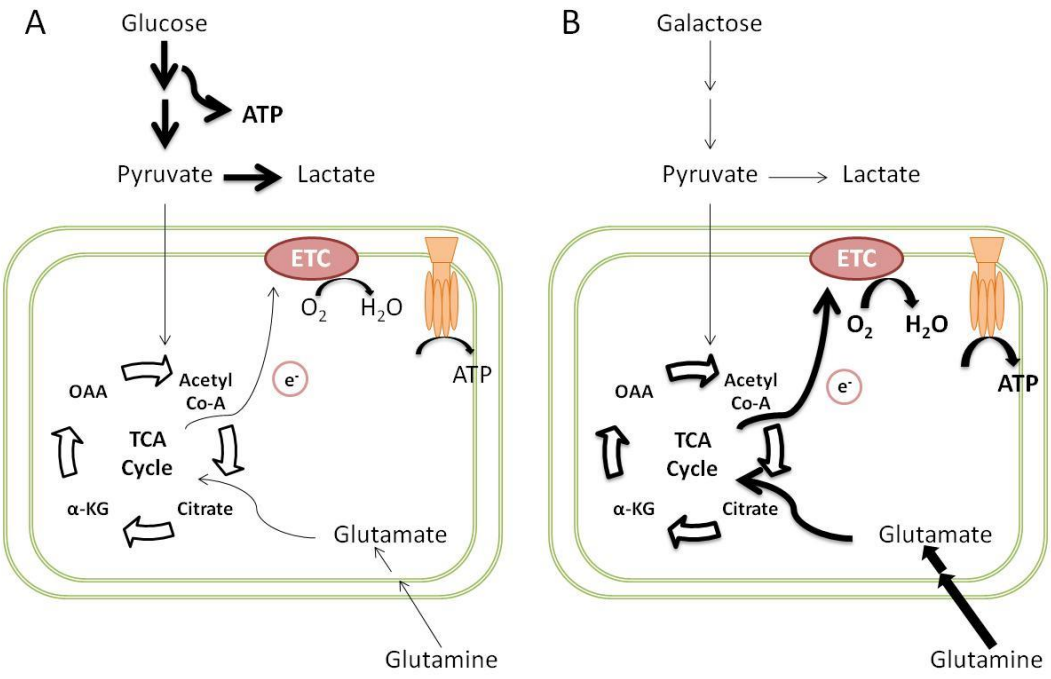


**Figure 3.12: Diagrammatic representation of the metabolism of glucose and galactose in culture.**

**(A) Cells in culture mostly utilise glucose through glycolysis to generate ATP and lactate as a by-product. (B) Cells utilise glutamine and pyruvate in the media, which after initial metabolism enters the TCA cycle, generates reducing equivalents, such as NADH and $FADH_2$ that transport electrons to the ETC and generate ATP through OxPhos. Figure adapted from (Gohil et al., 2010).**

Through metabolomic analysis of intracellular metabolites, the cellular uptake of respective energy substrates was confirmed. HCT116 cells were cultured under high glucose-DMEM (here on referred to as glucose) or glucose free, galactose-substituted DMEM (here on referred to as galactose) for at least 24 hours prior to measurements. HCT116 cells were cultured in glucose or galactose, harvested and subject to dual-phase extraction and a broad panel of intracellular metabolites were analysed using magnetic resonance spectroscopy (MRS), at the Institute of Cancer Research (ICR), Sutton, UK by Dr Yuen-Li Chung.

Figure 3.13 shows the intracellular metabolite profile of HCT116 cells under the two culture conditions (glucose or galactose). A significantly increased concentration of intracellular glucose was observed in cells cultured in glucose compared with galactose (Figure 3.13A). Conversely, in cells cultured in galactose there was a significantly increased level of

intracellular galactose observed, as anticipated (Figure 3.13B). Together, these data suggest that cells are taking up their respective carbon source (glucose or galactose), and the culture conditions promotes a more oxidative phenotype in the presence of galactose compared with glucose.

To evaluate cellular metabolic change under glucose and galactose culture conditions, total cellular ATP was measured in HCT116 cells after the addition of metabolic inhibitors using a bioluminescent assay. HCT116 cells were cultured in the presence and absence of the $F_1F_O$-ATPase inhibitor, oligomycin to inhibit OxPhos and glyceraldehyde-3-phosphate dehydrogenase (GAPDH) inhibitor, iodoacetic acid (IAA), to inhibit glycolysis. Oligomycin and IAA were added in combination to inhibit both OxPhos and glycolysis. This assay allowed assessment of the relative contributions of OxPhos and glycolysis to total cellular ATP levels. Figure 3.13C shows that in glucose the addition of oligomycin had no significant effect on cellular ATP levels (red bar) compared to non-inhibitor treated control cells (blue bar). However, IAA significantly reduced ATP levels (green bar), indicating that HCT116 cells are highly glycolytic under high glucose culture conditions. Cells cultured in galactose for 24 hours were significantly more sensitive to oligomycin, suggesting a greater contribution of OxPhos to total cellular ATP levels (Figure 3.13C). These data confirm the distinct culture conditions are promoting their respective metabolic phenotype.

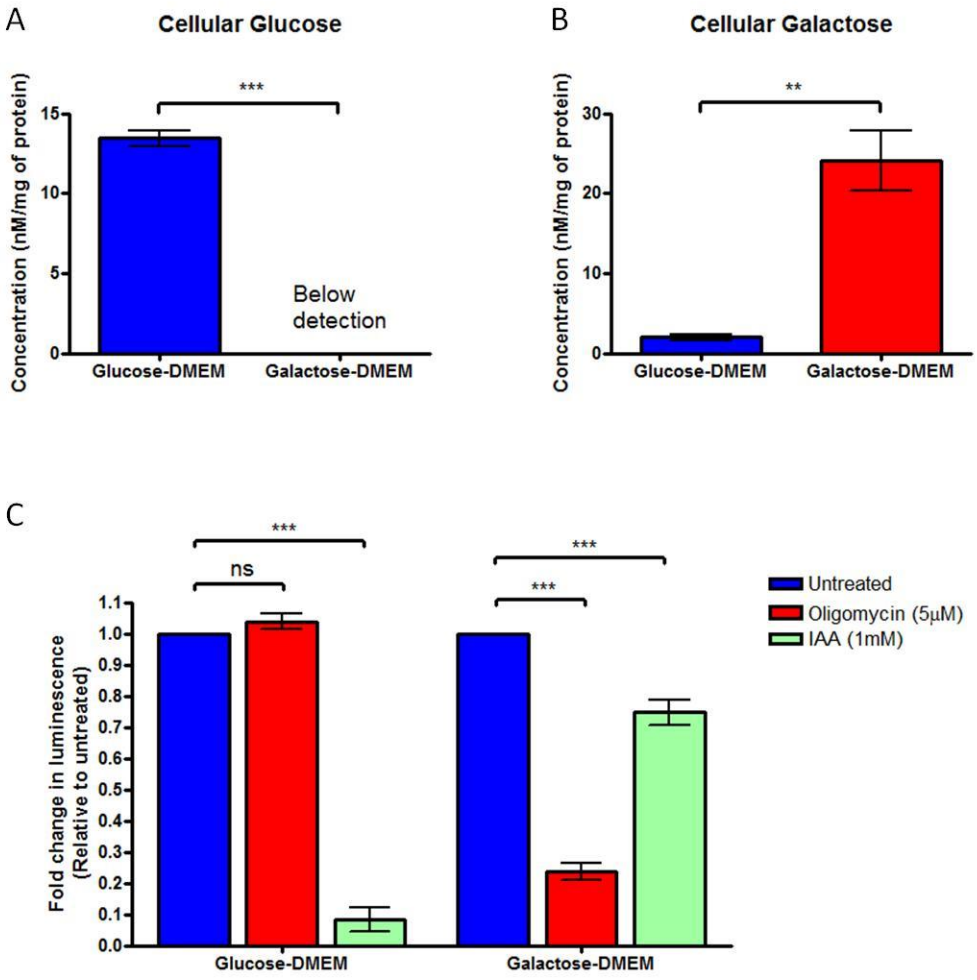


**Figure 3.13: Effects of manipulating cellular culture conditions on intracellular metabolites and ATP synthetic pathways.**

**Metabolomic analysis of HCT116 cells cultured in high glucose (glucose-DMEM, blue) or glucose free-galactose substituted media (galactose-DMEM, red) for 24 hours. Graphs show the concentration of intracellular glucose (A) and galactose (B) in cells (concentration, nM/mg protein). Values are mean +/- S.E.M (n=4). (*** p<0.001; **p<0.01) and data analysed using paired, two-tailed t-test). (C) Graph shows the fold change in luminescence (relative to untreated) as a measure of total cellular ATP levels for cells incubated in glucose-DMEM (left) and galactose-DMEM (right). Cells were untreated (blue), or treated with either oligomycin (5μM, red) or IAA (1mM, green). Values are mean +/- S.E.M (n=3). Data analysed using paired, two-tailed t-test (*** p<0.01, ns p>0.05).**

To determine the metabolic/energetic consequence of the change in OCR precipitated by acute treatment of cells with DMOG, cellular ATP was measured using a bioluminescent assay. Under the glucose and galactose culture conditions detailed above, compartmental

ATP production was measured over time in HCT116 cells. Compartmental ATP was measured using a transiently transfected firefly luciferase ATP reporter construct, targeted either to the mitochondria, using a mitochondrial targeted sequence derived from cytochrome c oxidase subunit VIII (COX-VIII) (mitochondrial probe), or using an untargeted cytosolic probe (Jouaville et al., 1999). With the addition of D-luciferin in the presence of oxygen, cells expressing the luciferase protein in their respective cellular compartments generate light that is proportional to the amount of ATP present in the transfected cell. HCT116 cells were maintained at 37°C during the assay and luminescence was measured over time using an automated kinetic luminometer. After a 15 minute baseline stabilisation period, 1mM DMOG was injected into respective wells and luminescence measured every 60 seconds. After 60 minutes incubation there was a small but significant increase in both cytosolic and mitochondrial luminescence in glucose, suggesting an increase in ATP over this period (Figure 3.14A). This result was replicated in those cells cultured in galactose for 24 hours prior to the assay (Figure 3.14B), suggesting that the increase in ATP observed in figure 3.14A was generated independently of glycolysis. An experiment with vehicle only was run separately and had no effect on luminescence (data not shown). Collectively, these data indicate that despite a decrease in OCR, DMOG is able to maintain cellular ATP levels, either by promoting its synthesis or reducing hydrolysis of ATP. Data was corrected for background luminescence, obtained through combined injection of oligomycin and IAA and normalised to luminescent values prior to DMOG injection to account for variations in luciferase expression and luminescent signal between repeats.

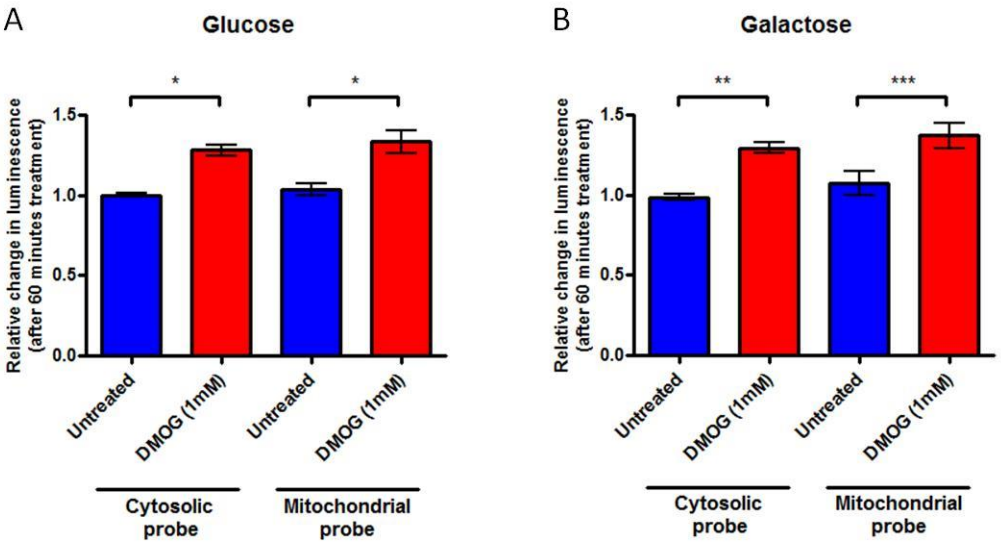


**Figure 3.14: Effect of DMOG on mitochondrial and cytosolic ATP levels.**

**HCT116 cells were transfected with luciferase constructs targeted to the mitochondria or cytosol (untargeted) in either (A) glucose or (B) galactose culture conditions. Reaction substrates were added and luminescence measured at 60 second intervals. Data is presented as fold change in luminescence after 60 minutes DMOG incubation relative to baseline immediately before addition. Graphs show a significant increase in ATP luminescence by 60 minutes DMOG (1mM, red) treatment compared to untreated (blue) in both cytosolic and mitochondrial compartments in glucose and galactose culture conditions. Values are mean +/- S.E.M (n=4). Data was analysed using paired, two-tailed t-test (*p<0.05, ** p<0.01, *** p<0.001).**

### 3.7.3 *The maintenance of cellular ATP levels in response to DMOG treatment is independent of HIF-1α*

To assess the contribution of HIF-1α to DMOG-induced maintenance of ATP, mitochondrial and cytosolic ATP was measured using the targeted luciferase construct as described above (Figure 3.14). Cells were transfected with either siRNA targeted towards *HIF-1α* or a non-silencing control (NSC) siRNA, and luminescence was measured over time. DMOG was injected after 15 minutes and the change in luminescence was followed for 60 minutes at 2 minute intervals. Despite effective silencing of *HIF-1α* (Figure 3.15C), treatment with DMOG continued to result in a significant increase in luminescence in both compartments under glucose and galactose conditions (Figure 3.15A and B). These data suggest the increase or maintenance of ATP observed in figure 3.14 is independent of HIF-1α. Data was corrected for background luminescence, obtained through combined injection of oligomycin and IAA

and normalised to luminescent values prior to DMOG injection to account for variations in luciferase expression and luminescent signal between repeats.

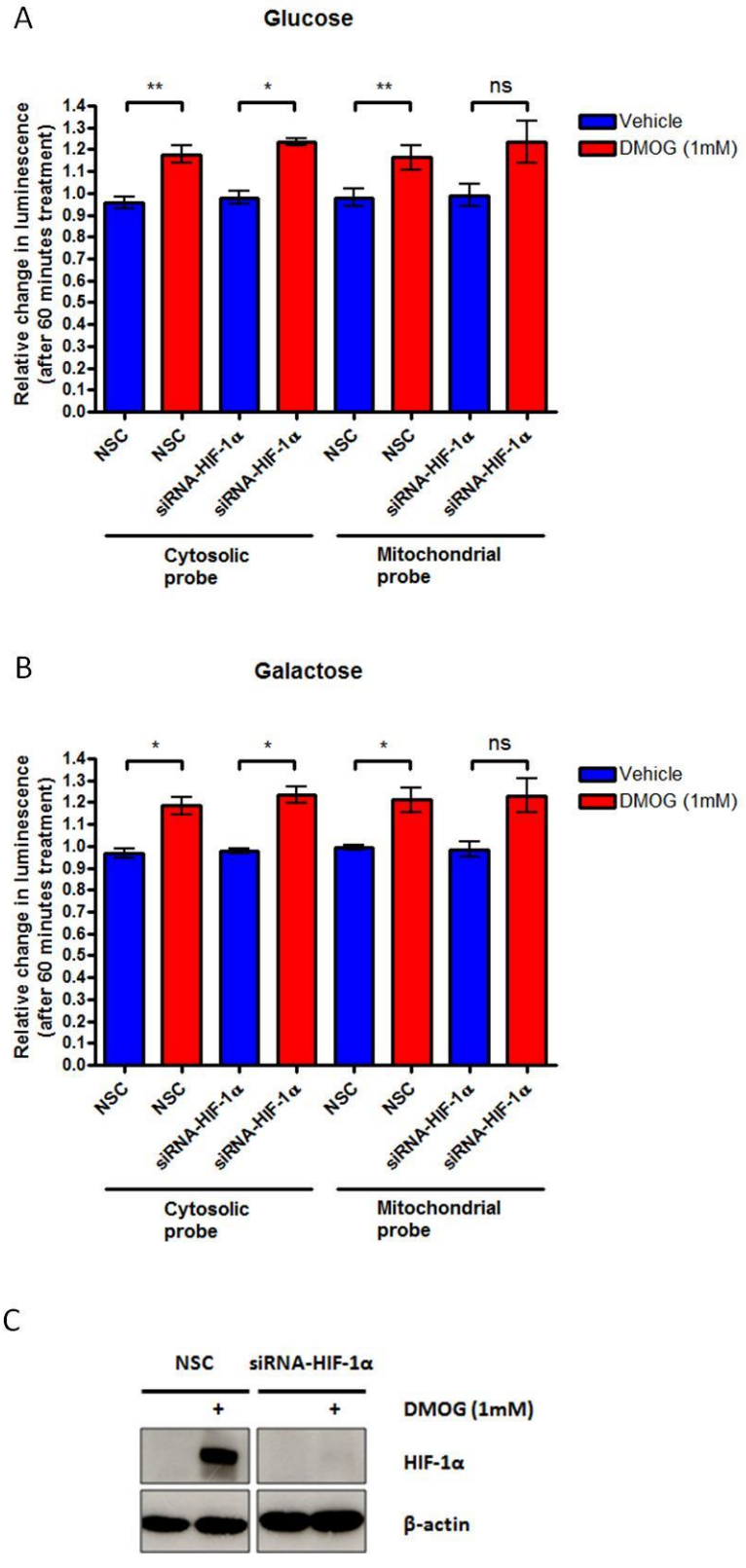

**Figure 3.15: Maintenance of cellular ATP levels in response to DMOG are independent of HIF-1α.**

***HIF-1α* was silenced in HCT116 cells and then cells were subsequently transfected with luciferase constructs targeted to mitochondria or cytosol (untargeted) in either (A) glucose or (B) galactose culture conditions. Reaction substrates were added and luminescence measured at 2 minutes intervals. Data is presented as fold change in luminescence after 60 minutes DMOG treatment relative to baseline immediately before addition. Graphs show increases in ATP luminescence after 60 minutes DMOG (1mM, red) compared to untreated (blue) in both cytosolic and mitochondrial compartments in the presence of non-silencing control (NSC) siRNA or *HIF-1α* siRNA in glucose and galactose culture conditions. Values are mean +/- S.E.M (n=4). Data was analysed using paired, two-tailed t-test (** p<0.01, * p<0.05, ns p>0.05). (C) Western blot shows confirming knockdown of HIF-1α protein. In parallel with experiments in A-B, HCT116 cells were treated with DMOG for 1 hour (+, 1mM). The absence of HIF-1α protein after DMOG treatment in the presence of the siRNA suggests effective silencing. β-actin was used as a load control.**

### 3.7.4 *Effects of DMOG treatment on mitochondrial inner membrane potential*

Mitochondrial inner membrane potential ($\Delta\psi_m$), together with a small pH gradient, forms the proton electrochemical potential, generated across the mitochondrial inner membrane. The serial transfer of electrons through membrane associated complexes along the ETC is coupled to the pumping of protons against their concentration gradient into the IMS. Mitochondrial membrane potential is an important indicator of cell viability and ultimately dictates the cellular capacity to generate ATP by OxPhos (Acton et al., 2004). Mitochondrial inner membrane potential can be measured by fluorescent microscopy using the cationic lipophilic dye, TMRM. TMRM accumulates in areas of negative potential based on its charge and is a well characterised tool to study mitochondrial membrane potential (Brand and Nicholls, 2011). Figure 3.16A shows the effect of addition of 1mM DMOG on mitochondrial inner membrane potential using TMRM and fluorescent time-lapse microscopy. HCT116 cells were equilibrated in TMRM for 45 minutes after which the assay was commenced with a 30 minute baseline imaging period. The addition of 1mM DMOG to cells cultured in glucose caused no significant difference observed in fluorescence over a period of 90 minutes (Figure 3.16A).

To further explore the effects on DMOG treatment on mitochondrial membrane potential, an alternative approach to TMRM measurement was also undertaken, which allowed membrane potential to be measured over longer periods of DMOG treatment. $DIOC_6(3)$ is also a well characterised membrane potential-sensitive dye and suitable for flow

cytometric analysis. HCT116 cells were treated for 1, 4 or 24 hours with DMOG, before trypsinisation and equilibration with the $DIOC_6(3)$. Median fluorescence was then measured by flow cytometric analysis. Figure 3.16B shows no change in fluorescence up to 24 hours DMOG treatment, confirming the data obtained using TMRM and suggesting no likely relationship between the changes observed in OCR and membrane potential. Together these data suggest that despite a decrease in OCR, DMOG is maintaining cellular ATP levels and mitochondrial membrane potential.

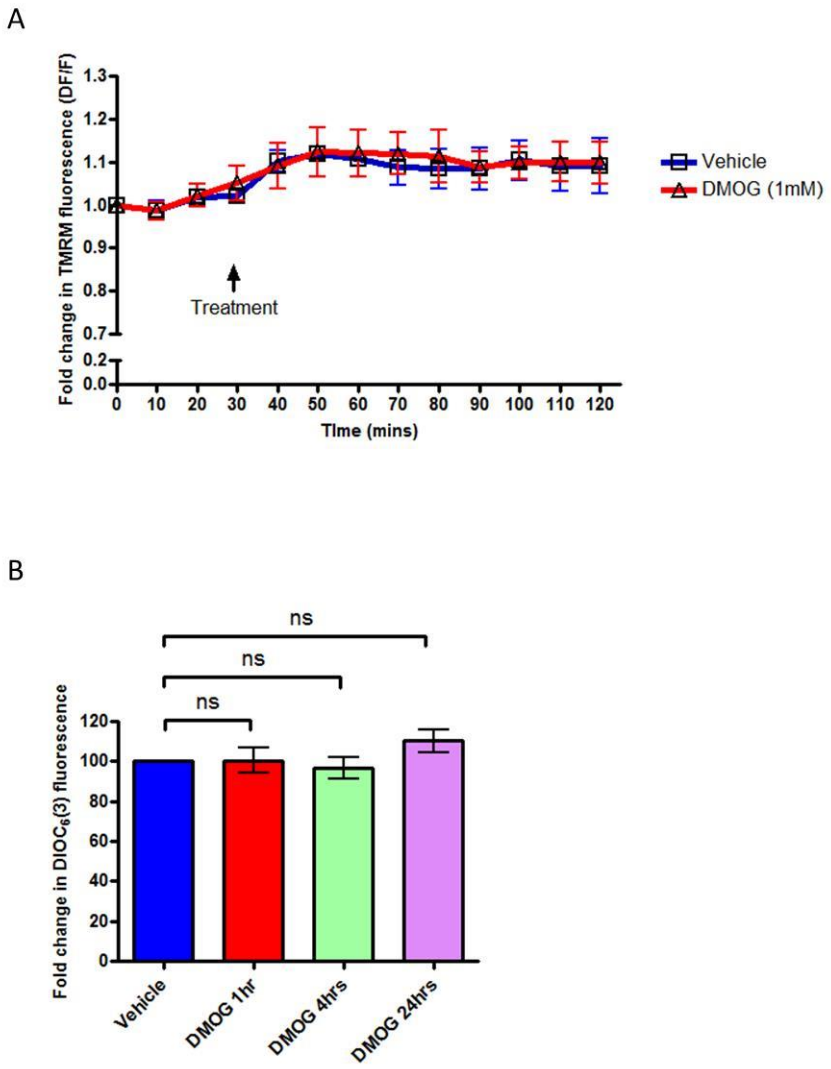


**Figure 3.16: Effect of DMOG on mitochondrial inner membrane potential.**

**(A) HCT116 cells were incubated with TMRM (50nM) and equilibrated for 45 minutes and measurements were then taken at 10 minute intervals. Values were normalised to fluorescence change from the first frame (DF/F). DMOG (1mM, red) or vehicle (blue) was added after 30 minutes and cells imaged for a total duration of 2 hours. Cells in each condition were imaged from two parallel wells using 3 fields of view per well, with average intensity calculated from three regions of interest, with background correction. Analysis was performed using Image Pro Plus software (Media Cybernetics, Rockville, USA). Values are mean +/- S.E.M (n=3). (B) HCT116 cells were incubated with $DIOC_6(3)$ (0.2nM) equilibrated for 30-45 minutes before analysis by flow cytometry using a Beckman Coulter CyAn™ ADP Analyser. Graph shows the fold change in median fluorescence with DMOG compared to vehicle alone for the times indicated (ns. $p>0.05$). Values are mean +/- S.E.M (n=3). Data was analysed using paired, two-tailed t-test.**

## 3.8 Evaluation of the effects of a second PHD inhibitor on mitochondrial parameters

### 3.8.1 *Evaluation of a second PHD inhibitor on HIF-1α protein stabilisation*

DMOG is a well-characterised inhibitor of the PHD proteins/α-ketoglutarate-dependent dioxygenases enzymes that activate the hypoxic response. As such, DMOG is widely used to investigate HIF-1α stabilisation and downstream effectors of the oxygen-sensing pathway (Elvidge et al., 2006). However, to determine that the mitochondrial effects observed in response to DMOG treatment are due to PHD inhibition (Figure 3.11, Figure 3.14 and Figure 3.16), we tested a second inhibitor of the PHD proteins (designated PHD-I). The structure of PHD-I is unrelated to that of DMOG (Figure 3.17A-B). Chemically, PHD-I is a hydroxyquinolone and has previously been demonstrated to inhibit the PHD proteins with an $IC_{50}$ = 2μM in a cell-based assay (Smirnova et al., 2010) (reference compound: D2 #8), that utilised a stably transfected reporter comprising the HIF-1α ODD domain fused to luciferase and assessed for intracellular proline hydroxylation (Smirnova et al., 2010). PHD-I works through chelation of $Fe^{2+}$ at the PHD active site, a mechanism distinct from non-specific iron chelation (Smirnova et al., 2010). DMOG is an analogue of α-ketoglutarate and a competitive inhibitor for the α-ketoglutarate binding site on the PHD proteins (Mole et al., 2003). DMOG is also an inhibitor of distinct α-ketoglutarate-dependent dioxygenases (Rose et al., 2011), thus lacks specificity for the PHDs.

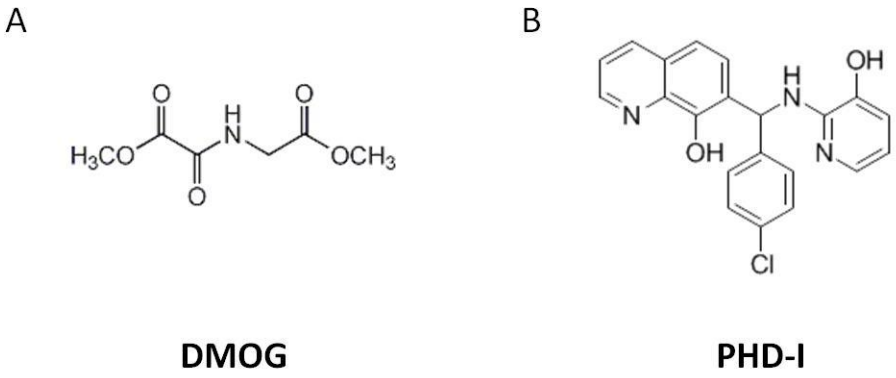


**Figure 3.17: Structural comparison of PHD inhibitors, DMOG and PHD-I.**
**(A) The structure of DMOG and (B) PHD-I. The two structures are unrelated, PHD-I being a hydroxyquinolone and DMOG an analogue of α-ketoglutarate. Structures sourced from www.calbiochem.com.**

First, it was important to determine that PHD-I was behaving as expected. In order to determine a working concentration of PHD-I and confirm inhibitory activity, as previously described for DMOG (Figure 3.10), HCT116 cells were incubated for 20 hours with PHD-I, in the presence and absence of 10μM MG132 (which was added for the final four hours of PHD-I treatment to inhibit the proteasome). HIF-1α protein was robustly induced by PHD-I at a concentration of 2.5-5μM and the disappearance of the hydroxylated species of HIF-1α at 5μM PHD-I confirmed the effective inhibition of the PHD proteins (Figure 3.18A). Therefore a dose of 5μM PHD-I was used in further experiments.

To investigate the kinetics of the HIF-1α response to PHD-I, HCT116 cells were incubated with 5μM PHD-I over time and western blot analysis was performed to assess HIF-1α stabilisation (Figure 3.18B). PHD-I rapidly and robustly stabilised HIF-1α protein by 60 minutes with the kinetics of the stabilisation being similar to that observed for DMOG (Figure 3.10B and Figure 3.18B). The effects of PHD-I on mitochondrial function were then assessed in order to compare these with effects observed with DMOG treatment.

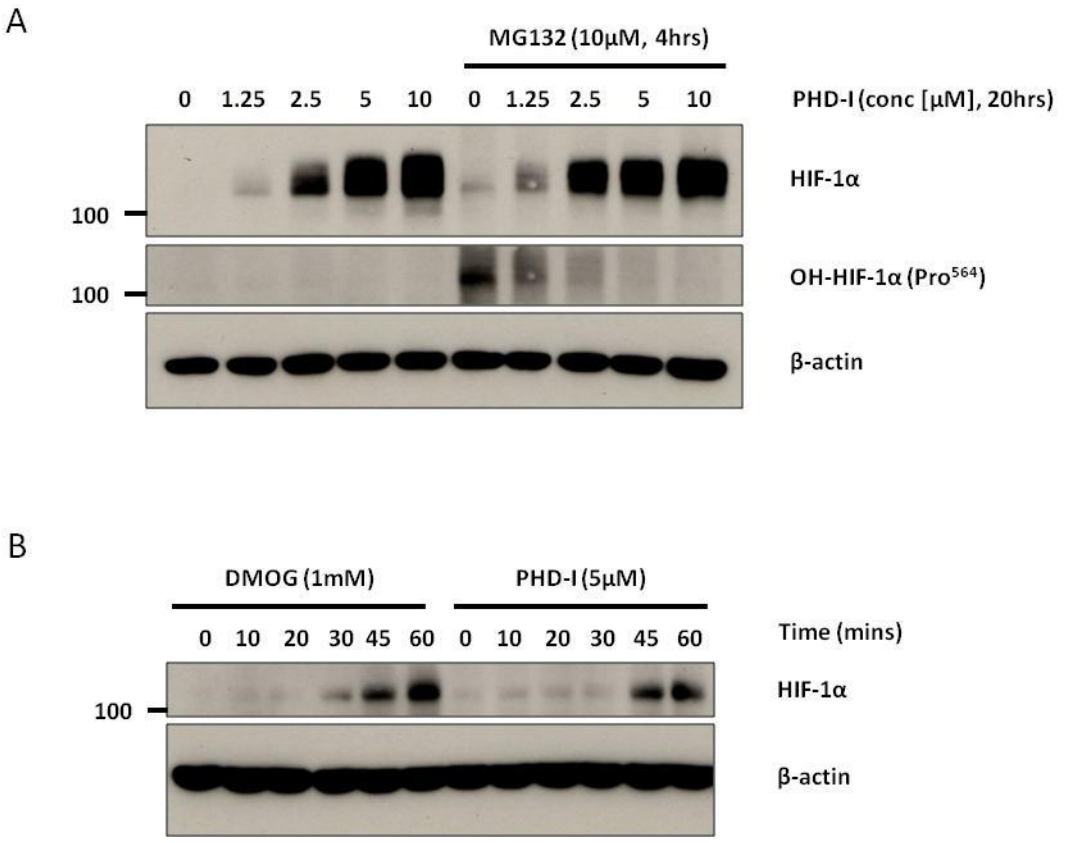


**Figure 3.18: Dose and time-dependent effects of PHD-I on HIF-1α protein.**

**Western blot analysis of HCT116 cells treated over a concentration titration of PHD-I (20 hours) in the presence and absence of the proteasome inhibitor MG132 (10μM), for the final 4 hours. (A) Western blot shows inhibition of the proteasome by MG132 prevents the degradation of the hydroxylated species of HIF-1α, and PHD-I blocks the hydroxylation of HIF-1α protein. Hydroxylated HIF-1α species fully disappeared at 5μM suggesting effective inhibition of the PHD proteins. (B) Western blot shows time course comparison of HIF-1α protein induction for DMOG (1mM) and PHD-I (5μM) treatment over a period of 60 minutes. Western blot analysis demonstrating HIF-1α protein is significantly induced at 45 minutes for both compounds. β-actin is used as a load control for both experiments.**

### 3.8.2 *Investigation into the role of PHD-I on mitochondrial function*

In addition to the Seahorse XF24 bioanalyser, the Oroboros Oxygraph 2K (O2K) was used to measure oxygen consumption rate in intact cells. The advantage of the O2K is the capacity to add sequential volumes of compound to cells in suspension, so one can carefully titrate the concentration of agents in order to define the maximum respiratory capacity. The Oroboros O2K is a modular system for high-resolution respirometry, combining a two-

parallel chamber, closed-system into which cells are added and dissolved oxygen in the buffer measured by polarographic oxygen sensors and rate calculated. Effect of PHD-I on OCR was measured over time. PHD-I was injected after an initial baseline stabilisation period and the OCR of HCT116 cells was followed over time. Figure 3.19A shows no change in baseline OCR in HCT116 cells cultured in glucose after injection of 5µM PHD-I over a period of 30 minutes. There was also no change in leak respiration (after the addition of oligomycin) or maximum respiratory capacity (after the addition of FCCP) (Figure 3.19). Re-oxygenation was necessary to replenish consumed oxygen in the respiration buffer. To do this the chamber was opened for a few minutes while oxygen concentration returned to starting concentrations. These data raise the possibility that the change in OCR observed with DMOG (Figure 3.11) was not due to inhibition of the PHD proteins but due to some off target affect not recapitulated by PHD-I, which is a relatively more specific PHD inhibitor.

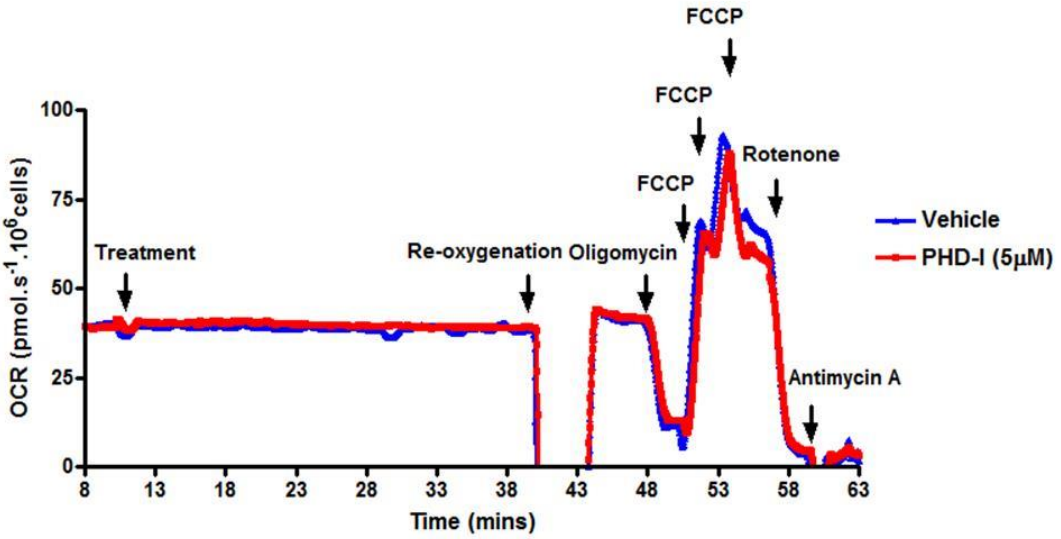


**Figure 3.19: Effect of PHD-I on OCR in HCT116 cells.**

**Graph shows OCR (pmol.$s^{-1}$.$10^6$ cells) measured over time in minutes (mins) using the Oroboros O2K in HCT116 cells. OCR was allowed to stabilise for approximately 10 minutes before the addition of PHD-I (5µM; red) or vehicle (blue) for 30 minutes. Oligomycin (2µg/ml) was added to determine the oxygen consumed that is coupled to ATP synthesis, FCCP titration (0.5µM increments) allowed estimation of maximum respiratory rate and rotenone (0.5µM) and antimycin A (2.5µM) allowed correction for non-mitochondrial respiration. There is no change in basal OCR in cells cultured in glucose conditions.**

DMOG also caused a small but significant increase in ATP levels when measured using targeted ATP-sensitive luciferase constructs (Figure 3.14). This experiment was repeated using PHD-I. After an initial baseline period for stabilisation of the signal, 5μM PHD-I was injected and the luminescence followed over time. There was no significant difference observed by 60 minutes of PHD-I treatment compared to control in either cytosolic or mitochondrial compartments in glucose conditions (Figure 3.20A). Similar findings were also observed in the cytosolic compartment in those cells cultured in galactose. However, there was a very small but significant decrease in luminescence in the cytosolic signal in cells cultured in galactose (Figure 3.20B). Oligomycin and IAA were injected at the end of the experiment to determine background luminescence. Data was collated from four independent experiments and presented as fold change in luminescence after background correction, normalised to values immediately prior to drug injection, to account for variations in transfection efficiency between conditions and experiments.

These data suggest that the small but significant increase in luminescence observed after DMOG treatment is not mimicked by PHD-I. This result, when combined with the absence of an effect of PHD-I on OCR is suggestive of distinct mechanisms through which these inhibitors are affecting mitochondrial function, one which is unlikely to be through a common mechanism of action, since they do not produce identical results.

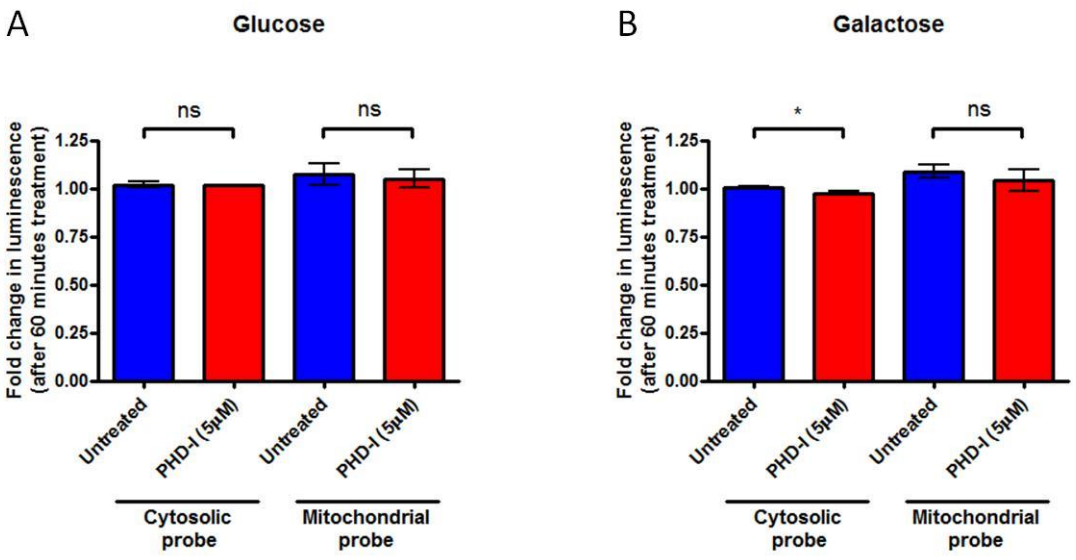


**Figure 3.20: Effect of PHD-I on compartmental ATP levels.**

**HCT116 cells were transfected with luciferase constructs targeted to mitochondria or cytosol (untargeted) in either (A) glucose or (B) galactose conditions. Reaction substrates were added and luminescence measured at 60 second intervals. Data is presented as fold change in luminescence after 60 minutes PHD-I incubation relative to baseline immediately before addition. (A) Graph shows there was no significant increase in luminescence by 60 minutes PHD-I treatment (5μM, red) compared to untreated (blue) in both cytosolic and mitochondrial compartments (ns $p>0.05$). (B) Graph shows there was a small significant decrease in luminescence in the cytosol after PHD-I treatment only in galactose conditions (cytosolic probe * $p<0.05$, mitochondrial probe ns $p>0.05$). Values are mean +/- S.E.M (n=4). Data was analysed using paired, two-tailed t-test.**

The data presented above led us to conclude that DMOG was affecting metabolism through functions independent of its established role as a PHD protein inhibitor. As DMOG is structurally related to α-ketoglutarate, it was possible that DMOG was acting through the TCA cycle (Figure 3.21).

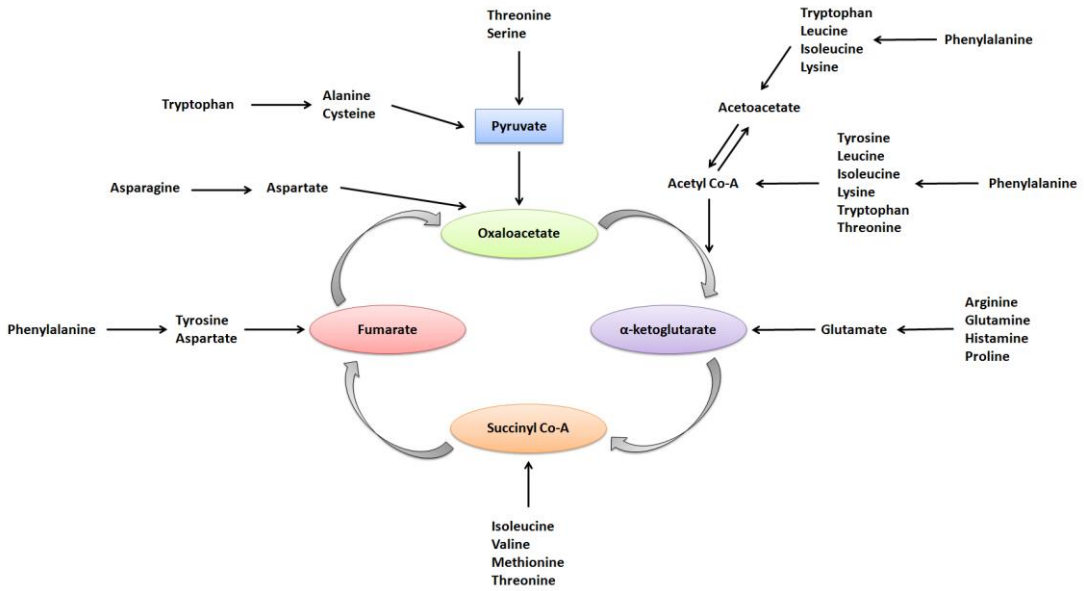


**Figure 3.21: Catabolism of amino acid skeletons and their entry into the TCA cycle.**

**The structural similarities between DMOG and α-ketoglutarate make the TCA cycle a potential target for DMOG-mediated metabolic effects.**

To understand the mechanism through which DMOG was producing a bioenergetic phenotype, potentially independent of the PHD proteins, metabolomic analysis was undertaken. HCT116 cells were cultured either in the presence or absence of 1mM DMOG for 2 hours, under either glucose or galactose culture conditions. Media was replaced prior to the addition of DMOG to allow analysis of cellular uptake and excretion of metabolites in the 2 hour treatment window. After 2 hours, media was removed and frozen. The cells were repeatedly washed before being subjecting to dual phase extraction to separate water-soluble, protein and lipid-soluble metabolites. Metabolomic profiling was undertaken using magnetic resonance spectroscopy (MRS) at the Institute of Cancer Research (ICR), Sutton, UK by Dr Yuen-Li Chung. Aqueous and lipid phases were analysed and designated "cellular metabolites". Analysis of media samples were designated "media metabolites", with negative values denoting the excretion while positive values denoted the uptake of named metabolites. Total protein was quantified from the cell samples to allow normalisation of metabolite concentration to cellular protein content. The full metabolic analysis is included in the appendix. The analyses showed significant changes in cellular (Figure 3.22) and media (Figure 3.23) metabolites. Figure 3.22A shows that the addition of DMOG significantly reduced the cellular fumarate concentration in both glucose

and galactose culture conditions. Fumarate is a TCA cycle intermediate, formed by the oxidation of succinate by succinate dehydrogenase and contributes to maintaining the supply of reducing equivalents to the ETC. Reduction of fumarate would affect electrons entering the ETC at complex I and as a result potentially reduce oxygen consumption rate. The reduction of fumarate upon DMOG treatment raises the possibility that since the structure of DMOG is analogous to that of α-ketoglutarate, another TCA cycle intermediate; DMOG may be affecting the TCA pathway through competitive inhibition. When cells are cultured in galactose, they will be more reliant on the TCA cycle, since pyruvate and glutamine will be the primary metabolic substrates. A reduction in flux through the TCA cycle would be expected to decrease the supply of electrons to the ETC and potentially be the underlying mechanism for the decreased OCR observed in DMOG treated cells.

Levels of intracellular glucose were also reduced after DMOG treatment, in those cells cultured in glucose (Figure 3.22B). This is possibly a compensatory mechanism due to a block in TCA cycle, and a mechanism through which cells can produce ATP by glycolysis and maintain membrane potential through the reverse mode of the $F_1F_O$-ATPase and ATP hydrolysis. Interestingly, significant differences were also observed in aspartate levels (Figure 3.22E). HCT116 cells cultured in glucose exhibited an increase in cellular aspartate by 2 hours DMOG treatment. Conversely, cells cultured in galactose demonstrated a significant decrease in aspartate by 2 hours DMOG treatment. The initial levels of aspartate were also different between the culture conditions in the absence of the DMOG. Figure 3.23 shows the extracellular metabolic changes that occurred in the media of HCT116 cells, as a result of increased uptake or excretion of metabolites in response to DMOG treatment. Valine, threonine, iso-leucine and phenylalanine all increase in response to DMOG treatment in those cells cultured in galactose. Collectively, there are clear differences in cell metabolism when HCT116 cells are treated with DMOG which occur within minutes to hours of treatment, suggestive of a non-transcriptional response and one mediated through perhaps a combination of the PHD proteins and non-specific off target effects of DMOG.

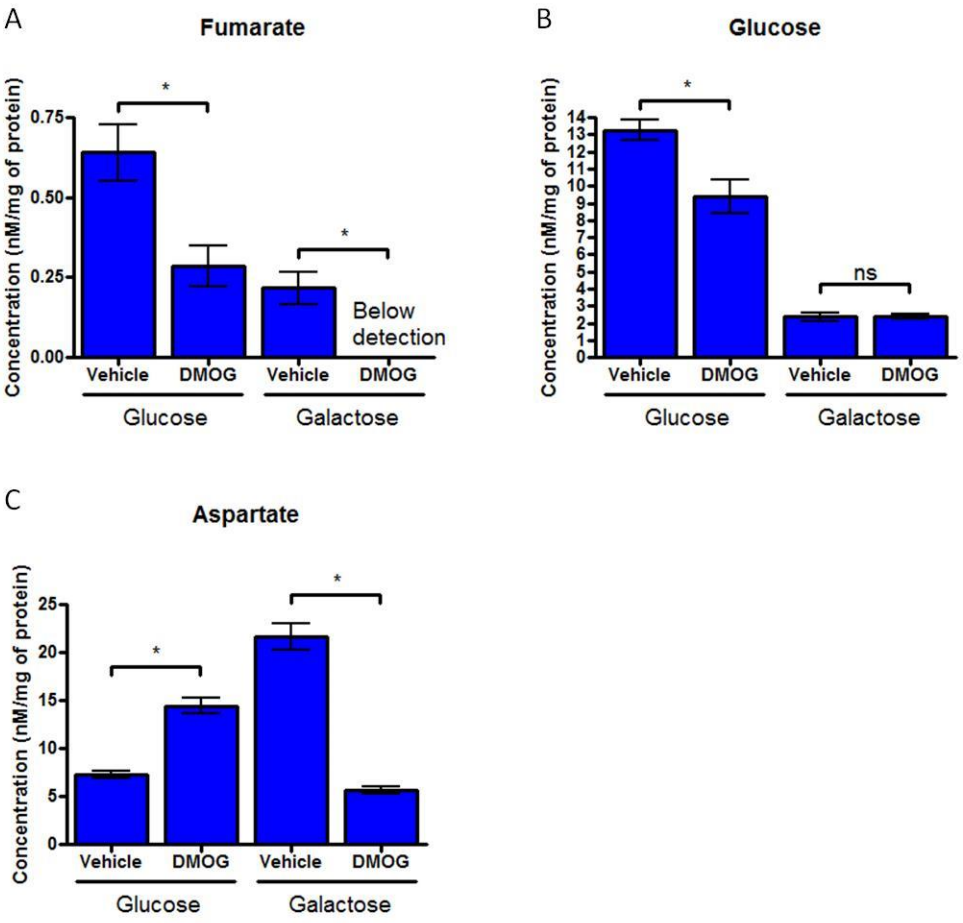


**Figure 3.22: Metabolomic analysis of intracellular metabolites.**

**HCT116 cells were cultured under either glucose or galactose conditions for 24 hours. DMOG (1mM) or vehicle was added to freshly replaced media for 2 hours. Media was removed and immediately frozen for analysis. Cells were washed and protein and metabolites separated through dual phase extraction. Metabolites were quantified by MRS (performed at the ICR, Sutton, UK) and presented as a concentration per mg of protein (nM/mg). Values are mean +/- S.E.M (n=3) (* $p<0.05$, ns $p>0.05$).**

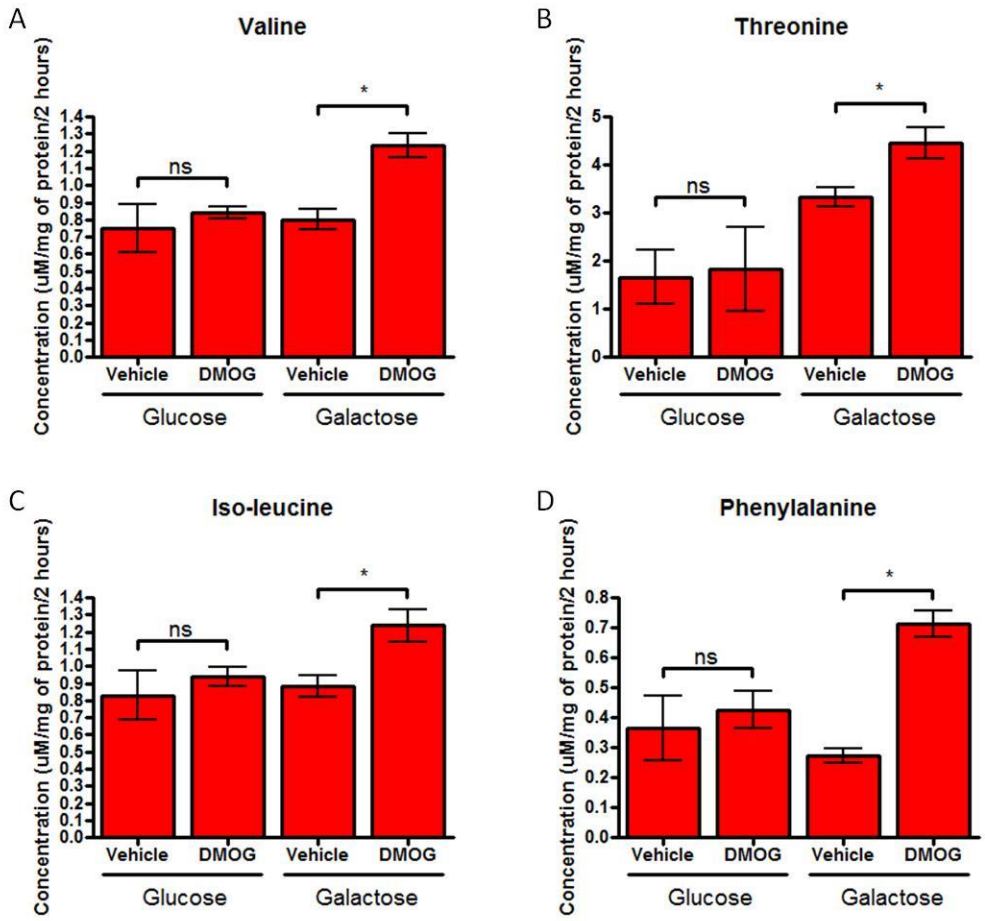


**Figure 3.23: Metabolomic analysis of metabolites found in the media.**

**HCT116 cells were cultured under either glucose or galactose conditions for 24 hours. DMOG or vehicle was added to freshly replaced media for 2 hours. Media was removed and immediately frozen for analysis. Media metabolites were quantified by MRS (performed at the ICR, Sutton, UK) and presented as a concentration per mg (µM/mg) of protein over 2 hours. Values are mean +/- S.E.M (n=3) (* $p<0.05$, ns $p>0.05$).**

## 3.9 Discussion

The role of HIF-1 has been extremely well characterised since its discovery as a central mediator of the cellular response to hypoxia in 1992 (Semenza and Wang, 1992). Since then, HIF-1 has been observed to play an essential role in cardiovascular biology. The cardiovascular role of HIF-1 has been examined in many systems, including cell and tissue culture, *ex vivo* models, such as the Langendorff isolated perfused heart and *in vivo* (Date et al., 2005, Cai et al., 2008, Kido et al., 2005). Using each of these approaches HIF has been

identified to have a role in development, normal healthy physiology as well as under pathophysiological conditions.

### 3.9.1 *HIF-1 in maintaining cardiovascular physiology and function*

Despite its title as an 'inducible factor', basal HIF transcription has been identified as important and necessary for correct functioning of the heart. HIF-1 is required for basal gene transcription under physiological conditions in normoxia, for the maintenance of ion signalling, vascularity and energy metabolism (Huang et al., 2004). Additionally, basal HIF-1α transcription has been observed as being crucial in the acute phase of ischaemic pre-conditioning (Loor and Schumacker, 2008, Cai et al., 2008). A transgenic mouse model of HIF-1α constitutive over-expression in the myocardium demonstrated increased VEGF-mediated angiogenesis, a reduction in infarct size and improved cardiac mechanics and function 4-weeks post coronary artery occlusion (Kido et al., 2005). Improvement in cardiac function was also observed using intramyocardial injection of small hairpin RNA (shRNA) toward PHD2, demonstrating enhanced neoangiogenesis and improved ventricular function in a mouse model of myocardial infarction (Huang et al., 2008). Taken together, this suggests that the control of HIF levels and maintenance of appropriate basal transcription is vital in cardiac dynamics and function. These observations are important as this chapter has aimed to explore the acute/short term consequences of activation of the oxygen-sensing pathway, through inhibition of the PHD proteins on metabolism and mitochondrial function. HIFs role in cardiac pathology has also been characterised (Lee et al., 2000). HIF-1α is up regulated in response to chronic ischaemia, its mRNA levels and expression of the HIF target gene *VEGF* are both increased after coronary artery occlusion (Lee et al., 2000).

### 3.9.2 *HIF-1 in cardioprotection*

Activation of HIF/hypoxia pathway in several studies has been demonstrated to exhibit a cardioprotective role, attributed to HIF-dependent downstream target genes, such as *haem oxygenase-1* (*HO-1*), *VEGF* and *inducible nitric oxide synthase* (*iNOS*) (Loor and Schumacker, 2008, Hyvarinen et al., 2010, Eckle et al., 2008, Dawn and Bolli, 2005).

Cardioprotection has been demonstrated in *Phd2* hypomorphic mice. *Phd2* hypomorphs have decreased activity of PHD2 through a gene trap insertion cassette and expresses tissue-dependent amounts of *Phd2* mRNA, with only 8% of control expression in the heart (Hyvarinen et al., 2010). These mice show chronic HIF-1α stabilisation in the heart and improved mechanical recovery after 20 minutes global ischaemia and 45 minutes

reperfusion. A reduction in infarct size was evidenced by decreased lactate dehydrogenase release. Hyvarinen *et al* suggested that the congestive heart failure observed in the broad spectrum conditional *Phd2* knockout mouse model (Minamishima et al., 2008), was due to indirect polycythemic pathology and enhanced angiogenesis as consequence of systemic factors - as neither were evident in the heart of the hypomorphic mice (Hyvarinen et al., 2010).

Intriguingly, non-lethal rounds of ischaemia-reperfusion, pre-ischaemic insult or rounds of reperfusion/reoxygenation immediately post ischaemia, have been shown to be protective - processes known a pre- and post-conditioning respectively (IPC and IPost) (Taylor and Pouyssegur, 2007, Murry et al., 1986). IPC has both an immediate/early and delayed component leading to protection (Arstall et al., 1998). Early phase protection occurs in minutes and lasts up to a few hours post stimulus. Early phase protective events are mediated by ion channels and other signalling molecules with a delayed transcriptional response occurring within 12-24 hours and lasting as long as 3-4 days (Date et al., 2005). HIF-1 has been shown to be involved in both these situations; predictably the transcriptional response (Date et al., 2005), mediated through the up-regulation of HIF-specific gene expression. However HIF-1 is thought to be involved in an immediate/early phase non-transcriptional response (Cai et al., 2008).

In 2005, Date *et al* observed HIF-1α to be protective and also play a role in late phase response to ischaemic pre-conditioning (Date et al., 2005). HIF-mediated protection was observed *in vitro* using a hypoxia-reoxygenation approach, examining constitutively stable hybrid forms of HIF-1α and after determination of the influence on myocardial viability and gene expression (Date et al., 2005). In 2008, Cai *at al* reached the same conclusion (Cai et al., 2008). Cai *et al* identified relief of protection from hypoxic preconditioning using mice heterozygous for *Hif-1α* in a model of ischaemic injury. Cai *et al* identified that this HIF-dependent protection was dependent on *Hif-1α* gene dosage and HIF-1α induced mitochondrial ROS production. Cai *et al* also demonstrated a role of HIF-1 in the early phase of cardiac protection, after observing an increased infarct size after IPC and ischaemic injury in the *Hif-1α*$^{+/-}$ (Cai et al., 2008). The HIF-dependent early phase protection was concluded not to be the acute activation of HIF-1 target genes, but the HIF-dependent basal expression of genes required for the mechanism behind the preconditioning stimulus.

Therefore loss of HIF-1 would interrupt the signalling pathway that in the presence of HIF-1α would mediate protection (Cai et al., 2008).

Studies showing that HIF-1 elicits protection in ischaemic preconditioning and cardioprotection were performed using intraventricular infusion of siRNA, targeted towards *Hif-1α* and *Phd2* and pharmacological HIF-1 activation using DMOG. Eckle *et al* highlighted the increased purigenic signalling through the A2B adenosine receptor (A2BAR) under conditions of HIF-1α stabilisation and loss of protection in *A2BAR*$^{-/-}$ mice (Eckle et al., 2008).

Numerous problems can be identified with respect to targeting PHD2 and the suggestion that resultant HIF-1α stabilisation is responsible for the observed protective effect. Firstly PHD3, not PHD2 is the prominent isoforms in the heart, and there is increasing expression with age (Rohrbach et al., 2005). Secondly, a body of evidence suggests that the PHD proteins have functions outside their regulation of HIF-α (Table 4; below) and it may be interruptions to these distinct pathways which is responsible for the phenotypic changes associated with the cellular resistance to ischaemic injury.

HIF-1 and HIF-2 have distinct roles in cardioprotection. HIF-1 regulates the transition in metabolism from aerobic respiration to glycolysis in the early phase of ischaemic preconditioning through up-regulating genes such as *PDK-1* and mediating the cytochrome oxidase subunit switch. In the late phase, HIF-1 functions to up-regulate genes dictating vascular changes and cell survival such as *VEGF*, *HO-1* (Dawn and Bolli, 2005, Ockaili et al., 2005), *cyclooxygenase-2* (Bolli et al., 2002), *iNOS* (Guo et al., 1999) and the *A2B receptor* (Synnestvedt et al., 2002). HIF-2 appears comparatively understudied and believed to be involved in maintaining mitochondrial and antioxidant homeostasis and regulating more adaptive responses (Shohet and Garcia, 2007). A delicate balance exists between glycolytic and aerobic metabolism and HIF-1 is central in directing these transitions. In the heart, these metabolic processes have been linked to cardioprotection against ischaemic injury and the involvement in ischaemic preconditioning. It therefore remains possible that the HIFs are having more of a direct role on metabolism, although precisely how, is yet to be elucidated.

Although the involvement of HIF in cardioprotection is evident and effects multi-factorial, it has yet to be identified as the common pathway. Additionally, the concept of ischaemic

preconditioning still remains a complex subject and one that needs to be delineated if there is to be any therapeutic significance to this cytoprotection.

### 3.9.3 *Characterisation of HL-1 cardiomyocytes*

The first part of this chapter aimed to utilise the HL-1 cell line as a model system and tool to study fully differentiated adult cardiomyocytes and to further probe the HIF-mitochondria interface. HL-1 cells were developed by William Claycomb and established from atrial tumour cells derived from the AT-1 mouse in which the SV40 large T antigen has been targeted to atrial myocytes using the ANF promoter (Claycomb et al., 1998). HL-1 cells were isolated from an AT-1 subcutaneous tumour and display characteristics of a fully differentiated cardiomyocyte with respect to morphology, biochemistry and electrophysiology (Claycomb et al., 1998). HL-1 cardiomyocytes possess the ability to spontaneously contract and can be serially passaged in culture, making them a useful model to initially characterise HIF responses as a prerequisite to the isolation and characterisation of primary cells.

Under hypoxia, oxygen, the essential substrate for the generation the hydroxyproline in the ODD domain of HIF-α becomes limiting and hydroxylation is inhibited. Inhibition of hydroxylation allows HIF-1α to escape pVHL-mediated targeting and proteasomal degradation, stabilising the HIF-α protein. The response of HIF-1α to hypoxia was successfully validated in the HL-1 cells, shown by a robust increase in HIF-1α protein observed over time in 1% oxygen. Additionally, we confirmed HIF-1α protein stabilisation after inhibition of the PHD proteins. The α-ketoglutarate analogue, DMOG, prevents hydroxyproline formation by competing with the α-ketoglutarate and at the co-factor binding site. HL-1 cells therefore demonstrate a characteristic response to both hypoxia and PHD inhibition; demonstrate reproducible HIF-1α induction and HIF-1-dependent target gene expression after 24 hours, making this a useful model system in which to study the potential role of HIF-1α in a cardiomyocyte background.

IGF-1 is produced in every tissue, constitutively expressed and mediates autocrine-paracrine-endocrine actions on cell survival, differentiation and proliferation (Suleiman et al., 2007). The IGF-system consists of two ligands (IGF-1 and -2), two receptors (IGF-1R and -2R) and IGF-binding proteins, which function in tandem to allow receptor-mediated responses under tight regulation (Suleiman et al., 2007). IGF-1 is a survival factor and a HIF-1 target gene, encoding a functional HRE present in intron 1 (Tazuke et al., 1998). IGF-1

stimulation can equally induce HIF-1α protein synthesis in tumour cells (Feldser et al., 1999). Circulating, non-bound IGF-1 binds its cognate receptor on the cell membrane and activates either the MAPK or the PI3K-AKT/PKB signalling pathways. To confirm growth factor signalling to HIF-1α as we have previously described (Bardos et al., 2004), IGF-1 was successfully demonstrated to induce HIF-1α protein synthesis after 2 hours treatment, increasing over time in HL-1 cells. The importance of this lies in ensuring well characterised pathways leading to effects on HIF exist and are operating as expected in this cell line.

The HL-1 cell line provided a good model for characterisation of the mitochondrial association of the HIFs. However, these cells do not behave exactly like primary cardiomyocyte. HL-1 cells rely heavily on glycolysis and less on OxPhos for their energy production (Monge et al., 2009). They have decreased cytochrome content, decreased respiratory chain complex activities, particularly complex I (Monge et al., 2009, Eimre et al., 2008). For further analysis of the functional consequence of HIF-1α association with mitochondria and its potential effects on mitochondrial function with respect to cardiac biology, it would be necessary to use primary cardiomyocytes derived from rat or mouse, which would provide a more physiological context with respect to the balance between glycolytic and OxPhos metabolism.

### 3.9.4 *Mitochondrial association of the HIFs*

The second part of this chapter aimed to illustrate alternative, non-transcriptional roles of the HIF-1α protein outside of its traditional nuclear role. There is a significant amount of evidence to suggest extensive cross-talk between the HIF pathway and mitochondria (Briston et al., 2011, Yang et al., 2012, Fukuda et al., 2007, Zhang et al., 2008, Rane et al., 2009). It is not only evident that mitochondrial respiration plays a role in regulating HIF activity, but HIF activation also controls mitochondrial metabolism and cellular metabolic adaptation to hypoxia (Ebert et al., 1995, Papandreou et al., 2006, Kim et al., 2006, Fukuda et al., 2007). This indirect response is mediated through HIF-dependent expression of target genes, such as *GLUT-1*, *PDK1*, *LON* and *COX4-2* (Ebert et al., 1995, Papandreou et al., 2006, Kim et al., 2006, Fukuda et al., 2007). The question of whether there is more immediate and/or role for the HIFs within minutes to hours of hypoxia or pharmacological activation is an area still yet to be fully explored, particularly in relation to mitochondria.

In addition to work from our own lab (Briston et al., 2011), to date only one other group has suggested the possibility that HIF-1α protein associates with mitochondria (Rane et al.,

2009). In this work, Rane *et al* demonstrated that in rat primary cardiomyocytes HIF-1α can be co-purified with mitochondria after a period of hypoxic preconditioning, however not after 24 hours hypoxia alone (Rane et al., 2009). Our observations extend these studies and indicate that after activation of this pathway, there is rapid accumulation of the stabilised HIF-1α protein observed in mitochondrial fractions. The kinetics for stabilisation of HIF-1α protein *in vivo* in response to hypoxic preconditioning may provide an explanation as to why Rane and colleagues did not observe mitochondrial HIF-1α at 24 hours hypoxia. It is perhaps that the direct molecular association of HIF-1α protein with mitochondria is transient, and forms part of the early immediate response to hypoxia, prior to the activation of gene transcription.

In a number of experiments and conditions we have observed HIF-1α to be present in mitochondrial fractions. It is clear that HIF is central in mediating transcriptional adaptive responses to hypoxia, however it is plausible that in line with other transcription factors and distinct from its nuclear role that HIF-1α may associate with mitochondria. This mitochondrial association may directly affect mitochondrial metabolism in a more acute setting (Rane et al., 2009).

HIF-1α is constitutively transcribed and regulated on the level of protein stability. In normoxia, despite a short protein half-life and low abundance, HIF-1α is transcriptionally active, as we found that HIF-1α knockdown in normal, ambient oxygen concentrations reduced the expression of validated HIF-1 target genes (data not shown). Western blot analysis has limited sensitivity and in the results obtained from cells in culture, HIF-1α protein can only be observed in mitochondrial fractions after inhibition of the PHD protein-mediated hydroxylation. There remains the possibility that HIF-1α is associated with mitochondria in normal, ambient oxygen concentrations and is below the limit of detection by western blotting. The isolation and purification of mitochondria from liver tissue allowed for analysis of the HIF-1α/mitochondrial association in a more physiological environment. The liver is a highly aerobic organ (Lemasters et al., 1992) and in spite of this, in the purified mitochondrial fractions HIF-1α protein can be readily detected, suggestive of enrichment in this fraction. Careful examination of the western blot from liver tissue (Figure 3.6), demonstrated distinct differences in the banding pattern of HIF-1α compared to that from hypoxia in HL-1 cells (compare lanes 1 and 2) and that found in the purified mitochondrial fraction (lane 4). The diffuse HIF-1α band in hypoxic HL-1 cells is likely a result of heavy

post-translational modification. The different banding patterns observed in enriched mitochondria isolated in these experiments from cells exposed to hypoxia versus tissue may arise from distinct alterations in these post-translational modifications between tissues and/or cellular compartments.

It must be noted and is important to consider, that there are clear limitations associated with fractionation protocols and methods for purifying mitochondria. Results from these experiments must be carefully interpreted; there resides the inherent probability of fraction contamination, a limitation which can be overcome to some degree through sucrose gradient separation, but remains present nonetheless. Therefore to confirm the subcellular fractionation data, further work and analysis would be necessary. Biochemical fractionation after ultracentrifugation and immunoblotting would be appropriate to confirm the organelle fractions in which the HIF-1α protein can be observed. Analysis of HIF-1α by immunogold labelling and electron microscopy would allow *in situ* analysis of cellular localisation. Additionally, protease protection assays of mitochondrial fractions, would allow determination of intra-mitochondrial localisation. This would entail proteinase K digestion of mitochondrial outer membrane tethered proteins and sodium carbonate extraction of matrix components to delineate HIF-1α protein mitochondrial topology. Immunoprecipitation of HIF-1α from purified mitochondrial fractions and mass spectrometry of the proteins would allow identification of the protein in addition to analysis of any post-translational modifications. This approach would allow determination of whether a specifically modified form of HIF-1α resides in or with mitochondria. These analyses would also allow determination of whether HIF-1α protein exists as a complex within mitochondria with its beta subunit or other mitochondrial protein(s). Finally, mitochondrial import assays could be utilised to assess uptake of radiolabelled *in vitro* translated HIF-1α protein into isolated intact mitochondria.

A second interesting observation is the identification of HIF-1β in mitochondrial fractions obtained from both cells and tissue. HIF-1β identification, raises the possibility of the alpha and beta isoforms complexing on the outer mitochondrial membrane or intra-mitochondrially and functioning in partnership. RNA interference experiments or using null cells to investigate loss of HIF-1β may reveal more information with respect to this localisation. Further examination would allow determination of whether the paralleled association HIF-1β with HIF-1α is firstly necessary for mitochondrial association of HIF-1α

and secondly whether this has any immediate consequence on mitochondrial function after hypoxic insult or pharmacological inhibition of the PHD proteins. Interestingly in HL-1 cells, after 2 hours DMOG treatment, mitochondrially-associated HIF-1β protein decreases. This mitochondrially-associated decrease in HIF-1β protein may reflect that HIF-1β localisation at this time point is most likely to be nuclear, where it will dimerise with HIF-1α and form the transcriptional complex. Previous studies have shown that HIF-1β is nuclear, due to the presence of a putative nuclear localisation sequence in the N-terminal domain (Holmes and Pollenz, 1997, Pollenz et al., 1994); however, as yet, there are no published reports describing mitochondrial association of HIF-1β protein.

Identification of a hydroxylated species of HIF-1α protein in mitochondrial fractions raises a number of intriguing questions and possibilities. Firstly, it is perhaps plausible that HIF-1α is functionally hydroxylated within or immediately surrounding the mitochondria. The mitochondria are the primary consumers of oxygen within the cell and as such under non-pathological conditions are well supplied with oxygen. It is therefore not surprising, if HIF-1α is present at the mitochondrial interface for it to be hydroxylated due to the abundance of available substrate for the PHD proteins. Secondly, if future work proves the localisation of HIF-1α protein to be intra-mitochondrial, it would be interesting to investigate whether the hydroxylation of HIF-1α is a pre-requisite for import or exclusion from the organelle.

The next challenge would be the functional assessment of HIF-1α protein-mitochondria association. For future work, HIF-1α protein could be fused with a mitochondrial targeting sequence (MTS). Albeit an over-expression system, though these experiments it would be possible to identify if and how HIF-1α affects mitochondrial function directly. An extremely interesting possibility is that in keeping with HIF-1α's role as a transcription factor, it may be regulating mitochondrial gene transcription under specific conditions. Assessing mitochondrial gene expression in combination with the over-expressed MTS-tagged protein would allow delineation of alterations in mitochondrial gene expression by RT-qPCR. Finally, using techniques such as electrophoretic mobility shift assay (EMSA) or chromatin immunoprecipitation (ChIP) assays, identification of the HIF-1α protein binding mitochondrial DNA could be established.

A second proposed model as to the function of the HIF-mitochondria association is one of direct protein binding. A model could be proposed whereby HIF-1α is binding directly to mitochondrial outer-membrane or intra-mitochondrial proteins and by some undefined

mechanism affecting or maintaining mitochondrial function. Work from our lab has described the human CHCHD4/MIA40 mitochondrial protein family, a novel regulator of HIF-1α (Yang et al., 2012). CHCHD4.1 is identical to human MIA40, which is an IMS protein and contains structurally and functionally essential conserved cysteine domains necessary to participate in IMS protein import. As discussed, we have shown that CHCHD4/MIA40 regulates cellular oxygen consumption rate and ATP synthesis and that CHCHD4/MIA40 is essential for regulating HIF-1α stabilisation in response to hypoxia (Yang et al., 2012). CHCHD4/MIA40 knockdown prevents HIF-1α induction and transcriptional activity, decreases oxygen consumption rate in normoxia, ATP biosynthesis and inhibits tumour growth and angiogenesis *in vivo* (Yang et al., 2012). Unpublished observations from our lab, show HIF-1α to be present in a complex with CHCHD4 and this is hypothesised to limit electron flow through the disulphide relay system, affecting flux through to cytochrome c and indirectly affecting oxygen consumption. Questions however still remain as to the relationship between HIF-1α and mitochondria. The endeavour to provide solutions to the proposed questions will uncover novel molecular and mechanistic insights into the role of HIF-α in regulation of metabolism and mitochondrial function. Despite the limitations of the techniques described in this work, collectively these observations pave the way to better understand the functional and physiological significance of the HIF-mitochondria association.

### 3.9.5 *HIF-independent roles and mitochondrial association of the PHD proteins*

EGFP-tagged PHD protein constructs have previously determined cellular topology of the exogenous PHD proteins (Metzen et al., 2003). Metzen *et al* demonstrated nuclear localisation of PHD1, PHD2 distributed throughout the cytosol and PHD3 was observed in both nuclear and cytosolic compartments (Metzen et al., 2003). Using the same constructs, our data confirm the data published by Metzen and colleagues (Metzen et al., 2003). The rat orthologue of PHD3, SM-20 has been observed in mitochondria, however unlike human PHD3, SM-20 encodes an additional mitochondrial targeting sequence (Lipscomb et al., 2001). PHD2 has been described to co-localise with the adapter protein FKBP38 in mitochondria and ER (Barth et al., 2009) and PHD2 and PHD3 have been observed to demonstrate mitochondrial localisation in rat hepatocytes (Khan et al., 2006). The protein aggregation observed after EGFP-PHD3 expression is consistent with that reported by Metzen *et al* where it was concluded to be a consequence of over-expression (Metzen et al., 2003). PHD protein aggregation however, has recently been observed with endogenous

PHD3 and mediated through SQSTM1/p62 (p62) which promotes cytosolic aggregation of proteins, an effect lost in hypoxia (Rantanen et al., 2013).

In addition to the studies on HIF-1α, we have also presented that both PHD2 and PHD3 are present in mitochondrial fractions under physiological conditions. Our data confirms published observations for PHD2 (Barth et al., 2009) but is novel for human PHD3. Further experiments are however necessary to characterise their exact sub-mitochondrial localisation, determine mitochondrial topology and eliminate outer-mitochondrial membrane association, using the same approach as discussed for HIF-1α. Our data on PHD subcellular localisation remain subject to the same limitations as outlined above, such that more detailed investigation would be necessary to confirm intra-mitochondrial localisation. Collectively, our observations are however most intriguing and raise questions regarding PHD-mediated HIF-1α modifications within mitochondria or potential HIF-independent roles of the PHD proteins.

The HIF-independent roles of the PHDs are still under investigation and to date a growing number of distinct substrates have been identified (Cummins et al., 2006, Mikhaylova et al., 2008, Kuznetsova et al., 2003, Koditz et al., 2007, Xie et al., 2009). To date, PHD3 has the most interacting partners outside of the HIFs. It has been observed to hydroxylate the $\beta_2$-adrenergic receptor to mediate pVHL-dependent ubiquitination and subsequent degradation (Xie et al., 2009). PHD3 has also been observed to be pro-apoptotic under certain circumstances (Lee et al., 2005) as well as binding to and regulating activity of activating transcription factor-4 (ATF-4) in a pVHL-independent manner (Koditz et al., 2007). PHD3 interacts with mitogen activated protein kinase organiser-1 (MORG-1) (Hopfer et al., 2006), human homologue of the *Caenorhabditis elegans* biological clock protein CLK-2 (HCLK2) (Xie et al., 2012) and p62 (Rantanen et al., 2013).

Additionally, the large subunit of RNA polymerase II (RPB1) has been demonstrated to be regulated by pVHL, after both PHD1 and PHD2 were co-immunoprecipitated with RPB1 in response to oxidative stress. Interplay has also been demonstrated between PHD1 and NF-κB signalling through PHD1-mediated inhibition of inhibitor of nuclear factor kappa-B kinase (IKKβ) and linking hypoxia to NF-κB signalling (Cummins et al., 2006). Table 4 summarises these investigations and additional HIF-independent roles of the PHD proteins.

| | Partner | Model | Function | Reference |
|---|---|---|---|---|
| **PHD1** | **RPB1** | **Human** | Hydroxylation of RPB1 is necessary for oxidative stress induced phosphorylation of RPB1 | **(Mikhaylova et al., 2008)** |
| | **IKKβ** | **Human** | Hydroxylation of IKKβ promotes activation of NF-κB signalling | **(Cummins et al., 2006)** |
| | **SPRY2** | **Human** | Hydroxylation necessary for pVHL mediated degradation | **(Anderson et al., 2011)** |
| | **ATF-4** | **Human** | Stabilisation of ATF-4, through hydroxylation independent binding and control of transactivation activity | **(Hiwatashi et al., 2011)** |
| **PHD2** | **RPB1** | **Human** | Loss of PHD2 stimulates hydroxylation necessary for oxidative stress induced phosphorylation of RPB1 | **(Mikhaylova et al., 2008)** |
| | **ING-4** | **Human** | Direct interaction involved in the regulation of HIF-1α activity in hypoxia | **(Colla et al., 2007)** |
| **PHD3** | **MORG-1** | **Human** | MORG-1 interacts with PHD3 proposed to act as molecular scaffold providing a framework between HIF regulation and potentially other signalling pathways | **(Hopfer et al., 2006)** |
| | **BCL-2** | **Rat** | Interacts with BCL-2, inhibits the formation of BCL-2-BAX complex and inhibits the anti-apoptotic effect of BCL-2 | **(Liu et al., 2010)** |
| | **$\beta_2$-AR** | **Human** | Hydroxylation necessary for pVHL recognition and proteasomal degradation | **(Xie et al., 2009)** |
| | **ATF-4** | **Human** | Binding to ATF-4, hydroxylation independent control of transactivation activity through ATF-4 destabilisation | **(Koditz et al., 2007)** |
| | **p62** | **Human** | p62 required for normoxic aggregation of PHD3 which is lost in hypoxia. Regulates expression, localisation and activity of PHD3 | **(Rantanen et al., 2013)** |
| | **PKM2** | **Human** | PKM2-PHD3 interaction enhances binding of PK-M2 to HIF-1α facilitating role as potential co-activator | **(Luo et al., 2011)** |
| | **PAX-2** | **Human** | Binds PAX-2 and hydroxylation activity necessary for PAX-2 degradation | **(Yan et al., 2011)** |
| | **PRP19** | **Human** | Complexes and inhibits PHD3 mediated apoptotic cell death under prolonged hypoxia | **(Sato et al., 2010)** |
| | **HCLK2** | **Human** | Hydroxylation necessary for HCLK2 interaction with ATR allowing activation of ATR/CHK1/p53 and apoptotic cell death in response to DNA damage | **(Xie et al., 2012)** |

**Table 4: HIF-independent regulatory roles of the PHD proteins.**

**Table detailing the model system in which the interaction was elucidated, the function of the relationship and the reference from which the information was derived. BCL-2 = B-cell lymphoma 2, PAX-2 = Paired box gene-2, SPRY2 = Sprouty-2.**

Interestingly, from a metabolic perspective, knockout of PHD1 has been shown to re-programme basal metabolism in skeletal muscle, reducing oxygen consumption through

controlling the switch from glucose oxidation to a more glycolytic phenotype in generating ATP (Aragones et al., 2008). Mice null for *Phd1* are better adapted to survive acute ischaemic/hypoxic insults as they consume less oxygen (Aragones et al., 2008). Consequentially *Phd1*-null mice generate less oxidative stress, preventing damage to mitochondria and continue to maintain OxPhos, albeit at a low residual level. This effect is mediated through PPARα, HIF-2α and increased expression of multiple isoforms of pyruvate dehydrogenase kinase (Aragones et al., 2009, Aragones et al., 2008).

Due to the relatively low affinity of the PHDs toward oxygen, many of the cellular responses to low oxygen occur at concentrations well above those that limit oxidative mitochondrial ATP production and prevent the cell from metabolic crisis. In this situation PHD activation could be seen as a more anticipatory response or early warning system (Sridharan et al., 2008). What is interesting about the PHDs is their presence in many other organisms including those which either do not have a HIF orthologue or in oxygen generating (photo-synthetic) organisms, which may suggest an important physiological role independent of HIF (Boulahbel et al., 2009). In addition to this and also interesting to note is their seeming unnecessary redundancy in terms of HIF regulatory activity, with PHD2 being the principle negative regulator and PHD1 and PHD3 only playing a small role (Boulahbel et al., 2009).

### 3.9.6 *Effects of DMOG treatment and PHD protein inhibition on mitochondrial function*

The final part of this chapter aimed to investigate the short-term or acute effects (within minutes to hours) of activation of the oxygen-sensing pathway and determine if any phenotype could be attributed to the mitochondrial localisation of HIF-1α. To begin to explore the functional effects of HIF-1α stabilisation and activation of the oxygen-sensing pathway on mitochondria, several mitochondrial parameters were assessed. Most notably, oxygen consumption immediately decreased upon addition of the PHD inhibitor DMOG. This effect increased over time and a large significant effect on the maximum respiratory rate was also recognised.

HCT116 cells are highly glycolytic, a phenotypic characteristic of tumour cells. This observation was validated with the ATP data presented here. HCT116 cells appear to generate most, if not all their ATP through glycolysis (Warburg effect; (Warburg, 1956)). Predominantly glycolytic ATP production was confirmed by the negligible decrease in total cell ATP levels after the addition of oligomycin and the significant decrease after the addition of the glycolysis inhibitor IAA. In response to DMOG treatment over a period 60

minutes, total cellular ATP appeared to be maintained. There was a small but significant increase in cytosolic and mitochondrial ATP over the first hour of DMOG treatment, notwithstanding the significant decrease in OCR. Together these data suggest that cells are able to maintain their ATP levels while utilising less oxygen.

DMOG treatment caused no change in mitochondrial membrane potential. We have also demonstrated that the reduction in OCR with DMOG treatment cannot be reversed with pre-treatment with a HIF-1α inhibitor (data not shown). The maintenance of ATP after DMOG treatment was also found to be HIF-1α-independent. DMOG produced a small but significant increase in mitochondrial and cytosolic ATP in the presence of *HIF-1α* silencing.

To date there are two papers from Gary Wright's group detailing the metabolic HIF-1α-dependent and -independent effects of over 20 hours PHD inhibition (Sridharan et al., 2007, Sridharan et al., 2008). Initially Sridharan *et al* observed that inhibition of the PHD pathway is cytoprotective. Treatment of cardiomyocytes with PHD inhibitors allows maintenance of mitochondrial membrane potential during metabolic inhibition (MI), induced after cardiomyocyte culture in glucose-free media containing potassium cyanide (KCN) with or without 2-deoxyglucose (2-DG). There was significantly less toxicity in the presence of the PHD inhibitors DMOG and ethyl 3,4-dihydroxybenzoate (EDHB). Post metabolic insult and 2 hours recovery, PHD inhibitor treatment afforded maintenance of ATP levels and increased 3-(4,5-dimethylthiazol-2-yl)-2,5-diphenyltetrazolium bromide (MTT) reducing capacity, compared to pre-MI values, suggestive of a mechanism other than an increase in anaerobic glycolysis. Mitochondrial membrane potential decrease after cardiomyocyte culture in MI medium reduces less after the activation of the PHD pathways and also increases to a greater degree after 2 hours recovery. Membrane potential maintenance was not affected by oligomycin, eliminating the reverse mode of the $F_1F_O$-ATPase and ATP hydrolysis for mechanism of maintenance. The major observation is that in the absence of PHD inhibition, KCN is sufficient to depolarise the membrane, however the addition of rotenone is necessary in the PHD treated cells, suggesting that complex I is still active during and after MI. OCR was also reduced to 15% of controls and extracellular acidification rate (ECAR) increased after 22 hours DMOG treatment (Sridharan et al., 2007).

In their second paper (Sridharan et al., 2008), Sridharan *et al* observed that treatment with DMOG causes a decrease in cardiomyocyte ATP turnover by reducing contractility and a reduced oxygen consumption rate. After the addition of the uncoupler, dinitrophenol

(DNP) to cardiomyocytes treated with DMOG, Sridharen *et al* observed a significant decrease in maximum respiratory rate, an effect which interestingly was reversed when HIF-1α was knocked down (Sridharan et al., 2008). This suggests that the reduction in basal OCR was not just a consequence of the reduced ATP turnover, but is actively "clamped" under conditions of PHD inhibition. Intriguingly, the initial reduction in basal ATP turnover and reduced basal OCR in PHD inhibitor treated cells is HIF-1α-independent. HIF-1α-independence suggests differential and distinct roles for the PHDs in controlling the direct suppression of OxPhos and the down-regulation of ATP turnover (by a reduction in contractile activity of cardiomyocytes) through HIF-1α-independent and -dependent roles respectively (Sridharan et al., 2008). To summarise, PHD inhibitor-mediated;

- ↓ basal OCR and ↓ ATP turnover → HIF-1α-independent
- ↓ max respiratory rate → HIF-1α-dependent

Therefore, flux through the ETC in the presence of PHD inhibition is independent of the stabilisation and activity of HIF-1α. The PHD-mediated decrease in OCR and ATP maintenance correlates with what was observed in our system, whereby the acute treatment with DMOG resulted in an immediate and significant decrease in OCR, which continued to fall over a 30 minute period. This may suggest we are observing the immediate effects that ultimately mediated the final 85% reduction in the basal OCR observed by Sridharan *et al* (Sridharan et al., 2007, Sridharan et al., 2008). Sridharen *et al* propose a mechanism, through inhibition of the PHD proteins increasing flux through the purine nucleotide cycle, which re-generates adenosine monophosphate (AMP) from inosine monophosphate (IMP), consumes aspartate and produces fumarate and ammonium as by products (Sridharan et al., 2008). Fumarate then is reduced at complex II to succinate. This PHD-mediated adaptation would allow cells under periods of metabolic inhibition to utilise fumarate as the terminal electron acceptor when complex IV is inhibited. This also makes sense of their observation in that in PHD inhibitor-treated cells, rotenone is also required in addition to KCN to depolarise the mitochondrial membrane, as complex I retains activity and complex II provides an outlet for electrons. These findings correlate with our data. Here, we observe a reduction in aspartate levels in galactose culture conditions and reduced fumarate in both glucose and galactose conditions, possibly suggesting the involvement of complex II and fumarate being used as a terminal electron acceptor. We would have to measure succinate levels to be confident of this. However, under high

glucose conditions the increase in aspartate does not correlate with that observed by Sridharen *et al* and what we observe in galactose. These are however two separate systems, one being a highly oxidative cardiomyocyte and other a highly glycolytic tumour derived cell line and perhaps the comparison of HCT116 culture in galactose is more reflective of the oxidative cardiomyocyte.

The maintenance in ATP, despite the DMOG-induced decrease in OCR, may be dependent on decreased ATP utilisation, in contrast to increased ATP biosynthesis. ATP turnover was demonstrate to be reduced in cardiomyocytes by reducing contraction in a HIF-1α-independent fashion (Sridharan et al., 2008). There is no parallel process in the HCT116 colon cancer cell line, so an alternative explanation is necessary. The major cellular consuming processes of ATP are translation (protein synthesis) and the $Na^+/K^+$-ATPase. There are no reports suggesting that inhibition of the PHD proteins for 2 hours affects translation, however in one study DMOG was observed to inhibit the $Na^+/K^+$-ATPase after 24 hours treatment, without altering expression or membrane localisation (Ward et al., 2011) – this effect could account for the maintenance of ATP in the HCT116 cells.

Although there are strong correlations with the data presented here and that presented by Sridharan *et al* (Sridharan et al., 2008), one could also hypothesise that the PHD proteins are not responsible for the DMOG induced changes in metabolism. Treatment of cells with second PHD inhibitor (PHD-I), failed to reproduce those effects observed by DMOG with respect to OCR and ATP. Other dioxygenases which are potentially inhibited by DMOG include FIH, JmjC domain containing protein 2A (JMJD2A), PHD finger protein 8 (PHF8) and γ-butyrobetaine hydroxylase (BBOX1) (Rose et al., 2011). BBOX1 is involved in carnitine biosynthesis and is localised to mitochondria. Inhibition of BBOX1 would result in decreased fatty acid metabolism (Rose et al., 2011). Possibly reducing OCR, however the extent to which these cells rely on fatty acid metabolism is unknown. Performing the total cellular ATP assay in the presence of additional fatty acid metabolism inhibitor would allow clarification of this. Additionally, simultaneous knockdown of each of the PHD proteins would be necessary to elucidate their precise role and determine the exact mechanism.

Chemically, DMOG is an α-ketoglutarate analogue, which raises the possibility that interference with the TCA cycle directly may be responsible for the decrease in oxygen consumption rate observed in response to DMOG. To test this, we employed a second, none chemically related PHD inhibitor, PHD-I. Unfortunately the same phenotype was not

observed with this inhibitor. PHD-I did not reduced OCR, had no effect on ATP or affect mitochondrial membrane potential. This may suggest that DMOG is having off-target effects and influencing metabolism independent of the PHD proteins or HIF-1α. Metabolomic analysis suggests large significant decreases in cellular fumarate after 2 hours DMOG treatment. Decreased fumarate may be indicative of a block in the TCA cycle, preventing the re-synthesis of fumarate through competitive inhibition of α-ketoglutarate dehydrogenase. However fumarate depletion, does not affect the maintenance of ATP and possibly co-incidental or compensatory mechanisms are in play. However, based on the observations outlined above (Sridharan et al., 2007, Sridharan et al., 2008), the potential still exists that fumarate is being reduced at complex II and oxygen is not being consumed at complex IV, causing a decrease in OCR. Fumarate respiration is only likely to be used when respiration clamped and glycolysis is insufficient to maintain ATP levels, for example when DMOG treated HCT116 cells were cultured in galactose. However, in our system we also see a decrease in fumarate levels in glucose conditions, perhaps suggesting an alternative cause.

A number of questions remain;

(i) Why does DMOG reduce OCR in our system?

(ii) Where is the ATP coming from to allow maintenance of levels despite decreased OCR?

(iii) PHD inhibition ensures ATP is maintained by reducing turnover by inhibiting cardiomyocyte contraction. What is the parallel process in non-cardiomyocytes?

(iv) Why does PHD-I not produce the same phenotype as DMOG?

Interestingly, significant differences were also observed in aspartate levels after DMOG treatment. HCT116 cells cultured in glucose-DMEM exhibited an increase in cellular aspartate and conversely, cells cultured in galactose demonstrated a significant decrease. Aspartate can be metabolised to oxaloacetate, raising the possibility that to overcome the block in the TCA cycle, cells are increasing their consumption of this amino acid as a compensatory mechanism. Valine, threonine, iso-leucine and phenylalanine all increase in response to DMOG treatment in those cells cultured in galactose. A hypothesis may be that as a consequence of a non-functional TCA cycle, metabolites that would otherwise feed the pathway are not necessary, present in excess and excreted. Without profiling of the

complete set of metabolites and understanding of the unique properties and metabolism, the data is hard to interpret. Additionally, the metabolomic profile of PHD-I would be useful to interpret these findings with DMOG to allow validation and separation of those metabolites which are changing as a result of PHD protein inhibition and those which change with DMOG alone, to delineate the PHD protein-independent effects of the compound.

Future work would involve metabolomic analysis of the second PHD inhibitor to confirm which of the metabolite changes are common between inhibitors and to investigate the underlying mechanisms behind those pathways and metabolite changes. To confirm the predicted effect of DMOG on the TCA cycle, the transfer of reducing equivalents to the ETC could be measured. The intrinsic auto-fluorescent properties of the TCA cycle product, NADH can be exploited for this purpose. This may demonstrate that in the presence of DMOG, output from the TCA cycle appears to change, characterised by a decrease in fluorescence. This would however also be the situation if DMOG and PHD inhibition was directing fumarate to be used as a substrate for complex II.

Is important to note that DMOG is the prototypical PHD inhibitor and routinely the 'go to' compound to activate the oxygen-sensing pathway. It has been used to probe the effect of HIF-1α on cellular function and therefore data gained using this inhibitor must be carefully evaluated in light of its HIF-independent effect on metabolism.

## 3.10 Summary

How mitochondria interface with the HIF oxygen-sensing machinery is of great interest. The possibility that HIF or other components of the oxygen-sensing pathway perform yet unidentified novel mitochondrial functions that may result in cell survival/homeostasis will be key to investigate and a number of important questions remain:

(i) Is HIF-1α present within mitochondria; does it associate with any mitochondrial proteins what is its function?

(ii) Would the presence of HIF-1α and HIF-1β in mitochondria affect mitochondrial gene expression?

(iii) Do the PHD proteins have HIF-α-independent mitochondrial functions?

(iv) Should DMOG continue to be used as a tool to study the HIF/hypoxic response given the absence of a common metabolic phenotype with a second inhibitor of the PHD proteins?

The observation that a number of key regulators of the hypoxic response associate with mitochondria, hopefully will ignite work and open people's eyes toward investigating an alternative paradigm as to the role of HIF in hypoxia. Key details are still unknown; however exploration of a more direct relationship between the oxygen-sensing pathway and mitochondria, functioning either in the acute phase or in parallel to the traditional hypoxic response, would allow us to build on our initial findings.

# Chapter 4: The role of pVHL in the maintenance of mitochondrial homeostasis

## 4.1 Introduction

Normoxic regulation of the HIF-α subunits (HIF-1α and HIF-2α) is under the control of the von Hippel-Lindau (pVHL) tumour suppressor, the protein product of the *VHL* gene (Maxwell et al., 1999). Inactivating germline mutations of the *VHL* gene are responsible for the development of visceral cysts, particularly in the kidney giving rise to VHL disease (Shen and Kaelin Jr, 2013). Tumours arise in VHL patients after somatic inactivation of the second wild type *VHL* allele in the susceptible cell. The aetiology of many sporadic clear cell renal carcinomas is also due to biallelic inactivation of the *VHL* tumour suppressor gene and has been estimated to be present in a large percentage of patients with disease (Lai et al., 2011, Kaelin, 2008, Shen and Kaelin Jr, 2013).

*VHL* is transcribed as two isoforms, derived from two in-frame initiation codons within the *VHL* gene, $VHL_{19}$ and $VHL_{30}$. $VHL_{19}$ lacks the N-terminal acidic domain present in $VHL_{30}$, however still serves as the recognition component of the E3-ligase machinery (Lai et al., 2011). pVHL forms the substrate recognition and catalytic component of an E3-ligase complex, along with elongins B and C, RBX1 and cullin 2 functions to poly-ubiquitinate the HIF-α subunits targeting them for destruction by the 26S proteasome (Stebbins et al., 1999, Iwai et al., 1999, Maxwell et al., 1999). Studies of the *VHL* gene and the gene product have gone a long way to help understand the signalling pathways that allow cells to sense and respond to changes in oxygen tension (Kaelin, 2002).

There has been much interest in uncovering protein targets of pVHL other than HIF-α and to date, this search has uncovered a number of candidates (Pal et al., 1997, Lai et al., 2011, Mukhopadhyay et al., 1997). Analysis of gene expression has identified a number of putative pVHL targets and an overlapping but also distinct number of genes regulated by pVHL and/or hypoxia (or HIF) (Kaelin, 2002, Harten et al., 2009, Jiang et al., 2003). pVHL has been observed to interact and suppress the SP1 transcription factor (Mukhopadhyay et al., 1997) and bind to isoforms of atypical protein kinase C (Pal et al., 1997), fibronectin and the ARF tumour suppressor (Lai et al., 2011). It has also been observed to have HIF-independent roles in the maintenance of primary cilia, control of extracellular matrix formation and regulation of apoptosis (Kaelin, 2008).

pVHL has previously been described to affect mitochondrial function. pVHL-dependent mitochondrial effects have been demonstrated using renal carcinoma cell lines devoid of functional pVHL and direct comparison with stable functional wild type pVHL re-expression

(Hervouet et al., 2005, Hervouet et al., 2008). Hervouet *et al* observed that re-expression of pVHL increases protein expression of a number of ETC subunits, increases oxygen consumption and ETC enzyme activity. Re-expression of pVHL also increases mitochondrial DNA copy number, proposed to be via a TFAM-mediated mechanism (Hervouet et al., 2005). A follow up study demonstrated the effects of pVHL loss could be rescued through simultaneous knockdown of HIF-2α in pVHL-deficient cells (Hervouet et al., 2008).

pVHL has been demonstrated to localise to mitochondria when over-expressed (Shiao et al., 2000). Shiao *et al* observed enlarged mitochondria in the presence of wild type over-expressed pVHL, detected using immunogold labelling and electron microscopy (Shiao et al., 2000). However, the immunogold signal was exclusive to the mitochondria, making the observations speculative, as pVHL has been shown to be mainly cytosolic, but capable of trafficking to the nucleus *in vitro* at low cell density (Lee et al., 1996).

In order to explore the role of pVHL in the regulation of mitochondrial homeostasis, renal adenocarcinoma derived cell lines, devoid of functional pVHL have been widely used (Hervouet et al., 2005, Hervouet et al., 2008). The 786O clear cell renal cell carcinoma (CCRCC) cell line has a single *VHL* allele with a single nucleotide deletion, resulting in a frameshift mutation (Gnarra et al., 1994). Transfection of pVHL into these cells was originally demonstrated to suppress tumour formation in nude mice (Iliopoulos et al., 1995), the first observation as to the role of pVHL in tumourigenesis. Patient derived 786O cells have constitutively stabilised HIF-2α and do not express HIF-1α (Maxwell et al., 1999), allowing elimination of confounding effects of both HIF-1α and HIF-2α stabilisation on interpretation of the data. pVHL re-expressing 786O cells have been vital in understanding the role of pVHL in oxygen-sensing and in the delineation of HIF-dependent function. In this work, these cells were used as a model to investigate how re-expression of functional pVHL (786O-VHL); with parallel control of empty pCMV vector (786O-EV), in a pVHL defective background affects the mitochondrial phenotype.

Figure 4.1 demonstrates that in the 786O cells, HIF-2α protein levels are reduced to basal levels upon stable re-expression of functional pVHL. The 786O cell model allows mitochondrial function of pVHL to be assessed in the absence of the well described mitochondrial and metabolic actions of HIF-1α (Zhang et al., 2008, Fukuda et al., 2007, Papandreou et al., 2006). The 786O cells therefore provide a model by which the role of pVHL protein expression can be easily delineated, providing rationale for their use.

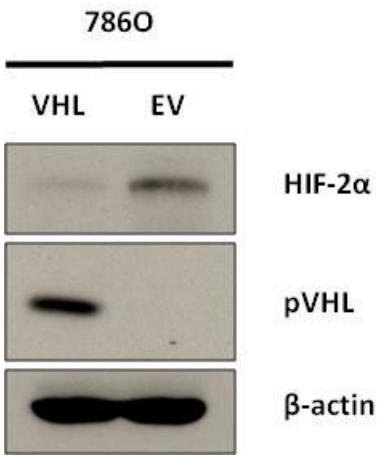


**Figure 4.1: Re-expression of functional pVHL protein in 786O renal carcinoma cells reduces HIF-2α protein to basal levels.**

**Western blot analysis shows 786O (786O-VHL (VHL, stably re-expressing pVHL) and 786O-EV (EV, vector control)) cells and demonstrates the presence of stably transfected pVHL and the effect on the constitutive stabilisation of HIF-2α observed in the 786O-EV cells. β-actin was used as a load control.**

## 4.2 Hypothesis

pVHL status regulates mitochondrial function.

## 4.3 Aims

1. To use matched pVHL positive and negative 786O cell lines to assess the effects of pVHL on mitochondrial function.

2. To evaluate the effects of pVHL mutation on mitochondrial function.

## 4.4 The effect of pVHL status on the expression of nuclear and mitochondrially encoded electron transport chain proteins

With respect to the relationship between pVHL and mitochondria, the most striking observation to date is the selective loss of mitochondrial ETC proteins in cells devoid of functional pVHL (Hervouet et al., 2005). Hervouet *et al* have observed that re-expression of pVHL in a pVHL defective background increases the protein expression of select ETC subunits (Hervouet et al., 2005).

To confirm the role of pVHL status in regulating mitochondrial ETC protein expression, protein levels of key ETC subunits were assessed using SDS-PAGE and western blot analysis on protein samples harvested from 786O cells. Analysis demonstrated clear differences in protein expression of both mitochondrial and nuclear encoded subunits of complex IV (mtCO-2 and COX-IV) after pVHL re-expression in the 786O-VHL cells compared to the 786O-EV cells (Figure 4.2). The protein expression of VDAC1, heat shock protein-60 (HSP60) and ATPB were similar in both 786O cell lines (Figure 4.2).

Observations from figure 4.2 extend published literature (Hervouet et al., 2005, Craven et al., 2006, Sarto et al., 1997), which previously demonstrated decreases in the complex I protein, NADH-ubiquinone oxidoreductase, complex III proteins (core II, iron sulphur protein (ISP), ubiquinol-cytochrome c reductase complex core protein 2 and 13kDa protein) and ATP6, a mitochondrially encoded subunit of the $F_O$ channel of the $F_1F_O$-ATPase in cells devoid of pVHL when compared to cells with pVHL stable re-expression. Notably, protein changes in the alpha subunit of the $F_1$-ATPase and adenine nucleotide translocase-1 (ANT1) were not observed (Figure 4.2)(Hervouet et al., 2005, Craven et al., 2006, Sarto et al., 1997). Interestingly, pVHL stable re-expression appeared to increase the expression of ETC proteins of both nuclear and mitochondrial genetic origin, while the expression of a number distinct non-electron transporting mitochondrial proteins were unaffected by VHL status (Figure 4.2).

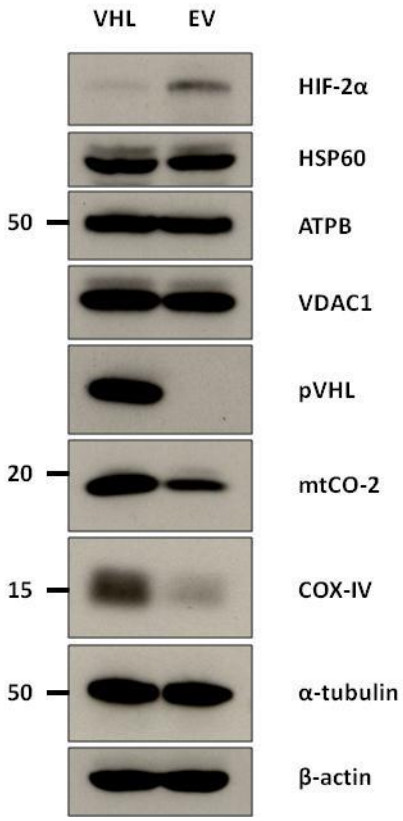


**Figure 4.2: Expression of mitochondrial proteins is differentially affected by pVHL status. Western blot analysis of 786O-EV (EV, vector control) cells and 786O-VHL (VHL, stably re-expressing pVHL) cells demonstrating changes in the expression of multiple complex IV ETC proteins (mtCO-2 and COX-IV) and absence of changes in distinct non-electron transporting mitochondrial proteins (VDAC, ATPB and HSP60). α-tubulin and β-actin were used as load controls.**

## 4.5 The effect of pVHL status on cellular bioenergetics and energy homeostasis

Mitochondrial respiration is highly regulated and controls a large number of cellular processes, such as ion regulation and membrane potential and hence is a key controller of cellular homeostasis (for review see (Pesta and Gnaiger, 2012). A previous study into the bioenergetic role of pVHL was unable to show statistical significance when investigating the effect of pVHL re-expression on cellular oxygen consumption rate (OCR) in a pVHL defective background, however there was a trend toward an increase in OCR after wild type pVHL re-expression in matched cells (Hervouet et al., 2005). To determine the functional effects of the pVHL-dependent ETC protein expression (Figure 4.2) and to further characterise any

mitochondrial phenotype associated with stable re-expression of pVHL in 786O cells, OCR was measured.

To assess mitochondrial respiration the Oroboros O2K was used. This equipment facilitates closed chamber, high resolution respirometry and was used previously to characterise the effects of PHD inhibition on mitochondrial respiration (see chapter 3; Figure 3.19). Respirometry allows the measurement of oxygen dissolved in the respiration medium by polarographic oxygen sensors and calculation the oxygen consumed as a function of time, producing a rate. The O2K design allows for sequential titrations of compound to determine their effects on respiration and better understand ETC function (Pesta and Gnaiger, 2012). Careful titration of compound allows the dissection of metabolic fluxes with respect to *in situ* mitochondria and whole cellular physiology.

To assess the role of pVHL status on cell respiration, 786O cells were trypsinised, washed, counted twice and re-suspended in HEPES-buffered DMEM. Using intact cells, multiple aspects on mitochondrial respiration were investigated. Routine respiration is supported by the metabolites in the cell culture media (glucose-DMEM). In 786O cells stably re-expressing pVHL (786O-VHL) basal oxygen consumption rate was significantly higher compared to 786O-EV control cells (Figure 4.3A). The addition of oligomycin and inhibition of the $F_1F_O$-ATPase allows calculation of the leak respiration. Significant increases in leak respiration (non-phosphorylating respiration, mainly controlled by and compensating for the proton leak across the inner membrane) were observed in the 786O-VHL cells compared to the 786O-EV cells (Figure 4.3B). Increased leak respiration reflects that in cells with stable pVHL re-expression, a greater volume of total oxygen consumed is not coupled to ADP phosphorylation at the $F_1F_O$-ATPase. Increased leak respiration in the presence of pVHL is perhaps to be expected as routine respiration also increases (Figure 4.3A-B). Maximum respiratory capacity (after titration of FCCP) is also observed to increase in the presence of function pVHL protein (Figure 4.3C). Non-mitochondrial respiration was determined through the combined administration of rotenone and antimycin A to inhibit complexes I and III respectively (Figure 4.3).

From the described parameters the respiratory flux ratios were calculated. Flux ratios are ratios of oxygen flux under different respiratory states, normalised for a maximum flux in a common reference state (normally maximum respiratory capacity). Ratios are therefore independent of mitochondrial content and cell size, with each experiment serving as its

own internal control (Pesta and Gnaiger, 2012). Routine control ratio (R/E) is defined as the ratio of routine respiration to maximum respiratory capacity in the non-coupled state. The routine control ratio is a measure of how close routine respiration operates to maximum respiratory capacity under the specific condition of the assay (Pesta and Gnaiger, 2012). There is no significant different between 786O-EV and 786O-VHL cells, suggesting they are both respiring at approximately 30-35% of maximum capacity (Figure 4.3D) and indicates no limitation in substrate oxidation in 786O-EV cells compared to 786O-VHL cells.

The leak control ratio (L/E) is defined as the ratio of leak respiration to maximum respiratory capacity. It is an index of uncoupling at constant ETC capacity. L/E increases with uncoupling from a theoretical minimum of 0.0 for a fully coupled system, to 1.0 for a fully uncoupled system (Pesta and Gnaiger, 2012). In the 786O-VHL cells, the ETC functions as a more coupled system compared to the 786O-EV cells (Figure 4.3D).

Net-routine control ratio (R-L)/E calculates the proportion of routine respiration that is being used to drive ATP synthesis corrected for maximum flux. The net-routine control ratio remains constant, if uncoupling is fully compensated by an increase of routine respiration and a constant rate of oxidative phosphorylation (OxPhos) is maintained (Pesta and Gnaiger, 2012). Net-routine control ratio is less in cells devoid of functional pVHL (786O-EV), compared to 786O cells stably re-expressing pVHL (786O-VHL), hence a smaller proportion of the maximum capacity was being used to drive ATP synthesis, possibly because of increased leak/uncoupling or less ATP demand (Figure 4.3D). A representative trace for the 786O cells, from the Oroboros O2K is shown in figure 4.3E.

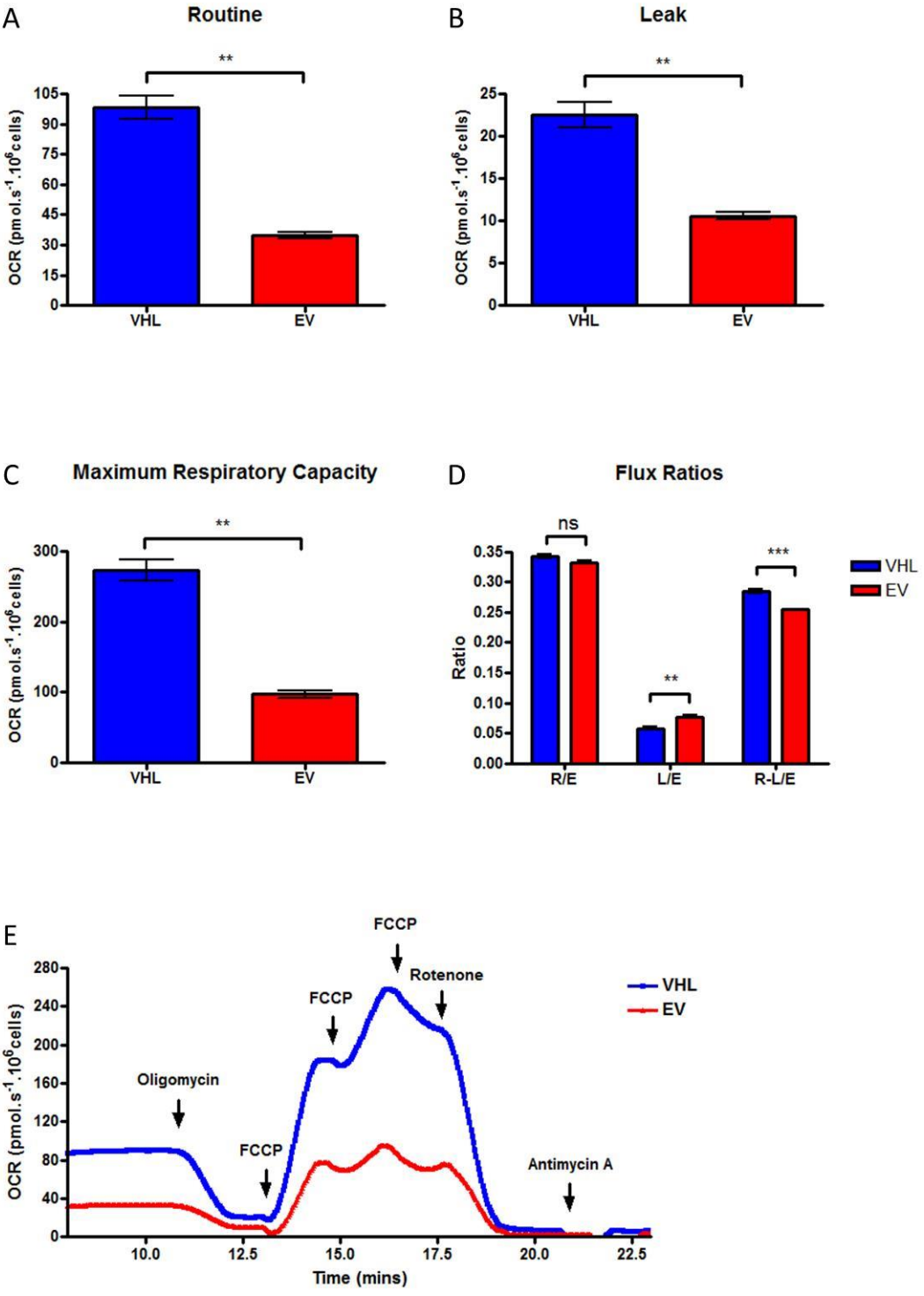
A
Routine
**
OCR (pmol.s-1.10^6cells)
105
90
75
60
45
30
15
0
VHL
EV
B
Leak
**
OCR (pmol.s-1.10^6cells)
25
20
15
10
5
0
VHL
EV
C
Maximum Respiratory Capacity
**
OCR (pmol.s-1.10^6cells)
300
200
100
0
VHL
EV
D
Flux Ratios
ns
***
**
Ratio
0.35
0.30
0.25
0.20
0.15
0.10
0.05
0.00
R/E
L/E
R-L/E
VHL
EV
E
FCCP
Rotenone
FCCP
Oligomycin
FCCP
Antimycin A
VHL
EV
OCR (pmol.s-1.10^6cells)
280
240
200
160
120
80
40
0
10.0
12.5
15.0
17.5
20.0
22.5
Time (mins)

**Figure 4.3: pVHL status affects routine OCR and associated bioenergetic parameters.**

**786O (786O-EV (EV, red) and 786O-VHL (VHL, blue)) cells were analysed using the Oroboros O2K, and OCR (pmol.s$^{-1}$.10$^{6}$ cells) corrected for cell number and non-mitochondrial respiration. (A) Graph shows stable re-expression of pVHL significantly increases basal OCR (** p<0.01). (B-C) Graph shows leak respiration and maximum respiratory capacity are significantly increased in the presence of pVHL (** p<0.01). (D) Graph shows bioenergetic ratios affected by pVHL status (*** p<0.01, ** p<0.01 and ns p>0.05). Values are mean +/- S.E.M (n=4). Data analysed using paired, two-tailed t-test. (E) Graph shows a representative trace of OCR using the Oroboros O2K comparing 786O-EV (EV, red) and 786O-VHL (VHL, blue) cells. R/E = routine control ratio, L/E = leak control ratio and R-L/E = net-routine control ratio.**

In search of a potential explanation for the difference in the degree of ETC coupling in the presence and absence of functional pVHL, the expression levels of the uncoupling proteins (UCPs) were examined. UCP1 is specifically expressed in adipocytes of brown adipose tissue (Brand and Esteves, 2005), therefore mRNA expression of *UCP2* and *UCP3* was analysed using real time-quantitative polymerase chain reaction (RT-qPCR). A small but significant increase in *UCP3* mRNA expression was observed in 786O-EV cells compared to 786O-VHL cells, which may contribute to the changes in the degree of uncoupling observed (Figure 4.4).

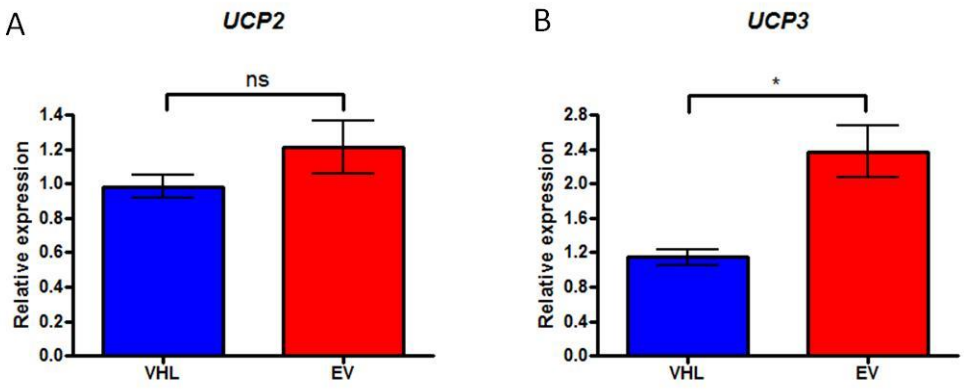


**Figure 4.4: pVHL status affects the mRNA expression of *UCP3* in 786O cells.**

**Graphs show transcript analysis of (A) *UCP2* and (B) *UCP3* using RT-qPCR in 786O-EV (EV, red) and 786O-VHL (VHL, blue) cells. *UCP3* expression is up-regulated in 786O-EV cells compared to 786O-VHL cells (* p<0.05 and ns p>0.05). Data was analysed using the comparative Ct method after normalisation to a single experimental repeat. Values are mean +/- S.E.M (n=4) and data analysed using paired, two-tailed t-test.**

The degree to which cells rely on glycolysis for ATP production relative to their need for mitochondrially-generated ATP influences the extent to which cells respire and consume oxygen. Therefore the experiments described above (Figure 4.3) were performed in cells that had been cultured in glucose-free galactose media for 24 hours, as described previously (chapter 3). As anticipated, under galactose conditions, routine respiration increased due to the increased reliance on OxPhos (Figure 4.3A and Figure 4.5A; compare axis).

After culture in galactose, significant increases were also observed in leak respiration and maximal respiratory capacity in 786O cells (Figure 4.5A-C). The trend between 786O cell lines was the same for flux ratios obtained in both glucose and galactose culture conditions (Figure 4.3D and 4.5D), however in galactose conditions a significant difference between 786O-EV and 786O-VHL cells for leak and net-routine controls ratios was not observed (Figure 4.5D). pVHL status did not affect the routine control ratio in galactose, suggesting that both cell lines are respiring at the same fraction of their maximum capacity, correlating with the observation in glucose. Forcing these cells to become more oxidative does however decrease the difference between routine respiration and maximal respiratory capacity, from approximately 30-35% of maximum capacity in the glycolytic environment (glucose conditions) compared to 40-45% in the galactose-induced oxidative conditions (R/E; Figure 4.5D). This is predictable as cells are relying more heavily on their mitochondria for ATP production. A representative trace is shown in figure 4.5E.

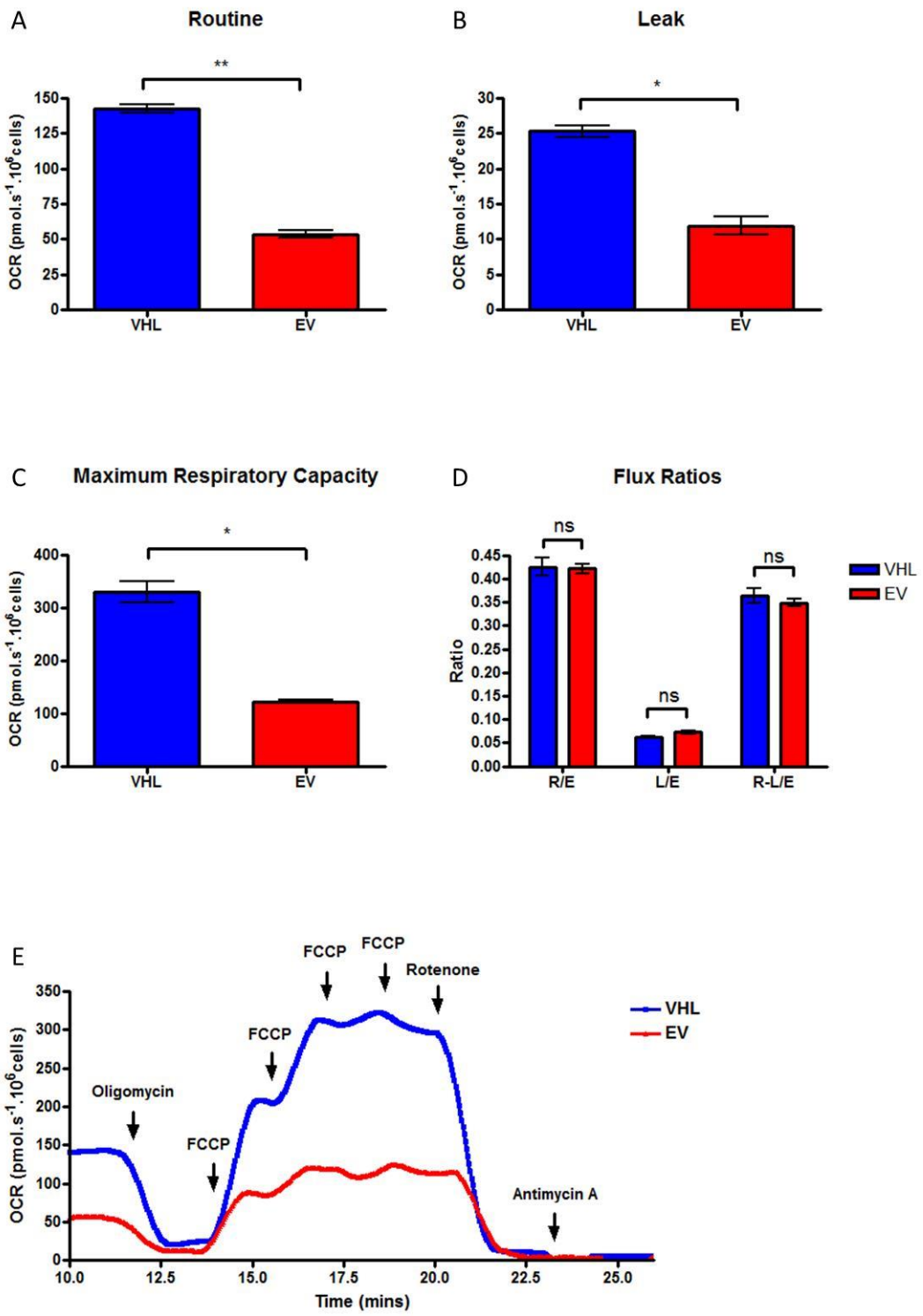
A
Routine
**
OCR (pmol.s-1.10^6cells)
VHL
EV
B
Leak
*
C
Maximum Respiratory Capacity
D
Flux Ratios
ns
Ratio
R/E
L/E
R-L/E
E
FCCP
Rotenone
Oligomycin
Antimycin A
Time (mins)

**Figure 4.5: pVHL status affects routine OCR and associated bioenergetic parameters after culture in galactose for 24 hours.**

**786O (786O-EV (EV, red) and 786O-VHL (VHL, blue)) cells were analysed using the Oroboros O2K, and OCR (pmol.$s^{-1}$.$10^6$ cells) corrected for cell number and non-mitochondrial respiration. (A) Graph shows stable re-expression of pVHL significantly increases basal OCR (** p<0.01). (B-C) Graph shows leak respiration and maximum respiratory capacity are significantly increased in the presence of pVHL (* p<0.05). (D) Graph shows effect of pVHL status on bioenergetic ratios (ns p>0.05). Values are mean +/- S.E.M (n=4). Data analysed using paired, two-tailed t-test. (E) Graph shows a representative trace of OCR using the Oroboros O2K comparing 786O-EV (EV, red) and 786O-VHL (VHL, blue) cells having been cultured in galactose for 24 hours. R/E = routine control ratio, L/E = leak control ratio and R-L/E = net-routine control ratio.**

To assess the consequences of pVHL status on total cellular ATP and to correlate the significant differences in OCR to a functional end point, cellular ATP was measured using a luminescent assay described previously (chapter 3). Cells were counted and suspended to equal concentration across lines. Assay reagent was then added and the luminescence measured. In the presence of functional pVHL protein there was a significant increase in luminescence, suggesting higher cellular ATP concentration of per cell compared to those cells devoid of functional pVHL (Figure 4.6A). This is potentially a consequence of the increase in OCR and increased expression of a number of key mitochondrial ETC complex proteins.

Having observed an increase in cellular ATP levels in 786O-VHL cells compared to 786O-EV cell, the mechanism through which pVHL status affects the pathways of cellular ATP maintenance was investigated. Utilising the same luminescent assay as above, inhibitors of glycolysis (IAA) and OxPhos (oligomycin) were added for 30 minutes and the change in luminescence interpreted. As described previously (chapter 3), IAA was used to inhibit glycolytic and oligomycin to inhibit mitochondrial ATP synthesis. Interestingly the cells without functional pVHL (786O-EV) were more sensitive to oligomycin and significant differences were observed in luminescence after 30 minutes treatment (Figure 4.6B). Unlike HIF-1α, HIF-2α does not up-regulate glycolytic target genes, such as *PDK* and *LDH* (Hu et al., 2003). These observations reflect that, despite stabilisation and activation of HIF-2α after loss of pVHL, the 786O-EV cells are more reliant on mitochondrially generated ATP. An oxidative phenotype associated 786O cells over-expressing HIF-2α has previously been observed (Biwas et al, 2010), where 786O cells over-expressing HIF-2α were grown as

xenographs and displayed a metabolic profile associated with lower glycolytic and greater mitochondrial metabolism (Biswas et al., 2010).

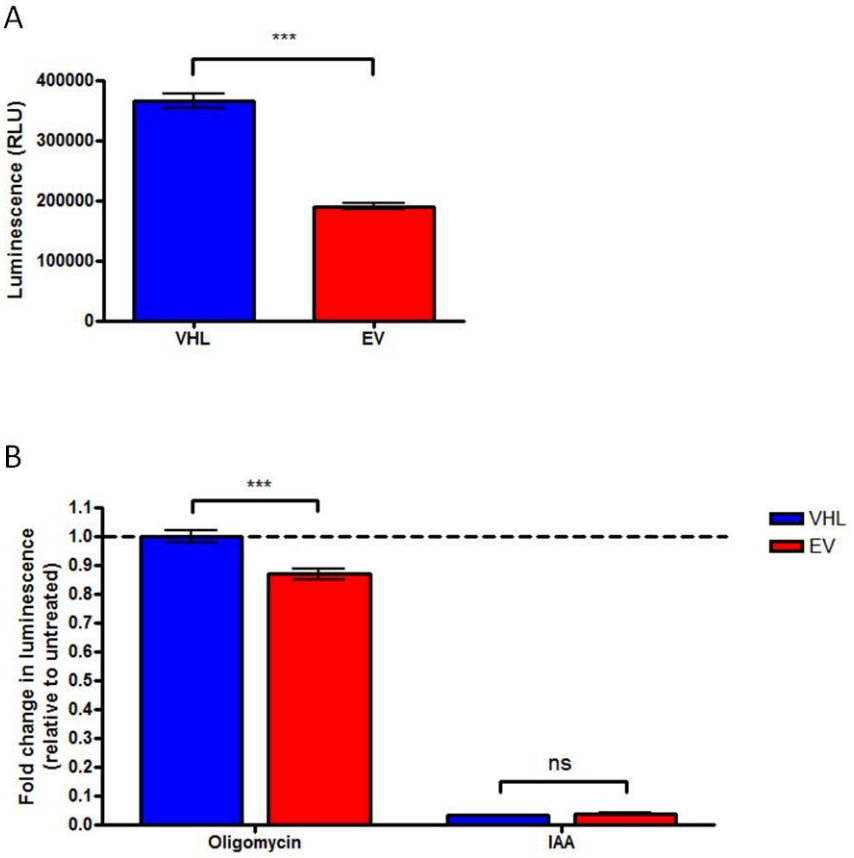


**Figure 4.6: pVHL status affects total cellular ATP levels and the pathways of ATP synthesis.**

**(A) Graph shows total cell ATP content in significantly increases in 786O-VHL (VHL, blue) compared to 786O-EV (EV, red) (*** p<0.001). 500,000 cells/ml were counted for each cell line before lysis is assay reagent. Luminescence was measured after 10 minutes stabilisation period. Data presented is raw luminescence values of the mean of 3 well replicates over 3 independent experiments (n=3) +/- S.E.M and analysed using a paired, two-tailed t-test. (B) Graph shows pVHL status affects the contribution of the ATP synthetic pathways to total cell ATP. Total cell ATP assay was performed in 786O (786O-VHL (VHL, blue) and 786O-EV (EV, red)) cells in the presence and absence of inhibitors of glycolysis (IAA; 1mM) and OxPhos (oligomycin; 5µg/ml) for 30 minutes. A combination of both inhibitors was used to determine background luminescence. Graph shows there is a significant difference between 786O-VHL and 786O-EV cells in the presence of oligomycin (*** p<0.001 and ns p>0.05). Values are mean of 3 well replicates over 3 independent experiments, relative to untreated control (n=3) +/- S.E.M and data analysed using a paired, two-tailed t-test.**

## 4.6 The effect of pVHL status on mitochondrial DNA maintenance

Each mitochondrion contains multiple copies of mitochondrial DNA, which unlike nuclear DNA, is continually replicated independent of cell division (Smits et al., 2010). The mitochondrial genome contains approximately 16,600 base pairs and in humans encodes proteins from four of the five respiratory complexes, a number of transfer RNAs and two ribosomal RNAs. Altered mitochondrial DNA copy number (the number of mitochondrial DNA copies per cell), can occur either through variations in biosynthesis or DNA maintenance. The depletion of mitochondrial DNA can produce a dysfunctional in ETC, involving complex I, III and IV dysfunction and has been associated with a variety of diseases (Venegas and Halberg, 2012, Clay Montier et al., 2009).

Mitochondrial DNA copy number can be estimated through calculation of the ratio between a single copy nuclear gene, such as beta-2-microglobulin (β2M) and a region of the mitochondrial genome by RT-qPCR as previously described (Venegas and Halberg, 2012). A significant increase in mitochondrial DNA copy number was observed in 786O-VHL cells compared to 786O-EV cells (Figure 4.7). These data suggest that there are significantly fewer copies of the mitochondrial genome in cells devoid of functional pVHL, a phenotype which could cause the reduced mitochondrial protein expression observed in these cells (Figure 4.2). Mitochondrial DNA copy number has previously been demonstrated to be reduced in the absence of functional pVHL and a reduction in the protein expression of the mitochondrial transcription factor A (TFAM) proposed as the mechanism (Hervouet et al., 2005). Mitochondrial DNA content has also been demonstrated to decrease in clear cell renal carcinoma in tissue from patients (Simonnet et al., 2002, Selvanayagam and Rajaraman, 1996).

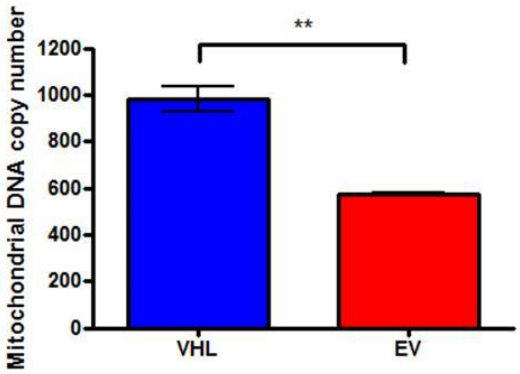


**Figure 4.7: pVHL status affects mitochondrial DNA copy number.**

**The graph shows mitochondrial DNA copy number calculated through analysis of expression of the single copy nuclear gene, *β2M* and mitochondrial *ND1* by RT-qPCR. Ct values were obtained for gene and the ratio calculated as described (Venegas and Halberg, 2012). There is a significant increase in mitochondrial DNA copy number in the 786O-VHL (VHL, blue) cells compared to the 786O-EV (EV, red) cells (** p<0.01). Values are mean +/- S.E.M (n=5) and data analysed using paired, two-tailed t-test.**

A large number of proteins are implicated in the replication, integrity and maintenance of the mitochondrial genome (Smits et al., 2010). The protein machinery is unique to mitochondria and disruptions to which are well documented through mutation analysis of patients with mitochondrial disease (Venegas and Halberg, 2012). Regulators of mitochondrial DNA maintenance include, TFAM (Ekstrand et al., 2004), the mitochondrial DNA helicase TWINKLE, encoded by the *PEO-1* gene and the mitochondrial DNA polymerase gamma (POLG). Other proteins include the single stranded DNA binding protein (mtSSB) and a number of accessory proteins (Venegas and Halberg, 2012, Falkenberg et al., 2007).

To determine whether known mitochondrial regulators, such as TFAM, POLG and TWINKLE are altered in 786O cells, gene expression was analysed using RT-qPCR. A small but significant increase in *TFAM* expression was observed in 786O-VHL cells compared to 786O-EV cells (Figure 4.8A), consistent with a previously reported increase in TFAM protein expression associated with pVHL (Hervouet et al., 2005). No differences were identified in the expression of *PEO*-1 and *POLG* was slightly but non-significantly increased after pVHL re-expression (Figure 4.8B and C). These results indicate that pVHL status affects *TFAM*

expression and highlight a mechanism through which pVHL regulates mitochondrial DNA copy number in the 786O cells.

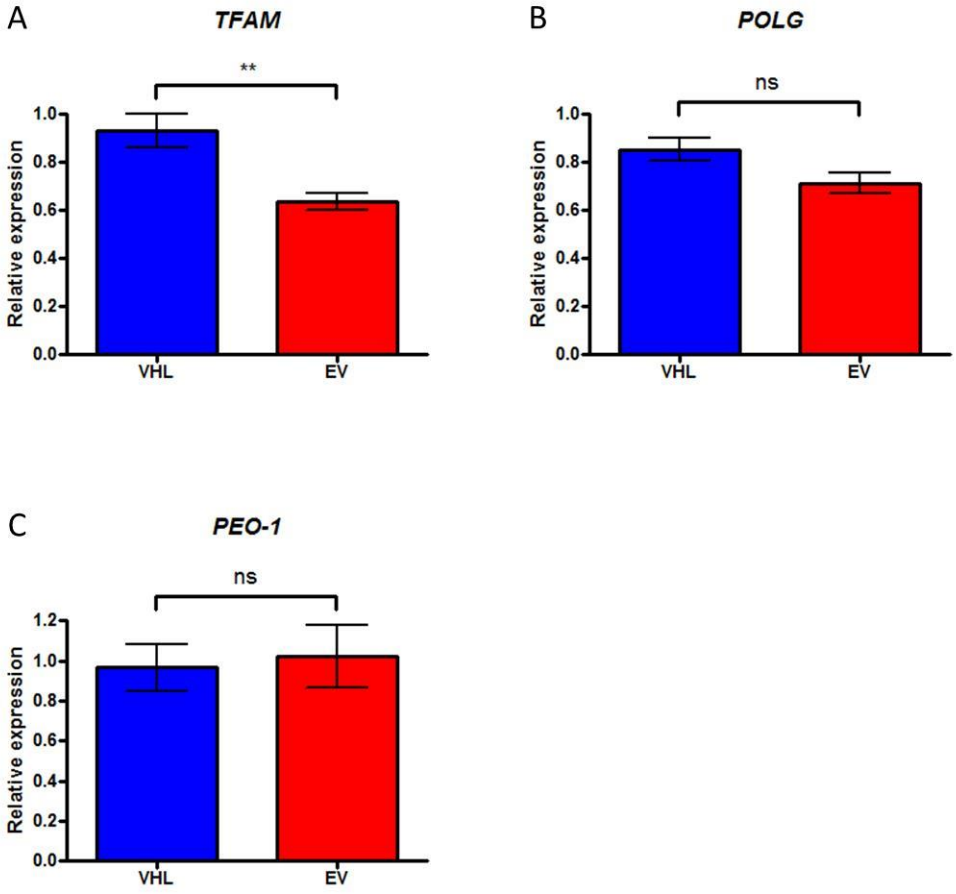


**Figure 4.8: Effect of pVHL status on the expression of factors involved in mitochondrial DNA replication and maintenance.**

**Graphs show relative expression of mRNA transcripts (*TFAM*, *POLG* and *PEO-1*) involved in the regulation mitochondrial DNA replication analysed using RT-qPCR. Graphs show (A) small significant increase in *TFAM* expression (** p<0.01) and (B and C) no change in *PEO-1* or *POLG* expression between 786O-EV (red) and 786O-VHL (blue) cells (ns p>0.05). Data analysed using the comparative Ct method after normalisation to a single experimental repeat. Values are mean +/- S.E.M (n=4-8). Data analysed using paired, two-tailed t-test.**

## 4.7 The effect of pVHL status on the control of mitochondrial biogenesis

To further investigate how pVHL status affects mitochondria, mitochondrial mass was analysed in 786O cells. Mitochondrial mass can be measured using fluorescent probes and flow cytometric analysis, where notably, the uptake of probe is independent of

mitochondrial membrane potential. To analyse mitochondrial mass in 786O cells, mitoview green was used. Mitoview is a membrane permeable dye that binds to mitochondrial phospholipids and insensitive to changes in membrane potential. The major mitochondrial lipid is cardiolipin (CL) which composes approximately 12-20% of a mitochondrial inner membrane total phospholipid content (Chicco and Sparagna, 2007, Hatch, 2004). OxPhos complex integration and assembly is dependent on CL and as such, mitochondrial lipids are vital for the efficient coupling of respiration and mitochondrial function. CL is synthesised in and exclusive to mitochondria (Ventura-Clapier et al., 2008).

786O cells were trypsinised, re-suspended and incubated in mitoview green for 30 minutes at 37°C before analysis by flow cytometry. A small shift in mitoview green fluorescence was observed in 786O-VHL cells compared to 786O-EV cells (Figure 4.9), suggesting an increase in mitochondrial mass or CL content.

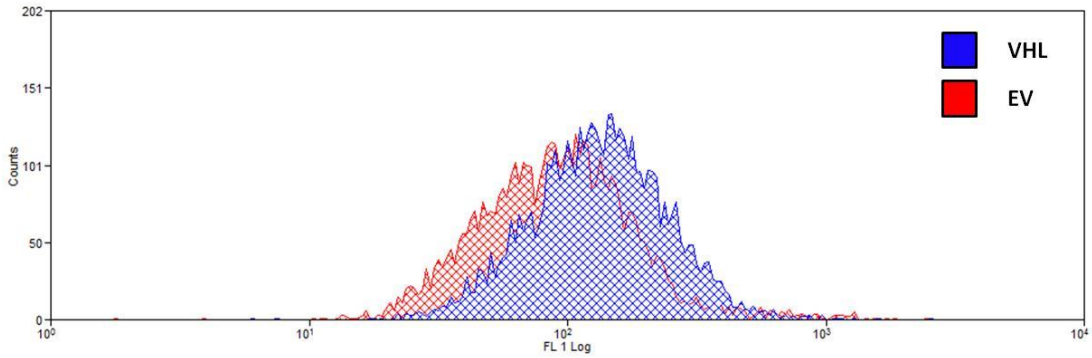


**Figure 4.9: pVHL status affects mitochondrial mass.**

**Graph shows flow cytometric analysis of mitochondrial mass analysed using mitoview green fluorescence. A small increase in median cell fluorescence was observed in 786O-VHL cells (blue) compared to 786O-EV cells (red). Data presented is representative of 3 independent experiments. Over 5000 cells were analysed per experimental repeat (n=3).**

Mitochondrial biogenesis is regulated by a number of transcription factors and their co-activators, most notably the peroxisome proliferator activated receptor co-activator (PGC) family of proteins. These include PGC-1α and PGC-1β co-activators, which interact with a number of transcription factors to regulate the expression of a large number of mitochondrial genes (Ventura-Clapier et al., 2008). The *TFAM* promoter contains binding

sites for both the nuclear respiratory factors -1 and -2 (NRF-1 and NRF-2), which are nuclear encoded transcriptional factors and are among a number of proteins which are involved in orchestrating nuclear control of mitochondrial biogenesis. The co-activation of these factors by PGC-1α results in the up-regulation of mitochondrial biogenesis, a circuit highly active in oxidative tissue or rapidly induced in response to exercise and increased energy demand (Ventura-Clapier et al., 2008).

To explore the possibility that transcriptional regulation of nuclear encoded mitochondrial genes is affected by pVHL status, mRNA expression of *PGC-1α*, *PGC-1β*, *NRF-1* and *NRF-2* was analysed by RT-qPCR. There were no significant differences observed in either *PGC-1α* or *PGC-1β* expression (Figure 4.10A-B) in the presence or absence of functional pVHL protein in the 786O cells. Likewise, there was also no significant difference in *NRF-1* or *NRF-2* expression between the 786O cell lines (Figure 4.10C-D). These data suggest that the changes observed in mitochondrial mass are likely not due to altered expression of mitochondrial transcriptional controllers.

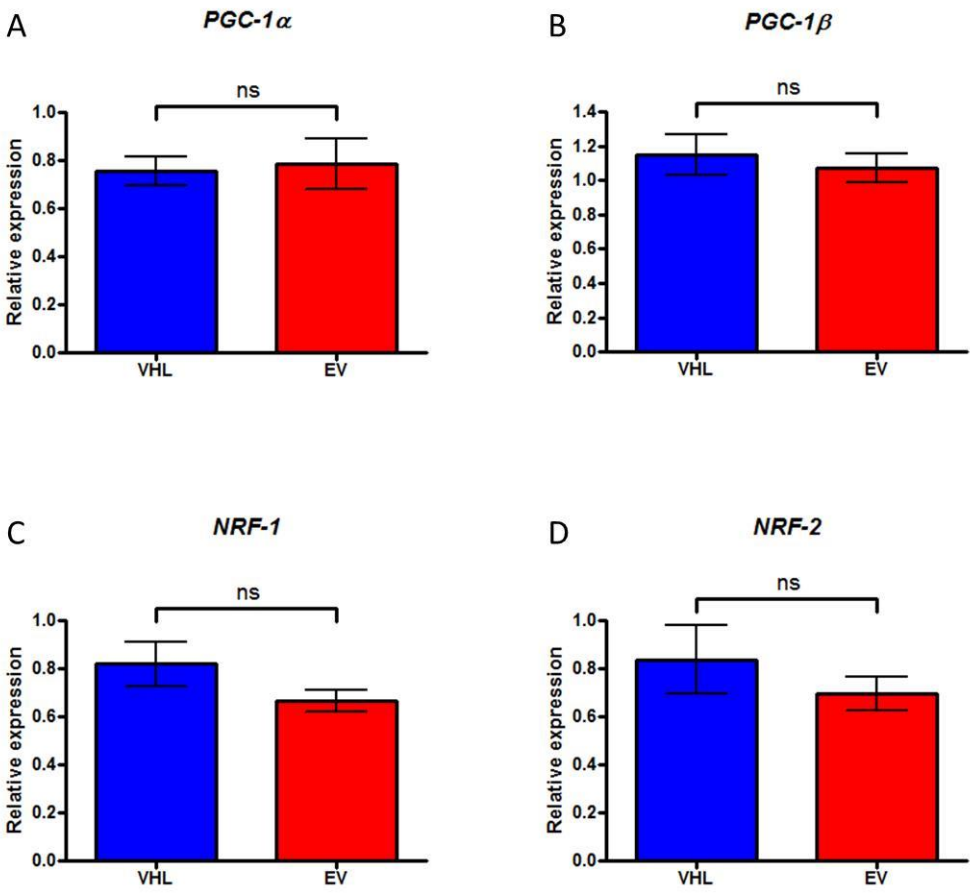


**Figure 4.10: pVHL status does not affect transcript expression of major regulators of mitochondrial biogenesis.**

**(A-D) Graphs show relative expression of mRNA transcripts (*PGC-1α*, *PGC-1α*, *NRF-1* and *NRF-2*) involved in mitochondrial biogenesis analysed using RT-qPCR. No significant difference was observed between 786O-EV (EV, red) and 786O-VHL (VHL, blue) cells. Data analysed using the comparative Ct method after normalisation to a single experimental repeat. Values are mean +/- S.E.M (n=4) and data analysed using paired, two-tailed t-test (p>0.05).**

## 4.8 The effect of pVHL status on mRNA expression of mitochondrially localised proteins

In light of the increase in mitochondrial ETC protein expression and increased mitochondrial DNA copy number in the 786O-VHL cells compared to the 786O-EV cells, it is likely that there could also be a parallel increase in mitochondrial gene transcription. Although the major controllers of mitochondrial gene transcription have been assessed,

there are distinct mechanisms through which mitochondrial genes can be induced and PGC-1α is highly regulated through post-translational modifications.

A panel of genes were selected that comprise both nuclear encoded (*SDHA* and *COX-IV*) and transcripts encoded by the mitochondrial genome (*ND6*, *cytochrome b* and *mtCO-2*). At least one subunit of each of the electron transporting complexes was selected for analysis. RT-qPCR was performed and demonstrated no significant effect of pVHL status on the expression of all genes analysed (Figure 4.11). Only a sample of the ETC subunits were analysed, however a number of the genes analysed (Figure 4.11) correlated with proteins previously demonstrated to be altered by pVHL status on the protein level (Figure 4.2) and elsewhere (Hervouet et al., 2005). Interestingly, the 786O-EV cells express mitochondrially-derived mRNA transcripts at a similar level as the 786O-VHL cells, despite their being fewer copies of the genome per cell in the 786O-EV cells. Together these data suggest that a decrease in mRNA expression is not the causal factor for the observed difference in mitochondrial ETC protein expression in the 786O cells (Figure 4.2).

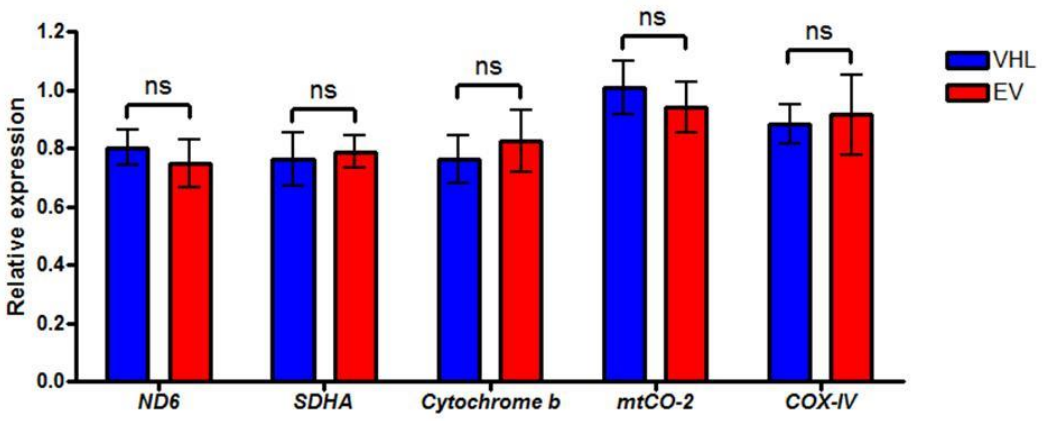


**Figure 4.11: pVHL status does not affect the transcript expression of nuclear and mitochondrially encoded genes.**

**Graph shows relative expression of mRNA transcripts (*ND6*, *SDHA*, *cytochrome b*, *mtCO-2* and *COX-IV*) analysed using RT-qPCR. No significant difference was observed between 786O-EV (EV, red) and 786O-VHL (VHL, blue) cells. Data analysed using the comparative Ct method after normalisation to a single experimental repeat. Values are mean +/- S.E.M (n=4-8) and data analysed using paired, two-tailed t-test (ns p>0.05).**

## 4.9 The effect of pVHL status on the expression of genes involved in mitochondrial protein translation

The process of ribosomal translation sits between gene transcription and protein folding and mitochondria contain their own machinery for the translation of mitochondrial genome derived transcripts. As a potential mechanism for the discrepancy between protein and mRNA expression of ETC complexes observed in the 786O cells (Figure 4.2 and

Figure 4.11), the mitochondrial translational machinery was investigated. Notably, both proteins of mitochondrial and nuclear origin are affected by pVHL status, raising the possibility that synthesis of mitochondrially encoded proteins is impaired and as a consequence affecting the protein expression and/or turnover of those nuclear encoded. The pVHL-dependent change in mitochondrially encoded ETC subunits may cause incomplete assembly of ETC complexes and possibly increase degradation of those incompletely assembled.

To investigate whether pVHL status mediates effects on the mitochondrial translational machinery, RT-qPCR was performed to examine the expression of key genes involved in this pathway. Translation initiation, involves mitochondrial initiation factors-2 (TIF2), elongation requires mitochondrial elongation factor-Tu (TUFM) and elongation factor G1 (GFM1). The final stages of termination and mitochondrial ribosomal recycling require mitochondrial ribosomal release factor (MRRF1) (Christian and Spremulli, 2012).

No significant differences observed in the mRNA expression of any of the translational machinery analysed in the 786O cells (Figure 4.12). These data suggest that the transcript levels of the mitochondrial translational machinery are likely unaffected by pVHL status, however until the process of translation is measured, the precise effect of pVHL status on mitochondrial translation cannot be fully determined.

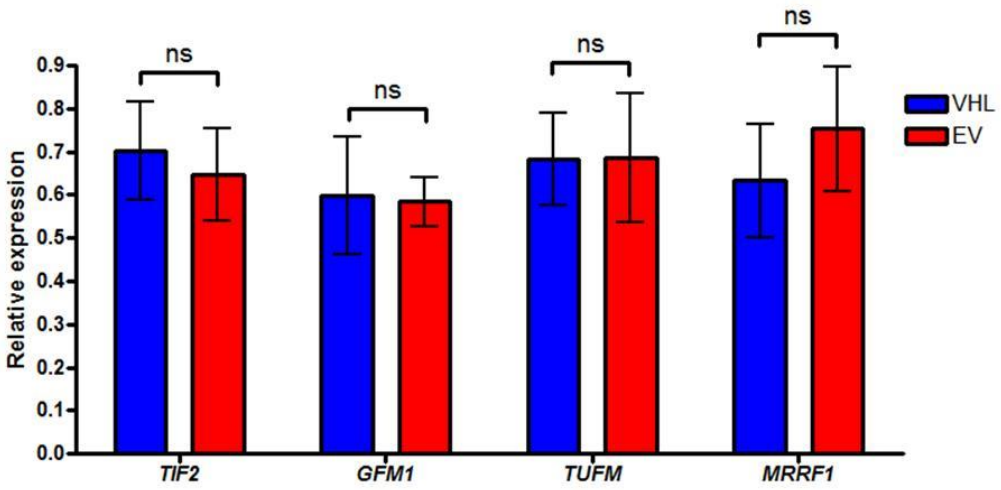


**Figure 4.12: Effect of pVHL status on the transcript expression of major regulators of mitochondrial translational.**

**Graphs shows relative expression of mRNA transcripts (*TIF2*, *GFM1*, *TUFM* and *MRRF1*) analysed using RT-qPCR. No significant difference was observed between 786O-EV (EV, red) and 786O-VHL (VHL, blue) cells. Data analysed using the comparative Ct method after normalisation to a single experimental repeat. Values are mean +/- S.E.M (n=4-8) and data analysed using paired, two-tailed t-test (ns p>0.05).**

A number of gene arrays have been generated comparing the presence and absence of pVHL in various renal cell backgrounds (Hervouet et al., 2008, Harten et al., 2009). Analysis of these micorarrays reveals an abundance of mitochondrial ribosomal protein (MRP) large (L) and small (S) subunits to be significantly up-regulated after re-expression of pVHL. Changes in mitochondrial ribosomal protein expression are subtle but remain significant at between a 1.2 and 2 fold induction. In 786O cells, *MRPS35* ($p<0.01$), *MRPS18C*, *MRPL30* isoform A and *MRPL30* isoform B ($p<0.05$) are all up-regulated when pVHL is re-expressed (Hervouet et al., 2008). In RCC10 cells with re-expression of wild type pVHL, *MRPL17*, *MRPL35*, *MRPL42*, *MRPL46*, *MRPL50*, *MRPL21* and *MRPS33* are all up-regulated at a significance of $p<0.01$ and an additional 19 distinct subunits at a significance of $p<0.05$ (Harten et al., 2009). Therefore it was thought appropriate to validate microarray data with respect to the role of pVHL status in the expression of mitochondrial ribosomal subunits. Mitochondrial ribosomes are distinct from cytoplasmic ribosomes, they are nuclear encoded, imported and specific to the translation of the 13 mitochondrially encoded protein transcripts (O'Brien, 2003). The ribosomal genes *MRPS35* and *MRPL30* were selected for analysis on the basis of their appearance in a gene array performed in 786O

cells (Hervouet et al., 2008) and the remaining genes were arbitrarily selected as they were absent from significance in either array. Interestingly, the expression of three from seven mRNA transcripts were significantly decreased in the 786O-EV cells compared to the 786O-VHL cells (Figure 4.13), two of which have been identified previously through microarray analyses ((Hervouet et al., 2008); Figure 4.13). These data suggests that pVHL status affects the expression of ribosomal subunits, an observation that correlates which the pVHL-dependent changes in mitochondrial ETC protein expression.

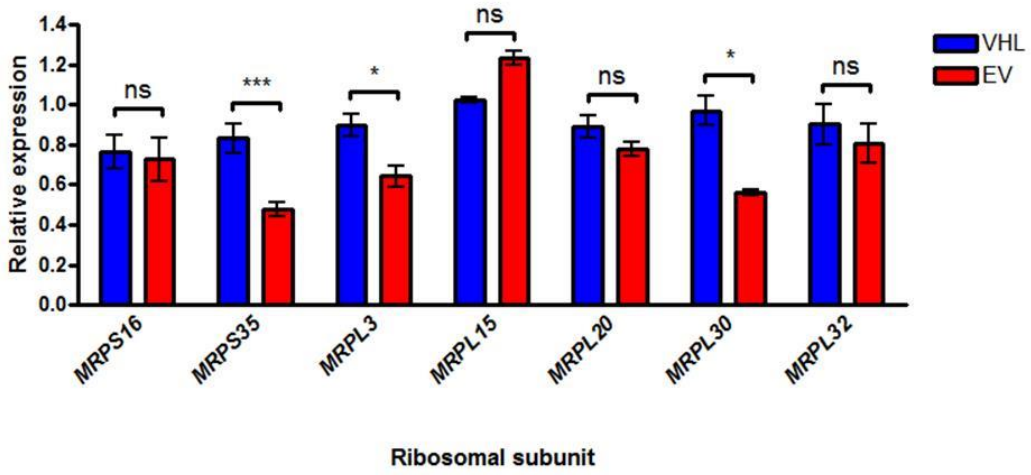


**Figure 4.13: Effect of pVHL status on the expression of mitochondrial ribosomal subunits. Graph shows relative expression of mRNA transcripts (*MRPS16*, *MRPS35*, *MRPL3*, *MRPL15*, *MRPL20*, *MRPL30* and *MRPL32* analysed using RT-qPCR in 786O (786O-EV (EV, red) and 786O-VHL (VHL, blue)) cells. Data analysed using the comparative Ct method after normalisation to a single experimental repeat. Values are mean +/- S.E.M (n=4-8) and data analysed using paired, two-tailed t-test (ns p>0.05). ADDED LEGEND**

## 4.10 The effect of silencing *HIF-2α* on pVHL-dependent changes in mitochondrial ETC protein expression

A previous report suggests silencing *HIF-2α* in 786O-EV cells, increases mitochondrial ETC protein expression (Hervouet et al., 2008). To explore the role of HIF-2α on mitochondrial protein expression, *HIF-2α* was silenced using RNA interference (RNAi) as described previously (Carroll and Ashcroft, 2008) and the expression of ETC proteins was examined. There were no observed changes in the expression level of pVHL-affected ETC proteins,

COX-IV and mtCO-2 in the 786O-EV cells despite effective knockdown of HIF-2α protein for 48 hours (Figure 4.14). These data indicate that the pVHL-dependent changes in ETC protein expression in 786O cells are likely independent of the stabilisation and transcriptional activity of HIF-2α and dependent on a role of pVHL outside that of its negative regulation of HIF-α.

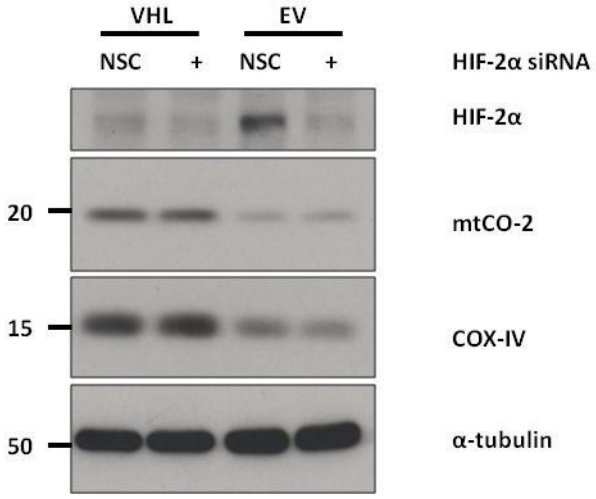


**Figure 4.14: Effect of *HIF-2α* knockdown on mitochondrial protein expression.**
**Western blot analysis of ETC proteins (mtCO-2 and COX-IV) in 786O (786O-EV (EV) and 786O-VHL (VHL) cells, in the presence of non-silencing control (NSC) siRNA or *HIF-2α* siRNA (+). α-tubulin was used as a load control.**

## 4.11 Analysis of mitochondrial parameters in pVHL positive and negative RCC10 cells

To determine if the pVHL-dependent mitochondrial effects described above could be observed in a distinct cell line, further investigation was undertaken using RCC10 cells. RCC10 cells, like 786O cells are human renal carcinoma derived cells, which lack functional pVHL (Harten et al., 2009, Maxwell et al., 1999). In contrast to the 786O cells, RCC10 cells express both HIF-1α and HIF-2α subunits.

Pooled RCC10 cell lines were previously generated that stably express wild type and mutant forms for the pVHL protein (Bond et al., 2011). The R200W mutation in *VHL* is associated with polycythemia and homozygotes for the mutation present with stabilised HIF-1α and

HIF-2α protein, elevated blood haematocrit and increases in HIF downstream targets such as EPO and VEGF (Hickey et al., 2007), a phenotype known as Chuvash polycythemia. There is a single substitution at base pair 598 which results in tryptophan to arginine change in the carboxyl-terminus of pVHL at codon 200 (Hickey et al., 2007). Mutations in the extreme C-terminal of pVHL decreases, but does not eliminate the ability of pVHL to bind and negatively regulate HIF-1α (Lewis and Roberts, 2003). The D126N and S183L mutations were identified in a single patient after sequencing of the *VHL* gene in a young boy (Bond et al., 2011). When these mutants are over-expressed in a pVHL null background they display an intermediate phenotype with relation to HIF-1α stabilisation and role in regulating metabolic function/glycolysis (Bond et al., 2011). The N78S mutation is an inactivating pVHL mutation; it lacks the capacity to negatively regulate HIF-1α and behaves similarly to the R200W mutant with respect to HIF-α induction. Unlike the 786O cells, the RCC10 express HIF-1α and as such distinct differences will exist between the cell lines due to the contribution of HIF-1α.

Figure 4.15A demonstrates the effect of expression of pVHL mutants on the stabilisation of HIF-α protein subunits and downstream target (GLUT-1). Parallel analysis of the expression of the HIF target gene *PHD3*, was used as confirmation of the genotype (Figure 4.15B). From these four pVHL mutants, the R200W and N78S were taken forward for further study.

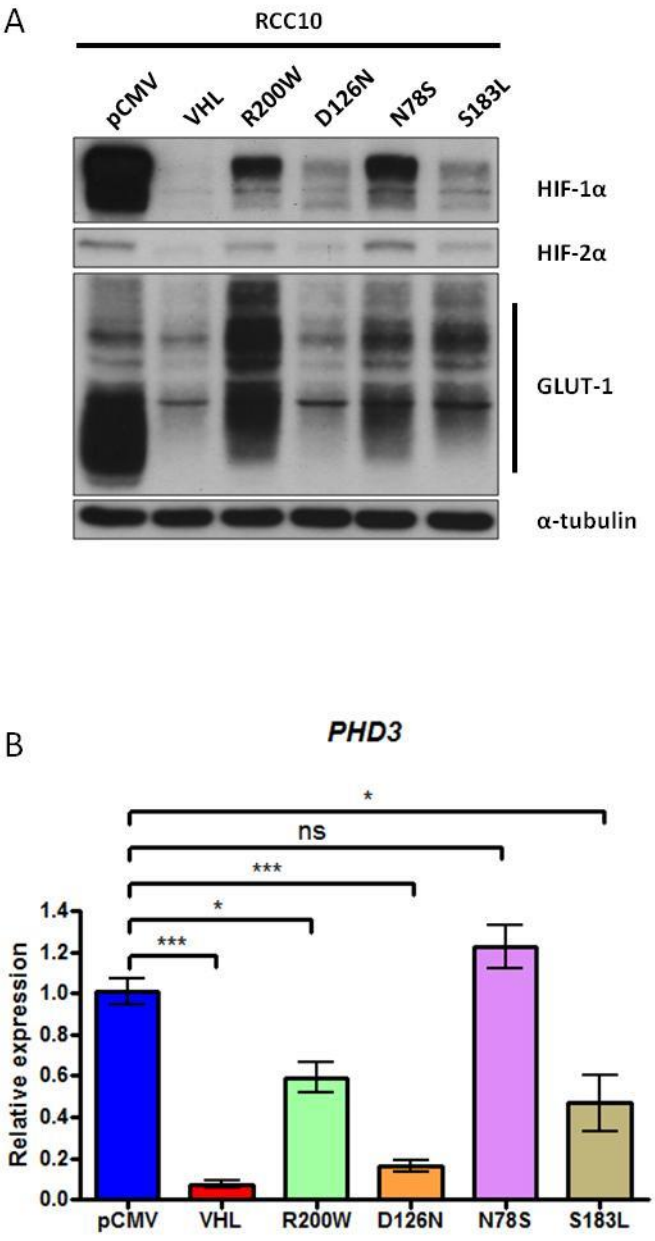


**Figure 4.15: Introduction of wild type pVHL or pVHL mutants differentially affects the stabilisation of HIF-1α, HIF-2α protein and target gene expression.**

**(A) Western blot analysis demonstrating the effect of wild type pVHL (VHL) and mutant pVHL (R200W, D126N, N78S, S183L) protein expression in RCC10 cells on the constitutive stabilisation of HIF-α (HIF-1α and HIF-2α) protein, compared to control (pCMV). α-tubulin was used as a load control. (B) Graph shows relative expression of HIF target gene *PHD3* analysed using RT-qPCR in cells described in A. Data analysed using the comparative Ct method after normalisation to a single experimental repeat. Values are mean +/- S.E.M (n=4) and data analysed by paired two-tailed t-test.**

pVHL status in the 786O cells had significant effects on mitochondrial DNA content. Similar observations were found in the RCC10 cells (Figure 4.16). There was a significant increase in mitochondrial DNA copy number in RCC10-VHL cells compared with RCC10-pCMV. Despite stabilisation of HIF-1α and HIF-2α (Figure 4.15), expression of the R200W mutant also produced a significant increase in mitochondrial DNA copy number to a value comparable with that of wild type pVHL expression in the RCC10 cells (Figure 4.16). Stable re-expression of the N78S mutant in RCC10 cells produced a small and non-significant increase in mitochondrial DNA copy number compared to RCC10-pCMV, producing an intermediate phenotype (Figure 4.16). These data suggest that the pVHL-induced increase in mitochondrial DNA copy number is independent of HIF-1α or HIF-2α stabilisation and the ability of pVHL to bind and negatively regulate HIF-α.

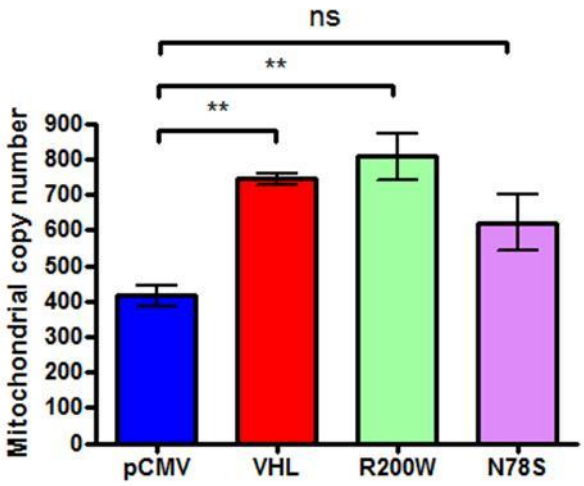


**Figure 4.16: pVHL status affects mitochondrial DNA copy number in RCC10 cells.**

**Graph shows mitochondrial DNA copy number calculated through analysis of expression of the single copy nuclear gene *β2M* and mitochondrial *ND1* by RT-qPCR in control (pCMV), wild type pVHL (VHL) and mutant pVHL (R200W, N78S) RCC10 cells. Ct values were calculated for each and the difference calculated as described (Venegas and Halberg, 2012). There is a significant difference between the wild type pVHL and pCMV-empty vector (** p<0.01). There are differential effects on mitochondrial DNA copy number dependent on the mutation in pVHL (** p<0.01, ns p>0.05). Values are mean +/- S.E.M (n=5). Data analysed by paired, two-tailed t-test.**

Next, total cellular ATP was measured using a luminescent assay, described previously. In the RCC10-pCMV cells there was a significant reduction in luminescence compared to the RCC10-VHL cells, as observed previously in the 786O cells (Figure 4.6A), suggesting lower total cellular ATP concentration per cell (Figure 4.17). Correlating with the previous data, the RCC10-R200W mutant demonstrated a phenotype similar to re-expression of wild type pVHL and the RCC10-N78S mutant was more intermediate (Figure 4.17).

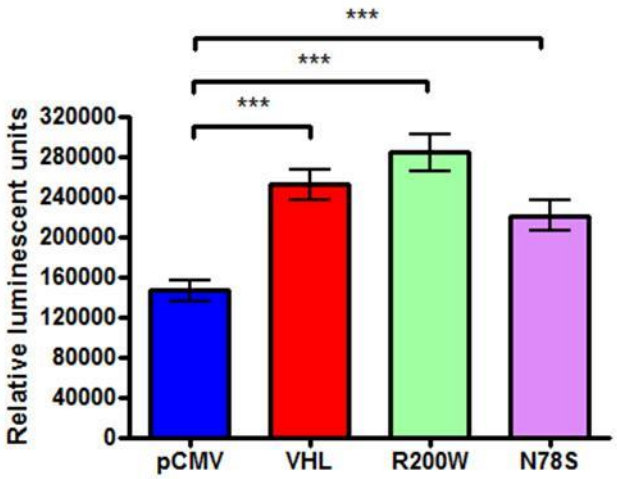


**Figure 4.17: pVHL status affects total cellular ATP levels in RCC10 cells.**

**Graph shows total cellular ATP content in control (pCMV), wild type pVHL (VHL) and mutant pVHL (R200W, N78S) RCC10 cells. There is a significant difference between the luminescence generated in wild type pVHL and mutant pVHL cells (R200W and N78S) and that generated in the pCMV-empty vector cells (*** p<0.001). Values are mean +/- S.E.M (n=3). Data analysed by paired, two-tailed t-test.**

pVHL status was previously observed to affect protein expression of a select number of ETC proteins of both of nuclear and mitochondrial origin (Figure 4.2). To investigate whether mitochondrial ETC protein expression was also affected in RCC10 cells, protein samples were subject to SDS-PAGE and western blotting. In the absence of wild type pVHL, a reduction in both mt-CO2 and COX-IV expression was observed in the RCC10-pCMV cells compared to RCC10-VHL cells, correlating well with that in the 786O cells (Figure 4.18; lanes 1 and 2). Additionally no differences in other mitochondrial proteins, including those involved in OxPhos, such as ATPB, SDHA, VDAC1 and prohibitin-1 (PHB1) were observed.

Intriguingly, mutant pVHL in RCC10 cells had differential effects. Analysis of the RCC10-R200W and RCC10-D126N mutants revealed a phenotype similar to that of wild type pVHL expression. An increase in mtCO-2 and COX-IV expression was observed in the RCC10-R200W and RCC10-D126N mutants compared to RCC10-pCMV cells (Figure 4.18; lanes 3 and 4). Analysis of RCC10-N78S and RCC10-S183L demonstrate an intermediate phenotype between observed changes in the RCC10-pCMV and after wild type pVHL expression (RCC10-VHL) (Figure 4.18; lane 5).

Together these data suggest that the changes in mitochondrial protein expression are independent of the stabilisation or abundance of either HIF-α subunit and that the changes are dependent on pVHL but not on its ability to recognise the HIF-α subunits. Consistent with the 786O data, re-expression of pVHL in RCC10 cells increases mitochondrial ETC protein expression, cellular ATP and mitochondrial DNA copy number.

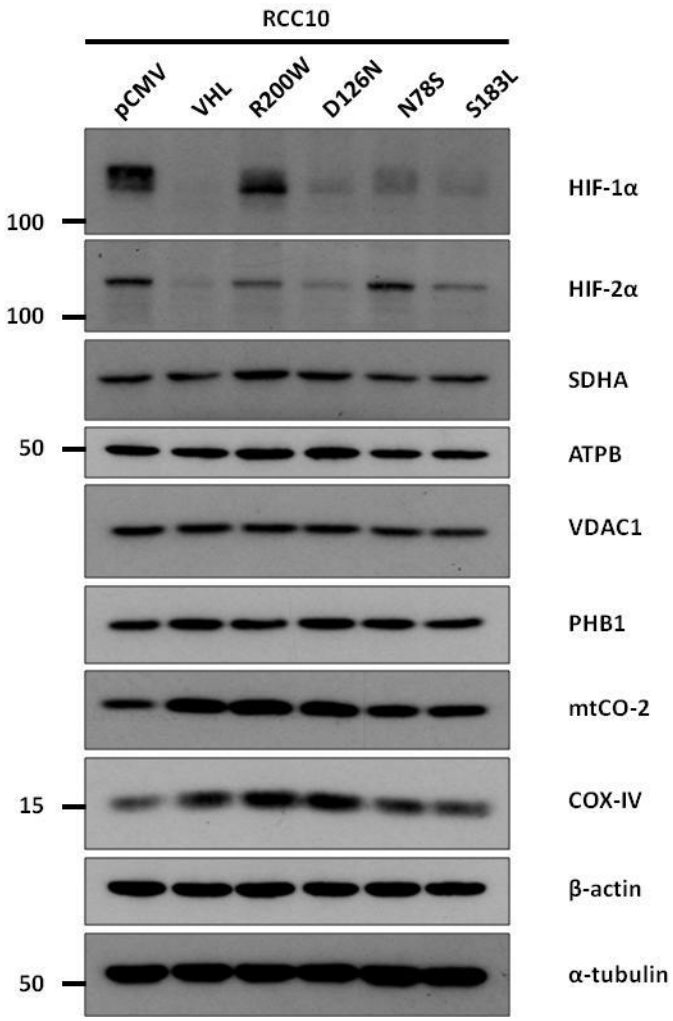


**Figure 4.18: pVHL status affects mitochondrial ETC protein expression in RCC10 cells.**

**Western blot analysis of RCC10 cells expressing empty vector control (pCMV), wild type pVHL (VHL) or pVHL mutants (R200W, D126N, N78S and S183L) and their effect on the expression of mitochondrial proteins (SDHA, ATPB, VDAC1, PHB1, mtCO-2 and COX-IV). β-actin and α-tubulin were used as load controls.**

## 4.12 Discussion

VHL disease is an autosomal dominantly inherited, multi-system hereditary cancer syndrome, where affected individuals are predisposed to the development of a spectrum of vascularised tumours. Tumours can affect both the central nervous system in addition to visceral organs. The disease is the leading cause of inherited renal cell carcinoma and *VHL* mutation has been associated sporadic renal cell carcinoma, originating from the proximal

tubule, which are highly aggressive (Lai et al., 2011, Kaelin, 2008, Shen and Kaelin Jr, 2013, Simonnet et al., 2002).

Details regarding the role of pVHL status and influence on mitochondrial homeostasis are still in their infancy. To date, there have been a small number of studies detailing the role of pVHL in mitochondrial function, all of which have focussed on renal carcinoma derived cells (Hervouet et al., 2005, Hervouet et al., 2008). The negative regulation of the HIF-α subunits by pVHL has understandably been the focus of most attention and study, however novel HIF-independent functions of pVHL are emerging (Li and Kim, 2011). The emerging evidence suggests an apparent a role for pVHL in the regulation of mitochondrial function (Hervouet et al., 2005, Hervouet et al., 2008, Li and Kim, 2011). However, the importance and biological significance of this less characterised function of pVHL remains a mystery. Exploring this novel aspect of pVHL function, may ultimately provide some further insight into the pathophysiology of renal disease.

Loss of pVHL in CCRCC has been shown to specifically reduce the expression of a number of OxPhos proteins, decrease ETC complex *in vitro* activity and affect OCR without influencing membrane potential or $F_1$-ATPase activity (Hervouet et al., 2005). A significant decrease in mitochondrial DNA copy number in cells and tissue has also been documented to be influenced by pVHL status, as has an effect on oxidative stress *in vitro* (Hervouet et al., 2005, Hervouet et al., 2008).

An interesting comparison has been made between these CCRCC and oncocytomas (Simonnet et al., 2002). In CCRCC, observations suggest that OxPhos and mitochondrial impairments are increased in parallel with the tumour aggressiveness; however oncocytomas, which originate in the renal collecting duct, rarely cause metastatic disease and interestingly have increased mitochondrial density and DNA content. This has led to the hypothesis that a down-regulation of OxPhos enables a growth advantage and increased ability to metastasise (Simonnet et al., 2002). It would be interesting to explore the role of proliferating versus metastatic cancer cell phenotype in terms of mitochondrial characteristics and function, whether manipulation of epithelial to mesenchymal transition (EMT) state would affect mitochondrial function, morphology or bioenergetics. Alternatively, it would be interesting to assess whether modulation of mitochondrial function can promote or inhibit the metastatic potential or the proliferative capacity of cancer cells.

In this work we aimed to link previous observations relating to the role of pVHL (Hervouet et al., 2005, Hervouet et al., 2008, Craven et al., 2006) and to further explore a potential mechanism behind the effects on mitochondrial ETC protein expression, bioenergetics and mitochondrial DNA maintenance. Through expression of wild type pVHL and pVHL mutants and detailed investigation into a broad range of parameters that relate to mitochondrial function, in this chapter we have observed a number of novel functions relating to the role of pVHL in modulating mitochondrial homeostasis.

### 4.12.1 *pVHL re-expression affects the expression of mitochondrially and nuclear encoded ETC proteins*

Here, we observed a decrease in the expression of number of integral mitochondrial proteins in renal carcinoma cell lines devoid of pVHL function compared with cells stably re-expressing pVHL. Most notably was reduced protein expression of mtCO-2 and COX-IV. This is in addition to published observations that ISP, core II and 13kDa protein of complex III and ATP6 are also decreased in cells devoid of pVHL function. $F_1$-ATPase-α and $F_1$-ATPase-β however, were not affected and expressed at similar levels irrespective of pVHL status (Hervouet et al., 2005). A second proteomic study, in UMRC2 cells with stable pVHL re-expression, also identified increases in ubiquinol-cytochrome c reductase complex core protein 2 of complex III and identified effects on complex I (Craven et al., 2006). A full list of mitochondrial ETC proteins identified as changing in a pVHL-dependent manner identified in cell culture is included in the table below (Table 5).

Alterations in protein expression appeared to be limited to those proteins involved in electron transport, while the expression of proteins with functions outside the ETC appeared not to change in the 786O cells. HSP60, VDAC1 and PHB1 proteins are all expressed at comparable levels and not affected by pVHL status. Published observations also suggest that adenine nucleotide translocase (ANT) expression is also maintained in the presence and absence of pVHL (Hervouet et al., 2005). Collectively these observations raise the question as to why a select number of ETC proteins are decreased in the absence of functional pVHL compared to its re-expression. A more substantial proteomic approach of mitochondrial proteins would be beneficial in determining the full complement of affected proteins and ETC complexes to aid in the elucidation of a potential mechanism.

Interestingly, the alterations in protein expression comprise elements which are both mitochondrially and nuclear encoded, and all ETC complexes identified with alterations in

protein expression contain elements that are mitochondrially encoded. Complex II, of which all four subunits are nuclear encoded, was interestingly not measured in all published analyses (Hervouet et al., 2005, Hervouet et al., 2008, Craven et al., 2006, Sarto et al., 1997) and does not change in the RCC10 cells (Figure 4.18). The data presented here with respect to the effect of pVHL status on ETC protein expression correlates well with previous observations (Hervouet et al., 2005), and indicating the data is robust and reproducible.

| Complex | Protein | Genetic origin | Change in expression after stable pVHL re-introduction | Ref. |
|---|---|---|---|---|
| I | NADH-ubiquinone oxidoreductase 24 kDa (NDUFV2) | Nuc | Increased | (Sarto et al., 1997) |
| I | NADH-ubiquinone oxidoreductase 39 kDa (NDUFA9) | Nuc | No change (cells) increased (tissue) | (Craven et al., 2006) |
| III | Ubiquinol cytochrome c reductase core protein 2 (UQCRC2) | Nuc | Increased | (Craven et al., 2006) |
| III | Ubiquinol cytochrome c reductase core protein 1 (UQCRC1) | Nuc | Increased | (Craven et al., 2006) |
| III | 13kDa protein | Nuc | Increased | (Hervouet et al., 2005) |
| III | Core II | Nuc | Increased | (Hervouet et al., 2005) |
| III | Iron sulphur protein (ISP) | Nuc | Increased | (Hervouet et al., 2005) |
| IV | Cytochrome c oxidase subunit 2 (mtCO-2) | Mito | Increased | (Hervouet et al., 2005) |
| IV | Cytochrome c oxidase subunit 4 (COX-IV) | Nuc | Increased | (Hervouet et al., 2005) |
| V | ATP synthase, $F_O$ subunit 6 (ATP6) | Mito | Increased | (Hervouet et al., 2005) |
| V | ATP synthase, mitochondrial $F_1$ complex, alpha (ATP5A) | Nuc | No change | (Hervouet et al., 2005) |
| V | ATP synthase, mitochondrial $F_1$ complex, beta (ATP5B) | Nuc | No change | (Hervouet et al., 2005) |

**Table 5: Effects of pVHL re-expression on mitochondrial protein expression in renal carcinoma cells.**

**Table detailing the protein, genetic origin and change in response to pVHL re-expression. The re-expression of pVHL has been identified in a number of proteomic and biochemical analyses to affect mitochondrially localised proteins of both nuclear (Nuc) and mitochondrial (Mito) origin. References are indicated.**

Analysis of ETC complex assembly would be necessary to determine if the pVHL-dependent change in mitochondrial protein abundance is paralleled by a reduction in OxPhos protein assembly. Blue-native poly acrylamide gel electrophoresis (BN-PAGE) is a tool that allows protein complexes to be separated in their native conformation. This also allows separation of respiratory super-complexes and identifies failures in complex synthesis and/or assembly. BN-PAGE would be beneficial not only to determine if the decreased expression of the ETC proteins correlates with reduced complex assembly, but also using this same approach, in-gel activity assays could be undertaken investigate the specific activities of each complex. As a comparable and/or complementary approach, spectrophotometric assays could be performed to measure the activity of each ETC complex, using a combination of substrates and inhibitors of each complex.

Being the principal negative regulator of HIF-α subunits, pVHL governs the cellular abundance of stabilised HIF-1α and activity of the HIF complex, thus indirectly controls target gene expression. 786O cells express HIF-2α only and loss of pVHL in these cells leads to constitutively stabilised and active HIF-2α. Differences observed after pVHL re-expression need first to be interpreted in relation to their HIF-α status in order to determine the potential involvement of stabilised HIF-α (HIF-1α and/or HIF-2α). Thus for the 786O cell system differences in mitochondrial parameters described in this chapter are independent of any role of HIF-1α and only consideration of stabilised and transcriptionally active HIF-2α is necessary. A previous report suggests that silencing of *HIF-2α* in 786O-EV cells increases ETC protein expression in 786O cells, but not to the same degree of expression as observed after pVHL re-expression (Hervouet et al., 2008). Data from Hervouet *et al*, suggests the increase in ROS observed in 786O-EV cells and the HIF-2α-dependent expression of manganese superoxide dismutase (Mn-SOD), increases mitochondrial $H_2O_2$ and propose this increase in oxidative stress is responsible for the reduction in complex protein expression (Hervouet et al., 2008). Our studies failed to confirm the observations by Hervouet *et al*. After silencing of *HIF-2α* in 786O-EV cells, we observed no change in mitochondrial protein expression, indicating that the effects on mitochondrial ETC protein expression are mediated through pVHL-dependent, HIF-2α-independent processes. Additionally, the incubation of these cells over night with the antioxidant N-acetyl cysteine fails to rescue the decrease in ETC proteins in the 786O-EV cells (data not shown), suggesting that increased oxidative stress (ROS) produced in the 786O-EV cells is likely not responsible for the effects of pVHL on mitochondrial ETC protein

expression observed. Finally, data obtained in pVHL mutant expressing cells, particularly RCC10-R200W cells, suggest that despite the presence of constitutively stabilised HIF-2α in these cells compared to cells re-expressing wild type pVHL (RCC10-VHL) there was no difference on their respective ability to effect mitochondrial protein expression.

A striking observation from the changes in protein abundance between the pVHL positive and negative cell lines is that ETC proteins of both nuclear and mitochondrial origin were affected by pVHL status. Since the control of mitochondrial genome transcription is distinct from cellular control of nuclear transcription, it is likely that the change of protein expression is happening post-transcriptionally or from alterations in mitochondrial DNA/RNA processing. Approaches were first used to fully characterise the mitochondrial phenotype, understand how the alterations in protein expression affected function and attempts made to correlate these with pVHL status.

### 4.12.2 *pVHL re-expression affects mitochondrial bioenergetics and cellular energy processing*

The reduced mitochondrial respiration in the 786O-EV cells compared to the 786O-VHL cells is likely a function of reduced ETC protein expression. In this chapter we have demonstrated a significant increase in OCR when pVHL is re-expressed in 786O cells. This correlates with significant increases in leak respiration and maximum respiratory capacity in the 786O-VHL cells. The increased OCR in 786O-VHL cells is maintained under galactose-induced oxidative conditions. Determination of the flux ratios allows interpretation of more subtle effects on bioenergetics. Under both glucose and galactose conditions, independent of pVHL status, cells were respiring at a similar proportion of their theoretical maximum rate, as ascertained by the routine control ratio. In galactose, as predicted respiration was slightly closer to the maximum capacity. The coupling of the ETC appears to significantly increase in the presence of pVHL determined by the leak control ratio. The biological significance of this however is less clear.

Analysis of mRNA transcripts of the UCPs demonstrates a significant up-regulation of *UCP3* expression in the 786O-EV cells compared to the 786O-VHL cells, possibly promoting an uncoupling effect. However, evidence suggests that these channels only promote proton conductance in the presence of specific activators (Brand and Esteves, 2005). Hence UCPs catalyse only an inducible proton conductance and notably fatty acids and products of ROS metabolism have been observed to activate the channels (Brand and Esteves, 2005). We

and others (Hervouet et al., 2008) have observed mitochondrial oxidative stress to be increased in the absence of pVHL in 786O cells (data not shown) and activation of UCPs could potentially be a mechanism to promote uncoupling and function to reduce superoxide production. Increased uncoupling would attenuate mitochondrial ROS and protect cells from reactive species induced damage (Brand and Esteves, 2005). The net-routine control ratio estimates the proportion of the maximum capacity coupled to ATP synthesis. The net-routine control ratio is reduced in the absence of pVHL function and may be suggestive of a number of cellular characteristics, potentially less ATP demand or as a consequence of uncoupling. The differences in ratios are small and biological significance needs to be carefully interpreted and more data necessary to draw solid conclusions.

A biological consequence of the significant increase in OCR and ETC protein expression in the 786O-VHL cells compared to the 786O-EV cells is an augmentation in cellular ATP levels. 786O-VHL cells have a greater cellular concentration of ATP, a phenotype mimicked in the RCC10-VHL cells. The energetic profile of the RCC10 cells demonstrates a parallel relationship with respect to the role of pVHL status on cellular ATP levels and as observed in the 786O cells, re-expression of pVHL increases total cellular ATP. Initial characterisation of the bioenergetics in the RCC10 cells also reveals parallel observations and increased OCR after wild type pVHL re-expression. This confirms a pVHL-dependent, HIF-1α-independent mechanism controlling the OCR phenotype. Interestingly, the RCC10-R200W mutant has an equivalent cellular concentration of ATP as wild type RCC10-VHL and preliminary investigation of bioenergetics reveals comparable rates of respiration. The RCC10-N78S mutant has a total cellular ATP intermediate between RCC10-pCMV and wild type pVHL expression. The pathway through which this ATP is produced is to date unknown. However with the constitutively stabilised HIF-1α in these two mutant lines, and high levels of glycolysis would be predicted to be a contributory factor.

Interestingly, despite 786O-VHL cells consuming more oxygen, as a proportion of their basal ATP concentration, these cells are slightly, but significantly less reliant of OxPhos for ATP synthesis compared to the 786O-EV cells. Conversely, 786O-EV cells are slightly but significantly more reliant on OxPhos for biosynthesis of ATP, demonstrated by their increased sensitivity to oligomycin. This has been observed elsewhere in tumour xenographs using the same cell line devoid of functional pVHL and with constitutively stabilised HIF-2α (Biswas et al., 2010). HIF-2α over-expressing xenographs displayed a

metabolic profile associated with lower glycolytic and greater mitochondrial metabolism and perhaps greater tolerance to mitochondrial ROS-dependent damage (Biswas et al., 2010).

Further experiments using the Oroboros O2K would be worthwhile. Permeabilisation of the cells and treatment with exogenous respiratory substrates would allow further analysis of respiration. Using a combination of glutamate, malate, pyruvate and succinate and inhibitors of complexes I and II (rotenone and malonate) it would be possible to determine the contribution of complexes I and II to ADP-stimulated respiration. Inhibition at complex III and addition of ascorbate and N,N,N',N'-tetramethyl-p-phenylenediamine dihydrochloride (TMPD) would allow complex IV activity to be analysed in isolation. The experimental protocol could also be extended to using isolated mitochondria, whereby the metabolism of saturating exogenous substrates could be assessed in the absence of extra-mitochondrial control and regulation. This would allow the precise mitochondrial bioenergetic phenotype to be assessed in detail. Spectrophotometric assays have been performed in the presence and absence of pVHL with reference to citrate synthase and succinate cytochrome c reductase. Interestingly, there was no change in citrate synthase activity after the re-expression of pVHL; this is normally used as an indicator of mitochondrial number, however a significant reduction in succinate cytochrome c reductase activity, a measure of combined activity of complexes II and III was observed. The ATP hydrolysis of the $F_1$-ATPase does not change after pVHL re-expression (Hervouet et al., 2005). These data suggest that minimal/absent deficit in TCA cycle function and down-regulation of OxPhos in cells devoid of functional pVHL.

### 4.12.3 *pVHL re-expression affects mitochondrial DNA maintenance*

Mitochondrial DNA copy number is a measure of mitochondrial DNA content. Mitochondrial DNA content has been quantified in a number of tumours and decreases have been observed in breast, prostate, hepatocellular and gastric tumours (Chandra and Singh, 2011). Decreased mitochondrial DNA copy number in tumours has been associated with increased invasiveness and high-grade aggressive disease in a number of situations (Chandra and Singh, 2011, Simonnet et al., 2002). Conversely, increased mitochondrial DNA copy number and bioenergetic function have been associated with increased invasiveness of oesophageal squamous cell carcinoma cells (Lin et al., 2012, Mambo et al., 2005). Hence the story of mitochondrial function and relation to tumour progression is complex.

A previous study along with observations from our own laboratory (Figure 4.7 and

Figure 4.16) suggest that mitochondrial DNA copy number is reduced in the absence of functional pVHL in renal carcinoma cell lines (Hervouet et al., 2005). A reduced mitochondrial DNA copy number implies there is a lower number of copies of the mitochondrial genome per cell, however usually does not provide any information on the number of the copies of the mitochondrial genome per mitochondria, i.e. no relationship with mitochondrial mass. Additionally, the organisation of DNA molecules remains unknown and analysis of nucleoid DNA content and cellular distribution may reveal additional insight into pVHL-dependent effects on mitochondrial DNA maintenance.

The RCC10 cells again display parallel characteristics with respect to the 786O cells and mitochondrial DNA copy number. Re-expression of wild type pVHL (RCC10-VHL) significantly increases mitochondrial DNA copy number compared to RCC10-pCMV. RCC10-R200W mutation retains a mitochondrial DNA copy number similar to that of wild type pVHL, consistent with the results for ATP, ETC protein expression and preliminary respirometry. The RCC10-N78S mutant reproducibly displays an intermediate phenotype, again consistent with results for ATP and early respirometry data.

Further investigation into the role of pVHL in the maintenance of mitochondrial DNA may be informative. In addition to studies on mitochondrial DNA organisation and localisation, depletion of mitochondrial DNA using ethidium bromide and tracking rate of re-population could reveal insights into the role of pVHL in mitochondrial DNA replication.

Despite this change in mitochondrial DNA copy number, observations suggest that mitochondrially encoded transcripts can be maintained in the 786O-EV cells. The mRNA expression of the mitochondrial transcription factor *TFAM* is significantly reduced in 786O-EV cells compared with 786O-VHL cells. Transcript expression of neither *POLG* nor *PEO-1* was affected by VHL status. TFAM has been linked to mitochondrial genome maintenance and levels of TFAM protein have been observed to be proportional to the quantity of mitochondrial DNA present (Ekstrand et al., 2004, Campbell et al., 2012). Therefore, the lower mitochondrial DNA copy number observed in the 786O-EV cells compared with the 786O-VHL cells could be a result of a correlative lower level of the *TFAM* transcript (Hervouet et al., 2005). However, the mechanism underlying how pVHL affects *TFAM* expression remains to be investigated. It has been observed that TFAM over-expression in

mice results in an increase in mitochondrial DNA copy number, but changes to mitochondrial mass and respiratory chain are not observed. This suggests a separable role for TFAM in regulation of biogenesis/transcript expression versus mitochondrial DNA copy number/mitochondrial DNA replication, and highlights that mitochondrial DNA copy number changes do not always directly relate to changes in mitochondrial activity (Falkenberg et al., 2007, Ekstrand et al., 2004).

*TFAM* mRNA expression is regulated via PGC-1α. PGC-1α lacks DNA binding capacity but interacts and co-activates a number of transcription factors, including the nuclear respiratory factors (NRFs) (Ventura-Clapier et al., 2008). The NRFs are a family of transcription factors, linked to the transcriptional control of many mitochondrial genes (Scarpulla, 2008). However there are no changes in the expression of these factors observed after transcript analysis in the 786O cells.

PGC-1α has been explored in a number of situations relating to its role in renal carcinoma and to date, through microarray, serial analysis of gene expression (SAGE) and direct RT-qPCR, changes in its expression have failed to be identified (Hervouet et al., 2005). However, PGC-1α is heavily post-translationally modified by number of proteins including p38MAPK, AMPK and SIRT1 (Ventura-Clapier et al., 2008, Fernandez-Marcos and Auwerx, 2011), giving rise to the possibility that since activity is not necessary regulated on the level of mRNA or protein expression, that changes in PGC-1α post-translational modification could potentially be playing a role. *TFAM* is among a number of PGC-1α targets that change with loss of pVHL. MFN1, *MRPS35* and OPA-1 are also targets which we have observed change either on the transcript or protein level in pVHL positive and negative cells. However, our analysis of the expression of other PGC-1α genes, such as *PEO-1* and *SDHA* showed they were not affected by pVHL status change, making a conclusion as to the role of co-activation difficult.

To understand the role of PGC-1α and its activation status, a larger number of target genes would need to be analysed (Yao et al., 2013). The Mitocarte database (Broad Institute; (Pagliarini et al., 2008)) holds information on the degree of PGC-1α-dependent induction of mitochondrial proteins, after PGC-1α over-expression. The Mitocarte database can be used to cross reference changes observed in a number of analysed transcripts with the degree of induction by PGC-1α, to possibly delineate any relationship.

The expression of *PGC-1β* was also not significantly affected by VHL status. *PGC-1β* expression is under the control of c-MYC, and loss of PGC-1β has been observed to reduce respiration in pVHL-deficient renal cells that express HIF-1α (Zhang, 2007). However despite HIF-2α having been shown to activate c-MYC (Gordan et al., 2007), there is no difference in the expression of this co-activator across the 786O cells. Collectively, these observations suggest that in the absence of pVHL, constitutively stabilised HIF-2α is not affecting c-MYC-dependent PGC-1β activity.

### 4.12.4 *pVHL re-expression affects nuclear and mitochondrial transcription and translation*

As discussed above, regulation of the PGC family of co-activators occurs mainly on the post-translational level, therefore we explored the possibility that the observed pVHL-dependent changes in ETC protein levels was occurring upstream of protein expression. To determine that the decreased mitochondrial protein expression observed in the 786O-EV cells compared to the 786O-VHL cells was potentially a result of reduced gene transcription, RT-qPCR was performed. Genes encoding at least one protein of each ETC complex was analysed in addition to genes transcribed from both mitochondrial and nuclear genomes. There were no significant differences observed, suggesting a post-transcriptional mechanism. Despite the decreases in protein abundance of mtCO-2 and COX-IV, their mRNA was expressed at similar levels between cell lines.

Since there was no significant alteration in ETC gene transcription between cell lines and in search of a mechanism responsible for the observed deficiencies in ETC protein expression in the absence of pVHL protein in 786O cells, the mitochondrial translational machinery was investigated. As mitochondria contain their own distinct equipment for translation, including a discrete set of ribosomes (Christian and Spremulli, 2012) and a large spectrum of clinical presentations and cellular phenotype have been documented relating to dysfunction in these processes (Rötig, 2011), investigation seemed appropriate. Deficiencies in the synthesis of mitochondrially encoded proteins may lead to mis-assembly and/or deficiency in assembly of ETC holoenzymes and increased turnover of other subunits, as observed elsewhere (Fernández-Vizarra et al., 2009), hence why changes in nuclear encoded proteins may also be observed. There are distinct phases to mitochondrial translation and genes encoding the auxiliary factors involved in each process were selected to study. Translation begins with initiation, whereby the start site on the mRNA is selected

and the initiator methionine-tRNA occupies the p-site of the ribosome. Translation initiation involves mitochondrial initiation factors-2 and -3 (TIF2 and TIF3). Elongation involves mitochondrial elongation factor-Tu (TUFM), elongation factor-Ts (TSFM) and elongation factors G1 and G2 (GFM1 and GFM2) which are responsible for directing the sequential additions of amino acids to the growing polypeptide, corresponding to the specific codons in the mRNA transcript. The final stages are translational termination and mitochondrial ribosomal recycling. It is during these phases, the full-length polypeptide is released and ribosomes are disassembled, mitochondrial ribosomal release factor (MRRF1) is involved at this stage (Christian and Spremulli, 2012). Analysis of transcript expression of these auxiliary factors revealed no significant difference between the 786O-VHL and 786O-EV cells, indicating that pVHL status has no effect on the expression of the mitochondrial translational machinery. However this analysis is limited to those transcripts analysed and is not evidence of the translational process being functional.

In this chapter we have also investigated the effects on the transcript levels of mitochondrial ribosomes. Mitochondria contain a discrete set of ribosomes, distinct from that in the cytoplasm. These are responsible for the translation of mRNA transcripts derived from mitochondrial DNA and could potentially be a factor in the discrepancy between protein and transcript expression observed in mitochondrial ETC subunits in the presence and absence of pVHL. Ribosomal proteins are themselves nuclear encoded and differ in their RNA content and physical properties to cytoplasmic ribosomes (O'Brien, 2003). In this chapter, we have observed significant alterations the expression of a number of mitochondrial ribosomal protein subunits, including *MRPS35*, *MRPL3* and *MRPL30*. These findings are consistent with data obtained from SAGE analyses and micro-arrays detailing the effects of pVHL re-expression in renal carcinoma cells (Harten et al., 2009, Jiang et al., 2003, Hervouet et al., 2008). There are at least 78 proteins that compose the mitochondrial ribosomes, organised in to small (28S) and large (39S) subunits and clearly analysis of them all would require a high through-put method.

Analysis of mitochondrial ribosome assembly may however reveal the global and cellular effects of alterations in expression and clearly confirmation of corresponding changes in protein expression need to be determined. Interestingly, a number of mitochondrial ribosomal proteins also have a distinct moonlighting roles and involvement in cellular processes distinct from structural regulation of mitochondrial translation. MRPS29, also

known as death associated protein-3 (DAP3) has been observed to be involved in apoptosis and (Koc et al., 2001). Mutations have also been documented in a number of these proteins, including *MRPL3*, which presented as mitochondrial cardiomyopathy, associated with decreased ETC activity, ETC protein expression and complex assembly (Galmiche et al., 2011).

*In vitro* mitochondrial translation assays would be necessary to determine the exact effects of loss of pVHL on mitochondrial translation. At this stage, this analysis is outside the scope of this thesis. However, using chloramphenicol to inhibit mitochondrial protein translation would be a preliminary experiment to determine if the effects of pVHL re-expression could be related to mitochondrial protein translation.

### 4.12.5 *pVHL re-expression affects mitochondrial biogenesis*

#### *4.12.5.1 pVHL status affects mitochondrial mass*

In this chapter we have also observed mitochondrial mass to be altered in a manner dependent on pVHL status; the significance of this difference is however difficult to interpret, as the assay is limited by the absence of an independent positive control. However, it can be concluded that the re-expression of pVHL increased median cell fluorescence as detected by mitoview green staining and flow cytometric analysis. The uptake of mitoview green is independent of mitochondrial membrane potential as it binds lipids in the mitochondrial membrane. This observation is intriguing as a decrease in mitochondrial mass would likely explain the decrease in OCR, simply because there is a smaller mitochondrial density, but cannot explain the difference between mitochondrial protein and mRNA expression or the fact that some mitochondrial proteins are significantly affected by pVHL status while others are not. Additionally, there are similar levels of VDAC1 and other integral mitochondrial proteins across the cell lines, which are often and justifiably used as markers for mitochondrial load in a number of assays. Finally, there is a documented maintenance of citrate synthase activity between the cell lines, often used as a measure and control for mitochondrial abundance (Hervouet et al., 2005).

Mitoview green, however does not directly measure mitochondrial number or amount and hence mitochondrial mass *per se*, but mitochondrial lipid content. It would be appropriate to repeat the mitochondrial mass experiments using the well characterised generic nonyl acridine orange (NAO). When a single molecule of CL is excited at 488nm it emits a green

fluorescence which is typically measured and reported as a measure of mitochondrial mass. However, it has been observed that two molecules of NAO can bind one molecule of CL which results in a red fluorescence, when excited under the same conditions. This red fluorescence has been demonstrated to be a more accurate indicator of the true CL content of a cell as it is a function of the unusual diacidic nature of CL compared to other lipids. Menadione could be used as a positive control as it has been shown to decrease CL content through the production of ROS (Davis, 2002, Garcia Fernandez et al., 2004). There is however still confusion over whether the uptake and distribution of NAO is truly membrane potential independent (Jacobson et al., 2002) and therefore results must be carefully considered and if differences are present, full lipid analysis by mass spectrophotometry (MS) or radio-labelled phosphorous may be appropriate. Even analysis using NAO in fixed cells by flow cytometry would perhaps be worthwhile to pursue in future experiments.

The number and characteristics of the mitochondrial proteins affected raises the question of whether the lipid composition of the inner membrane is affected by pVHL status. The expression of proteins that comprise the $F_1$-ATPase complex do not change in the absence of pVHL, yet this is a component of the OxPhos machinery and the ATP6 subunit protein expression does change. The $F_1$-ATPase can however exist as a separate entity, detached from the channel and has even been shown to be present outside the mitochondria and potentially moonlights as a cell surface receptor for apolipoprotein A1 and angiostatin among other ligands (Champagne et al., 2006).

Other proteins investigated are not inner membrane associated, such as VDAC1, which is outer membrane, PHB1 and HSP60. To explore the possibility that the changes in protein expression in the OxPhos subunits are related to inner membrane integrity or composition, distinct proteins of the mitochondrial inner membrane need to be explored, TIMM10, a translocase of the mitochondrial inner membrane for example. Published data also suggests that ANT1, the inner membrane translocase is unaffected through pVHL re-expression (Hervouet et al., 2005). It may however be the role of CL in the organisation and assembly of higher order oligomeric complexes and super complexes, that is responsible for the ETC protein differences between pVHL positive and pVHL negative cell lines (Wittig and Schägger, 2009).

#### *4.12.5.2 Potential role of cardiolipin in the expression of ETC protein expression*

CL is an interesting and unique tetra-acyl phospholipid that is unique to mitochondria composing approximately 12-20% of a mitochondrial inner membrane total lipid content (Chicco and Sparagna, 2007, Hatch, 2004). To date there is no data directly linking pVHL with the synthesis or maintenance of CL and initial characterisation of the role of pVHL on transcript expression of enzymes involved in the synthesis of CL gave no significant results (data not shown). There are however striking similarities between defects in the CL synthetic pathway in yeast and the phenotype we observe with loss of pVHL in the 786O cells. Genetic loss of phosphatidylglycerophosphate synthase (*PGS1*) in yeast, which gives rise to loss of phospatidylglycerol and CL causes translational defects whereby proteins of nuclear and mitochondrially encoded subunits of complex IV fail to be translated. This was associated with changes in mitochondrial morphology, failure to grow on non-fermentable carbon sources and eventually loss of mitochondrial DNA (Ostrander et al., 2001). A later study using mitochondrially targeted GFP fused to the *COX4* promoter and re-introduction of *PGS1* led to translation of the COX4-mt GFP suggesting that restoration of mitochondrial lipid restores translation (Su and Dowhan, 2006). There are also similarities with Chinese hamster ovary (CHO) mutant cells deficient for CL. Intracellular ATP was reduced, as was oxygen consumption and complex I activity (Ohtsuka et al., 1993). Other complex activities were however not significantly modified.

CL is required for proper assembly of respiratory super-complexes and their insertion into the membrane. Defects in cardiolipin synthesis or remodelling, as in the case of Barth syndrome and *tafazzin* mutation, levels of individual complexes are affected as well as super-complexes, affecting the efficient coupling between complexes of the ETC (Gonzalvez et al., 2013). Native page would again be useful here to determine if complex and higher-order super-complex assembly of the ETC proteins is affected in addition to their individual protein subunits in the 786O cells.

### 4.12.6 *pVHL and the ECV E3-ligase complex: Mechanism behind the differential effects of pVHL mutants on mitochondria?*

Data obtained in RCC10 cells expressing wild type pVHL and a panel of pVHL mutants revealed a number of interesting insights into the potential mechanism behind the role of pVHL in mediating the mitochondrial ETC protein expression phenotype described in this chapter. Reassuringly there was a direct correlation between the observations in 786O cells

and those in the RCC10 cells. In both lines, the expression of COX-IV and mtCO-2 proteins were higher in pVHL positive compared to pVHL negative cells while expression of VDAC1 and ATPB proteins were unaffected by pVHL status. Additionally, in the RCC10 cells there was no difference observed in the expression of either SDHA or PHB1 proteins across wild type and mutant pVHL cell lines.

Stabilised HIF-2α and downstream target expression has been proposed as the mechanism behind the selective loss of mitochondrial ETC proteins (Hervouet et al., 2008). Intriguingly however, here we found that despite constitutively stabilised HIF-2α in the RCC10-R200W mutant, the phenotype is highly representative of that observed after wild type pVHL expression in both the 786O and RCC10 cell lines (Figure 4.18). The RCC10-R200W mutant is deficient with respect to HIF-α binding capacity (Hickey et al., 2007), however we still observed ETC protein expression at levels equivalent to that of wild type pVHL. The RCC10-N78S mutation gave rise to an intermediate phenotype. COX-IV and mtCO-2 protein levels were between that that of RCC10-pCMV and RCC10-VHL cells, while the levels of ATPB and VDAC1 proteins were unaffected. There are also intriguing distinctions after the introduction of RCC10-D126N and RCC10-S183L mutants, with the former behaving as RCC10-R200W and wild type pVHL and the latter giving rise to a phenotype similar to RCC10-N78S and RCC10-pCMV.

pVHL is a component of the ECV E3-ligase complex, responsible for maintaining substrate specificity and interactions with target proteins. The E3-ligase complex contains RBX1, cullin 2 (Cul2) and elongins B and C (Stebbins et al., 1999, Iwai et al., 1999, Kibel et al., 1995). pVHL directly links to elongin C and this heterodimer interacts with cullin 2-RBX through the scaffold elongin B. This arrangement serves as the mechanism through which the E2-ubiquitin conjugating enzyme is brought into proximity of the pVHL bound substrate (Hacker et al., 2008).

The crystal structure of pVHL was solved in 1999 by Stebbins *et al* (Stebbins et al., 1999), who observed two domains within pVHL, an N-terminal domain, rich in β-sheets and smaller α-helical domain, separated by small polypeptide linking regions. Interactions between pVHL and elongin C were observed within a large portion of the α-domain and small number of amino acids in the β-domain being also necessary for the interaction. The β-domain extends between residues 63-154. The α-domain of pVHL, residues 155-192, contains three α-helices and a fourth helix from elongin C fits in to this arrangement. pVHL

residues 154-156 and 189-194 are linker regions of the protein that separate the α and β domains (Stebbins et al., 1999).

The H1 Helix within the α-domains of pVHL has been observed to make interactions necessary for the stable association of pVHL with elongin C, the most significant being between $Leu^{158}$, $Arg^{161}$ and $Cys^{162}$ (Figure 4.19). These residues are necessary for van der Waals bonding; contacts which are further augmented by $Lys^{159}$, $Val^{165}$, $Val^{166}$, and $Leu^{169}$ (Stebbins et al., 1999).

Contacts between the α-domains and elongin C are also made by $Leu^{178}$, $Ile^{180}$ and $Leu^{184}$, being the most extensive (Stebbins et al., 1999). These residues again sit in the α-domain of pVHL within the other two helices. $Ser^{183}$ sits immediately adjacent to this region and has been predicted to interact with elongin C. Using the Crescendo software programme, Forman *et al*, have predicted that the $Ser^{183}$ residue to interact with elongin C (Forman et al., 2009). Additionally with the proximity of the residue to $Leu^{184}$, mutation at the neighbouring site may alter the orientation of this serine residue and further affect binding. This suggests that the RCC10-S183L mutation may affect ECV complex assembly through interference with the pVHL-elongin C binding interface.

N78S mutation maintains a protein structure similar to that of wild type pVHL (Shmueli et al., 2013), however gives a mitochondrial phenotype that is intermediate and perhaps more reflective of loss of pVHL. This mutation effects the binding of pVHL to HIF-1α (Forman et al., 2009) and additionally predicted to have proximal atom pairs directed toward elongin C (Rechsteiner et al., 2011), suggesting a possible role in the binding and complex assembly. The N78S mutation has also been observed as unstable, hypothesised to be consequence of the lack of complex formation with elongins B and C (Bangiyeva et al., 2009). Inability to bind and complex leads to rapid turnover of pVHL protein by the proteasome (Schoenfeld et al., 2000a).

As predicated for N78S, the R200W mutation has minimal structural perturbations on pVHL protein. However the R200W mutation can maintain interaction with the whole ECV complex as when it is over-expressed its interaction with elongin C, elongin B, cullin 2 and RBX1 has been observed (Hacker et al., 2008). This would suggest that it is the E3-ligase activity of the complex and pVHL-elongin C interaction that is important for the observed mitochondrial phenotype, or at least the stability of the pVHL protein and potentially the

pVHL-mediated turnover and/or binding of an as yet unknown protein is responsible for the mitochondrial phenotype described in this chapter.

As D126N is a novel mutation, there is limited information of how it affects the structure of pVHL and its interaction with elongins B and C. Its position on the protein however is not adjacent to any interacting residues (Stebbins et al., 1999) and prediction suggest that the adjacent amino residues 123, 124, 125, 128 do not share proximal atoms pairs with elongin C (Rechsteiner et al., 2011). This adds weight to the hypothesis that the observed phenotype with loss of pVHL and pVHL mutations is independent of its capacity to recognise HIF-but instead maintain its ability to complex with elongin C and form the ECV E3-ligase machinery.

Interactions that have been observed as necessary for the HIF-α interaction are found in the β-domain of pVHL and extend to residues, $Tyr^{98}$, $Ser^{111}$ and $Trp^{117}$ all of which have been observed to abolish the pVHL recognition of pVHL-HIF-α binding. Ubiquitination however requires an intact α-domain (Ohh et al., 2000).

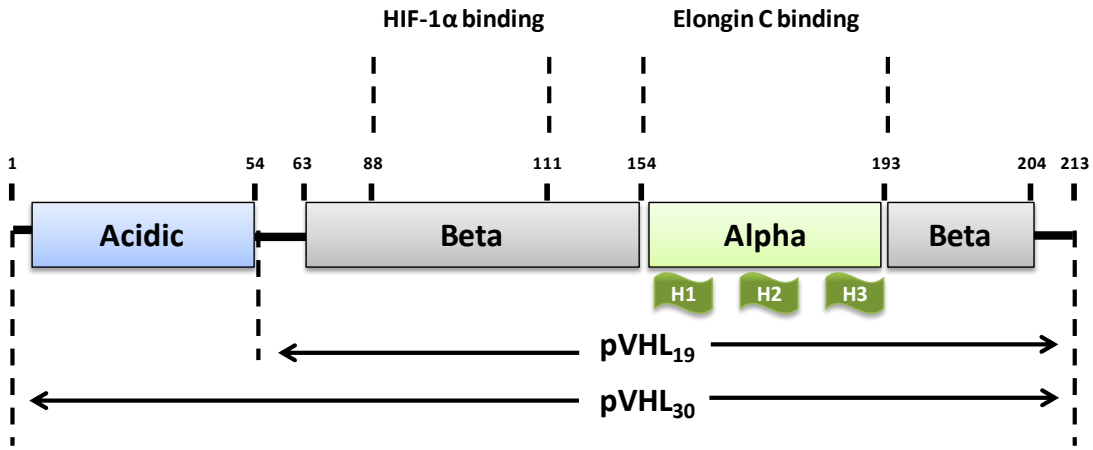


**Figure 4.19: Schematic representation of the pVHL protein.**

**Representation of the pVHL protein highlighting the alpha and beta domains and residues which are responsible for HIF-1α and elongin C binding. H = helix.**

Potentially the pVHL mutants in which we observed a mitochondrial phenotype distinct from wild type pVHL are more representative of an intermediate or pVHL deficient

phenotype, therefore those mutated residues may be less important in maintaining the interaction between pVHL and elongin C, but still playing a role. The mutations that behave similarly to wild type pVHL (R200W and D126N) are predicted not to be involved in this binding. To determine if the binding of pVHL to elongin C is important for the pVHL-mediated increase in mitochondrial protein expression and the observed mitochondrial phenotype, knockdown of elongin C or other component of the ECV E3-ligase complex, in the presence of wild type pVHL could be performed. Knockdown of a distinct ECV E3-ligase component, would allow determination of whether the effects of pVHL loss can be recapitulated. Helix one from the pVHL α-domain contains the most interactions with elongin C, the most significant contacts being $Leu^{158}$, $Cys^{162}$ and $Arg^{161}$ (Stebbins et al., 1999). Mutation of these residues in pVHL and/or the generation of alpha domain mutants and their subsequent expression in a pVHL null background would allow determination of whether the contact with elongin C is necessary for the observed effects on mitochondrial function and protein expression. Additionally, expression of these constructs, used above in a 786O background would be a useful comparator of phenotype where the role of pVHL could be assessed in the context of HIF-2α only and would be more representative, as many renal cell carcinomas have lost HIF-1α expression.

Co-immunoprecipitation or MS of the pVHL-elongin C complex would facilitate the identification of any relationship between disruptions of this interface with respect to the role of pVHL status on mitochondrial function. Determination of the effect of the mutant constructs on E3-ligase complex formation will reveal the extent to which the mutation affects the complex and assessment made as to its relationship between the mitochondrial phenotype observed. Over-expression of pVHL in a cell line already expressing wild type pVHL would prove a useful control as to the role of pVHL protein dose on any mitochondrial phenotype observed. High over-expression of the pVHL protein may be having effects beyond that which would be expected with physiological levels of pVHL.

### 4.12.7 *Potential model of pVHL-mediated effects on mitochondrial function*

It must be considered that pVHL is an extremely well-characterised component of an E3-ligase complex and therefore traditionally will affect processes post-translationally, by directing substrate recognition and turnover by proteasomal degradation. Interestingly inhibition of the 26S proteasome does not rescue this phenotype (data not shown), however pVHL has been observed to bind, sequester and inhibit proteins, including SP1 and

aPKC (Mukhopadhyay et al., 1997, Pal et al., 1997). Additionally, inhibition of the proteasome is likely to have a diverse range of effects on global protein turnover, so specificity toward the pathway of interest may be lost.

Having observed that there is lower expression of a number of ETC subunits in 786O-EV cells compared to 786O-VHL cells, a likely explanation, considering the function of pVHL function in negative regulation, is that pVHL is directing the turnover of distinct protein(s) also involved in negative regulation, perhaps a protease. This would create the phenotype in pVHL defective cells of increased expression of a negative regulator of proteins, therefore promoting turnover and degradation (Figure 4.20). A potential family of protease are the AAA-proteases found in the mitochondria. These are found bound to the inner mitochondrial membrane and participate in quality control of mitochondrial inner membrane proteins, such as those which are found in the ETC. Interestingly pVHL has been observed to interact with p97 (Barry, 2004), a AAA-protease involved in directing proteolytic turnover of MFN1 and MFN2 during parkin-mediated mitophagy (Tanaka et al., 2010).

A second hypothesis would be that pVHL works in concert with a binding partner to regulate the efficient turnover and replacement of damaged/dysfunctional proteins. This scenario could give rise to at least two possibilities: (i) pVHL binding is necessary for the activity of the protein complex, as observed in the ECV-E3 ligase complex, or (ii) the expression of pVHL suppresses the activity of the bound protein, as is observed for SP-1 (Mukhopadhyay et al., 1997). Interestingly, the m-AAA protease, composed of AFG3L2 and paraplegin in humans has been observed as necessary for MRPL32 processing and required for mitochondrial protein translation and ultimately respiratory capacity (Nolden et al., 2005). Protein synthesis is also necessary for the maintenance of mitochondrial DNA. Additionally loss of m-AAA protease in yeast, reduced mitochondrial protein expression and protein synthesis, yeast are respiratory deficient and there are defects in the proteolysis of non-assembled inner membrane proteins and the assembly of respiratory chain complexes, potentially linking a number of observed phenotypes (Arlt et al., 1998).

Intriguingly, selective turnover of mitochondrial ETC proteins has recently been described to be carried out by parkin E3-ligase (Vincow et al., 2013). The role of pVHL in mitochondrial dynamics and autophagy will be discussed in the next chapter (chapter 5); however change in parkin expression may clarify the discrepancy in mitochondrial protein

expression and explain the absence of changes in transcript expression. Finally, the loss of pVHL has been observed, through a number of microarrays and SAGE analysis to affect the expression of many genes, hence the pVHL dependent phenotype could be transcriptional.

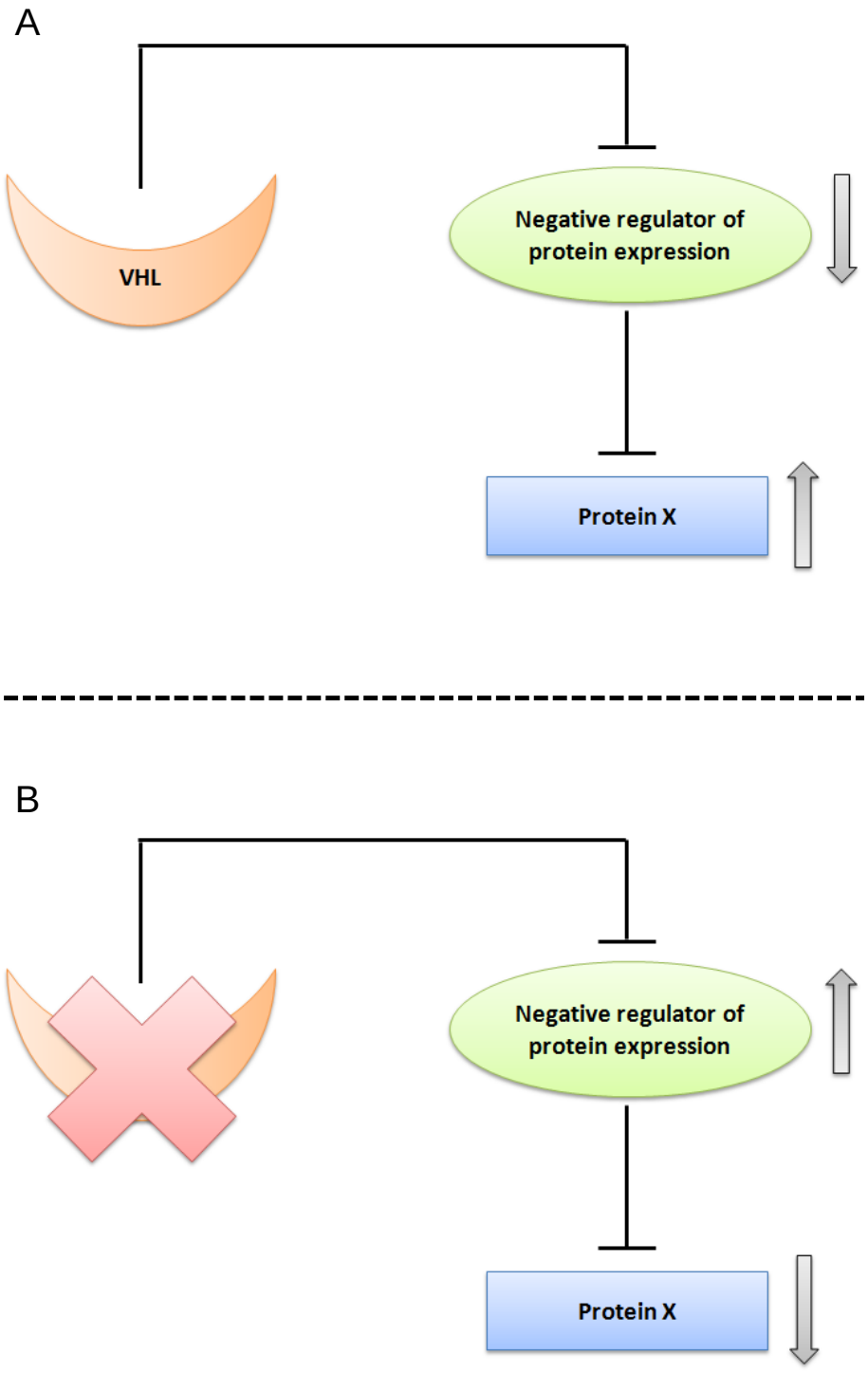


**Figure 4.20: Simplified hypothesis of the role of pVHL protein in the turnover of mitochondrial proteins.**

Future experiments in addition to those detailed above would include bioenergetic analysis of the pVHL mutant RCC10 lines. Preliminary data suggests that the R200W mutation behaves as wild type pVHL and the N78S mutant behaves like pCMV. These observations are in alignment with the data obtained for ETC protein expression, ATP levels and mitochondrial DNA content across the pVHL and mutant cell lines.

Using siRNA to silence elongins B or C, cullin 2 or RBX1 and investigation into whether the pVHL-dependent effects observed can be phenocopied. In line with this, co-immunoprecipitation and/or mass spectrometric analysis of the ECV complex with the relevant mutants would underscore the point of appropriate complex assembly as necessary for the mitochondrial phenotype. Re-expression of the same mutant constructs in to 786O background would eliminate the confounding effects of HIF-1α. Through the use of *VHL*$^{-/-}$ MEFs, interpretation of the effects of pVHL loss in a distinct cell line could be investigated while avoiding an over-expression system.

## 4.13 Summary

There is still much to consider with respect to the role of pVHL in the regulation of mitochondrial function. In this chapter we have observed changes in several mitochondrial parameters and a single causal link is yet to be established, however the data presented here provides the basis for further investigation of a number of potential mechanisms.

It is evident that the pVHL-dependent mitochondrial ETC protein phenotype is post-transcriptional, independent of HIF-1α and HIF-2α and likely independent of ROS. When considering data in this chapter, it is important to consider the true “wild type” cell line. The cells devoid of pVHL are patient derived and pVHL has been re-expressed. In the latter system, the pVHL protein will therefore most likely be present in excess. Further studies are therefore necessary. Using targeted siRNA toward pVHL and other distinct cell lines to determine effects on mitochondrial function are essential. These experiments will require additional consideration of the HIF-1α status. In much of this chapter we have avoided the confounding factor of stabilised HIF-1α and this has aided the delineation of the true, direct role of pVHL. The role of HIF-2α in regulating mitochondrial function will be considered in more detail the final chapter. There is clearly plenty to be resolved in terms of the signalling

pathway in which pVHL appears a major player and how this is affecting many different aspects of mitochondrial biology.

A number of important questions remain:

(i) Is the E3-ligase activity of the ECV E3-ligase complex necessary for the observed mitochondrial phenotype upon pVHL re-expression and can this phenotype be observed in pVHL positive cells lacking another component of the ECV complex?

(ii) Can we recapitulate this phenotype when we knockout or knockdown pVHL in a different cell line/context?

(iii) Is it the pVHL directed turnover of an as yet elusive protein that is responsible for the increase in ETC protein expression and relief of the negative pressure and regulation on mitochondrial proteases or complex assembly proteins?

(iv) Is the mechanism for the observed phenotype at the level of translation (mitoribosome), protein, ETC complex assembly (cardiolipin, assembly factors) or protein turnover?

Answering these questions will provide insight not only into a novel role for pVHL in mitochondrial homeostasis, but applicable to understand further the pathophysiology of CCRCC and VHL disease.

# Chapter 5: The role of pVHL on mitochondrial dynamics and cellular degradative pathways

## 5.1 Introduction

Mitochondria are dynamic organelles, capable of trafficking throughout the cell and able to undergo frequent cycles of fusion and fission that regulate their mass, bioenergetic capacity and turnover. Mitochondrial dynamics are intimately linked with cellular health and coordination of cellular processes. A number of pathologies are associated with disrupted mitochondrial dynamics, which have been extensively reviewed (Liesa et al., 2009). The morphological plasticity of mitochondria is mediated through the regulated expression, localisation and modification of a number of proteins. Specialised proteins such as dynamin-related protein 1 (DRP-1), fission-1 (FIS-1) and mitochondrial fission factor (MFF), mediate mitochondrial fission events and fusion is facilitated through mitofusins -1 and -2 (MFN-1 and MFN-2) and optic atrophy -1 (OPA-1).

Mitochondrial fusion antagonises fission and the balance of these two processes dictates mitochondrial morphology and function. DRP-1 is the master regulator of mitochondrial fission (Smirnova et al., 2001). DRP-1 localises mainly as distinct punctate structures of homo-oligomers in the cytoplasm, with a small proportion of protein associated with the mitochondrial outer membrane. Multimeric DRP-1 has been proposed to wrap around constriction points of the mitochondrion to promote division (Smirnova et al., 2001). Importantly, not all mitochondrially associated DRP-1 occupied sites undergo fission (Hoppins et al., 2007).

The GTPase activity of DRP-1 is essential for mitochondrial membrane constriction and tubulation, as addition of a non-hydrolysable GTP or mutation of the GTPase activity inhibits this function (Yoon et al., 2001). Therefore, DRP-1 mutations that inhibit GTP binding or alternatively the absence of GTP, reduce membrane association of DRP-1 and prevent self-assembly into spirals. In contrast, mutations that inhibit DRP-1 GTPase activity and hydrolysis result in tight and prolonged periods of mitochondrial membrane attachment, without scission. These malfunctions in DRP-1, function to inhibit mitochondrial division i*n vitro* (Hoppins et al., 2007, Yoon et al., 2001).

In addition to a number of other proteins, FIS-1 serves as a receptor for DRP-1 and is localised uniformly on the mitochondrial outer membrane (Losón et al., 2013, Chen and Chan, 2004). In the absence of FIS-1, the targeting and association of DRP-1 with mitochondria is compromised and results in an elongated mitochondrial morphology (Hoppins et al., 2007). However, the best characterised receptor for DRP-1 on the

mitochondrial outer membrane is MFF. The expression of MFF is necessary and essential for DRP-1 recruitment to the mitochondrial membrane, in contrast to FIS-1 where DRP-1 can be recruited in its absence (Losón et al., 2013, Otera et al., 2010). The molecular regulators of mitochondrial inner membrane fission are as yet unknown. There are also a number of proteins that have non-essential regulatory roles in mitochondrial division, including endophilin B1, ganglioside induced differentiation associated protein-1 (GDAP-1) and the mitochondrial ubiquitin ligase, MARCH5/MITOL (Hoppins et al., 2007).

Mitochondrial fusion is mediated through the combined efforts of the mitofusins (MFN-1 and MFN-2) and OPA-1. MFN-1 and MFN-2 are large transmembrane GTPases and although both function in mitochondrial fusion through the same mechanism, their relative activities differ, as does their tissue expression, with MFN-1 present at higher levels in the brain and MFN-2 in the heart and testes (Hoppins et al., 2007). Loss of a single mitofusin can be compensated for through expression of the other, however double knockout causes mitochondrial fragmentation (Chen et al., 2005). Mitofusins form homo- and hetero-dimeric complexes and are required on both adjacent mitochondrial membranes to mediate tethering, which promotes proximity and mitochondrial fusion (Chan, 2012).

OPA-1, also a transmembrane GTPase and related to dynamin, resides on the mitochondrial inner membrane. OPA-1 is responsible for the fusion of mitochondrial inner membrane and loss or mutation of OPA-1 results in mitochondrial fragmentation. Additionally, OPA-1 has been observed to play an important role in mitochondrial cristae maintenance (Chan, 2012, Meeusen et al., 2006).

Mitochondrial content exchange has emerged as an important consequence of mitochondrial fusion and fission events. Mitochondrial DNA is shared between mitochondria upon fusion and disruptions to this process result in respiratory deficits and mitochondrial genome instability (Parone et al., 2008, Vidoni et al., 2013, Chen et al., 2010). Fusion of mitochondria is hypothesised to allow complementation of mitochondrial DNA and protect mitochondria form consequences of accumulation of mitochondrial DNA mutations (Chan, 2012). Mitochondrial fusion and fission events have also been linked to apoptosis and adaptation to cellular stress (Frank et al., 2001). Mitochondria have been observed to elongate in response to nutrient deprivation (Rambold et al., 2011, Gomes et al., 2011), ultra violet radiation and after general inhibition of RNA translation or protein translation (Chan, 2012).

A dynamic relationship exists between mitochondrial bioenergetics and morphology. Inhibition of the ETC and OxPhos machinery has been observed to alter mitochondrial morphology and inhibition of fusion decreases mitochondrial oxygen consumption (Legros et al., 2002, Galloway et al., 2012, Chen et al., 2005). Conversely, inhibition of mitochondrial fission, through DRP-1 targeting, collapses mitochondrial membrane potential, reduces ATP and decreases oxygen consumption (Parone et al., 2008). These observations demonstrate the importance of maintaining a balance between fission and fusion, and the coordinated regulation of these opposing processes maintains cellular homeostasis.

In the last chapter (chapter 4), re-expression of pVHL in renal carcinoma cells was observed to increase cellular oxygen consumption rate, cellular ATP levels, mitochondrial mass and increase expression of a select number of mitochondrial proteins, namely components of the ETC. pVHL has also been observed to have differential effects on mitochondrial ribosomal protein mRNA expression and have significant effects on mitochondrial DNA content, through as yet an unknown mechanism (Hervouet et al., 2008). As yet, an unexplored question is how the loss of pVHL affects mitochondrial morphology. Mitochondrial morphology has been shown to affect bioenergetic capacity, mitochondrial DNA content and conversely cellular stress has been observed to mediate changes in mitochondrial morphology. The extent to which pVHL may govern these processes in renal cells however remains to be elucidated.

## 5.2 Hypothesis

pVHL status affects mitochondrial dynamics and morphology.

## 5.3 Aims

1. To explore the effects of pVHL on mitochondrial morphology.

2. To investigate the extent to which pVHL-mediated changes in morphology are paralleled across cell lines.

3. To determine the mechanism behind morphological changes mediated by pVHL and link these to cellular physiology.

## 5.4 The effect of pVHL status on mitochondrial morphology

Mitochondria are dynamic organelles, undergoing frequent fusion and fission cycles, which govern function and mitochondrial number. Equally mitochondrial function or dysfunction can affect the network and morphology, as such mitochondrial homeostasis relies on the appropriate communication between cell and organelle, disruption of which had been linked to dysfunction and disease.

In order to further explore the relationship between the pVHL and the mitochondrial phenotype described in chapter 4, 786O-VHL and 786O-EV cells were stained with mitoview green and imaged using confocal microscopy to assess mitochondrial morphology. Clear differences in mitochondrial morphology were observed across both 786O cell lines (Figure 5.1). 786O-EV cells exhibited a more fused and elongated mitochondrial phenotype compared to 786O-VHL which appeared to have smaller and more fragmented mitochondria (Figure 5.1). Interestingly, mitochondrial distribution appeared unaffected by pVHL status and mitochondria appeared equally dispersed throughout the cell in both 786O-EV and 786O-VHL cells (Figure 5.1). These data suggest that stable re-expression of functional pVHL in 786O cells increases mitochondrial fragmentation and alters the mitochondrial phenotype from an interconnected fused reticular network to a more ubiquitous distribution of smaller tubules (Figure 5.1).

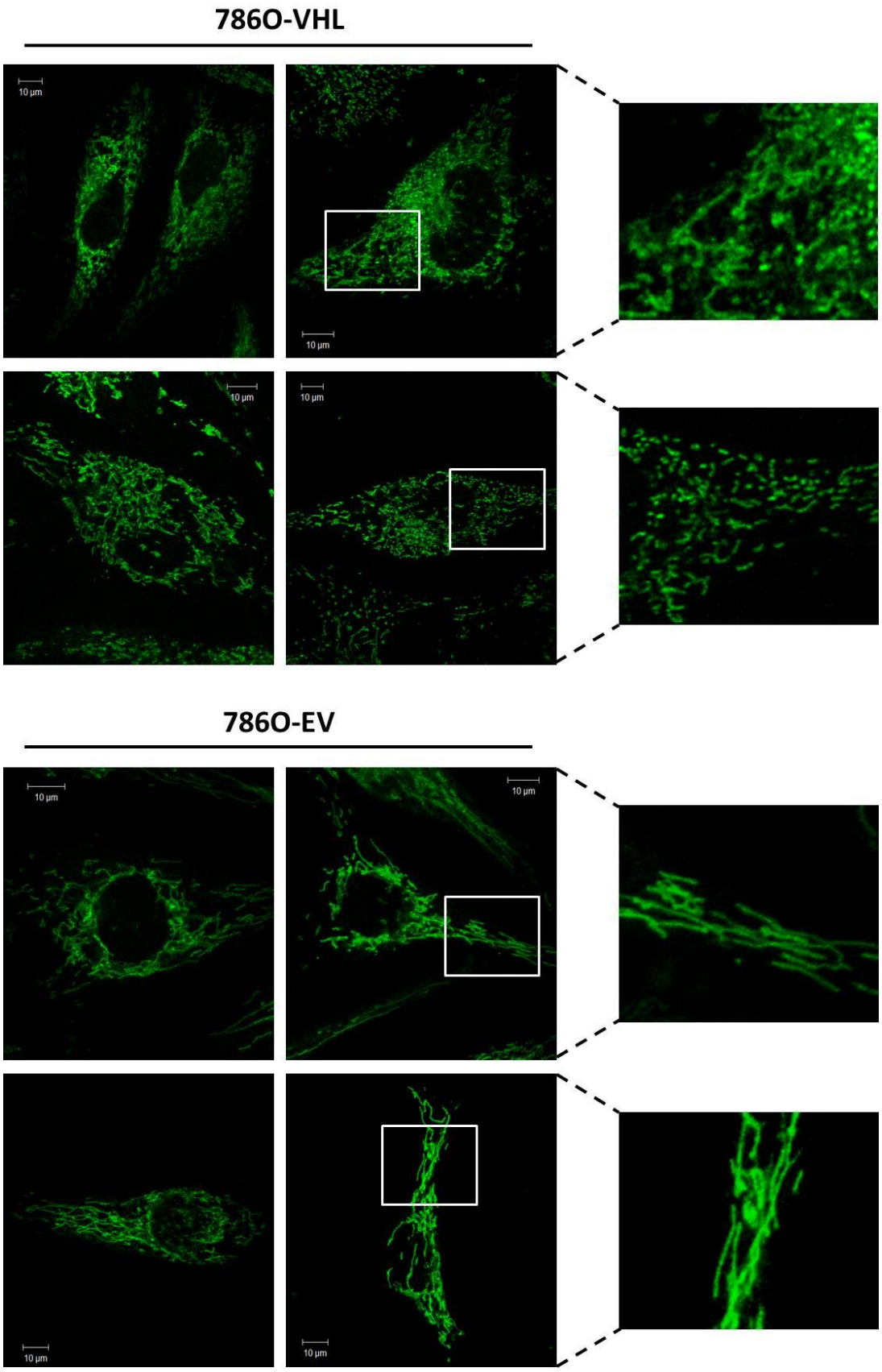
786O-VHL
10 µm
10 µm
10 µm
10 µm
786O-EV
10 µm
10 µm
10 µm
10 µm

**Figure 5.1: pVHL status affects mitochondrial morphology in 786O cells.**

**786O-EV and 786O-VHL cells were stained with 100nM mitoview green for 30 minutes washed and imaged by confocal microscopy. 786O-VHL cells exhibit a network of small mitochondrial units and limited tubular phenotype compared to 786O-EV cells which exhibit fused and elongated mitochondria. Images were acquired with a Zeiss 510 META confocal laser scanning microscope using a 63× oil objective and represent independent fields of view. Right panel shows higher magnified images.**

To further investigate the mitochondrial morphological changes in the 786O cells, electron microscopy (EM; carried out by Mark Turmaine, UCL, UK) was used to image cells and their mitochondria. In agreement with the images obtained by mitoview staining and live-cell imaging (Figure 5.1), ultrastructural analysis revealed that after pVHL re-expression in 786O cells (786O-VHL), mitochondria appeared smaller and more rounded (Figure 5.2A). This is in direct contrast to 786O-EV cells which are devoid of functional pVHL, in which mitochondria appear more elongated, thinner and more tubular (Figure 5.2B). Quantification of mitochondrial length, using Image J software (National Institute of Health, Maryland) measure tool, revealed a statistical difference between the two 786O cell lines (Figure 5.2C). Consistent with the imaging data (Figure 5.2A-B), the average mitochondrial length was significantly smaller in 786O-VHL cells (1.15μm) compared to 786O-EV cells (1.54μm) (Figure 5.2C). This analysis revealed that the length of mitochondria in 786O-VHL cells was approximately 25% smaller than those mitochondria in 786O-EV cells; collectively indicating that re-expression of functional VHL in 786O cells regulates mitochondrial morphology and length.

Overall assessment reveals that mitochondrial cristae appeared normal with equal density between the 786O cell lines. There are no other obvious mitochondrial abnormalities, beyond the difference in overall morphology between the cell lines. Nor are there any obvious changes in membrane contacts or mitochondrial distribution. Images were magnified to allow closer inspection of mitochondria (Figure 5.2A and B, lower panels). Taken together, these data suggest that the changes in morphology and size of mitochondria in pVHL re-expressing 786O cells may in part be responsible for the alteration in mitochondrial function observed previously in chapter 4.

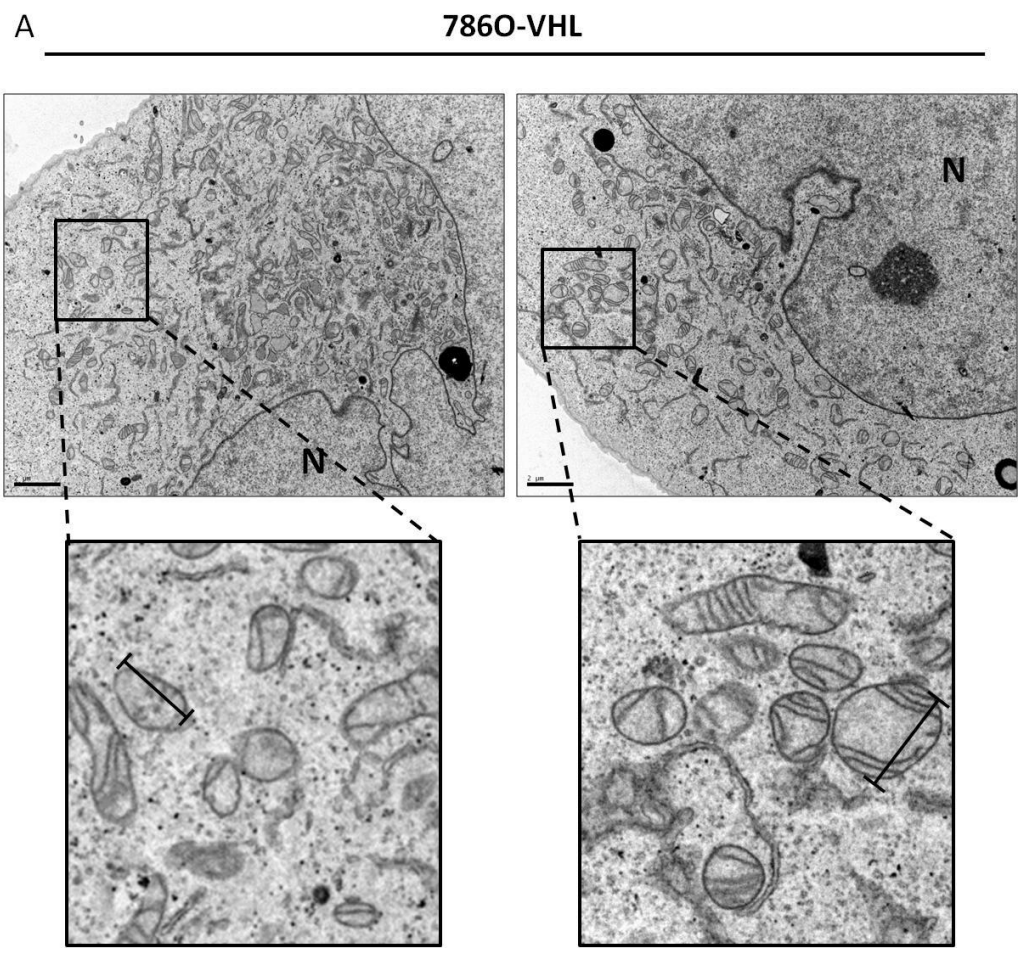
A
786O-VHL
N
N

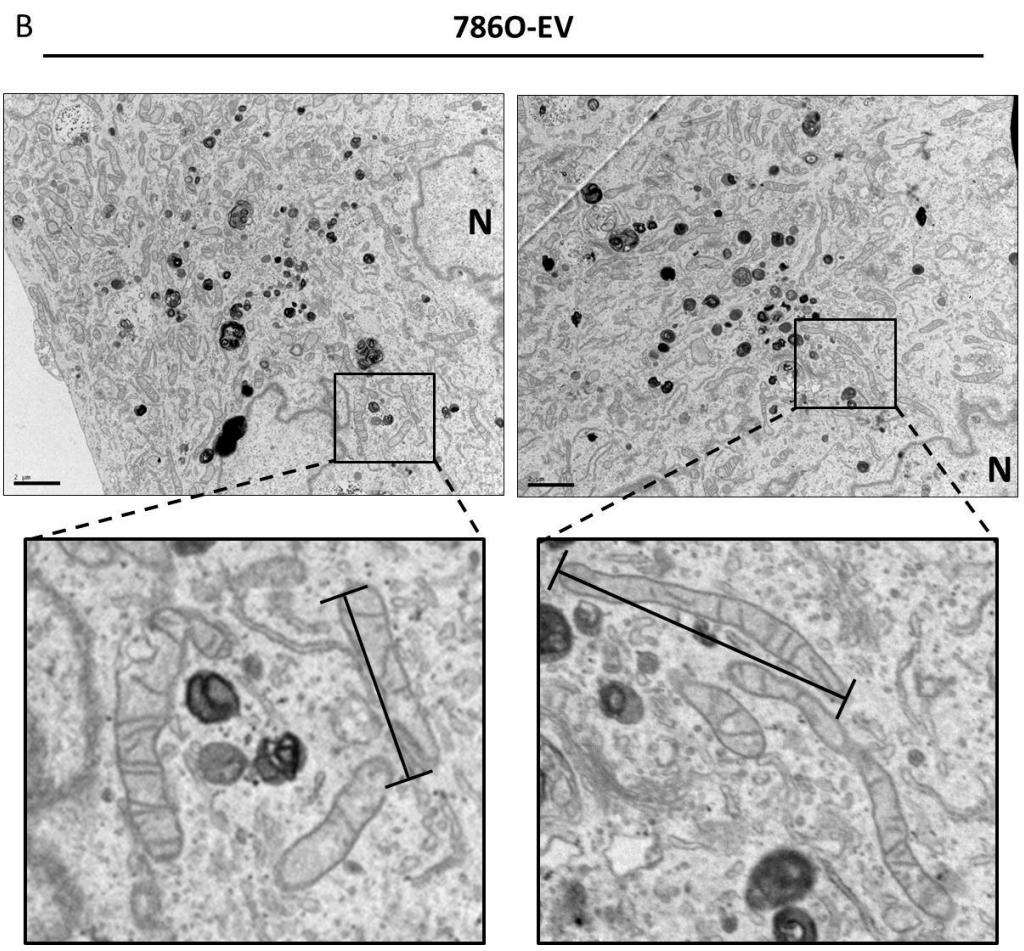
B
786O-EV
N
N

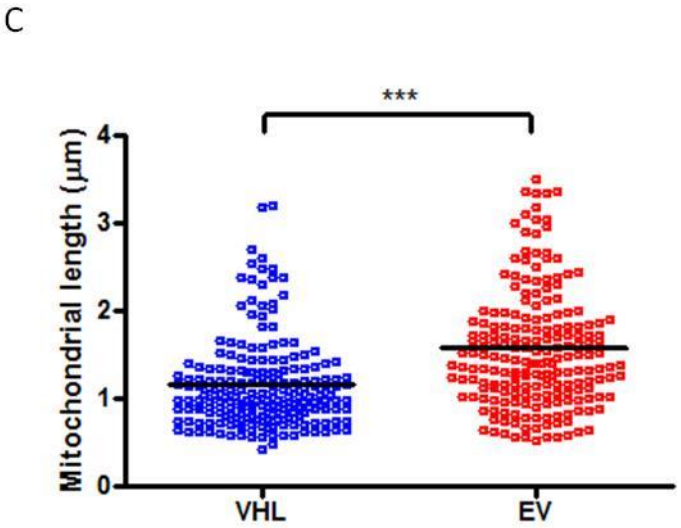
C
***
Mitochondrial length (μm)
0
1
2
3
4
VHL
EV

**Figure 5.2: pVHL status affects mitochondrial morphology and length.**

**786O (786O-EV and 786O-VHL) cells were fixed, sectioned and imaged by electron microscopy (EM). Preparation for imaging and microscopy was performed by Mark Turmaine at UCL. (A) EM images of 786O-VHL cells show small and round mitochondrial morphology. (B) EM images of 786O-EV cells show an elongated tubular mitochondrial network. N = nucleus (C) Graph shows mitochondrial length measured from EM images of 786O-EV (red) and 786O-VHL (blue) cells. Mitochondrial length was measured from the most highly curved membrane through the central axis to the periphery (as indicated, black bar). Measurements were calculated using Image J software (National Institute of Health, Maryland) after calibration of scale using the scale bar. Over 200 mitochondria were scored from single images of 9-10 cells. Data analysed using unpaired, two-tailed t-test (*** p<0.001).**

## 5.5 The effect of pVHL status on the protein expression, phosphorylation and sub-cellular localisation of controllers of mitochondrial fusion and fission

Mitochondrial and cellular homeostasis relies on the appropriate balance between fission and fusion. As discussed above, a number of key proteins, including DRP-1, MFN-1, MFN-2 and OPA-1 dictate mitochondrial morphology, governing the processes of mitochondrial fission and fusion respectively. DRP-1 protein is important in mediating outer membrane fission where FIS-1 protein serves in its recruitment to the outer mitochondrial membrane (Losón et al., 2013). Working in opposition, MFN-1 and MFN-2 are outer mitochondrial membrane proteins that in partnership with OPA-1 to regulate the fusion of outer and inner mitochondrial membranes respectively. The regulation of fission and fusion protein expression, their post-translational modification and turnover, coordinates the role that each protein plays in maintaining mitochondrial architecture, size and morphology.

To determine the contribution of the mitochondrial fusion and fission machinery to the morphological phenotype observed in pVHL re-expressing 786O cells, expression of fission and fusion proteins was investigated. Interestingly, in the 786O-EV cells a global reduction in all fusion and fission proteins assessed was observed, compared to 786O-VHL cells (Figure 5.3A-E). Reduction in isoforms of DRP-1 (Figure 5.3A), MFN-1 (Figure 5.3C), MFN-2 (Figure 5.3D) and OPA-1 (Figure 5.3E) were detected in 786O-EV cells compared to 786O-VHL cells. Interestingly, FIS-1 protein (Figure 5.3C) appears similar between pVHL positive and negative cells. A second interesting observation is that despite the lower levels of total DRP-1 protein in the 786O-EV cells compared to the 786O-VHL cells (Figure 5.3A), an

increase in the phosphorylation at $Ser^{637}$ of DRP-1 was observed (Figure 5.3A). This post-translational modification is a DRP-1 inactivating modification (Chang and Blackstone, 2007) and in the 786O-EV cells, an increase in the ratio of p-DRP-1 ($Ser^{637}$): DRP-1 (total) was detected (Figure 5.3A). DRP-1 $Ser^{616}$ phosphorylation is an activating modification, and was also found to be reduced in the 786O-EV cells compared to the 786O-VHL cells, reflective of protein abundance of total DRP-1 (Figure 5.3). Collectively, these data may suggest that the observed morphological phenotype in the 786O-EV cells compared with the 786O-VHL cells is a consequence of reduced fission, mediated through DRP-1 inhibition and not increased fusion.

There may also be differences in the expression of OPA-1 isoforms and differences in its processing. There are eight isoforms of OPA-1, which each undergoing differential processing due to the presence of cleavage sites in differentially spliced mRNA, giving rise to five bands on western blot (van der Bliek et al., 2013) (Figure 5.3E). The top two protein bands in figure 5.3E constitute the long form of OPA-1 and the lower three protein bands are the short form of OPA-1 (Figure 5.3E). All five OPA-1 protein forms were detected in the 786O cells (Figure 5.3E, labelled 1-5). Forms 2 and 4 of OPA-1 are expected to be present in a 50:50 ratio based on constitutive proteolytic cleavage; however in 786O-EV cells there appeared to be relative reduction in form 4, possibly suggesting differential mRNA splicing or altered proteolytic processing.

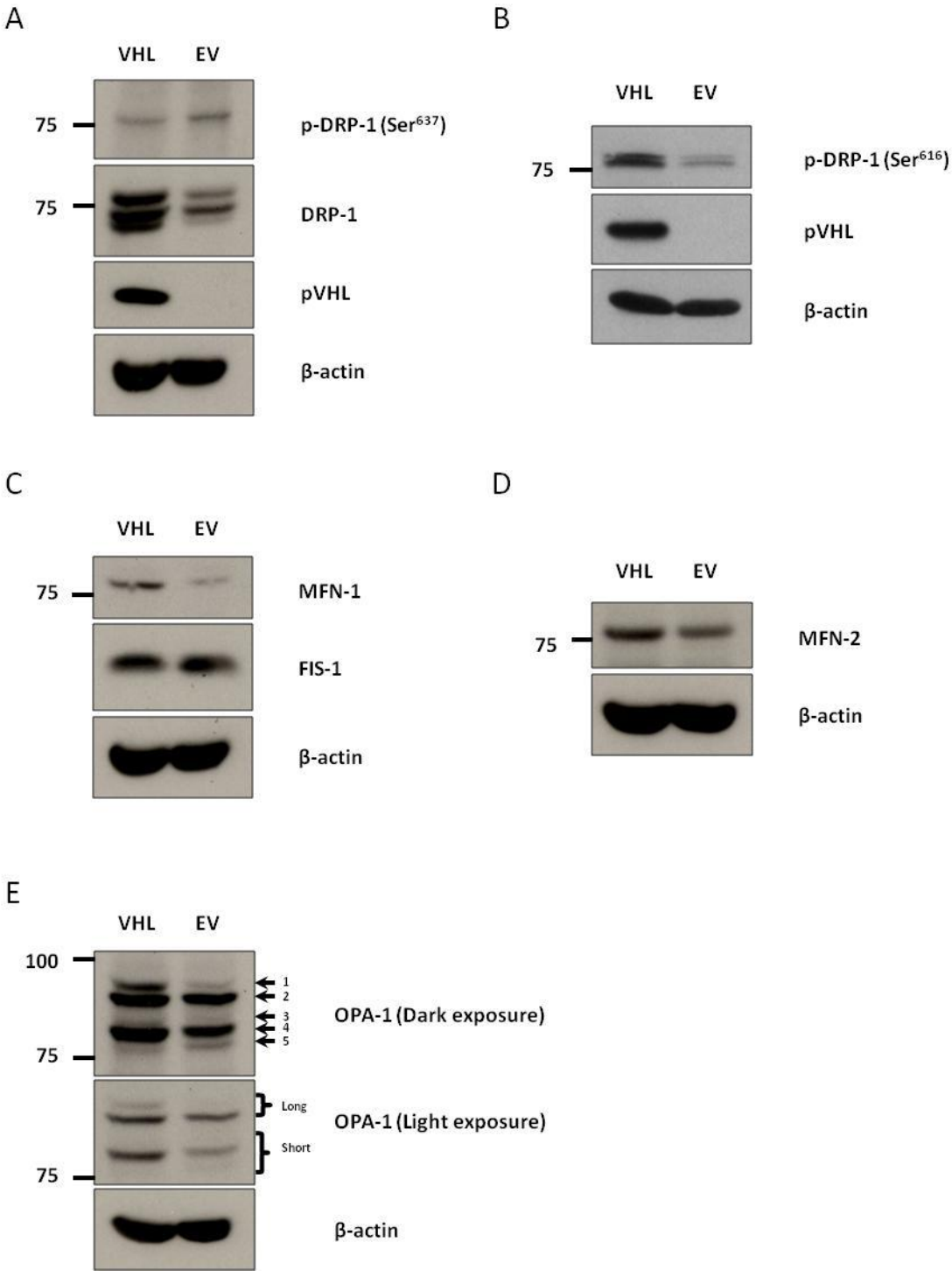
A
VHL
EV
75
75
p-DRP-1 (Ser637)
DRP-1
pVHL
β-actin
B
VHL
EV
75
p-DRP-1 (Ser616)
pVHL
β-actin
C
VHL
EV
75
MFN-1
FIS-1
β-actin
D
VHL
EV
75
MFN-2
β-actin
E
VHL
EV
100
75
75
1
2
3
4
5
OPA-1 (Dark exposure)
Long
Short
OPA-1 (Light exposure)
β-actin

**Figure 5.3: pVHL status affects expression and the post-translational modification of mitochondrial regulators of fusion and fission.**

**(A-E) Western blot analysis of the 786O (786O-VHL (VHL) and 786O-EV (EV)) cells demonstrating the differential effect on mitochondrial dynamic protein expression (DRP-1, MFN-1, MFN-2, FIS-1 and OPA-1) and post-translational modifications (p-DRP-1 ($Ser^{637}$), p-DRP-1 ($Ser^{616}$)). β-actin was used as a control for protein load and pVHL was assessed to confirm appropriate cellular expression.**

Typically DRP-1 resides in the cytosol and mediates mitochondrial fission, through a GTP dependent mechanism after binding to receptors located on the mitochondrial outer membrane (Smirnova et al., 2001). Therefore an alteration in total DRP-1 protein does not reflect that which is involved in mediating fission, as mitochondrially associated DRP-1 protein is not estimated.

To determine the influence of mitochondrially associated DRP-1, the subcellular localisation of endogenous DRP-1 protein was assessed in the 786O cells, in the presence and absence of re-expressed pVHL. As observed above (Figure 5.3C), there was increased total DRP-1 protein expression in the 786O-VHL cells compared to the 786O-EV cells (Figure 5.4; Load - lanes 1 and 2). Because of the clear difference in total DRP-1 protein expression between the 786O-VHL and 786O-EV cell lines, there was also a relative difference observed in the in DRP-1 protein in the cytosolic and mitochondrial fractions. Indeed, there was reduced DRP-1 protein in total, cytosolic and mitochondrial fractions in 786O-EV compared with 786O-VHL cells.

Interestingly, when comparing total DRP-1 protein levels with respect to total VDAC1, an outer membrane protein and mitochondrial marker, the ratio of total DRP-1 to VDAC1 present in the mitochondrial fraction was also increased in the 786O-VHL cells compared to the 786O-EV cells (Figure 5.4; Mito - lanes 5 and 6). Taken together, these data suggest that in the 786O-VHL cells there is more mitochondrially associated DRP-1 protein and highlights a potential mechanism through which pVHL may influence fission. Increased mitochondrially associated DRP-1 protein correlates with an increase in fragmented mitochondria observed in 786O-VHL cells, however how pVHL does this is yet to be determined.

Additionally, compared to the DRP-1 protein load for 786O-EV cells, there was an unexpected absence of DRP-1 protein observed in both cytosolic and mitochondrial

fractions, suggesting that DRP-1 protein may be localised in another compartment (e.g. nucleus). Indeed, DRP-1 protein has been observed to localise to the nucleus under hypoxia (Chiang et al., 2009). Additionally, in contrast to a previous study (Shiao et al., 2000), no pVHL protein was detected in the mitochondrial fraction, despite high pVHL expression in the 786O-VHL cells.

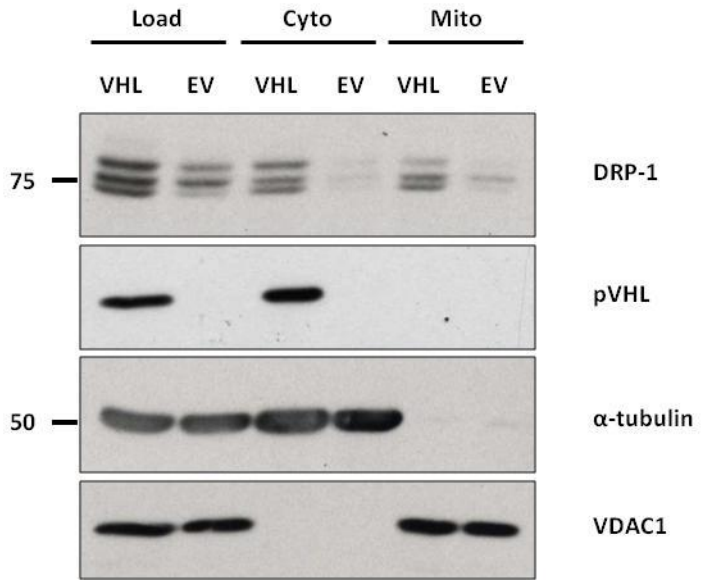


**Figure 5.4: pVHL status affects the subcellular distribution of DRP-1.**

**Subcellular fractionation of 786O (786O-EV (EV) and 786O-VHL (VHL)) cells and western blot analysis demonstrating increased ratio of DRP-1: VDAC1 in 786O-VHL cells compared to 786O-EV cells. α-tubulin and VDAC1 were used markers for the cytosol and mitochondria respectively, and pVHL was assessed to confirm appropriate cellular expression. Load = total cell homogenate, Cyto = cytosolic fraction, Mito = mitochondrial fraction.**

## 5.6 The effect of wild type and mutant pVHL re-expression on mitochondrial morphology in RCC10 cells

Since there were striking differences in the morphology of mitochondria in the presence and absence of functional pVHL protein in the 786O cells (Figure 5.1), it was important to assess other renal carcinoma cell lines and investigate the influence of pVHL mutations on the phenotype. As described previously, RCC10 cells are devoid of functional pVHL and after re-expression of wild type pVHL share a mitochondrial phenotype similar to that of 786O-VHL cells (chapter 4). After introduction of mutant pVHL protein, described

previously in chapter 4, the RCC10-R200W mutation appears to behave as wild type pVHL and RCC10-N78S mutant promoted a more intermediate phenotype (between wild type pVHL and empty vector) with respect to mitochondrial biology and the parameters assessed (chapter 4; Figure 4.16, Figure 4.17 and Figure 4.18).

In order to further assess mitochondrial morphology, RCC10 cells were fixed and the mitochondrial network examined using indirect immunofluorescence toward the ATPB subunit of the $F_1F_O$-ATPase. ATPB protein expression has previously been observed to be unaffected by pVHL status (chapter 4; Figure 4.2 and Figure 4.18). Confocal imaging demonstrated a similar morphological phenotype to that observed in the presence and absence of pVHL in the 786O cells. Like 786O-EV cells, RCC10-pCMV cells are devoid of functional pVHL and had more elongated and tubular mitochondria compared to the smaller more fragmented mitochondria observed in cells with wild type pVHL re-expressed (Figure 5.5 and Figure 5.1).

Interestingly, RCC10 cells expressing the R200W pVHL mutant appeared to exhibit a similar mitochondrial morphology to cells expressing wild type pVHL (Figure 5.5). Notably, mitochondria in both mutant RCC10-R200W and wild type RCC10-VHL cell lines appeared fragmented and less tubular to a similar degree, compared to the RCC10-pCMV cells. These data are consistent with the previously described similarities observed in mitochondrial DNA content, ATP levels and mitochondrial ETC protein expression between the pVHL R200W mutation and wild type pVHL (chapter 4; Figure 4.16, Figure 4.17 and Figure 4.18).

In contrast, the RCC10-N78S cells exhibited a mitochondrial morphology similar to the RCC10-pCMV cells (Figure 5.5). RCC10 cells expressing the N78S pVHL mutant, displayed a more elongated mitochondrial appearance compared to those expressing wild type pVHL, an observation suggesting an intermediate phenotype between RCC10-VHL and RCC10-pCMV.

Interestingly, cell shape is also affected by pVHL status. Loss of pVHL promotes a shift from an epithelial-like morphology to a more elongated cellular morphological phenotype, an observation that has been previously described and reflected in both the 786O and the RCC10 cell lines (Davidowitz et al., 2001). The possibility that the mitochondrial morphological changes observed in these cells are linked to cell shape is of particular

interest, given that mitochondrial dysfunction is associated with metastatic and aggressive disease.

Taken together, these data suggest that pVHL status affects mitochondrial morphology and this is evident across a number of renal carcinoma cell lines. Additionally, given that both wild type and R200W mutant pVHL protein have similar effects on mitochondrial morphology, it is possible that the role of pVHL in regulating mitochondrial morphology is distinct from its role in recognition of HIF-1α.

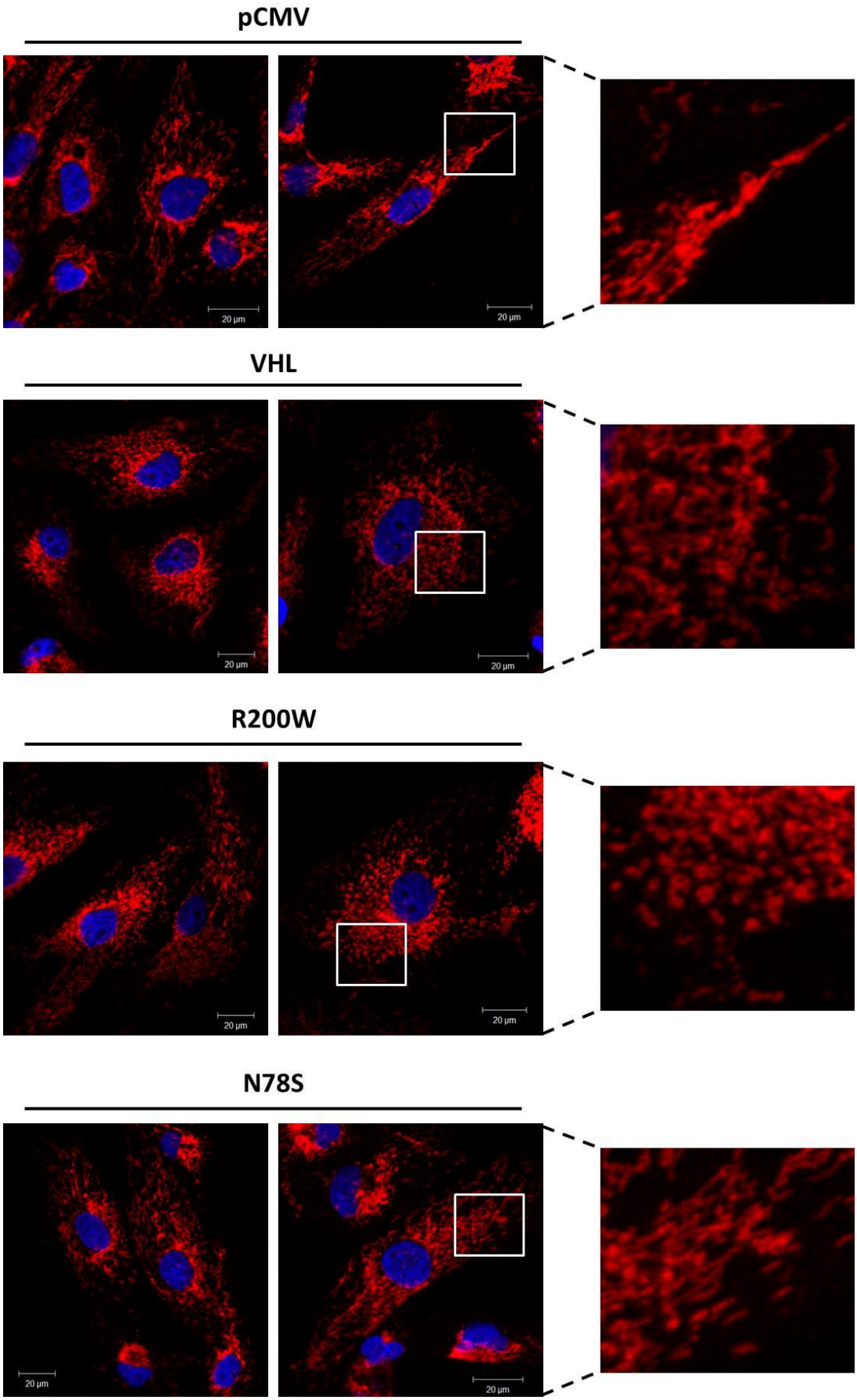
pCMV
20 µm
20 µm
VHL
20 µm
20 µm
R200W
20 µm
20 µm
N78S
20 µm
20 µm

**Figure 5.5: pVHL status affects mitochondrial morphology in RCC10 cells.**

**RCC10 cells expressing empty vector control (pCMV), wild type pVHL (VHL) or pVHL mutants (R200W and N78S) were stained using primary antibody towards ATPB and visualised using secondary antibody conjugated to Alexa Fluor 568 (red), nuclei were stained with DAPI (blue) and imaged using confocal microscopy. Images were acquired with a Zeiss 510 META confocal laser scanning microscope using a 63× oil objective and represent independent fields of view. Right panel shows higher magnified images.**

## 5.7 The effect of pVHL status in the regulation of autophagy

The mechanisms of mitochondrial fusion and fission have been characterised in great detail. However the mechanism of their regulation and the relationship between morphology, dynamics and cell physiology is only recently coming to light and remains comparatively less well understood.

DRP-1 has been implicated in mitochondrial fission necessary for promotion of apoptosis (Frank et al., 2001) and conversely the fusion machinery has been observed to delay or inhibit the process (Neuspiel et al., 2005). The cellular inheritance and intracellular distribution of mitochondrial nucleoids and DNA is also influence by mitochondrial fusion and fission events (Parone et al., 2008, Chen et al., 2010). Mitochondrial fusion has additionally been demonstrated to promote resistance to mitochondrial clearance by starvation-induced autophagy (Gomes et al., 2011, Rambold et al., 2011).

Interestingly, analysis of EM images of 786O cells revealed the presence of autophagosomes in 786O-EV cells and comparative lack of membrane vesicles in those cells expressing wild type pVHL (Figure 5.6A and B). These data suggest that pVHL status may affect autophagy. The magnified EM images (Figure 5.6B) indicated the presence of autophagosomal structures in 786O-EV cells that are consistent with previous studies (Eskelinen, 2008, Klionsky et al., 2012) (Figure 5.6B). The left panel in figure 5.6B highlights an early (Figure 5.6B; *) and late autophagosomal structures (Figure 5.6B; #) and right panel in figure 5.6B shows an early autophagosome (Figure 5.6B; *), with identifiable cytoplasmic structures encapsulated by a double membrane vesicle. Late autophagosomal structures are identified as being more electron dense than those earlier in the degradative pathway. A number of double membrane autophagosomes can also be observed in the non-magnified images in figure 5.6B, which contain clearly visible organelles (Figure 5.6B; arrow heads). These data suggest that, re-expression of pVHL in 786O cells affects the cellular appearance of markers of macroautophagy.

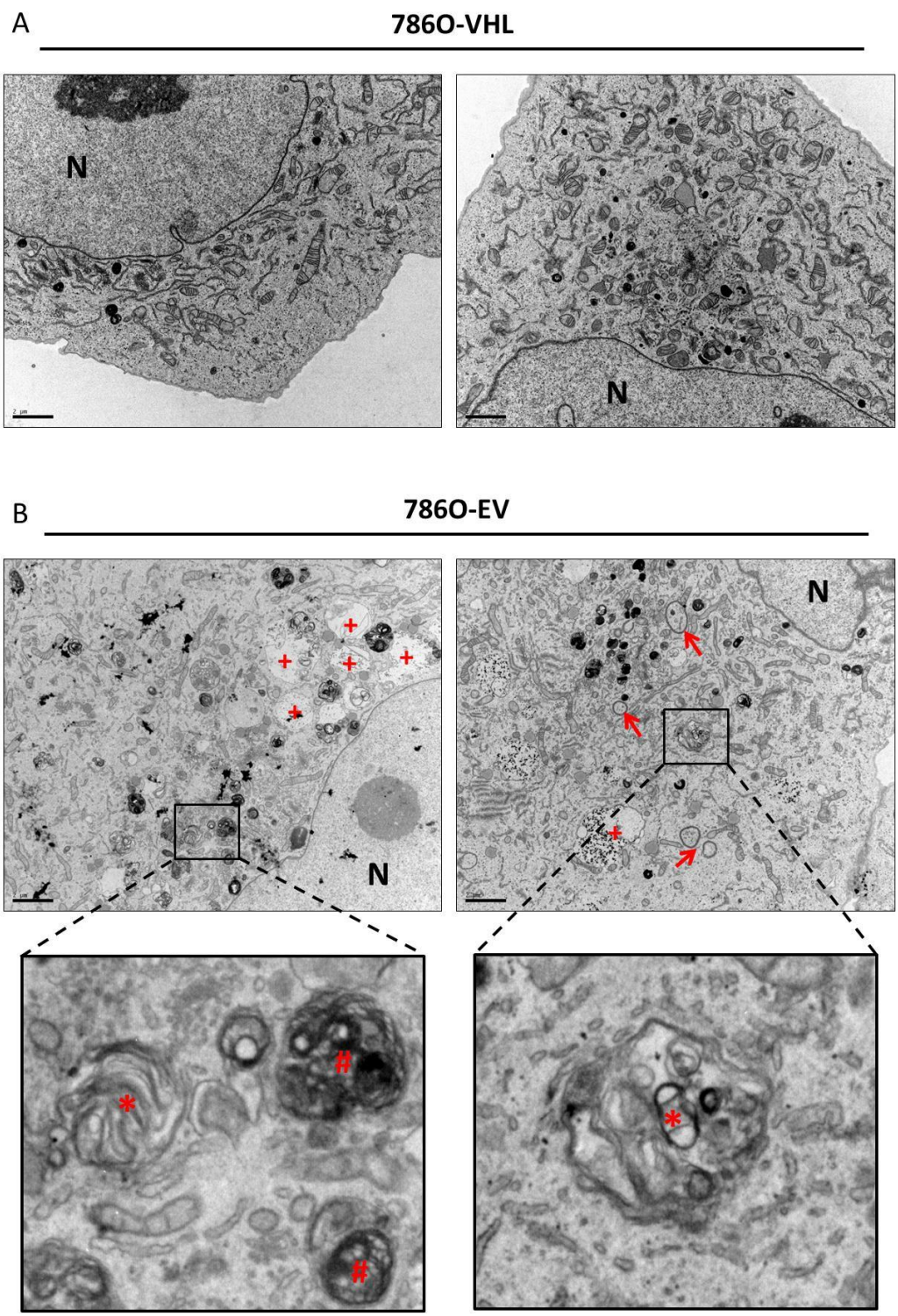
A
786O-VHL
N
N
B
786O-EV
N
N
#
*
#
*

**Figure 5.6: pVHL status affects the cellular appearance of markers of autophagy.**

**786O-EV and 786O-VHL cells were fixed, sectioned and imaged by electron microscopy (EM). Preparation for imaging and microscopy was performed by Mark Turmaine at UCL. EM images of (A) 786O-VHL cells and (B) 786O-EV cells show a reduced number of autophagosomes in A compared with B. N = nucleus, arrow = early autophagosomes, * = autophagosome, # = late autophagosome and + = lysosome. Autophagosomes were identified through comparison of images with published literature and in line with established opinions on structure identification (Eskelinen, 2008, Klionsky et al., 2012). ADDED CELL LABELS on image i.e. 786O-VHL, 786O-EV**

Autophagy is a highly evolutionarily conserved process by which a portion of the cytoplasm, including organelles such as endoplasmic reticulum (ER) and mitochondria, long-lived proteins and pathogens are surrounded non-selectively by a double membrane that forms the autophagosome. After membrane elongation and fusion, the contents are engulfed and sequestered. Autophagosomes are then directed toward the nucleus and the cargo degraded by the lysosome. Physiologically, autophagy occurs continuously at low levels. Various signalling events, in response to stress, such as starvation, hypoxia and infection can induce autophagy (He and Klionsky, 2009, Mizushima, 2007).

This complicated sequence of events, commencing with the selection and recognition of cargo, to formation and expansion of the autophagosomal membrane and ultimate fusion with and degradation by the lysosome is understandably highly regulated and a large number of protein mediators are involved. The ATG proteins are the principal controllers of the autophagic process and are conserved from yeast to mammals and function in a well-studied, coordinated sequence of reactions (He and Klionsky, 2009).

A method by which autophagy can be measured is through evaluation of the lipidation of LC3 protein, of which a number of isoforms exist, the best characterised being LC3B. As discussed in the introduction, LC3 is the only identified protein component of the inner autophagosome membranes. It is synthesised as a precursor and immediately cleaved in the cytoplasm at its C-terminus forming LC3-I. It is then covalently bound to phosphatidylethanolamine by the concerted efforts of ATG7 and ATG3 to form LC3-II, which allows its targeting to both sides of the autophagosome membrane where it is thought to be necessary for the expansion and final fusion of the autophagosome (He and Klionsky, 2009, Ravikumar et al., 2010). Autophagosomes then fuse with endosomes and finally the lysosome, involving lysosomal-associated membrane protein-2 (LAMP-2) and

RAB7. The contents of the autophagosome are degraded by the acid proteases and released back into the cytosol to be re-used in bio-synthetic pathways (He and Klionsky, 2009).

Despite lipidation of LC3B-I increasing the molecular weight of the protein, the increased hydrophobicity of LC3B-II causes the protein to migrate faster by SDS-PAGE, which can be readily observed as a band below the un-modified LC3B-I protein (Klionsky et al., 2012). To investigate the underlying mechanistic basis of the change in number of autophagosomes present after pVHL re-expression, protein from 786O cells was isolated and proteins involved in regulating autophagy were detected by western blot analysis. This revealed clear differences in the basal levels of lipidated LC3B (LC3B-II) protein (Figure 5.7A). There was lower levels of LC3B-II protein observed in 786O-VHL cells compared with 786O-EV cells, however no differences were observed in the levels of a number of other autophagic proteins, including beclin, ATG3 and ATG7 (Figure 5.7A) between the two cell lines. The LC3B-I to LC3B-II ratio is static, as is the presence of autophagosomes. Therefore, under non-stimulated conditions, the decrease in LC3B-II and decreased autophagosome identification by EM, observed with pVHL re-expression could suggest a number of scenarios. (i) There is a decrease in autophagosome formation, or (ii) increased autophagosome turnover, as both scenarios would result in lower protein levels of LC3B-II.

The activity and protein abundance of LC3B can also be regulated on the transcriptional level, hypothesised as a mechanism to replace protein stores during high levels of autophagic turnover (Rouschop et al., 2010). LC3B mRNA has been observed to increase under periods of ER stress and after activation of the unfolded protein response. It was therefore important to measure transcript expression of LC3B-II in the presence and absence of pVHL. To assess whether the changes in observed LC3B protein were due to alteration in the lipidation of the protein and not due to altered transcript expression, LC3B mRNA was analysed using RT-qPCR. Interestingly, there were significantly higher LC3B mRNA levels in 786O-VHL cells compared with 786O-EV cells (Figure 5.7B). These data suggest that higher levels of LC3B protein observed in the 786O-EV cells compared to the 786O-VHL cells are likely due to post-translational lipidation and not due to differences in LC3B mRNA expression.

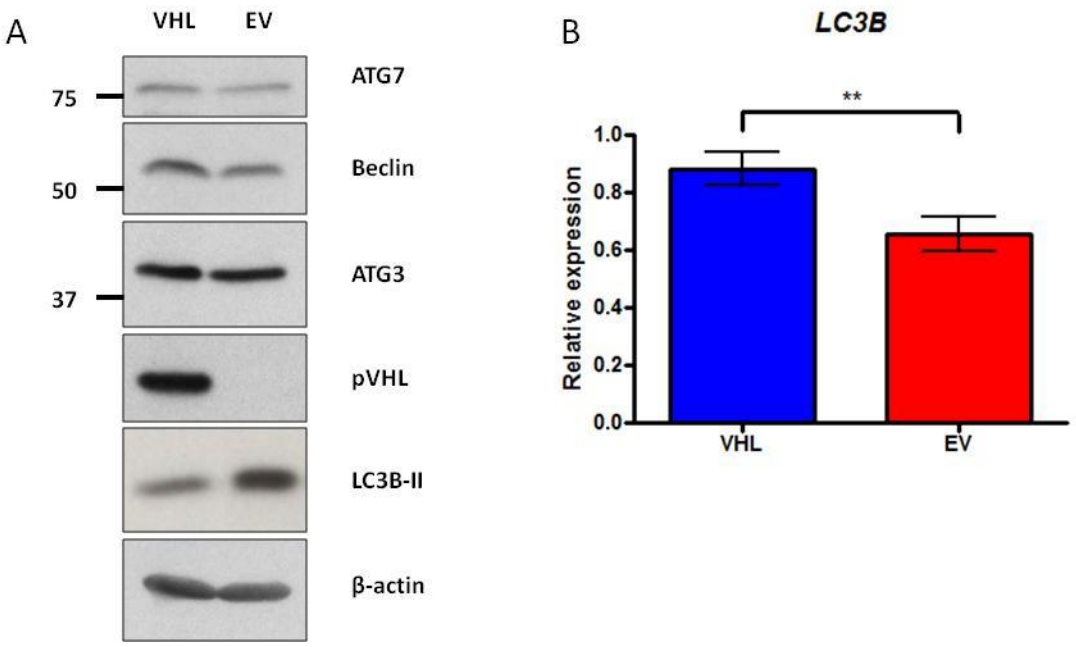


**Figure 5.7: pVHL status affects LC3B protein and mRNA expression.**

**(A) Western blot analysis of 786O (786O-VHL (VHL) and 786O-EV (EV)) cells and the differential effect on autophagic protein expression. Re-expression of pVHL decreases lipidated LC3B under basal conditions, without affecting other autophagic proteins. β-actin and was used as a protein load control and pVHL to confirm re-expression. (B) Graph shows the relative transcript expression of *LC3B* in 786O (786O-EV (EV, red) and 786O-VHL (VHL, blue)) cells using RT-qPCR. A significant difference in *LC3B* expression was observed in the 786O-VHL cells compared to the 786O-EV cells (** p<0.01). Data analysed using the comparative Ct method after normalisation to a single experimental repeat. Values are mean +/- S.E.M (n=4). Data analysed by paired, two-tailed t-test.**

Increases in the accumulation of autophagosomes and presence of LC3B-II under non-stimulated conditions is not representative of autophagic flux, as it could either be consequence of increased generation of autophagosomes (increased autophagy) or a block in the pathway and inhibition of autophagosomal maturation and/or turnover of LC3B-II (decreased autophagy) as discussed (Mizushima et al., 2010). Accumulation of autophagosomes may perhaps be due to delayed trafficking to the lysosomes, reduced fusion between compartments or impaired lysosomal proteolytic activity.

In order to examine the effects of pVHL status on autophagy, an autophagic flux assay was performed. Hanks balanced salt solution (HBSS) was used to induce autophagy, promoting starvation and chloroquine used to block lysosome-mediated proteolysis. Chloroquine increases LC3B-II protein, through neutralisation of the lysosomal pH and inhibition of

autophagosome degradation, increasing membrane associated LC3B-II. Failure to induce LC3B-II in the presence of lysosomal inhibition would suggest a defect or delay earlier in the autophagic process, prior lysosomal degradation (Barth et al., 2010). Chloroquine induced lipidation of LC3B-I is therefore reflective of intact autophagosome synthesis.

In the 786O cells, there was an increase in LC3B-II after the addition of chloroquine in both the presence and absence of pVHL (Figure 5.8). These data suggest that autophagosome synthesis is intact in both the 786O-VHL and 786O-EV cell lines. There remained an increased level of LC3B-II in the 786O-EV cells after chloroquine treatment compared with the 786O-VHL cells. It is likely that the increase in LC3B-II is occurring alongside autophagosome delivery to the lysosome, however LC3B-II synthesis may still be occurring in parallel with impaired lysosomal degradation (Rubinsztein et al., 2009).

Starvation is a mechanism through which autophagy can be induced. *In vitro,* the culture of cells for a number of hours in HBSS promotes autophagy and LC3B-I lipidation to LC3B-II. The addition of HBSS in combination with chloroquine should induce LC3B-II levels to a greater extent than that observed with chloroquine alone, indicating increased autophagic flux. However HBSS had no effect on promoting autophagy in the 786O cells (Figure 5.8). It is possible that the 786O cells are resistant to starvation-induced autophagy, as described elsewhere (Mizushima et al., 2010). Stimulation of autophagy is necessary to further elucidate effects on stress induced autophagic induction, using an alternative to HBSS to induce the pathway.

These data suggest that autophagosome synthesis is intact in both the 786O-VHL and 786O-EV cell lines. Interestingly, pVHL has previously been observed to be involved in autophagy, through regulating the expression of miR-204, inhibiting autophagy through the targeting of LC3B (Mikhaylova et al., 2012).

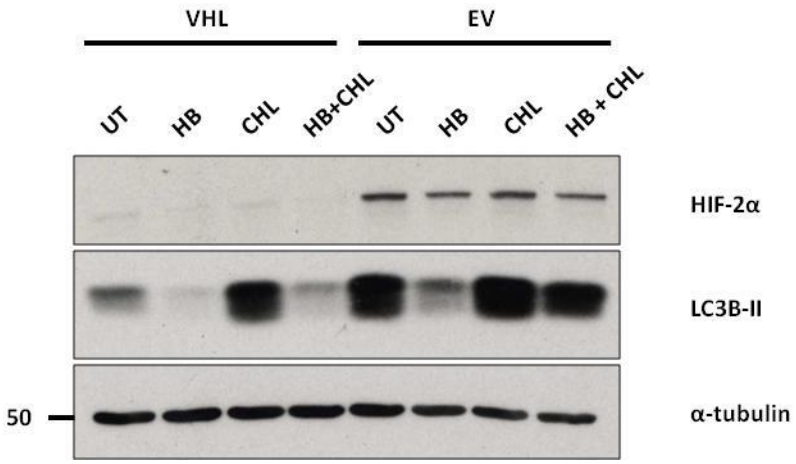


**Figure 5.8: Autophagosome synthesis is maintained in the presence and absence of pVHL. Autophagic flux assay and western blot analysis of 786O (786O-VHL (VHL) and 786O-EV (EV)) cells. Cells were incubated with either HBSS (HB), chloroquine (CHL; 20μM) or combination of both for 2 hours to assess autophagic flux. The increase in LC3B-II protein is representative of intact autophagosome synthesis in both cell lines. HIF-2α expression was assessed as confirmation of cellular phenotype, and α-tubulin was used as a load control.**

## 5.8 The effect of pVHL status on selective mitochondrial autophagy

Autophagy is considered a non-selective process and cytosolic components and organelles that reside in the area of autophagosome formation will be engulfed and degraded. This is in contrast to cargo-specific autophagy, that occurs under basal conditions to remove dysfunctional organelles and proteins (Youle and Narendra, 2011). One selective form of autophagy is the targeting and turnover of mitochondria, known as mitophagy (Lemasters, 2005). Having observed changes in mitochondrial morphology and autophagic parameters in the presence and absence of functional pVHL, experiments were undertaken to assess any effects of pVHL status on the mitophagic machinery.

There are a number of proteins whose role extends to mediating mitophagy. p62, also called sequestosome 1 (SQSTM1), is not specifically involved in mitophagy alone, however provides a molecular binding scaffold which links ubiquitinated substrates on the mitochondria to LC3B-II on the autophagosomal membrane (Pankiv, 2007). PINK1 is a serine/threonine protein kinase and the full-length protein is extremely difficult to detect by SDS-PAGE and western blotting as it is rapidly cleaved and processed under normal physiological conditions. Pharmacological uncoupling or alternative means of mitochondrial

inner membrane depolarisation stabilises the full-length PINK1 protein, through inhibition of the voltage sensitive protease PARL (Deas et al., 2011a). PINK1 accumulates rapidly on mitochondrial outer membrane, an event which promotes the PINK1-parkin dependent peri-nuclear trafficking of mitochondria (Vives-Bauza, 2010, Imai, 2012). Parkin is an E3-ubuquitin ligase and associates with mitochondrial outer membrane in response to stabilised PINK1. This translocation event promotes ubiquitination of mitochondrial outer membrane proteins, their recognition by p62 and autophagic turnover through LC3B-II binding and lysosomal degradation (Narendra et al., 2008, Kawajiri, 2010).

To analyse the expression of mitophagic proteins, 786O-EV and 786O-VHL cell lysates were analysed by SDS-PAGE and western blotting. This analysis revealed significant changes in parkin and p62 protein expression (Figure 5.9). In 786O-VHL cells, parkin protein was increased compared to 786O-EV cells (Figure 5.9A). To investigate whether changes in parkin mRNA was affected by pVHL status, mRNA levels from 786O-VHL and 786O-EV cells were quantified using RT-qPCR. There was an approximate 70% increase in parkin in 786O-VHL cells compared with 786O-EV cells (Figure 5.9B). Interestingly, parkin has also been shown to affect mitochondrial morphology and turnover of ETC proteins (Poole, 2008, Mortiboys et al., 2008, Vincow et al., 2013). In *Drosophila*, parkin mutation has been observed to affect mitochondrial morphology and cristae modelling (Poole, 2008) and in parkin mutant human fibroblasts, a more elongated and branched phenotype has also been noted (Mortiboys et al., 2008). In addition, parkin has recently been observed to mediate the selective turnover of mitochondrial ETC proteins *in vivo* (Vincow et al., 2013).

There was also a significant increase in p62 protein expression in 786O-VHL cells compared with 786O-EV cells (Figure 5.9C), with no significant change in mRNA (Figure 5.9D), suggesting that p62 is modified and/or turned-over at the protein level. Accumulation of p62 protein occurs when macroautophagy is inhibited and decreases under conditions of increased flux and steady-state levels have been used previously to asses autophagic flux (Klionsky, 2010, Klionsky et al., 2012). Steady state assessment of p62 protein levels is however questionable given the role of p62 in processes less well understood. The decrease in p62 protein in 786O-EV cells may confirm that there is increased autophagic flux in these cells compared to those with functional pVHL re-expression. Together these data would likely suggest the increase in LC3B-II in 786O-EV cells is due to increased macroautophagic flux.

Interestingly, p62 functions as a protein adaptor not just for ubiquitinated proteins on the mitochondrial outer membrane but for proteins present elsewhere in the cytosol. In addition to its role as an adapter that binds ubiquitinated substrates on the outer mitochondrial membrane and scaffolding to LC3B-II on the autophagosome membrane, p62 is a cargo receptor and also involved in aggregation of unfolded proteins, leading to their autophagic turnover (Puissant et al., 2012), suggesting alternative hypotheses for the effects of pVHL status on p62 protein abundance.

Collectively, these data demonstrate that pVHL status affects parkin mRNA and protein expression and that wild type pVHL re-expression in 786O cells leads to significantly increased parkin levels. Additionally, the significant difference in p62 protein could indicate increased autophagic turnover in 786O cells devoid of functional pVHL.

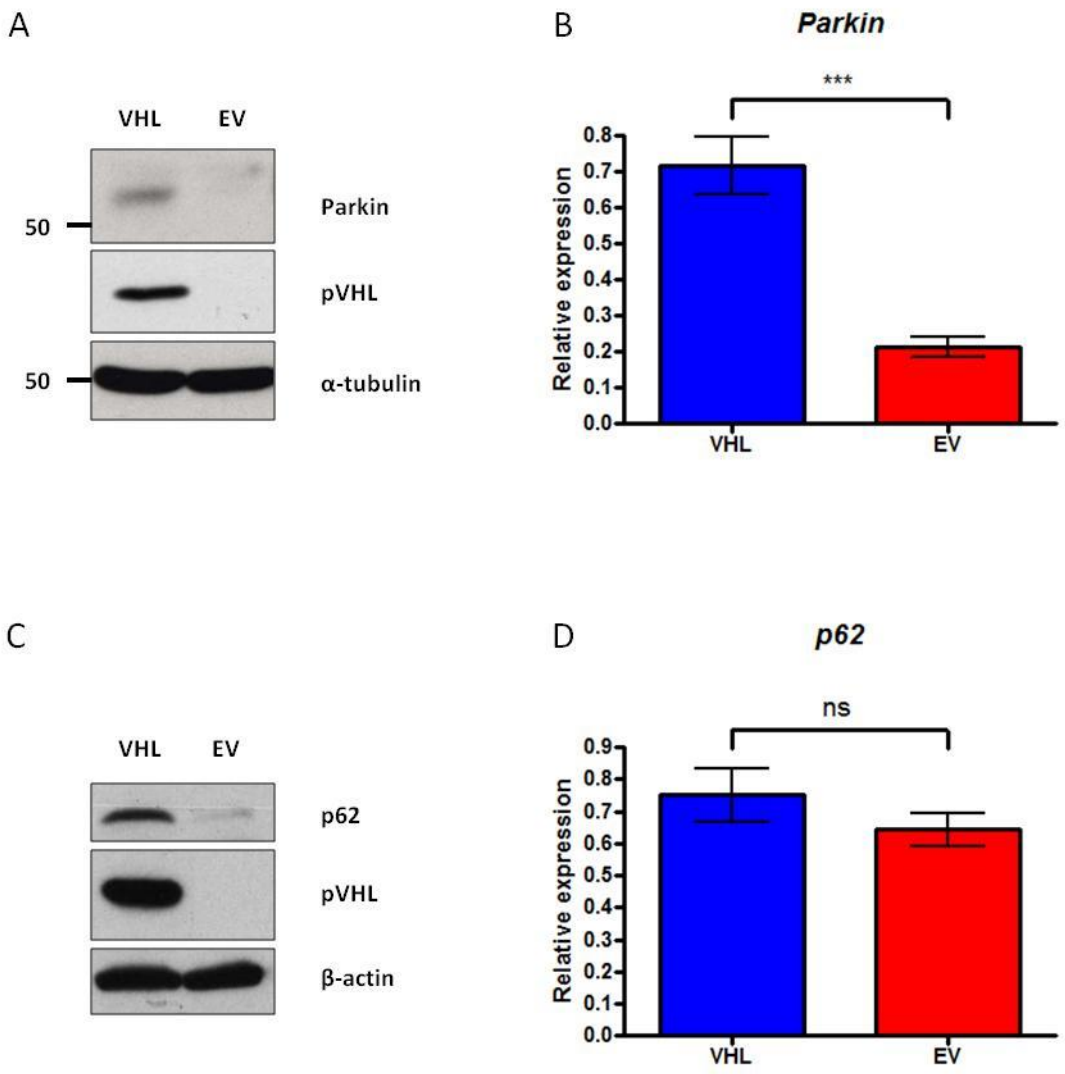


**Figure 5.9: pVHL status affects parkin and p62 expression.**

**(A and C) Western blot analysis of parkin and p62 protein expression in 786O (786O-VHL (VHL) and 786O-EV (EV)) cells, demonstrating an increase of both parkin and p62 protein in the 786O-VHL cells compared to the 786O-EV cells. β-actin was used as a load control and pVHL was assessed to confirm appropriate cellular expression. (B and D) Graphs show RT-qPCR analysis of *parkin* and *p62* from cells described in A, demonstrating a significant differences in *parkin* expression and no significant change in *p62* mRNA expression in the 786O-VHL cells compared with the 786O-EV cells (*** $p<0.001$ and ns $p>0.05$). Data analysed using the comparative Ct method after normalisation to a single experimental repeat. Values are mean +/- S.E.M (n=4). Data analysed by paired, two-tailed t-test.**

## 5.9 Discussion

In chapter 4, we have previously observed and described several biochemical and cell physiological differences in renal carcinoma cells after pVHL re-expression. 786O cells with and without functional pVHL protein have been used to explore the relationship between pVHL status and mitochondrial function. Here, we explore the relationship of pVHL status and mitochondrial morphology, with the aim to link these observations to the pVHL-dependent mitochondrial phenotype described in chapter 4. In this chapter, we have observed alterations in mitochondrial morphology, mitochondrial size and inter-connectivity to be dependent on pVHL, and have correlated these to a potential mechanism through the mitochondrial fusion and fission machinery. Understanding the mechanism of morphological plasticity alone is however insufficient. Efforts were therefore undertaken to highlight the importance of pVHL-mediated mitochondrial morphological alteration from a cellular context and gain insight into a potential molecular mechanism. In addition, we identified autophagy as a cellular process through which mitochondria and particularly mitochondrial morphology may be linked to pVHL status.

### 5.9.1 *Re-expression of pVHL alters mitochondrial morphology through affecting shape and reducing mitochondrial length*

The most striking phenotype observed throughout this investigation into the mitochondrial role of pVHL is the difference in mitochondrial morphology (Figure 5.1). Cells devoid of pVHL function have fused, tubular and elongated mitochondria. Conversely, cells re-expressing wild type VHL have fragmented, round, and distinct mitochondria. These morphological differences were clearly visualised by immunofluorescence and electron microscopy (Figure 5.1 and Figure 5.2). Analysis of the major regulators of mitochondrial dynamics highlighted a global change in the expression both fusion and fission machinery in the 786O cells that was pVHL-dependent, with the expression of the mitochondrially localised DRP-1 receptor FIS-1 remaining unchanged. Interestingly, FIS-1 is also involved in peroxisomal fission and determination of the amount of FIS-1 protein associated with mitochondria versus FIS-1 protein associated with peroxisomes might reveal more subtle differences with regard to the total FIS-1 protein levels. How the loss of any single protein (DRP-1, MFN1/2 and OPA-1) involved in mitochondrial fusion and fission affects the expression of other fusion and fission machinery is an interesting question. The possibility that cellular adaptation to loss of pVHL-dependent expression of a single fusion or fission protein has downstream compensatory effects on another fusion and fission protein

remains unknown. Interestingly loss of DRP-1 has been observed to decrease protein expression of MFN-1 and MFN-2 and alter OPA-1 processing (Ishihara et al., 2009, Möpert et al., 2009).

Although there is clearly less total DRP-1 protein in 786O-EV cells compared with 786O-VHL cells, the levels of phosphorylated ($Ser^{637}$) DRP-1 protein are comparatively higher. DRP-1 is the principal mediator of mitochondrial outer membrane fission and is regulated through a number of complex post-translational modifications, including phosphorylation, nitrosylation, SUMOylation and ubiquitination (Otera et al., 2013). DRP-1 is predominantly localised to the cytoplasm and recruited to mitochondria by receptor proteins, such as FIS-1 and MFF (Losón et al., 2013). DRP-1 is a dynamin-related GTPase and contains multiple domains including an amino-terminal GTPase domain and a regulatory region that resides on the carboxy-terminal end and comprises the GTPase effector domain (GED) (Cribbs and Strack, 2007, Hoppins et al., 2007).

Different cellular protein kinases control the activation state of DRP-1, through phosphorylation on a number of sites, including activation of DRP-1 at $Ser^{616}$ by protein kinase C delta (PKCδ) (Qi et al., 2011), CDK1/cyclin B (Taguchi et al., 2007) or $Ca^{2+}$/calmodulin-dependent protein kinase Iα (CAMK-Iα) (Han et al., 2008), and inactivation at $Ser^{637}$, by protein kinase A (PKA) (Chang and Blackstone, 2007). DRP-1 phosphorylation at a third site, $Ser^{693}$ in cells undergoing apoptosis is mediated through glycogen synthase kinase-3β (GSK3β) (Chou et al., 2012).

Our studies suggest that pVHL status affects the phosphorylation of $Ser^{637}$. Phosphorylation of DRP-1 on $Ser^{637}$ by protein kinase A (PKA) inhibits its capacity to induce mitochondrial fission (Chang and Blackstone, 2007). This post-translational modification inactivates the interaction between the GTPase and the GED of DRP-1, inhibits its GTPase activity and therefore inhibits mitochondrial fission (Chang and Blackstone, 2007). Additionally, increases in cellular cyclic adenine monophosphate (cAMP) have been shown under starvation conditions to activate PKA signalling and phosphorylation of DRP-1 $Ser^{637}$. Inhibition of DRP-1 produces a more fused network and mitochondria which are able to escape autophagic turnover through mitophagy (Gomes et al., 2011). To date, no association exists in the literature as to a relationship between pVHL status and PKA signalling. However future work will involve interrogation of this pathway, either through

use of assays for cyclic AMP and kinase activity, siRNA mediated approaches or pharmacological inhibition of PKA signalling.

Calcineurin is a serine/threonine protein phosphatase and has been demonstrated to dephosphorylate DRP-1 at $Ser^{637}$ and promote its recruitment to mitochondria and induce fission events (Cereghetti et al., 2008). There are no reported links detailing a direct relationship between calcineurin and pVHL, nor are there reports of changes in the calcineurin activating agents, calcium and calmodulin with relation to pVHL status. However, pVHL-mediated DRP-1 $Ser^{637}$ dephosphorylation through calcineurin signalling could just as likely be the mechanism controlling the activation state of DRP-1 in renal carcinoma cells. Understanding the relationship pVHL-calcineurin/calcium signalling may prove revealing in understanding these DRP-1 modification events.

Cycling of DRP-1 protein between the mitochondrial membrane and cytosol is determined by the rates of phosphorylation and dephosphorylation of DRP-1. This in turn controls the extent to which DRP-1-mediated mitochondria fission follows fusion, an event observed to occur *in vitro* in a similar place on the mitochondrion as early as 20 minutes after mitochondrial fusion (Twig, 2008, van der Bliek et al., 2013). DRP-1 recruitment to mitochondria is important for fission to occur. FIS-1 promotes DRP-1 recruitment and levels of FIS-1 at the mitochondrial outer membrane have been demonstrated to regulate mitochondrial morphology (Stojanovski et al., 2004). Enhanced binding of DRP-1 to FIS-1 on the mitochondrial outer membrane is also observed after DRP-1 phosphorylation at $Ser^{616}$ (Han et al., 2008).

In contrast to FIS-1, where knockdown does not completely abolish DRP-1 mitochondrial recruitment, MFF is necessary for DRP-1 mitochondrial localisation and DRP-1-mediated mitochondrial division (Otera et al., 2010). Loss of tumour necrosis factor α (TNFα)-receptor associated protein-1 (TRAP1) (also known as HSP75; heat shock protein 75) has been associated with reduced protein expression of DRP-1 and MFF, promoting mitochondrial fusion (Takamura et al., 2012). Intriguing, pVHL re-expression in 786O cells has been identified as increasing TRAP1 expression by SAGE analysis (Caldwell et al., 2002), potentially linking these observations to the pVHL-dependent morphological phenotype described in this chapter. Investigation in to how MFF expression is potentially determined by pVHL status may help in understanding the increased presence of DRP-1 protein in mitochondrial fractions, after pVHL re-expression in renal carcinoma cells.

There is clearly more phosphorylated ($Ser^{616}$) DRP-1 protein in the 786O-VHL cells compared with 786O-EV cells; this however may reflect the correlative difference in basal levels of total DRP-1 in the respective 786O cell lines. pVHL has been shown to interact directly with the delta and zeta isoforms of protein kinase C (PKCδ and PKCζ respectively) and sequester each in the cytoplasm (Pal et al., 1997). Cytoplasmic sequestration prevents the PKC isoforms from translocating to the plasma membrane and facilitating downstream effects on MAPK signalling. It has also been demonstrated that the activating phosphorylation at $Ser^{579}$ on DRP-1 isoform 3 (corresponding to $Ser^{616}$ on DRP-1 isoform 1 (Otera et al., 2013)) can be mediated through PKCδ (Qi et al., 2011). This raises the possibility that the presence of pVHL in the 786O-VHL renal cells, pVHL binding to PKCδ, maintaining its cytosolic localisation, proximity alone may promote association with cytosolic DRP-1 and subsequent phosphorylation, promoting fission. Importantly cytosolic pVHL-complexed-PKAδ maintains its activity (Pal et al., 1997). It would be interesting to explore the possibility of a pVHL-DRP-1-PKCδ complex which may promote mitochondrial fission. Inhibition of PKC signalling, using RNA interference or a specific inhibitor of the pathways would allow further dissection of the role of protein kinase signalling in the phenotype observed in the presence and absence of functional pVHL. pVHL re-expression in 786O cells has been demonstrated to decrease cyclin dependent kinase-1 (CDK-1) protein expression (Kim et al., 2011). Therefore, VHL-mediated phosphorylation of DRP-1 at $Ser^{616}$ in this scenario is unlikely due to a CDK1-dependent mechanism.

Subcellular fractionation was performed to determine the amount of total DRP-1 protein in the cytosol versus DRP-1 protein associated with mitochondria. The subcellular localisation of endogenous DRP-1 was assessed in the 786O cells, in the presence and absence of functional pVHL. This revealed an increase in the DRP-1: VDAC1 ratio in mitochondrial fractions in 786O cells re-expressing pVHL compared to 786O cells devoid of pVHL. This may suggest more mitochondrially associated DRP-1 protein and provide the mechanism mediating the increase in fragmentation observed in cells expressing wild type pVHL. However, these data must be carefully interpreted as there is clearly higher total DRP1 protein level in 786O-VHL cells compared to 786O-EV cells. Thus, accurately determining the differences in relative abundance DRP-1 protein at the mitochondria between the two cell lines is challenging.

Over-expression of wild type DRP-1 tagged to a fluorescent reporter and high resolution imaging would allow investigation into the degree of DRP-1 cytosolic versus mitochondrial association. Imaging techniques have been utilised to assess DRP-1 mitochondrial localisation after cell treatment with 0.001% digitonin, to rid the cell of the cytosolic pool of DRP-1 making the imaging of DRP-1 associated with mitochondria easier to measure and more quantifiable (Losón et al., 2013). Interestingly, in lung adenocarcinoma, DRP-1 has been observed as nuclear, an event correlating with poor prognosis and mediated through interaction with the human homologue of yeast protein Rad23 protein A (Chiang et al., 2009). Reduced cytosolic DRP-1 in the 786O-EV cells compared with 7860-VHL cells after subcellular fractionation may suggest an abundance of protein elsewhere localised in the cell, perhaps the nucleus. Further work may involve nuclear isolation and western blot analysis or immunofluorescence of endogenous or fluorescently tagged DRP-1 protein to determine subcellular localisation.

The RCC10-pCMV and RCC10-VHL cells exhibit similarities between the respective pVHL negative and positive 786O cell lines respectively, in terms of their mitochondrial morphology. Given that 786O cells do not express HIF-1α, it would suggest that the pVHL-mediated mitochondrial morphological phenotype observed is independent of HIF-1α. Expression of the R200W pVHL mutant shares a morphological phenotype similar to that observed after wild type pVHL re-expression. This is in spite of the differential stabilisation of HIF-2α (Figure 4.15), suggesting the abundance of HIF-2α protein present is not affecting this process and morphological changes appear HIF-2α independent. Expression of the N78S pVHL mutant appears to share morphological characters similar to those of RCC10-pCMV. Similarities between loss of function pVHL and N78S pVHL mutant expression and between wild type and R200W expression may suggest that the correct formation of the ECV E3-ligase complex is the factor responsible for the mitochondrial phenotype and not HIF-recognition (discussed in chapter 4). Morphological data also correlates with the data presented in the previous chapter (chapter 4), where similarities lie in mitochondrial protein expression, total ATP and DNA copy number between pCMV-RCC10 and N78S-RCC10 and between VHL-RCC10 and R200W-RCC10 (Figure 4.16, Figure 4.17 and Figure 4.18). As outlined in the previous chapter, future work will be aimed at delineating the relationship between pVHL mutation, ECV E3-ligase complex formation and mitochondrial phenotype. There is limited information available on the residues responsible and/or necessary for the recognition of substrates for pVHL beyond HIF-α. Identification of the

regions important in the binding to PKCδ may perhaps shed light on a mechanism for pVHL-dependent effects on mitochondrial morphology. Analysis of the DRP-1 phosphorylation states in the RCC10 cells may also confirm the alterations in mitochondrial fission being the mechanism regulating mitochondrial morphology in renal carcinoma cells.

It could be predicted that the increase in oxidative stress in cells with loss of pVHL function would affect mitochondrial morphology (Hervouet et al., 2008). Increased oxidative stress has been associated with mitochondrial fragmentation, contradictory to the data presented here (Wu et al., 2011). However, other reports suggest that through the oxidation of glutathione, mitochondrial fusion is stimulated (Shutt et al., 2012). Paradoxical observations, as to the role of oxidants in the regulation of mitochondrial morphology possibly reflect an early window of mitochondrial protection and resistance to autophagy before mitochondria ultimately yield to cellular stress. It is likely in our system that long-term oxidative stress, experienced in the absence of pVHL is not the cause of the mitochondrial morphological changes observed, as 786O-EV cells exhibit a highly fused network, more reflective of an acute glutathione response. These observations contribute to the evidence that ROS may not be responsible for the observed pVHL-mediated mitochondrial phenotype.

With the data presented here, it is difficult to determine whether re-expression of pVHL is mediating mitochondrial fragmentation, or in cells devoid of functional pVHL mitochondria become fused. One important aspect of future work will be to determine the universality of these pVHL-mediated effects on mitochondrial morphology. Knockdown of pVHL protein using siRNA to determine if the morphological observations can be phenocopied in distinct cell lines would be useful to determine if pVHL status is a determining factor in maintaining morphology outside of a pathological and over-expression system.

### 5.9.2 *Cell biological function of mitochondrial fusion and fission*

Mitochondrial dynamic proteins work in tandem to promote a balance of fusion and fission events and various cellular conditions have been shown to affect these processes. Oxidative stress promotes fusion in the early stages (Shutt et al., 2012) followed by fragmentation (Wu et al., 2011) and starvation has been observed to promote mitochondrial fusion (Rambold et al., 2011, Gomes et al., 2011). Mitochondrial fission is thought to allow distribution of mitochondria to daughter cells after cytokinesis, and observations have been made linking cell cycle progression to mitochondrial morphology

(Margineantu et al., 2002, Taguchi et al., 2007). Alternatively mitochondrial fusion allows for the exchange of mitochondrial components and substrates such as ATP and mitochondrial DNA, allowing complementation of DNA mutation or repair (Chen and Chan, 2004). It has been proposed that mitochondrial morphology can also influence mitochondrial DNA copy number and the balance of fusion and fission influences a nucleoid's access to proteins required for replication (Bogenhagen et al., 2008). Interestingly, cells with reduced mitochondrial fusion or increased mitochondrial fragmentation through genetic loss or reduction of OPA-1 or mitofusins have significantly reduced mitochondrial DNA content. Loss of fusion machinery also affects the mitochondrial capacity to control the distribution of nucleoids and mitochondria have been observed that contain no mitochondrial DNA and are respiratory deficient. There is also reduced respiratory capacity in mouse embryonic fibroblasts lacking mitofusins and OPA-1 (Chan, 2012, Chen et al., 2005).

Cells devoid of functional pVHL have a reduced mitochondrial DNA copy number compared to cells stably re-expressing pVHL. Parone *et al* have observed that knockdown of DRP-1 promotes mitochondrial and cellular dysfunction, without causing cell death (Parone et al., 2008). Upon loss of DRP-1, cells exhibit decreased respiration, ATP levels, mitochondrial membrane potential and growth rates with parallel increase in ROS and autophagy. Immunofluorescence analysis revealed that the increase in LC3 punctae did not co-localise with mitochondria, suggesting they were spared. Interestingly the DRP-1 knockdown also caused approximately 50% reduction in mitochondrial DNA copy number and reduced mitochondrial nucleoid staining (Parone et al., 2008). These observations correlate well with the phenotype observed in 786O cells in the absence of pVHL, suggesting that potentially re-expression of pVHL and promotion of mitochondrial fission is responsible for changes in bioenergetics, mitochondrial DNA maintenance and energy production.

pVHL protein levels change during the cell cycle and a reduction in both pVHL isoforms occurs at late G1 and during mitosis (Liu et al., 2011). It may be worth investigating the role of pVHL on mitochondrial morphology during cell cycle progression. Work in our own lab (Afshan Ahmed, unpublished) and data in the literature suggests that re-expression of pVHL has been shown to reduce the proportion of cells in S-phase (Hughes et al., 2007) and increase cells in G1. Cells in G1 have been observed to have more reticular, interconnected mitochondria than those in S-phase, which have a greater degree of mitochondrial

fragmentation (Margineantu et al., 2002). Mitochondria were shown to hyperfuse at the G1-S boundary and this morphology causes a build-up of cyclin E protein, necessary for S-phase transition (Mitra et al., 2009). The G1-S boundary corresponds with a decrease in pVHL protein and our observations that loss of pVHL promotes mitochondrial elongation (Liu et al., 2011). It may be worth exploring the relationship between mitochondrial morphology and cell cycle in relation to pVHL status. Investigating the levels of cyclin E in these cells and tracking morphology throughout the cell cycle, may allow dissection of any potential relationship.

Collectively, observations to date reflect that a balanced fusion and fission of mitochondria is necessary for cellular homeostasis and that perturbations in either direction are detrimental to the cell. From the data presented here, it is difficult to determine the degree to which mitochondria are dynamically regulated. Whether the 786O-EV cells remain fused or if they undergo frequent fusion and fission cycles is an important issue. Determination of fusion/fission cycling could be accomplished through live cell time-lapse imaging and creation of a mixed population of fluorescently labelled mitochondrial using a fusion assay. A number of methods have been developed to study the frequency of mitochondrial fusion and fission cycles *in vitro.* The first is to manufacture two parallel cultures of the same cell line artificially expressing probes to differentially label mitochondria, achieved through the stable expression of mitochondrial targeted fluorescent reporters. These cells can then be fused using polyethylene glycol, creating hybrid cells with respect to mitochondrial label and can be analysed for merging of colour and mitochondria. Photo-activatable fluorescent proteins have also been utilised to selectively label a subset of mitochondria within a cell and observe the transfer of this fluorescence to unlabelled mitochondria (Chan, 2012). One may hypothesise that cells without pVHL are more static and by not undergoing frequent fusion and fission cycles are unable to share proteins necessary for effective functioning and mitochondrial DNA maintenance and energy production.

It is likely that alterations in mitochondrial morphology dictated by the presence of pVHL are a consequence of more subtle effects on mitochondrial protein expression. Interestingly, a RNA interference screen in *Caenorhabditis elegans* demonstrated abnormal mitochondrial morphology exhibiting either fragmentation or elongation in over 80% of cases after mitochondrial gene knockdown (Ichishita et al., 2008). This suggests that a large proportion of integral mitochondrial proteins are important in regulating morphology and

mitochondrial protein disruption is likely to result in morphological alteration (Ichishita et al., 2008). Interestingly, only 25 of these proteins resulted in mitochondrial elongation, many involved in metabolism or transport of metabolites.

### 5.9.3 *Re-expression of pVHL decreases basal autophagy in cells devoid of functional pVHL protein*

Autophagy is an adaptive process by which the cell non-selectively degrades and recycles cytosolic components. Cellular proteins, organelles and cytoplasm are sequestered, delivered to the lysosome and subsequently degradation by acid hydrolyses (He and Klionsky, 2009). The engulfment of cellular components is accomplished through formation of an isolation membrane of unknown origin. This membrane elongates and encapsulates cytosolic material forming a double membrane vesicle, known as the autophagosome, a specialised unique organelle responsible for this engulfment of cellular protein and organelle recycling (Mizushima, 2007). Three types of autophagy are recognised; microautophagy, chaperone-mediated autophagy and macroautophagy. The process of macroautophagy is considered the main route of cytoplasm-to-lysosome delivery and widely termed “autophagy” (Mizushima, 2005).

Autophagy consists of a number of distinct phases and involves the orchestrated effort of a large number of protein controllers. Autophagy can either be triggered, for the production of amino acids under starvation conditions, known as “induced autophagy” or for the constitutive turnover of cytosolic components. This constitutive turnover is a quality control, homeostatic process involving the removal of damaged/aged organelles and long-lived proteins, known as “basal autophagy” (Mizushima, 2007). Autophagy is regulated by a large number of ATG proteins, which are recruited upon autophagic induction and are highly conserved between yeast and mammalian cells (Meléndez and Neufeld, 2008). Autophagy can be induced by nutrient starvation, such as amino acid and serum starvation in cell culture. The serine/threonine protein kinase mammalian target of rapamycin (mTOR) is considered the master regulator of nutrient sensing and signalling in the cell. Many signals that affect autophagic flux are mediated through mTOR and inhibitors of this pathway such as rapamycin, induce autophagy and are often used experimentally to study this pathway (Mizushima, 2007, He and Klionsky, 2009). Many pathways and proteins in addition to mTOR have also been shown to affect autophagy, including ROS and calcium

signalling, BCL-2 family proteins, AMP activated protein kinase (AMPK) and BNIP3, among others (Mizushima, 2007).

The initial sequence of steps of the process an isolation membrane forms, from an as yet unknown origin, elongates to form the pre-autophagosomal structure (PAS) and begins to engulf and trap cytosolic components before fusing and forming the double membrane vesicle known as the autophagosome (Ravikumar et al., 2010). Autophagosomes then fuse with endosomes to form an intermediate know as an amphisome before fusing with the lysosome and creating the autophagolysosome. The content of the autophagosome are then degraded by the acid proteases within the lysosomal compartment and amino acids recycled (Ravikumar et al., 2010).

Microtubule-associated protein 1 light chain 3 (LC3), is the only identified protein of the inner autophagosome membrane. Synthesised as a pre-cursor, it is cleaved at its C-terminus and forming LC3-I, which resides in the cell cytoplasm. ATG7 and ATG3 are involved in the lipidation of LC3-I with PE to form LC3-II, which allows targeting to both sides of the membrane of the elongating autophagosome. Membrane associated LC3-II is thought to control the membrane size, tethering and hemifusion and thought to be necessary for the expansion and final fusion of the autophagosome (He and Klionsky, 2009, Ravikumar et al., 2010). LC3-II on the outer autophagosome membrane gets recycled and that on the inner membrane degraded after lysosomal fusion. ATG5-ATG12 conjugation is also necessary for elongation and maturation of the of the autophagosome (He and Klionsky, 2009). Autophagosomes are not static structures and utilise the microtubules to traffic to the peri-nuclear region where there is greater abundance of lysosomes and disruption of this process will lead to inhibition of autophagy (Ravikumar et al., 2010). Autophagosomes will fuse with endosomes and then with lysosomes, which requires lysosomal-associated membrane protein-2 (LAMP-2) and RAB7. Autophagosome contents are degraded by the acid proteases and released for utilisation in cellular process to maintain cellular function in response to the autophagic trigger (He and Klionsky, 2009).

Here, we found that pVHL status affects the basal levels of lipidated LC3B protein. In the absence of any stimuli, stable re-expression of pVHL in 786O cells results in a decrease in lipidated LC3B (LC3B-II) under basal conditions compared with 786O cells devoid of functional pVHL. As discussed, interpretation of this could go a number of ways. Either there is increased autophagosome synthesis, or decreased turnover of autophagosomes, in

cells lacking functional pVHL. Newly synthesised LC3B is immediately cleaved to form cytosolic LC3-I. Under conditions that promote autophagy, LC3B-I is post-translationally modified through the addition of a PE group, by a ubiquitin-like system involving ATG7 and ATG3, forming the lipidated form, LC3B-II which becomes associated with the autophagosomal membrane.

Inhibition of the lysosome, achieved after incubation with chloroquine, promotes an increase in LC3B-II in both 786O-VHL and 786O-EV cell lines. The addition of chloroquine, clamps autophagosome degradation, so is a measure of LC3B-II/autophagosome synthesis (Rubinsztein et al., 2009). Independent of pVHL status, the addition of chloroquine increases LC3B-II protein levels, therefore loss of pVHL increases LC3B-II levels both in the presence and absence of lysosomal blockade. It is likely that the increase in synthesis likely occurs alongside delivery to the lysosome, however increased LC3B-II synthesis occurring parallel to decreased degradation may also be an explanation (Rubinsztein et al., 2009). Therefore, this suggests that in both cell lines, autophagosome synthesis is intact. Further analysis is however necessary to determine the extent to which rates of autophagy differ dependent on pVHL status.

Activation of the class III PI3K, VPS34 by the small GTPase RAB5 is required for the initiation of a new phagophore membrane and autophagosome (He and Klionsky, 2009, Ravikumar et al., 2010). VPS34 is a member of a multi-protein complex which includes beclin among others and it is this association which increases the activity of VPS34 (Ravikumar et al., 2010). Beclin can bind a number of proteins; however its availability to bind VPS34 affects autophagosome formation. One of the proteins that binds beclin is BCL-2. This relationship negatively regulates autophagy by sequestering beclin away from VPS34 under nutrient rich conditions and preventing free beclin inducing autophagy (Pattingre et al., 2005). 786O-VHL cells express higher levels of BCL-2 and BCL-XL (Schoenfeld et al., 2000b) and interestingly both BH3-domain proteins have been observed to bind beclin (Maiuri et al., 2007). Although our results demonstrate equal amounts of beclin between 786O-VHL and 786O-EV cells, a hypothesis would be that there is more available beclin in cells without functional pVHL, due the reduction in BCL-XL and BCL-2 protein expression. This may suggest there is proportionally greater free beclin in the 786O-EV cells, contributing to the increase in autophagosomal/autolysosomal structures observed in these cells. Co-

immunoprecipitation of the beclin-BCL-protein interaction may provide insight into this potential mechanism.

pVHL has recently been observed to play a role in regulating autophagy, through both HIF-α dependent and independent mechanisms (Mikhaylova et al., 2012). pVHL has been observed to positively regulate miR-204, independent of hypoxia or PHD inhibition (Mikhaylova et al., 2012). Treatment of cells with miR-204 significantly reduces the number of autophagosomes in pVHL negative cells without effect on those with stable pVHL re-expression. miR-204 inhibits the formation of autophagosomes, through a direct targeting of LC3B. Knockdown of LC3B resulted in significant inhibition of tumour growth *in vivo* suggesting that LC3B-mediated autophagy is necessary for RCC tumour growth. Additionally, through inhibition of HIF-2α, pVHL regulates the expression of LC3C, a paralogue of LC3B, which functions as a tumour suppressor and loss *in vivo* results in the increased incidence of small tumour growth in kidneys of nude mice. Hence there appears to be a distinction between anti-tumourigenic autophagy and pro-tumourigenic autophagy with the presence of pVHL promoting the first and suppressing the latter (Mikhaylova et al., 2012).

Interestingly, we have identified significant differences in the transcript levels of *LC3B* in the presence and absence of functional pVHL, however it is not currently established whether changes in the mRNA expression of autophagic proteins induces or inhibits the autophagic process (Klionsky et al., 2012). However, *LC3B* transcript expression has been shown to increase under conditions of ER stress and hypoxia through activation of the unfolded protein response (Rouschop et al., 2010). Our results demonstrate a reduced *LC3B* transcript expression in cells lacking functional pVHL. Under conditions of ER stress, it is hypothesised that the increase in *LC3B* expression compensates for the enhanced LC3B turnover after prolonged-hypoxia-induced autophagy (Rouschop et al., 2010). On this basis, the observed decrease in expression of *LC3B* mRNA could be an indicator of reduced autophagic flux and the cells requiring lower levels of transcript to replace degraded LC3B-II. However, other indicators suggest the autophagic flux in 786O-EV cells is higher than 786O-VHL. Based on our data, one could hypothesise that the rate of flux in the 786O-EV cells is higher than those with high levels of pVHL re-expressed and a cellular response is to stall the process, limiting excessive cellular autophagy, by reducing *LC3B* transcript

expression. Knockdown and over-expression of pVHL in a distinct cell line would be useful to test this hypothesis.

The observed sensitivity of pVHL negative cells to inhibition of autophagy supports the notion that they are more dependent on the autophagic process. Linking the altered mitochondrial morphology to the decreased autophagic flux after pVHL re-expression, may suggest that in the absence of pVHL, the increase in mitochondrial length and network elongation is a mechanism through which mitochondria are spared from autophagic degradation.

### 5.9.4 *Assays for monitoring autophagy and future work*

To further characterise the relationship between pVHL and autophagy additional work is necessary. Classically electron microscopy is performed after starvation with HBSS and addition of chloroquine to investigate the number of autophagosomes and autolysosomes observed. This would however require expertise in their identification and has often been published incorrectly (Eskelinen, 2008). Autophagosomes are identified as double membrane bound organelles or structure containing undigested cytosolic components and not fused with a lysosome (Mizushima et al., 2010). Autolysosomes are also difficult to identify, as often degradation of cytosolic components deposited from autophagosomes has proceeded to a degree that makes organelle and content identification impossible.

Fluorescence microscopy is a useful tool in studying autophagy. LC3B can be visualised using traditional immunofluorescence methods of endogenous protein or by over-expression of GFP-tagged construct. Punctate distribution would indicate autophagosomal formation as LC3B-II associates with both the inner and outer membrane of the autophagosomes (Mizushima et al., 2010). Changes in the number of punctae per cell could indicate changes in autophagosome number and flux can be determined by combining this approach with inhibition of the lysosome. Using the same GFP-LC3 construct, flux related changes in total LC3B can be interpreted quantitatively either through flow cytometry or qualitatively through SDS-PAGE and western blot. The GFP-LC3 construct is cleaved by the lysosomal proteases and results in free GFP which can be identified by GFP-specific antibodies by immunoblot (Mizushima et al., 2010).

The final assay to monitor autophagic flux would be through use of a red fluorescent protein (RFP) that is stable and unlike GFP not quenched by the lysosome. The tandem

construct would encode RFP-LC3B-GFP and autophagosomes could be tracked as yellow signals and autolysosomes as red (Mizushima et al., 2010). Increases in yellow and red signals would indicate increases increase in autophagic flux, however if red fails to increase, this suggests that there is interference at the terminal end of the process and autophagosome-autolysosome maturation (Mizushima et al., 2010).

The assays detailed above would be necessary first to confirm the increase in autophagy observed in the cells devoid of functional pVHL and that the pathway progresses to completion. It is also important to investigate the role of pVHL in another cellular context. Either through RNA interference and determine change in autophagic flux or over-expression in combination of autophagic induction and observe protection. Removal of mitochondria during periods of starvation is thought to induce a metabolic catastrophe, whereby cells resort to cytosolic ATP to maintain membrane potential, ultimately promoting bioenergetic crisis and cell death (Gomes et al., 2011). Working from the hypothesis that mitochondria elongate in the absence of pVHL to avoid turnover through non-selective autophagy, as observed elsewhere under cellular starvation (Gomes et al., 2011, Rambold et al., 2011), a number of experiments would provide insight in the relationship between pVHL status, mitochondrial morphology and autophagy. If this was the situation, over-expression of wild type DRP-1 in pVHL deficient cells would be expected to precipitate cellular dysfunction, through autophagic mitochondrial degradation and reduce viability. Alternatively, rather than promoting fission through DRP-1 over-expression, inhibiting mitochondrial fusion using RNA interference in cells devoid of functional pVHL, to target the mitofusins would precipitate unopposed fission and allow determination of cell survival/growth.

Inhibition of autophagy using 3-methyladenine (3-MA) and determination of mitochondrial morphology may provide insight into whether the observed tubular fused network present in the cells devoid of functional pVHL protein is a consequence of increased basal autophagy and cellular adaptation to stress through maintenance of mitochondrial functionality and ATP production. Rapamycin promotes autophagy by inhibition of mTOR. Treatment of 786O-VHL cells with rapamycin may provide a correlative link between mitochondrial elongation and autophagy in cells devoid of functional pVHL.

In light of the significant increase in parkin expression in pVHL positive 786O cells, mitophagic flux needs to be assessed. Mitophagic flux can be assessed using the same

assay as for analysis of autophagy, however FCCP and mitochondrial uncoupling is necessary induce the processes in place of HBSS or rapamycin. FCCP depolarises mitochondria, inhibits PINK1 cleavage and facilitates parkin recruitment and ubiquitination of mitochondrial substrates. It is to ubiquitinated proteins which the p62 adaptor protein binds and ultimately facilitates mitochondrial turnover and degradation by the lysosome. This assay would reveal an insight in to any effects on mitophagy regulated by pVHL of the effects on parkin expression.

### 5.9.5 *Re-expression of pVHL affects parkin mRNA and protein expression*

Mitochondrial fission is important for promoting clearance of damaged or depolarised mitochondria through mitochondrial specific autophagy or mitophagy. Having observed a dysfunctional mitochondrial phenotype in the absence of pVHL and the paralleled elongated morphology raises questions over mitochondrial quality control and maintenance of function. Hence, are dysfunctional mitochondrial avoiding mitophagic clearance through morphological changes and down-regulation of quality control proteins? Questions remain over the role of pVHL in the regulation of parkin, but the results are intriguing and knockdown of *VHL* in a distinct cell line and consideration of the presence of HIF-1α protein are required to understand this relationship further.

The increase in parkin expression in the 786O cells after pVHL re-expression is large and highly significant. Parkin is a RING-in-between-RING (RBR) E3-ubiquitin ligase and exhibits low activity *in vitro* and exists mainly in an auto-ubiquitinated conformation (Trempe et al., 2013, Chaugule et al., 2011). It is an unusual E3-ligase as it has multiple substrates, can bind multiple E2-ubiquitin ligases and has been demonstrated to play a role in multiple cellular processes, including mitophagy (Trempe et al., 2013). Why there is a decrease in parkin in these cells remains unanswered and is an interesting question. This reduction in parkin expression has been observed in a number of cancers, with parkin acting as a putative tumour suppressor protein (Veeriah et al., 2010), however not yet identified as being rescued through genetic manipulation as observed in this chapter after pVHL re-expression.

Parkin has also been shown to affect mitochondrial morphology. In *Drosophila melanogaster* the PINK1/parkin pathways has been observed to promote fission and/or inhibit mitochondrial fusion (Deng et al., 2008, Poole, 2008) and in rat hippocampal neurones, over-expression of parkin and PINK1 has been observed to increase mitochondrial number and decrease size, suggesting a role in mediating membrane fission

(Yu et al., 2011). In parkin mutant human fibroblasts, an elongated and branched morphological phenotype is also observed (Mortiboys et al., 2008). With reference to the 786O-VHL cells, the increase in parkin expression may be preventing fusion of mitochondria or promoting fission as described. Alternatively the decrease in the expression of parkin could be an advantage for the cancer cells to avoid autophagy and "hyperfuse" to prevent engulfment by the autophagosome, such as what happens under nutrient starvation (Rambold et al., 2011, Gomes et al., 2011).

There are a number of mechanisms though which parkin may affect the fusion and fission balance of mitochondria. FIS-1 has been identified as being ubiquitinated and physically interacting with parkin (Sarraf et al., 2013) and parkin has been observed to ubiquitinate and promote turnover of DRP-1, precipitating mitochondrial fusion (Wang et al., 2011). Both mitofusins have been observed to be ubiquitinated by parkin and degraded through a mechanism involving the AAA-protease p97 and the proteasome (Tanaka et al., 2010). Ubiquitination of mitofusins, prior to their proteasomal turnover, has been suggested to interfere with their tethering, a pre-requisite for mitochondrial elongation and interesting for the view of the fragmented mitochondria observed in the parkin expressing 786O-VHL cells (Ziviani and Whitworth, 2010). Finally, of note is the potential ubiquitination of MARCH5 by parkin. MARCH5 has been shown to ubiquitinate DRP-1 and mutant MARCH5 or knockdown has been observed to induce mitochondrial elongation (Reddy et al., 2011, Karbowski et al., 2007). The consequence of the parkin mediated ubiquitination of MARCH5 is unknown but remains a possibility for an indirect effect on mitochondrial morphology.

The mitochondrial-depolarisation dependent parkin ubiquitylome has identified a number of additional novel and interesting substrates for parkin, including proteins involved in mitochondrial function, including; import, metabolism, fission and fusion and trafficking (Sarraf et al., 2013). Parkin clearly appears to promote proteasomal turnover of a large number of proteins, however on distinct substrates parkin-mediated non-degradative ubiquitination may serve in signalling and cellular communication (Sarraf et al., 2013) and as such only time will reveal the true diversity and extent as to the role of parkin. Expression of wild type parkin into the 786O-EV cells would be evidence of a role for it in normal physiology if it were to have any influence on mitochondrial DNA copy number or morphology in the 786O cells. In acknowledgment of the decrease in the parkin in the 786O-EV cells compared to the 786O-VHL cells and its characterised role in mitophagy, it

would be useful to look at a time course of chemical uncoupler mediated membrane depolarisation and investigate turnover of established parkin substrates and how this impacts their clearance by autophagy/mitophagy. Experiments using the FK1 clone of anti-ubiquitin antibody and subsequent mitochondrial isolation and western blot analysis or immunofluorescence using a mitochondrial marker would allow investigation of the relative degree of protein ubiquitination in the presence and absence of parkin and pVHL.

It is however possible to link the observed decrease in parkin expression, mitochondrial morphology changes and effects on autophagy observed in the 786O cells in the presence and absence of pVHL. A reduction in parkin expression observed, efficiency of mitochondrial clearance may be limited. To maintain fidelity, mitochondria may be forced to undergo complementation and hence fusion to share components between healthy and dysfunctional mitochondria. This would produce a phenotype with elongated mitochondria, decreased mitochondrial DNA content and increase in ROS (Youle and van der Bliek, 2012).

Further work, expanding on these observations is necessary. A number of methods to monitor mitochondrial autophagy are available. Co-localisation of mitochondria and autophagosome can be employed to determine the delivery of mitochondria to the lysosomal compartment. Transfection with GFP-LC3 and visualisation of a mitochondrial protein, such as translocase of the outer membrane 20 (TOMM20) or VDAC1 and assessing co-localisation of the signal will give an indication of the degree of sequestration. Alternatively co-localisation of mitochondria with the lysosome could be analysed either in fixed cells using markers to each, such LAMP2 for the lysosome. In live cells this can be achieved using MitoTracker® and LysoTracker® dyes, where a merging of colours would indicate completion of fusion (Klionsky et al., 2012). EM would facilitate the identification of mitochondrial cargo within the autophagosomes and could be combined with lysosomal inhibitors to trap the structures. Finally, it may be necessary to induce mitochondrial depolarisation to facilitate an increase in mitophagic flux. It must be considered here though that this a chemical approach and not a physiological. Together these assays would be useful with regard to further delineating the significance of the increased parkin expression observed after pVHL re-expression, its role in mitochondrial function and ultimately renal disease.

Notably, all discussed ubiquitination events occur after mitochondrial depolarisation by pharmacological means and results may be not physiologically relevant as activity of parkin, at least *in vitro* without depolarisation is low. There is still much to learn about the functional consequence of parkin mediated ubiquitination and it is a rapidly expanding field. The observed difference in parkin expression in the 786O cells will undoubtedly have functional effect, but more work is necessary to determine what that is and to what cellular process they belong. Questions remain about the role of parkin without membrane depolarisation. Although it has been observed to have low activity under basal conditions, the altered parkin expression may be important in regulating low level ubiquitination events in the absence of stress and activation of autophagy. Vincow *et al* produced a brilliant study on the role of the PINK1-parkin pathway in *Drosophila melanogaster* to address the question as to the role of this mitophagic pathway *in vivo*, using a proteomic approach to assess mitochondrial protein turnover in parkin null flies (Vincow et al., 2013). They observed that in the absence of parkin, flies demonstrated a slower turnover and significantly prolonged half-life of mitochondrial proteins compared to controls, suggestive of decreased/impaired basal mitophagy. They performed the same study with *atg7* knockout flies and found that as expected mitochondrial protein turnover showed greater dependence on ATG7, as this acts downstream of parkin. However 40 mitochondrial proteins, demonstrated greater dependence on parkin, with electron transport chain components being over-represented in this group. More interestingly these included mitochondrially encoded ETC subunit proteins from all five complexes and a disproportionate number of membrane bound proteins. This suggests parkin has a role in addition to mitophagy, in the selective turnover of respiratory chain proteins, an effect which required PINK1 (Vincow et al., 2013). The authors propose that the selective turnover of these proteins may participate in the complex I pathologies observed with parkin and PINK1 loss of function studies, through mis-folding (Vincow et al., 2013). Parkin-dependent selective ETC protein turnover is also interesting from the perspective of the 786O cells and the lack of parkin the 786O-EV cells as the decreased abundance of ETC complex proteins in these cell may be result of mis-folding, due to decreased parkin-mediated turnover.

### 5.9.6 *The pVHL-p62 relationship*

Interestingly p62 has been shown as necessary for parkin-induced, peri-nuclear clustering of depolarised mitochondria (Okatsu, 2010), but not necessary for mitophagy to occur

(Narendra et al., 2010). Hence, p62 is dispensable and not rate-limiting for parkin-induced mitophagy, suggesting that there are p62 independent mechanisms that are capable of mitochondrial turnover (Narendra et al., 2010). In this chapter, we observed increased basal levels of p62 protein and no parallel change in the transcript levels in 786O cells stably re-expressing pVHL compared with 786O-EV cells. Similarly to LC3B, p62 has been demonstrated to be transcriptionally regulated during autophagy (He and Klionsky, 2009, Klionsky et al., 2012). The absence of a transcriptional change suggests the p62 phenotype observed is on the level of protein stability or turnover.

p62 is a ubiquitin scaffold binding protein and binds directly to LC3B (Bjørkøy et al., 2005). p62 is itself turned-over by the autophagic machinery and is proposed to be the mechanism through which ubiquitinated proteins are aggregated and targeted to the isolation membrane. Therefore p62 serves as the scaffolding protein between ubiquitin and LC3B-II on the autophagosome (Bjørkøy et al., 2009). p62 accumulates when autophagy is inhibited or there are defects in degradation and decreases under periods of autophagic induction. Therefore p62 protein levels are a useful indicator of flux in some scenarios and have been used as such in a number of studies (Klionsky et al., 2012). A role for ubiquitin and p62 in selective autophagy has been well reviewed elsewhere (Kirkin et al., 2009).

Western blot analysis of p62 under conditions of induced autophagy often demonstrates a reduction in protein levels, as observed in the 786O-EV cells compared with 786O-VHL cells, suggesting an increase in autophagic flux in these cells. Interestingly p62 containing aggregates are insoluble under certain lysis conditions, including Triton-X (Klionsky et al., 2012) and likely NP-40, as used throughout these experiments, as both have similar detergent properties. Future experiment would involve using NP-40 lysis buffer (as described in materials and methods) with the addition 1-2% SDS to analyse the p62 levels in the soluble and insoluble fractions in the absence and presence of functional pVHL. This would allow interpretation of the extent of p62 oligomerisation and aggresome formation (Klionsky et al., 2012). Parkin is required for the initial ubiquitination event that allows p62 targeting of mitochondria and subsequent clustering (Okatsu, 2010). Therefore immunofluorescence of p62 and the identification of aggresomes containing mitochondria, would give insight into the consequence of the differential parkin expression between the 786O cells.

## 5.10 Summary

The mechanistic basis underlying the changes in pVHL-mediated mitochondrial morphology, remain unknown, however we can speculate as to their being a role for basal autophagy, DRP-1 and potentially parkin. There is evidence to suggest that mitochondria elongate during autophagy, such that they are spared from degradation and able to maintain cellular viability. Under starvation, cAMP is increased and activates PKA to promote mitochondrial elongation (Gomes et al., 2011). Gomes *et al* identified that during starvation induced autophagy the phosphorylation of DRP-1 at $Ser^{637}$ promotes mitochondrial elongation by negative regulation of fission and maintaining a cytosolic localisation for DRP-1 (Gomes et al., 2011). In the 786O-EV cells, in the absence of functional pVHL, there is a clear increase in the number of autophagosomes and mitochondria appear more elongated compared to 786O cells stably re-expressing wild type pVHL. It is tempting to speculate that the increased basal autophagy is promoting DRP-1 phosphorylation at $Ser^{637}$ to maintain cellular integrity and viability.

Extending the observations of Vincow *et al* (Vincow et al., 2013), loss of parkin expression in cells devoid of functional pVHL may be responsible for the decreased ETC protein expression in these cells. Reduced selective turnover of proteins may precipitate dysfunctional complexes and mis-folding and bioenergetic deficiency. Fusion of dysfunctional mitochondria to allow complementation would link the loss of mitochondrial DNA content observed in the absence of pVHL.

It would be interesting and useful to explore by a proteomic approach pVHL ubiquitination or interacting targets, in a similar experiment to Lai *et al* (Lai et al., 2011) and Sarraf *et al* (Sarraf et al., 2013), to understand the extent of the diversity of pVHL targets and how these impact on mitochondrial biology. Targets of pVHL-mediated ubiquitination have already been observed to serve as recognition sites for the scaffold protein p62 and be targeted to the autophagosome through LC3B binding (Gao et al., 2010). Hence potentially pVHL-mediated ubiquitination of substrates, yet to be elucidated may also be regulated through this mechanism, linking pVHL status to cellular protein/organelle quality control.

Important questions remain:

(i) Does the bioenergetic state of 786O-EV cells dictate mitochondrial shape or does mitochondrial morphology dictate bioenergetic state?

(ii) Is the mechanism of pVHL-mediated mitochondrial morphological change at the level of DRP-1 and/or autophagy and what would be the consequences of reversing this?

(iii) How does the reduction in parkin expression affect mitochondrial turnover, morphology and function?

(iv) What is the relationship between parkin-mediated turnover of mitochondria and/or proteins and the biogenesis of new mitochondria?

(v) Do these observations extend to other forms of renal cell carcinoma and distinct cell lines?

At this stage it is difficult to elucidate cause from effect. Further work with respect to genes and proteins regulated by pVHL expression, analysis of downstream effectors and potentially consideration of pVHL-regulated microRNAs may provide insight into these questions.

# Chapter 6: The role of HIF-2α in the regulation of mitochondrial function and turnover

## 6.1 Introduction

HIF-1α and HIF-2α are highly related proteins, share 48% sequence similarity and are both induced in response to hypoxia (Tian et al., 1997, Hu et al., 2003). A number of gene sets regulated by HIF-1α and HIF-2α are identical; however individually each protein is capable of transactivating non-overlapping, distinct gene sets, suggesting diverse cellular phenotypes can be regulated by the HIFs. For example, HIF-1α specifically induces a variety of proteins involved in the up-regulation of glycolysis and this contributes to the Warburg effect in tumours (Hu et al., 2003), while HIF-2α has little role in promoting a glycolytic phenotype (Hu et al., 2003). Interestingly, differential binding of transcriptional co-factors within the N-terminal transactivation domain of HIF-α is a defining factor in the promotion of specific target gene expression thought to be responsible for different gene sets activated by either HIF-1α or HIF-2α (Hu et al., 2007).

The differential effect of HIF-1α and HIF-2α also extends to their role in tumourigenesis. A clear distinction can be made as to the role of HIF-α proteins in cancer, particularly with respect to renal cell carcinoma (RCC), where HIF-2α appears to function as a tumour promoter and HIF-1α a tumour suppressor (Shen and Kaelin Jr, 2013). Loss of HIF-1α is commonly observed in clear cell renal carcinoma, which frequently stems from deletion of chromosome 14q, on which HIF-1α resides (Shen and Kaelin Jr, 2013). Over-expression of HIF-1α in RCC cell lines, that are devoid of HIF-1α, but express HIF-2α, decreases their proliferation (Shen and Kaelin Jr, 2013, Raval et al., 2005). Conversely, to date most clear cell renal carcinomas analysed, with mutated pVHL express constitutive HIF-2α protein. Loss of HIF-2α protein rescues the tumourigenic phenotype in a similar fashion to pVHL re-expression and causes failure of tumour growth in nude mice (Kondo et al., 2003, Shen and Kaelin Jr, 2013). Interestingly however, HIF-2α has been observed as exhibiting tumour suppressor activities depending on the tumour context (Acker, 2005). The discrepancies between pro- and anti-tumour activities of HIF-2α function are not well understood, but the long-standing belief that HIF-1α and HIF-2α proteins exhibit largely overlapping functions has been dismissed. It is now clear that their roles, albeit coinciding in some instance, are non-redundant, can promote distinct phenotypes and may even have opposing roles when expressed in the same cell type (Keith et al., 2012). Interestingly, HIF-2α protein induction in hypoxia is detected for up to 48 hours, while HIF-1α protein declines by 24 hours (Holmquist-Mengelbier, 2006).

The HIFs form the crossroads of the adaptive response to hypoxia, allowing the cell to survive, proliferate and maintain homeostasis. Importantly, the transcriptional capacity of the HIFs has been observed even under ambient oxygen (Huang et al., 2004, Cramer and Johnson, 2003). Although the half-life of the alpha subunit is approximately three to five minutes, the basal transcriptional role of these factors has been observed as critical and necessary in the number of situations. For example, as discussed in chapter 3, HIF is important for correct heart function. Mice with cardiac-specific knock out of *Hif-1α*, using cre-lox technology and a myosin light chain promoter exhibited contractile dysfunction, due to altered calcium signalling, hypovascularity and changes in energy metabolism (Huang et al., 2004). Cramer *et al* have also observed basal HIF-1α transcription in myeloid cells (macrophages and neutrophils) (Cramer et al., 2003). Conditional loss of HIF-1α in the myeloid lineage leads to dramatically reduced expression of glycolytic genes and decreased cellular ATP pool, affecting myeloid cell activation and bacterial killing. Cramer *et al* suggest that HIF-1α is functioning as a controller of basal metabolism in these cells and has a role in mediating inflammatory capacity (Cramer et al., 2003). Together, these observations suggest that basal transcription through the HIF pathway is important in both physiology and pathophysiology.

When compared with HIF-1α, the role of HIF-2α has been understudied with respect to its role in mitochondrial function and homeostasis. HIF-2α has been shown to regulate antioxidant defence and ROS homeostasis through transcriptional regulation of *Sod2* in the *Epas1*/*Hif-2α*$^{-/-}$ mouse, which exhibits increased oxidative stress as well as a reduced response to oxidative stress (Scortegagna et al., 2003). Loss of HIF-2α protein also affects other mediators of the antioxidant response, such as haem oxygenase and glutathione peroxidise among others (Bertout, 2009, Scortegagna et al., 2003).

To date, only one study investigating the role of global knockout of *Epas1*/*Hif-2α*$^{-/-}$ and the consequence on mitochondria isolated from hepatocytes has been published (Oktay et al., 2007). The global knockout of *Epas1*/*Hif-2α*$^{-/-}$ mice display a mitochondrial disease-like phenotype; have mitochondrial ultra-structural abnormalities and compensatory up-regulation of succinate dehydrogenase and cytochrome c oxidase. The phenotype of these mice closely resembles the phenotype of the *Sod2* (Sod2$^{-/-}$) knockout mice (Oktay et al., 2007). SOD2 has previously been identified as a HIF-2 transcriptional target and is transcriptionally up-regulated by HIF-2α over-expression (Scortegagna et al., 2003).

Mitochondria isolated from *Epas1*/*Hif-2α*$^{-/-}$ mice exhibited increased oxidative stress, reduced respiration, sensitised mPTP opening and reduced activity of mitochondrial aconitase and α-ketoglutarate dehydrogenase (αKGDH), while ETC complex activities were retained (Oktay et al., 2007). The observed phenotype was a consequence of oxidative damage to αKGDH and down-regulation of the HIF-2α target gene, *frataxin*, a chaperone for aconitase. Loss of frataxin promoted oxidative damage to aconitase and highlighted the role of HIF-2α basal transcription in healthy physiology under ambient oxygen (Oktay et al., 2007).

In this chapter, as in chapters 4 and 5, the 786O cell model was utilised to understand the functional consequences of pVHL's effects on mitochondrial function. Patient derived 786O cells exhibit constitutively stabilised HIF-2α due to biallelic inactivation of *VHL*. The role of HIF-2α in the pVHL-dependent alterations in mitochondrial proteins has been addressed in chapter 4 and will be further explored in this chapter. Specifically, the role of constitutively expressed HIF-2α protein will be addressed with respect to distinct mitochondrial parameters after pVHL loss, including effects on bioenergetics, mitochondrial DNA maintenance, morphology and autophagy. Additionally the role of basal HIF-2α protein will be addressed using RNAi techniques.

## 6.2 Hypothesis

HIF-2α is important for the maintenance of mitochondrial homeostasis.

## 6.3 Aims

1. To characterise the role of HIF-2α in pVHL-mediated regulation of mitochondria.

2. To evaluate the effects of *HIF-2α* silencing on mitochondrial function and homeostasis.

3. To investigate the mechanistic basis for the role of HIF-2α in pVHL-dependent and -independent regulation of mitochondrial function.

## 6.4 The effect of silencing *HIF-2α* on target gene expression in the 786O cell model

The 786O cell model has proved a useful system for dissecting the role of pVHL in regulating mitochondrial function (chapters 4 and 5). Using the 786O cells, the effects of both constitutively stabilised HIF-2α, and loss of HIF-2α (using siRNA), can be investigated. 786O cells lack functional pVHL and HIF-1α protein, allowing specific dissection of the role of HIF-2α, without any compensatory or confounding effects of stabilised HIF-1α, providing rationale for their use. The evaluation of 786O cells stably re-expressing functional pVHL has also provided a platform to understand how pVHL influences mitochondrial function (chapters 4 and 5). This chapter aims to investigate the role of HIF-2α in the pVHL-dependent mitochondrial effects described previously (chapters 4 and 5).

To confirm the suitability and ease of manipulation of the 786O cell model, *HIF-2α* was silenced in both the 786O-EV and 786O-VHL cell lines and compared to a non-silencing control (NSC) siRNA. Protein samples were assessed by SDS-PAGE and western blot analysis to confirm *HIF-2α* knockdown and demonstrate consequential effects on HIF-2α downstream targets (GLUT-1). HIF-2α protein could be effectively knocked-down in the *HIF-2α* siRNA targeted cells compared to the NSC siRNA targeted cells (Figure 6.1A). Furthermore *HIF-2α* gene knockdown resulted in a decrease in constitutive GLUT-1 protein expression (Figure 6.1A). In parallel, 786O cells targeted with either *HIF-2α* siRNA or NSC siRNA were harvested, RNA was isolated and RT-qPCR performed. The RT-qPCR results validate those obtained on protein samples and confirm knockdown of *HIF-2α* by 70-75% compared to that of NSC siRNA control (Figure 6.1B). Interestingly, *HIF-2α* mRNA was found to be higher in the 786O-EV cells compared to the 786O-VHL cells (Figure 6.1B).

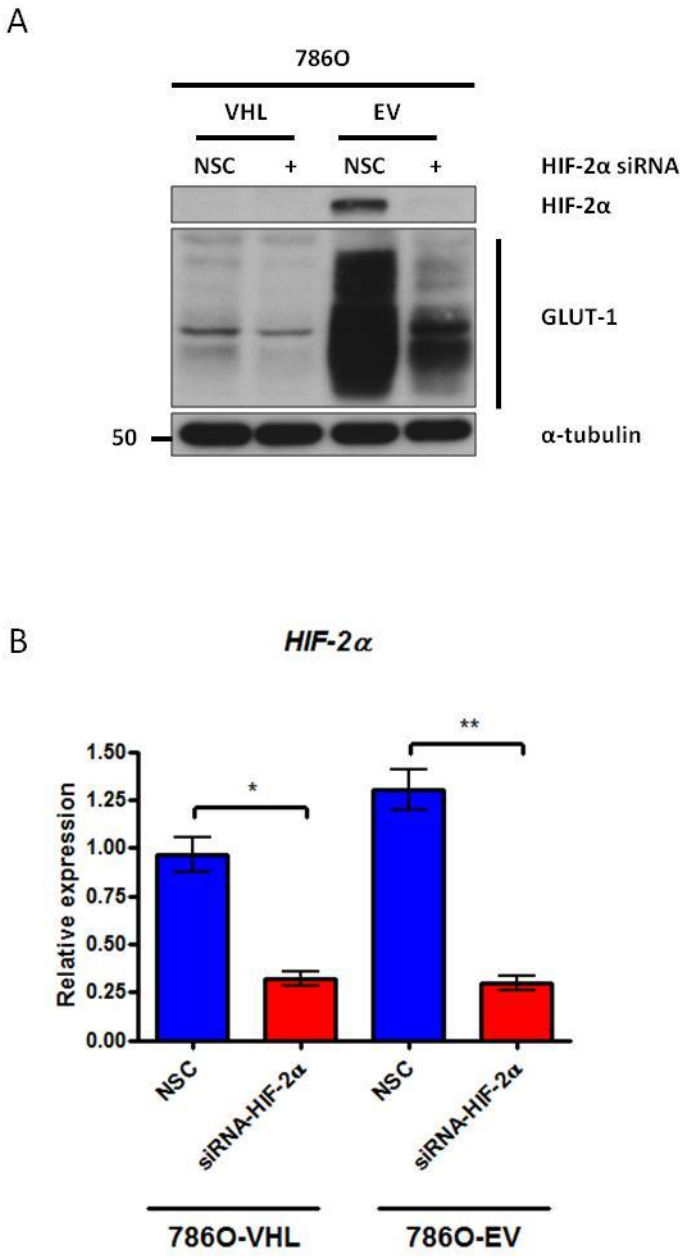


**Figure 6.1: Knockdown of HIF-2α and GLUT-1 in 786O cells.**

**(A) Western blot analysis of 786O (786O-EV (EV, red) and 786O-VHL (VHL, blue)) cells transfected with either a non-silencing control (NSC, 20nM) siRNA or a siRNA targeted toward *HIF-2α* ((+), 20nM, siRNA-HIF-2α). Western blot shows a significant knockdown of HIF-2α protein in the 786O-EV (EV) cells and a correlative reduction in GLUT-1 expression in both cell lines (VHL and EV). α-tubulin was used as a load control. (B) Graph shows relative expression of the *HIF-2α* transcript analysed by RT-qPCR from cells described in A. siRNA silencing of *HIF-2α* reduced transcript expression in both the 786O-VHL (* $p<0.05$) and 786O-EV cells (** $p<0.01$). Data analysed using the comparative Ct method after normalisation to a single experimental repeat. Values are mean +/- S.E.M (n=4) and data analysed by paired, two-tailed t-test.**

## 6.5 The effect of silencing *HIF-2α* on the expression of a panel of mitochondrial proteins

A previous study, linked to pVHL function (Hervouet et al., 2008), has shown that silencing *HIF-2α* in 786O-EV cells can increase the expression of mitochondrial ETC proteins, including COX-IV and core 2 of complex III. Indeed, chapter 4 described the findings that key mitochondrial proteins, including COX-IV and mtCO-2 were expressed at higher levels in the 786O-VHL cells compared to the 786O-EV cells (chapter 4; Figure 4.2). As an extension to the role of HIF-2α in the pVHL-mediated change in ETC protein expression (chapter 4; Figure 4.14), *HIF-2α* was silenced in 786O cells and protein samples subject to SDS-PAGE and western blot analysis. There was no effect of *HIF-2α* silencing on the expression of cytochrome c oxidase subunit protein expression (mtCO-2 and COX-IV) as reported previously (chapter 4; Figure 4.14). This analysis was expanded to include other mitochondrial proteins to investigate whether HIF-2α loss affected non-ETC protein expression. No effect on protein expression after HIF-2α silencing was observed for ATPB, PHB1 or VDAC1, despite knockdown of HIF-2α protein (Figure 6.2). Together, these data suggest that there is no role for HIF-2α in the regulation of expression of a number of mitochondrial proteins, however this does not eliminate the possibility there are effects on mitochondrial proteins that our analysis has not included.

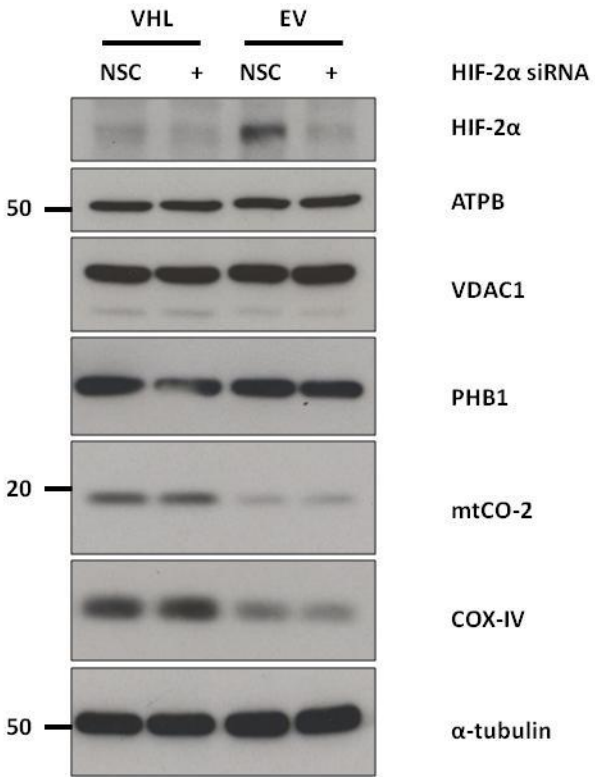


**Figure 6.2: Silencing of *HIF-2α* has no effect on the expression of a panel of mitochondrial proteins.**

**Western blot analysis of 786O (786O-VHL (VHL) or 786O-EV (EV)) cells each transfected with siRNA targeted towards *HIF-2α* (+, 20nM) or a non-silencing control siRNA (NSC, 20nM). Knockdown of HIF-2α has no effect on the protein expression of a select panel of mitochondrial proteins as indicated. NSC =. α-tubulin was used as a load control.**

## 6.6 The effect of silencing *HIF-2α* on organelle distribution and mitochondrial morphology

In chapter 5, a pVHL-dependent effect on mitochondrial morphology was observed in the 786O cells (chapter 5; Figure 5.1). To determine the role of HIF-2α in mediating the pVHL-dependent morphological change that was observed, *HIF-2α* was silenced in 786O cells. Cells were transfected with *HIF-2α* siRNA or NSC siRNA control and mitochondria imaged after fixation and primary antibody directed towards ATPB, as described previously (chapter 5; Figure 5.5). Immunofluorescence analysis showed no difference on the pVHL-dependent morphological changes observed in either 786O cell line, nor was there any global change in mitochondrial morphology after *HIF-2α* silencing (Figure 6.3A-B).

Although the gross morphology appeared not to change after *HIF-2α* silencing, mitochondrial localisation appeared more peri-nuclear in the *HIF-2α* siRNA transfected cells compared with those transfected with NSC siRNA control (Figure 6.3A). This peri-nuclear localisation was independent of pVHL status as it was observed in both 786O-VHL (Figure 6.3A) and 786O-EV cells (Figure 6.3B)

In order to determine the involvement of the microtubules in the *HIF-2α* siRNA-mediated peri-nuclear mitochondrial clustering, 786O-VHL cells were incubated with the anti-mitotic agent, nocodazole for two hours prior to fixation to de-polymerise the microtubules. Mitochondria are dependent on microtubules for their trafficking throughout the cell (Heggeness et al., 1978) and in the presence of nocodazole, *HIF-2α* siRNA failed to produce a peri-nuclear mitochondrial distribution. These data suggest microtubular involvement in this HIF-2α-dependent peri-nuclear mitochondrial process (Figure 6.3C). Staining of α-tubulin was used as a control on parallel coverslips to confirm the de-polymerisation of microtubules, compared to a vehicle treated control (Figure 6.3D).

Together these data suggest that, loss of *HIF-2α* by siRNA leads to peri-nuclear localisation of mitochondria, which is independent of pVHL status, but dependent on microtubule trafficking as indicated by depolymerisation after nocodazole treatment.

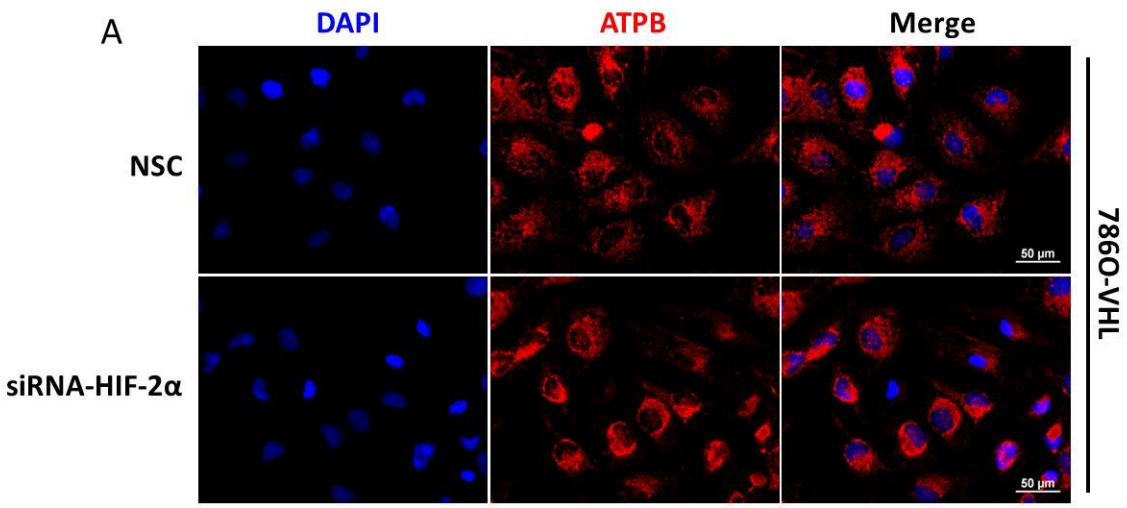
A
DAPI
ATPB
Merge
NSC
siRNA-HIF-2α
50 µm
50 µm
786O-VHL

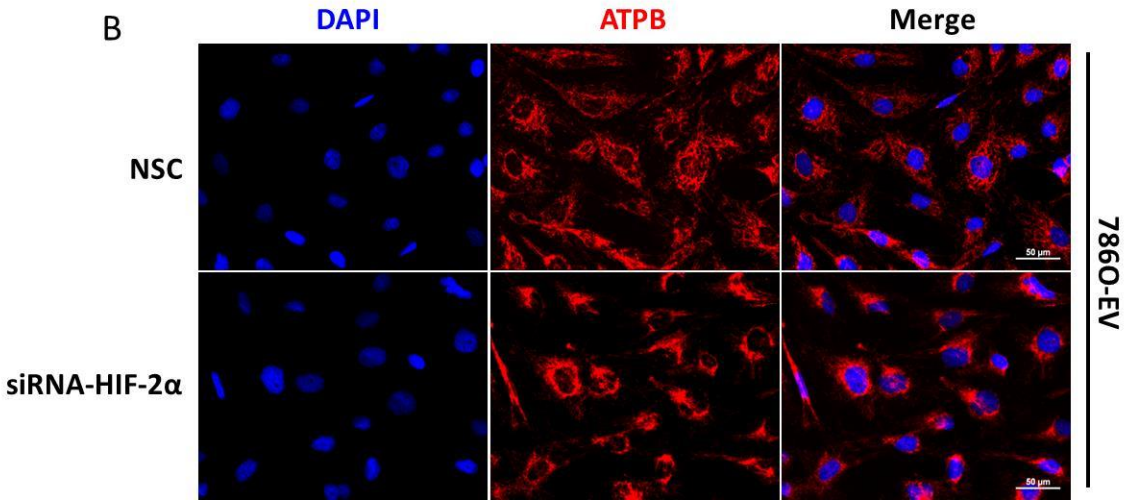
B
DAPI
ATPB
Merge
NSC
siRNA-HIF-2α
50 µm
50 µm
786O-EV

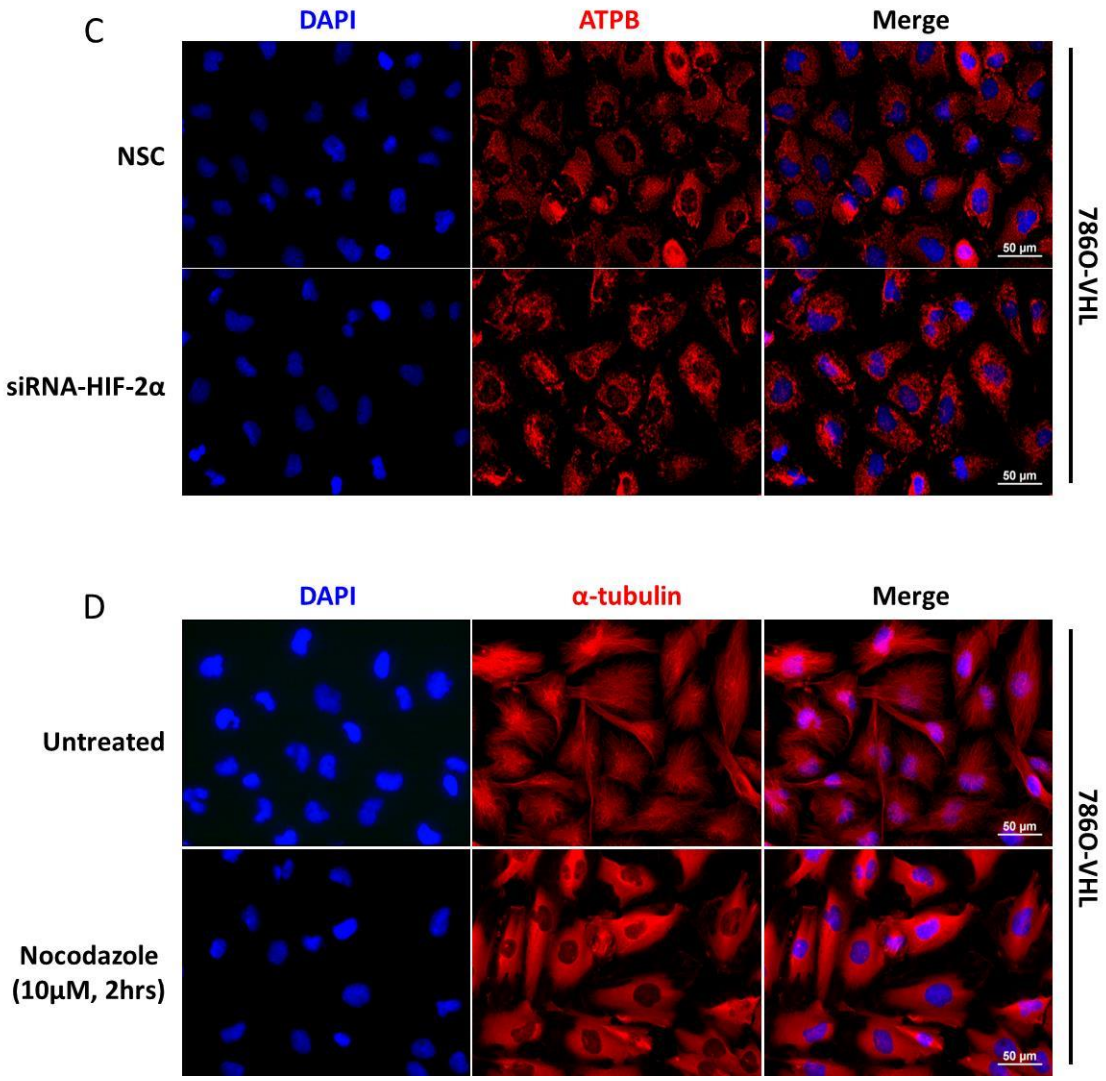


**Figure 6.3: Silencing of *HIF-2α* leads to a peri-nuclear localisation of mitochondria in 786O cells.**

**Immunofluorescence staining of (A) 786O-VHL and (B) 786O-EV cells transfected with non-silencing control (NSC; 20nM) siRNA or siRNA targeted towards *HIF-2α* (20nM, siRNA-HIF-2α). *HIF-2α* silencing promotes peri-nuclear clustering of mitochondria. (C) Immunofluorescence staining of 786O-VHL cells transfected with NSC siRNA or siRNA targeted towards *HIF-2α* in the presence and absence of nocodazole (10μM) for 2 hours. Depolymerisation of the microtubules prevents the peri-nuclear localisation of mitochondria induced by siRNA silencing of *HIF-2α*. Mitochondria were stained using primary antibody towards ATPB and Alexa Fluor 568 (red). (D) Treatment with nocodazole effectively depolymerises microtubules. α-tubulin antibody was used to visualise microtubules (red) and confirm effects of nocodazole treatment. Cells were visualised using Nikon Eclipse E600 upright microscope and 40x objective. Images are representative of 3 independent experiments.**

To further explore mitochondrial morphology and organelle subcellular distribution in response to HIF-2α knockdown, EM was used. *HIF-2α* was silenced in both 786O-VHL and 786O-EV cells and cells were processed for EM.

Consistent with the peri-nuclear localisation of mitochondria observed by immunofluorescence (Figure 6.3), EM analysis demonstrated a similar phenotype (Figure 6.4; carried out by Mark Turmaine, UCl, UK). However, to our surprise in addition to the re-distribution of mitochondria most other cellular organelles exhibited a peri-nuclear localisation after *HIF-2α* silencing (Figure 6.4A and B). Large areas of empty cytoplasm in cells transfected with *HIF-2α* siRNA were visible by EM, which was more obvious in the 786O-EV cells compared to the 786O-VHL cells (Figure 6.4B).

*HIF-2α* silencing also appeared to lead to a decrease in mitochondrial length in the 786O-EV cells (Figure 6.4B, right panel). Indeed, in the absence of pVHL (786O-EV cells), loss of *HIF-2α* decreased mitochondrial length, from 1.67μm to 1.48μm compared to cells expressing the NSC siRNA (Figure 6.4C). This phenotype was tending toward the smaller, rounder mitochondrial morphological phenotype observed in the 786O-VHL cells (Figure 6.4C compare 786O-EV/siRNA-HIF-2α with 786O-VHL/NSC siRNA. Importantly, these data suggest that the pVHL-mediated regulation of mitochondrial length in 786O cells is dependent on HIF-2α. Also notably, in the presence of re-expressed pVHL, loss of *HIF-2α* significantly increased mitochondrial length from 1.19μm in the NSC siRNA transfected cells to 1.6μm in those cells transfected with *HIF-2α* siRNA (Figure 6.4C)

These data suggest that there is a pVHL-HIF-2α-dependent mechanism regulating mitochondrial length. In the absence of functional pVHL protein, *HIF-2α* silencing failed to increase mitochondrial length, taken together suggesting an important role for HIF-2α in regulating the peri-nuclear localisation of organelles and in controlling mitochondrial length.

Interestingly, in 786O-VHL cells after *HIF-2α* silencing there was also a noticeable increase in the number of autophagosomal structures (Figure 6.4A; arrows) compared to the NSC siRNA transfected cells. Indeed, the increase in autophagosomes observed, suggests that basal HIF-2α protein expression may be involved and important in regulating autophagy.

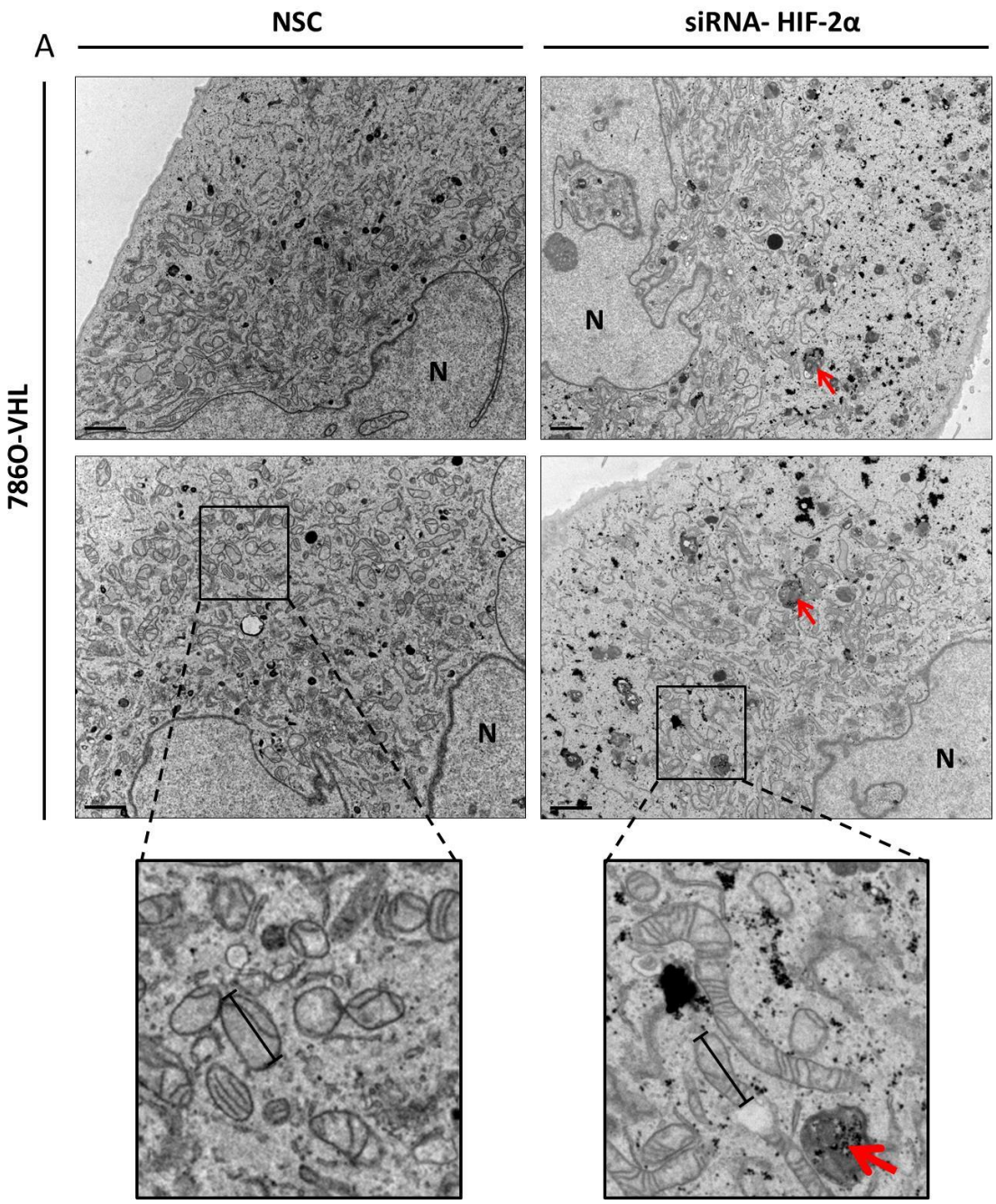
A
NSC
siRNA- HIF-2α
786O-VHL
N
N
N
N

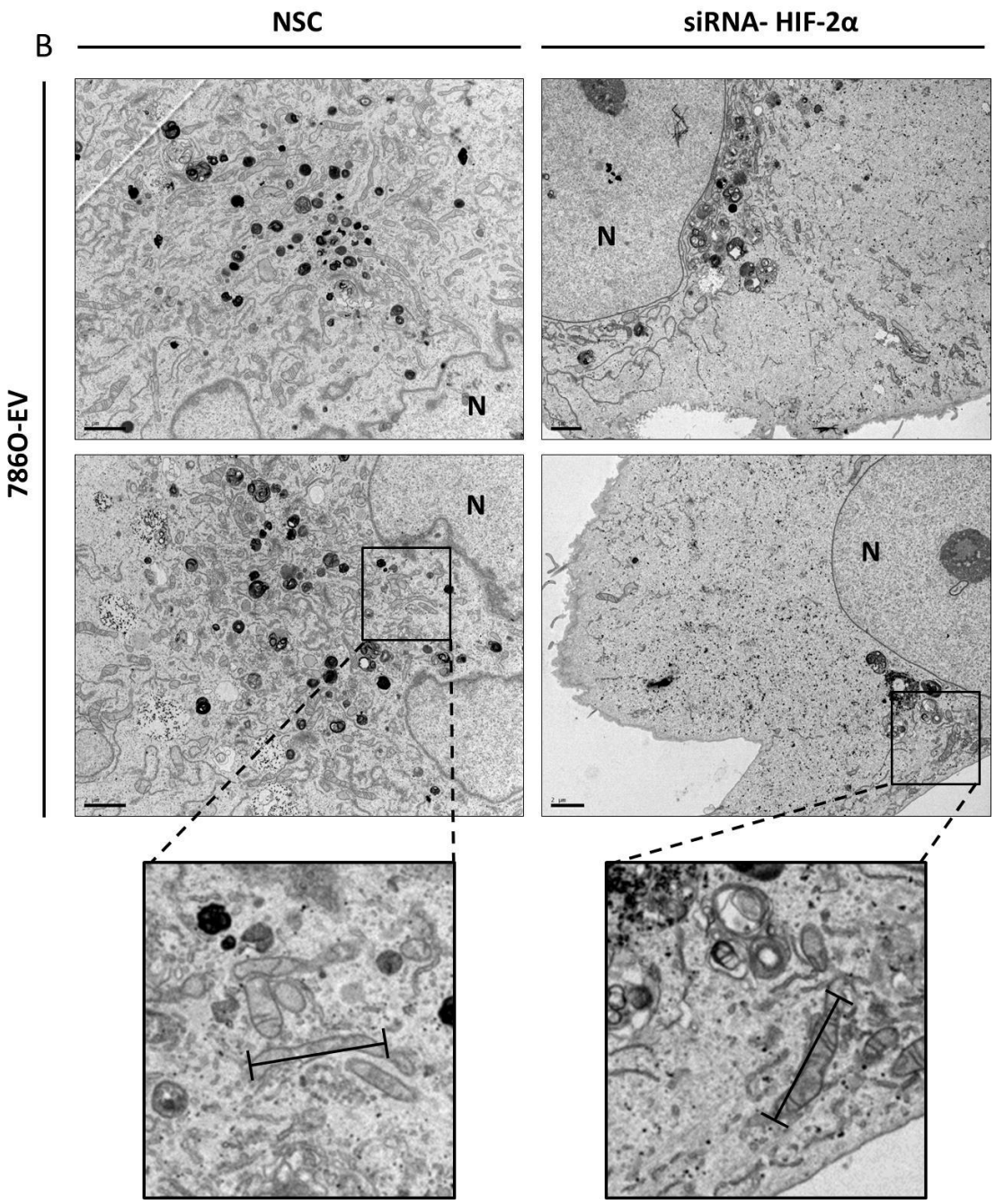
B
NSC
siRNA- HIF-2α
786O-EV
N
N
N
N

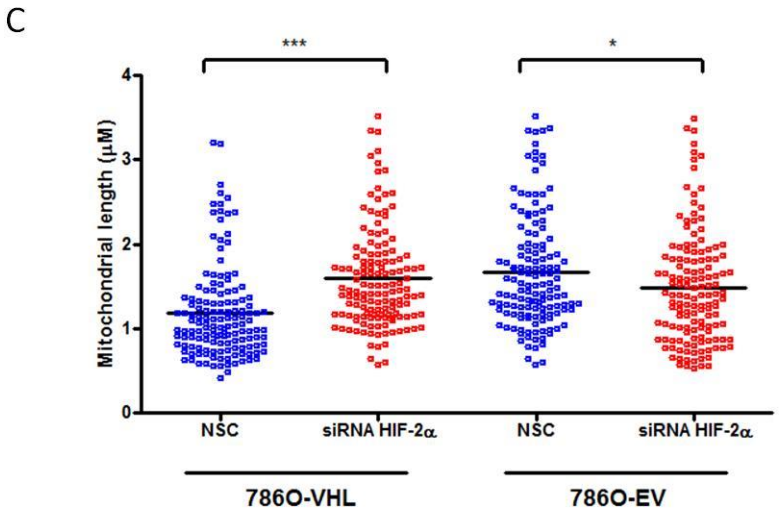


**Figure 6.4: Silencing of *HIF-2α* causes peri-nuclear localisation of organelles and affects mitochondrial length in a pVHL-dependent manner.**

**786O cells transfected with non-silencing siRNA control (NSC, 20nM) or siRNA targeted towards *HIF-2α* (20nM, siRNA-HIF-2α), were fixed, sectioned and imaged by electron microscopy (EM). Preparation for imaging and microscopy was performed by Mark Turmaine at UCL. EM images show (A) 786O-VHL cells and (B) 786O-EV cells. Lower panels are magnified EM images as indicated. N = nucleus, arrow = autophagosome (C) Graph shows quantification of mitochondrial length (µM) in 786O cells in the presence and absence of *HIF-2α* siRNA and pVHL re-expression. Mitochondria were measured using Image J software (National Institute of Health, Maryland), after scale bar calibration and measured from the most highly curved membrane through the central axis to the periphery (*** p<0.001 and * P<0.05). Over 140 mitochondria were scored from single independent images of 9-10 cells. Data analysed using unpaired, two-tailed t-test.**

## 6.7 The effect of silencing *HIF-2α* on autophagic protein expression

Previous studies have described that peri-nuclear distribution of organelles is associated with autophagy (Okatsu, 2010). Autophagosomes are transported along microtubules toward the nucleus where they are degraded by resident lysosomes (Ravikumar et al., 2010). HIF-2α has been observed previously to suppress autophagy in chondrocytes through regulation of mTOR and BCL-XL expression (Bohensky et al., 2009). The observations by Bohensky *et al* suggest that decreased HIF-2α protein expression in osteoarthritic tissue is associated with increased autophagy (Bohensky et al., 2009). To investigate the role of HIF-2α in the autophagic response in cancer cells, *HIF-2α* was silenced and the expression of a number of autophagic proteins was analysed after SDS-

PAGE and western blot analysis. No changes were observed in the expression of ATG5 or ATG3 and a small decrease in beclin expression after *HIF-2α* silencing in the 786O-EV cells compared with NSC siRNA was observed (Figure 6.5). In both the 786O-VHL and 786O-EV a reduction in LC3B-II expression was evident after *HIF-2α* silencing compared with NSC siRNA transfected controls (Figure 6.5A).

As discussed previously in chapter 5, the LC3B-I to LC3B-II ratio is a static measure of autophagosomal membrane, therefore in the absence of autophagic induction, a decrease in LC3B-II could suggest a number of possibilities. Either there is decreased synthesis/formation of autophagosomes or increased autophagosome turnover, as in both scenarios a reduced level of LC3B-II protein would be observed since both situations give rise to decreased autophagosomal membrane. While a mechanism for the change in LC3B-I to LC3B-II cannot be elucidated from these western data (Figure 6.5), it is clear however that loss of *HIF-2α*, independent of pVHL appears to affects LC3B processing and lipidation.

In addition to the post-translation lipidation of LC3B, the activity of LC3B can also be modulated at the mRNA level (Rouschop et al., 2010). It was therefore important to measure transcript expression of LC3B-II in the presence and absence of *HIF-2α* siRNA. Interestingly, no significant difference in LC3B transcript expression after silencing of *HIF-2α* compared to the NSC siRNA transfected cells in either the 786O-VHL or 786O-EV cells was observed (Figure 6.5B). Therefore indicating, that the change observed in LC3B protein is mediated at the post-translational level and independent of pVHL status.

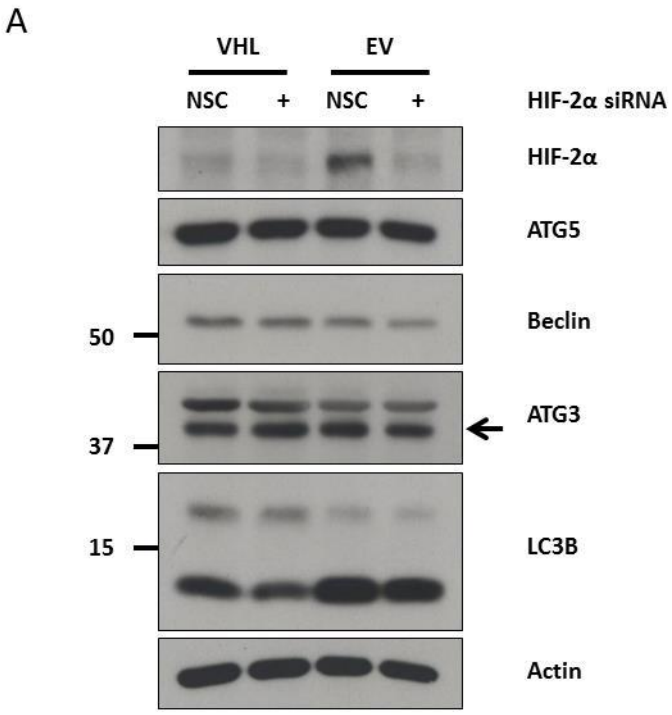
A
VHL
EV
NSC
+
NSC
+
HIF-2α siRNA
HIF-2α
ATG5
Beclin
ATG3
LC3B
Actin
50
37
15

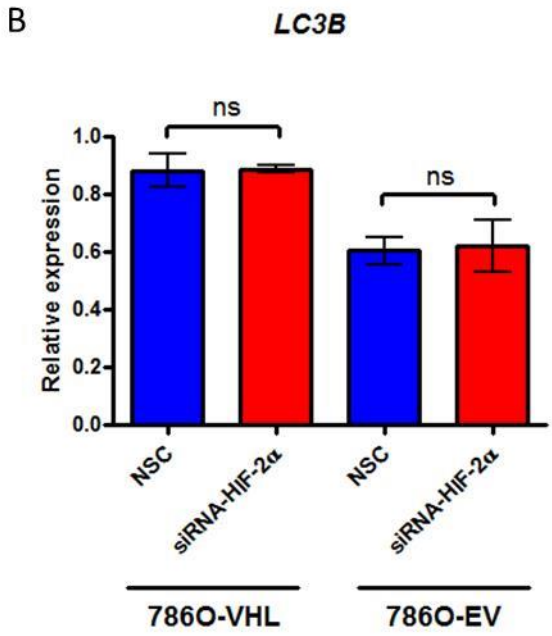
B
LC3B
ns
ns
Relative expression
1.0
0.8
0.6
0.4
0.2
0.0
NSC
siRNA-HIF-2α
NSC
siRNA-HIF-2α
786O-VHL
786O-EV

**Figure 6.5: Silencing of *HIF-2α* affects post-translational lipidation of LC3B.**

**(A) Western blot analysis of 786O cells transfected with non-silencing siRNA control (NSC, 20nM) or siRNA targeted towards *HIF-2α* (20nM, siRNA-HIF-2α). Knockdown of HIF-2α in each cell line decreases protein expression of LC3B-II without affecting other autophagic proteins (as indicated). β-actin was used as a load control (B) Graph shows relative expression of the *LC3B* transcript analysed by RT-qPCR from cells described in A. There was no significant difference in the presence of *HIF-2α* siRNA in each of the cell lines (ns p>0.05). Data analysed using the comparative Ct method after normalisation to a single experimental repeat. Values are mean +/- S.E.M (n=4) and data analysed by paired, two-tailed t-test**

## 6.8 The effect of silencing *HIF-2α* on mitophagy

Mitochondrial length has been observed to change, under conditions of autophagy and additionally during mitochondrial-specific turnover (mitophagy) (Gomes et al., 2011, Rambold et al., 2011, Tanaka et al., 2010). Mitophagy can be induced in response to mitochondrial dysfunction or damage and has been observed to be deregulated in a number of neurological conditions (Youle and van der Bliek, 2012).

To examine the role of HIF-2α in mitophagy, a number of proteins involved in the mitophagic process were investigated. Protein samples obtained after transfection with *HIF-2α* siRNA or NSC siRNA in 786O cells were prepared and subject to SDS-PAGE and western blot analysis. Confirming earlier observations (chapter 5; Figure 5.9) there was a difference in parkin protein levels between the 786O-VHL and 786O-EV cells (Figure 6.6A). Interestingly, after *HIF-2α* silencing an increase in parkin protein expression in 786O-VHL cells was observed (Figure 6.6A). A change in parkin expression was challenging to observe in 786O-EV cells since basal parkin protein levels were below levels of detection. Next, RT-qPCR was employed to deduce whether *parkin* mRNA levels were also changed. A small but reproducible increase in *parkin* transcript expression was observed in both 786O lines after silencing of *HIF-2α*, albeit not at statistical significance (Figure 6.5B), but potentially suggesting that the increase in parkin protein at least in part may be regulated through HIF-2α-dependent control of *parkin* gene expression.

*HIF-2α* silencing had little effect on the protein expression of the molecular adaptor p62 (Figure 6.6A). The abundance of p62 protein decreased in the 786O-EV cells compared to the 786O-VHL cells, confirming earlier observations (chapter 5; Figure 5.9). p62 protein is turned-over under conditions of increased autophagy and can be used marker of

autophagic flux, commonly in combination with other strategies (Bjørkøy et al., 2009, Klionsky et al., 2012).

Together, these data suggest that *HIF-2α* silencing affects the expression of parkin protein levels and leads to a small reproducible, but non-statistically significant change in *parkin* mRNA. These effects on parkin are independent of pVHL status. *HIF-2α* silencing interestingly, does not rescue the parkin deficit observed in the 786O-EV cells compared to the 786O-VHL cells.

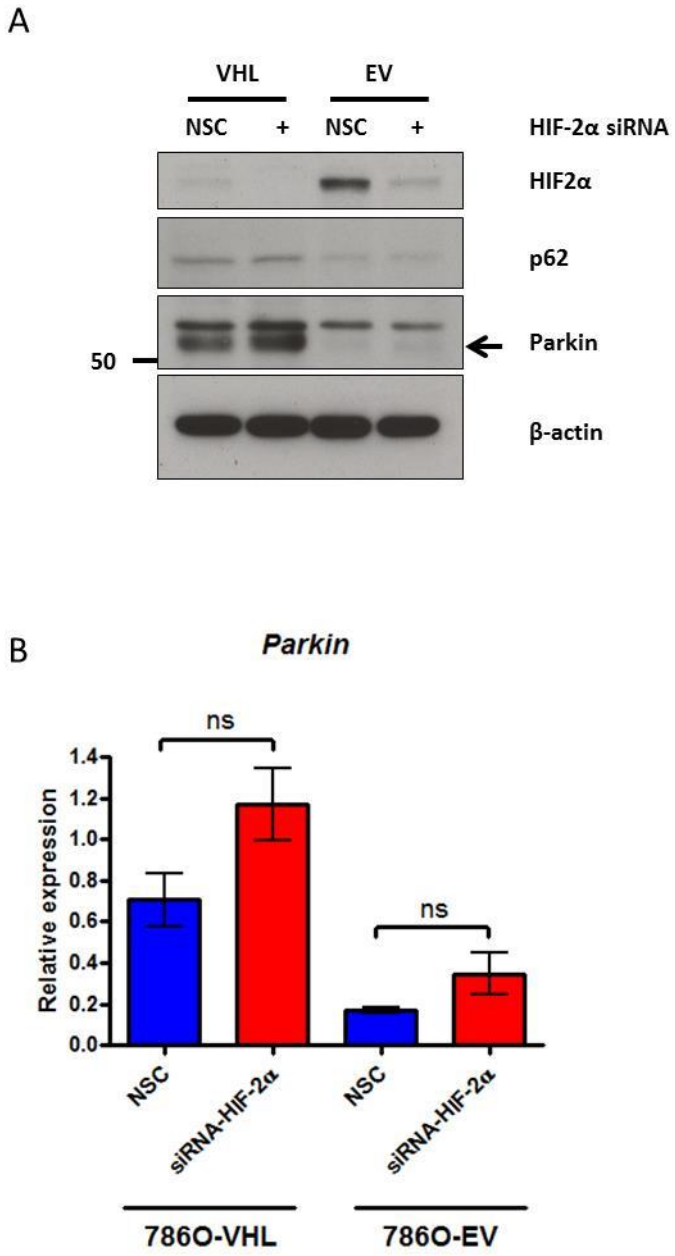


**Figure 6.6: Silencing of H*IF-2α* silencing affects parkin protein and mRNA expression.**

**(A) Western blot analysis of 786O (786O-VHL (VHL) and 786O-EV (EV)) cells transfected with non-silencing siRNA control (NSC, 20nM) or siRNA targeted towards *HIF-2α* (20nM, siRNA-HIF-2α). Knockdown of HIF-2α in each cell line leads to an increase in parkin protein expression. There is also a clear reduction in p62 protein levels between the 786O-VHL and 786O-EV cells as observed previously, however no influence of *HIF-2α* siRNA. β-actin was used as a load control. (B) Graph shows relative expression of the *parkin* transcript analysed by RT-qPCR from cells described in A. There was a small increase in *parkin* expression in both the 786O-VHL and 786O-EV cells in the presence of *HIF-2α* siRNA, however this was not statistically significant (ns p>0.05). Data analysed using the comparative Ct method after normalisation to a single experimental repeat. Values are mean +/- S.E.M (n=4) and data analysed by paired, two-tailed t-test.**

To correlate the observed changes in mitochondrial length, organelle subcellular distribution and parkin expression after *HIF-2α* silencing, the rate of HIF-2α-dependent mitophagic flux was assessed. 786O cells were transfected with either siRNA targeted toward *HIF-2α* or a NSC siRNA and treated with FCCP, to induce mitochondrial depolarisation and/or chloroquine, to inhibit the lysosome for 2 hours prior to analysis. A number of observations can be made from the data presented. Firstly and consistent with Figure 6.5, *HIF-2α* silencing led to a decrease in LC3B-II protein levels, compared to NSC siRNA control, in both 786O-VHL and 786O-EV cells (Figure 6.7A-B; lanes 1 and 5). The addition of chloroquine alone in both NSC and *HIF-2α* siRNA transfected cells leads to an increase LC3B-II protein levels compared to untreated cells, suggesting that HIF-2α is not important for LC3B-II/autophagosome membrane synthesis (Figure 6.7A-B; lanes 1 and 3 vs. 5 and 7). The addition of FCCP alone, which depolarises the mitochondrial inner membrane and promotes mitophagy, caused an increase in LC3B-II in both NSC and *HIF-2α* siRNA transfected cells (Figure 6.7A-B; lanes 1 vs. 2 and 5 vs. 6). Most interestingly, when autophagic flux was blocked with chloroquine, FCCP treatment increased LC3B-II protein levels in NSC transfected control cells, as anticipated (Figure 6.7A-B; lanes 2 vs. 4). However, in the presence of *HIF-2α* siRNA, FCCP treatment was unable to induce LC3B-II protein, when autophagosome degradation was blocked by chloroquine (Figure 6.7A-B; lanes 2 and 4 vs. 6 and 8). These data collectively suggest that HIF-2α is important for the induction of LC3B-II protein levels, specifically when mitophagy is induced and the lysosome is blocked, indicating that HIF-2α is regulating the maturation or terminal events of the autophagy process (Klionsky et al., 2012, Rubinsztein et al., 2009). Thus, when HIF-2α is knocked down, cells fail to increase LC3B protein levels after mitophagic induction with lysosomal inhibition which may suggest a block in autophagy/mitophagy at the terminal stages and decreased autophagosome degradation.

A

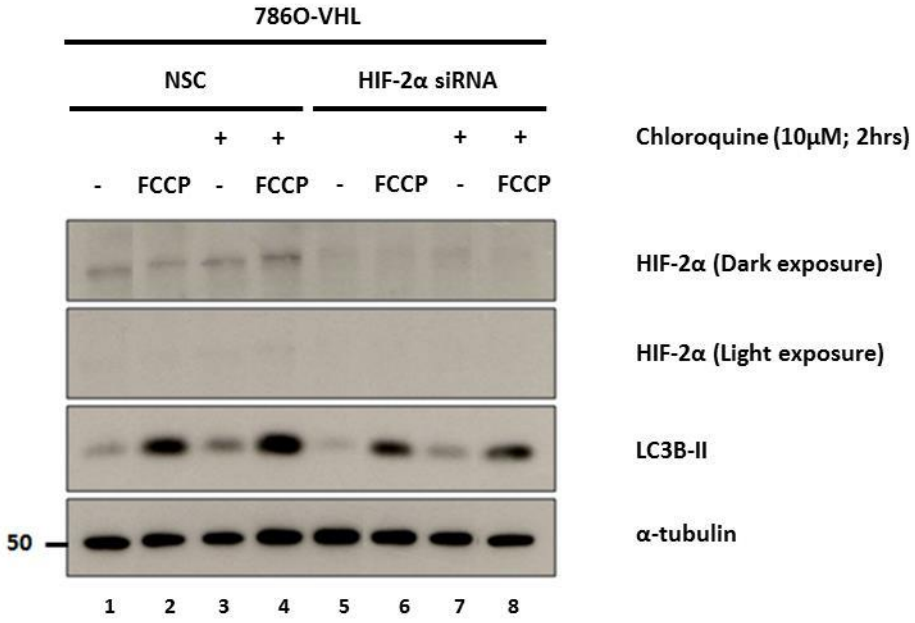
786O-VHL
NSC
HIF-2α siRNA
+ + + +
- FCCP - FCCP - FCCP - FCCP
Chloroquine (10μM; 2hrs)
HIF-2α (Dark exposure)
HIF-2α (Light exposure)
LC3B-II
α-tubulin
50
1 2 3 4 5 6 7 8

B

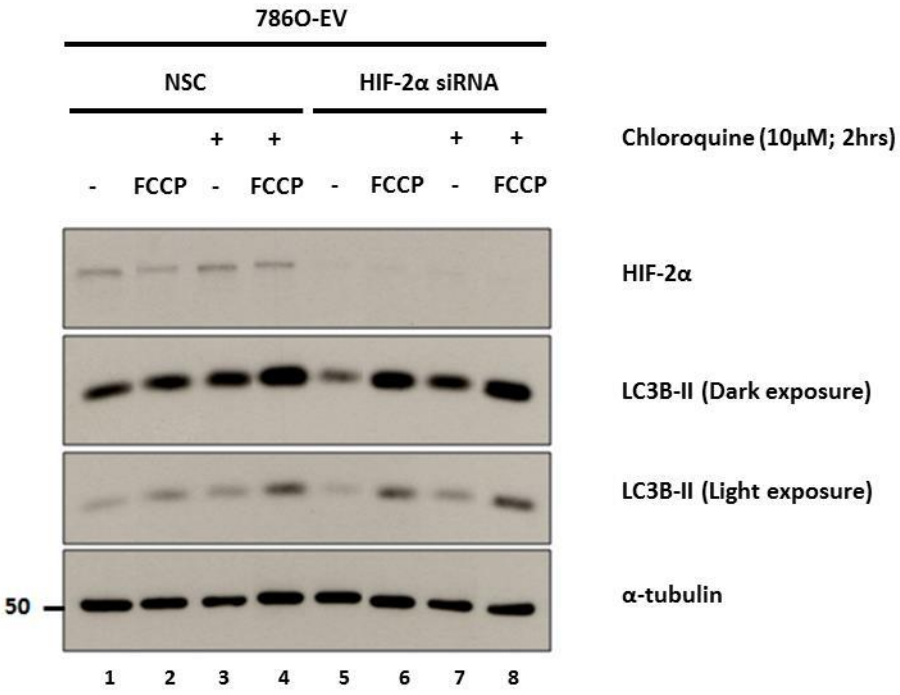
786O-EV
NSC
HIF-2α siRNA
+ + + +
- FCCP - FCCP - FCCP - FCCP
Chloroquine (10μM; 2hrs)
HIF-2α
LC3B-II (Dark exposure)
LC3B-II (Light exposure)
α-tubulin
50
1 2 3 4 5 6 7 8

**Figure 6.7: Silencing of *HIF-2α* affects mitophagic flux after pharmacological uncoupling with FCCP in 786O cells.**

**Western blot analysis of (A) 7860-VHL cells and (B) 786O-EV cells transfected with either NSC siRNA (NSC, 20nM) or siRNA towards *HIF-2α* (HIF-2α-siRNA, 20nM). Cells were incubated with FCCP (10μM) and chloroquine (10μM) as indicated (+) for 2 hours and the ratio of change in LC3B-II protein was analysed. α-tubulin was used as a load control.**

## 6.9 The effect of silencing *HIF-2α* on mitochondrial DNA copy number

Mitochondrial DNA copy number (the number of mitochondrial DNA copies per cell), can change either through variations in biosynthesis or mitochondrial turnover (Venegas and Halberg, 2012, Clay Montier et al., 2009). To investigate the role of *HIF-2α* silencing in 786O cells on mitochondrial DNA content, mitochondrial DNA copy number was estimated using RT-qPCR and estimation of the *β2M*:ND1 ratio as discussed in chapter 4 (chapter 4; Figure 4.7) (Venegas and Halberg, 2012).

*HIF-2α* silencing revealed a small but reproducible increase in mitochondrial DNA copy number compared to NSC siRNA transfected cells, however this increase was not statistically significant (Figure 6.8A). Reassuringly, a significant reduction in DNA copy number was observed in cells devoid of functional pVHL, validating earlier observations (chapter 4; Figure 4.7). *HIF-2α* silencing, in HCT116 cells revealed a similar increase in mitochondrial DNA copy number compared to NSC siRNA control (Figure 6.8B).

These data suggest that HIF-2α knockdown reproducibly, although non-significantly, leads to a small increase in mitochondrial DNA copy number, through a mechanism that is independent of pVHL and HIF-1α status. These data also reveal that the reduced mitochondrial DNA content observed in the absence of pVHL (786O-EV) compared to those cells stably re-expressing pVHL (786O-VHL), described earlier (chapter 4; Figure 4.7), failed to be reversed by *HIF-2α* silencing.

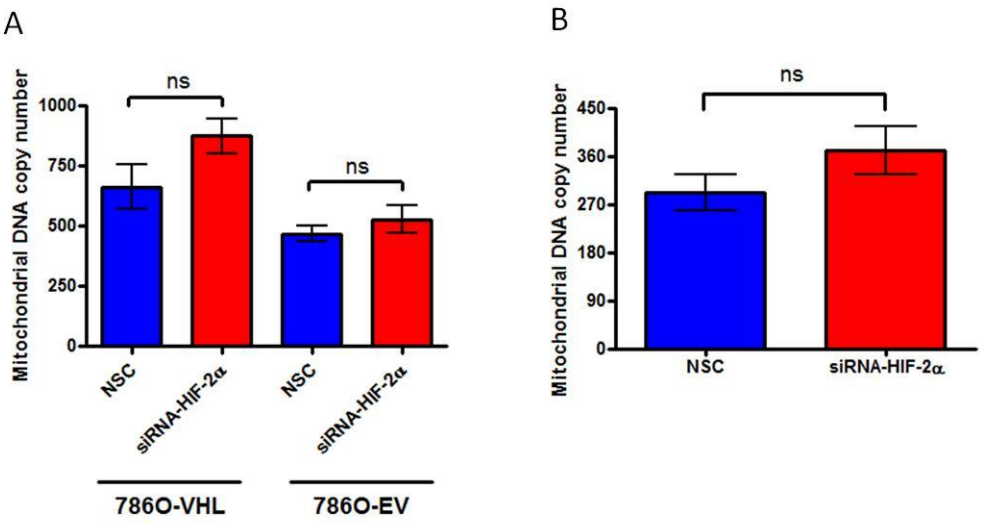


**Figure 6.8: Silencing of *HIF-2α* causes a small, reproducible, but non-statistically significant increase in mitochondrial DNA copy number.**

**Graphs show mitochondrial DNA copy number in (A) 786O (786O-VHL and 786O-EV) and (B) HCT116 cells, which was calculated through analysis of expression of the single copy nuclear gene *β2M* and mitochondrial *ND1* by RT-qPCR in cells transfected with either non-silencing control (NSC, 20nM) siRNA or siRNA towards *HIF-2α* (20nM, siRNA-HIF-2α). Ct values were calculated for each cell line and the ratio calculated as described in (Venegas and Halberg, 2012). Values are mean +/- S.E.M (n=5) and data analysed by paired, two-tailed t-test (ns P>0.05).**

## 6.10 The effect of silencing *HIF-2α* on mitochondrial bioenergetics

*Epas1*/*Hif-2α* loss has detrimental effects on mitochondrial function and adversely effects metabolism (Oktay et al., 2007). Oktay *et al* observed that knockout of *Epas1*/*Hif-2α* in mice decreases OCR and ETC activity in isolated mitochondria from hepatocytes, giving rise to a phenotype similar to that of the *Sod2*$^{-/-}$ mouse (Oktay et al., 2007). To investigate the role of transient *HIF-2α* loss on OCR, *HIF-2α* was silenced in 786O cells and effects on respiratory rate analysed using the Oroboros O2K. In the presence of *HIF-2α* siRNA, independent of pVHL expression, there was a significant increase in routine OCR compared with the NSC siRNA transfected cells (Figure 6.9A). Significant increases were also observed in leak respiration and maximum respiratory capacity (Figure 6.9B and C). A representative trace for 786O-VHL (Figure 6.9E) and 786O-EV cells is included (Figure 6.9F). Note, *HIF-2α* silencing was confirmed by RT-qPCR and found to be reduced by approximately 60% compared to control (Figure 6.9D).

These data suggest that in contrast to *HIF-2α* knockout, where respiratory capacity is diminished (Oktay et al., 2007), transient *HIF-2α* silencing increases mitochondrial respiration and ETC capacity. Notably, there was a highly significant increase in OCR in 786O-VHL cells compared to 786O-EV cells, confirming previous observations (chapter 4; Figure 4.3). These data also reveal that the reduced OCR observed in the absence of pVHL (786O-EV) compared to those cells stably re-expressing pVHL (786O-VHL), described earlier (chapter 4; Figure 4.3), failed to be reversed by *HIF-2α* silencing.

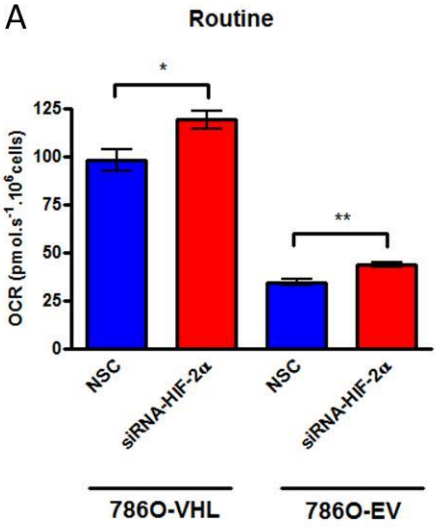
A
Routine
OCR (pmol.s-1.10^6cells)
NSC
siRNA-HIF-2α
786O-VHL
786O-EV

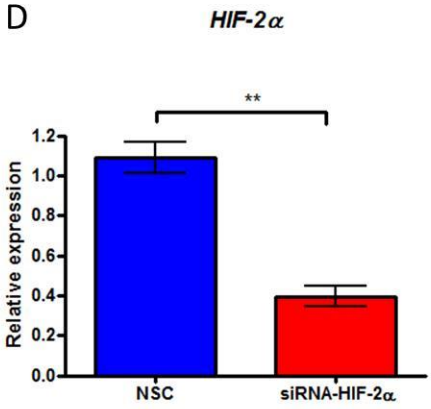
D
HIF-2α
Relative expression
NSC
siRNA-HIF-2α

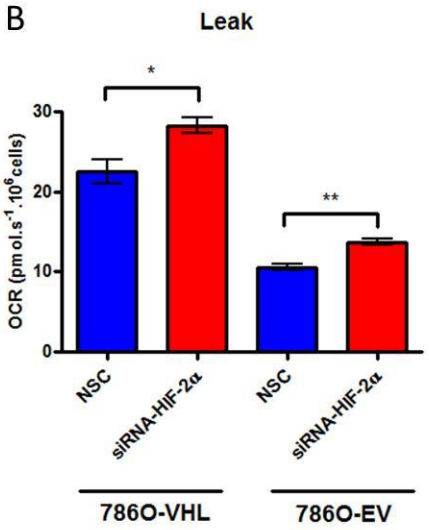
B
Leak
OCR (pmol.s-1.10^6cells)
NSC
siRNA-HIF-2α
786O-VHL
786O-EV

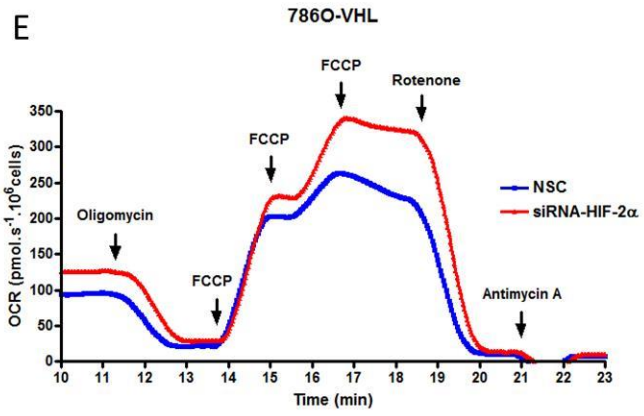
E
786O-VHL
Oligomycin
FCCP
FCCP
FCCP
Rotenone
Antimycin A
NSC
siRNA-HIF-2α
OCR (pmol.s-1.10^6cells)
Time (min)

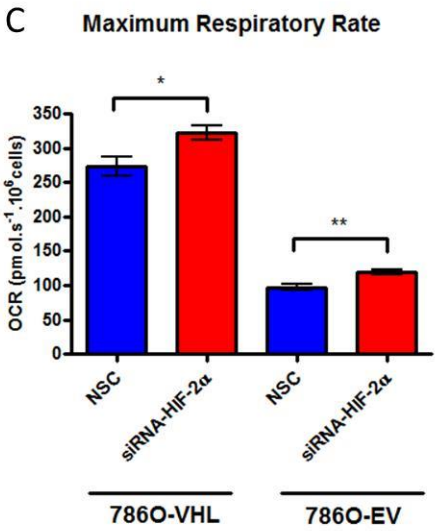
C
Maximum Respiratory Rate
OCR (pmol.s-1.10^6cells)
NSC
siRNA-HIF-2α
786O-VHL
786O-EV

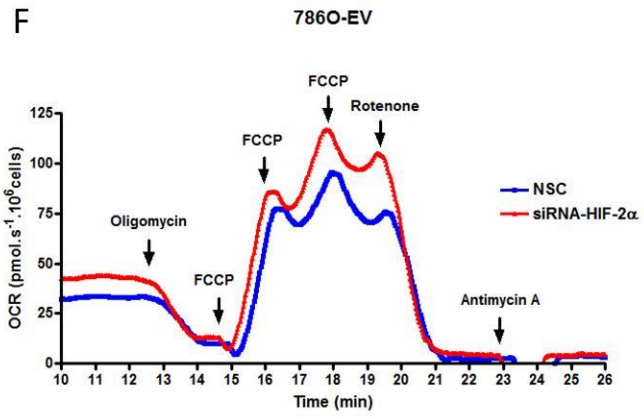
F
786O-EV
Oligomycin
FCCP
FCCP
FCCP
Rotenone
Antimycin A
NSC
siRNA-HIF-2α
OCR (pmol.s-1.10^6cells)
Time (min)

**Figure 6.9: Silencing of *HIF-2α* increase OCR in 786O cells.**

**786O (786O-VHL (VHL) and 786O-EV (EV)) cells transfected with non-silencing siRNA control (NSC, 20nM) or siRNA targeted towards *HIF-2α* (20nM, siRNA-HIF-2α) were analysed using the Oroboros O2K. Graphs show (A) routine respiration, (B) leak respiration and (C) maximum respiratory rate, corrected for cell number and non-mitochondrial respiration. (A-C) *HIF-2α* silencing significantly increased routine respiration and bioenergetic parameters. Values are mean +/- S.E.M (n=4). Data analysed using paired, two-tailed t-test (** P<0.01 and * p<0.05). (D) Graph shows relative expression of *HIF-2α* transcript analysed by RT-qPCR from cells described in A-C. *HIF-2α* was reduced by 60% in cells transfected with *HIF-2α* siRNA compared to NSC siRNA (* p<0.05). Data analysed using the comparative Ct method after normalisation to a single experimental repeat. Values are mean +/- S.E.M (n=4) and data analysed by paired, two-tailed t-test. (E-F) Representative graphs showing OCR (pmol.$s^{-1}$.$10^6$ cells) measured over time (minutes) for 786O cells described in A-C using the Oroboros O2K.**

Calculation of the bioenergetic flux ratios, described previously (chapter 4; Figure 4.3), allows more subtle changes in respiration to be investigated. Calculation and analysis of the leak and net-routine control ratios identified that there are no significant change in flux ratio in the presence after *HIF-2α* silencing compared to NSC siRNA control (Figure 6.10). These data indicate that: (i) there is no alteration in how close routine respiration operates in relation to maximum respiratory capacity after transient loss of HIF-2α protein, as indicated by the routine control ratio (R/E); (ii) there is no influence of HIF-2α status on the degree of uncoupling within the ETC, as indicated by the fact there was no change observed in the in the leak control ratio; (iii) HIF-2α status does not affect the proportion of the maximum capacity utilised to drive ATP synthesis, as indicated by the fact there was no change in net-routine control ratio (Figure 6.10).

These data also reveal that the effect on flux ratios observed in the absence of pVHL (786O-EV) compared to those cells stably re-expressing pVHL (786O-VHL), described earlier (chapter 4; Figure 4.3), failed to be revered by *HIF-2α* silencing.

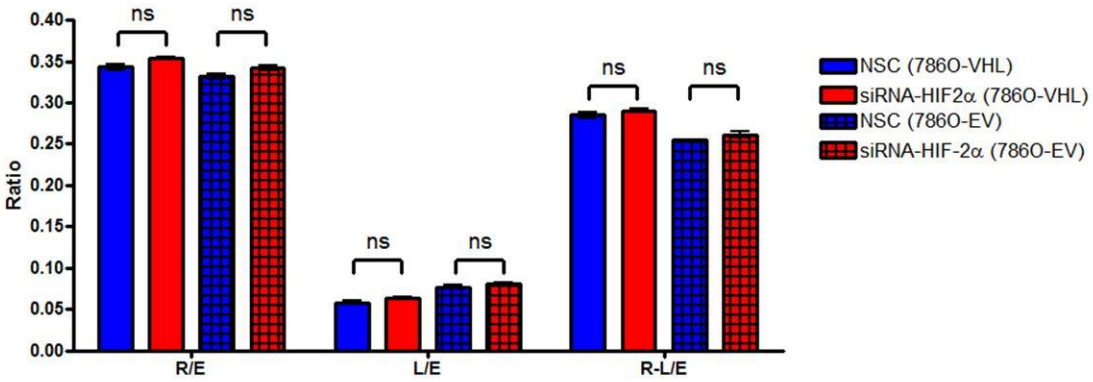


**Figure 6.10: Bioenergetic flux ratios are unaffected by *HIF-2α* silencing in 786O cells.**

**Flux ratios were calculated as previously described from the data presented in Figure 6.9. There was no significant difference in routine control ratio (R/E), nor where there significant differences observed in leak control ratio (L/E) or net routine control ratio (ns p>0.05). Values are mean +/- S.E.M (n=4) and data analysed using paired, two-tailed t-test.**

Oxygen consumption analysis performed in 786O cells was repeated using the HCT116 cell line to determine how the bioenergetic phenotype associated with *HIF-2α* silencing reproduced across cell lines. *HIF-2α* was silenced in HCT116 cells and OCR analysed using the Oroboros O2K. Analysis of routine respiration revealed that transient silencing of *HIF-2α* led to an increase in OCR (Figure 6.11A), consistent with previous observations in the 786O cells (Figure 6.9A). *HIF-2α* silencing also caused a significant increase in maximum respiratory capacity (Figure 6.11C), confirming data observed with the 786O cells (Figure 6.9C). A representative trace is shown below (Figure 6.11E). RT-qPCR analysis of samples confirmed *HIF-2α* silencing of approximately 80% in these experiments (Figure 6.11D).

Taken together, these data confirm that transient *HIF-2α* silencing leads to an increase in routine respiration and associated bioenergetic parameters, a phenotype that can be paralleled across cell lines. Transient knockdown of HIF-2α increases routine OCR, independently of pVHL or HIF-1α expression, and importantly leads to a corresponding increase in maximum respiratory flux, indicative of minimal mitochondrial toxicity after *HIF-2α* silencing.

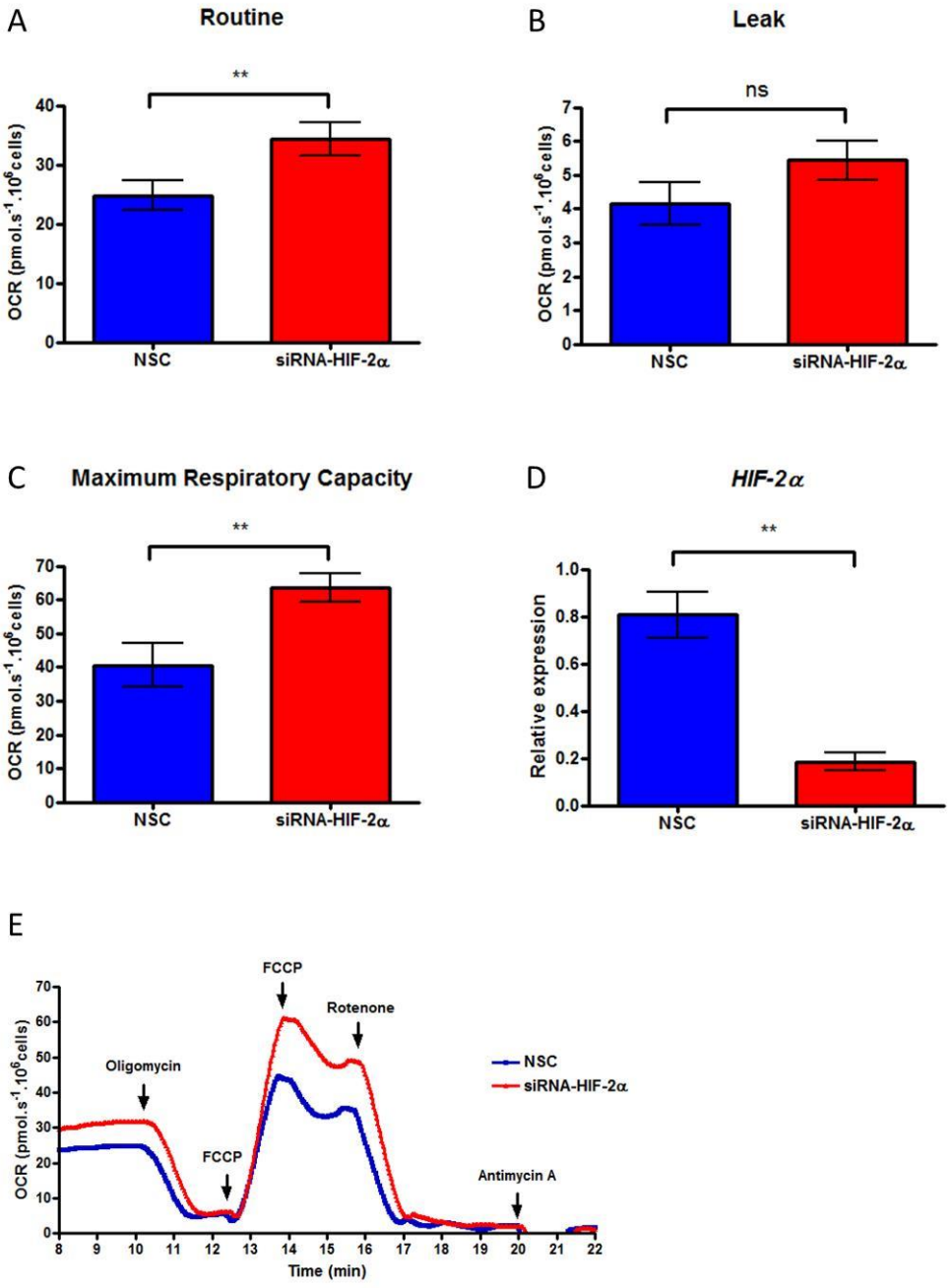
A
Routine
**
OCR (pmol.s-1.10^6cells)
NSC
siRNA-HIF-2α
B
Leak
ns
OCR (pmol.s-1.10^6cells)
NSC
siRNA-HIF-2α
C
Maximum Respiratory Capacity
**
OCR (pmol.s-1.10^6cells)
NSC
siRNA-HIF-2α
D
HIF-2α
**
Relative expression
NSC
siRNA-HIF-2α
E
FCCP
Rotenone
Oligomycin
FCCP
Antimycin A
NSC
siRNA-HIF-2α
OCR (pmol.s-1.10^6cells)
Time (min)

**Figure 6.11: Silencing of *HIF-2α* increases OCR in HCT116 cells.**

**Bioenergetic analysis of HCT116 cells transfected with either NSC siRNA or siRNA targeted toward *HIF-2α* (siRNA-HIF-2α, 20nM) analysed using the Oroboros O2K. Graphs show (A) routine respiration, (B) leak respiration and (C) maximum respiratory rate, corrected for cell number and non-mitochondrial respiration. (A-C) *HIF-2α* silencing significantly increased routine respiration and bioenergetic parameters. Values are mean +/- S.E.M (n=3). Data analysed using paired, two-tailed t-test (** P<0.01 and ns p>0.05). (D) Graph shows relative expression of *HIF-2α* transcript analysed by RT-qPCR from cells described in A-C. *HIF-2α* was reduced by 80% in cells transfected with *HIF-2α* siRNA compared to NSC siRNA (* p<0.05). Data analysed using the comparative Ct method after normalisation to a single experimental repeat. Values are mean +/- S.E.M (n=3) and data analysed by paired, two-tailed t-test. (E) Representative graphs showing OCR ($pmol.s^{-1}.10^6$ cells) measured over time (minutes) for cells described in A-C using the Oroboros O2K.**

## 6.11 Discussion

Metabolism has to be tightly regulated in hypoxia and a number of genes are involved in allowing cells to continue to produce ATP and adapt to periods of low oxygen. The HIFs are key mediators of metabolic control in hypoxia. HIF-1α is responsible for the down-regulation of oxidative metabolism and diversion of substrates away from mitochondria to promote glycolysis (Semenza, 2007b). Unlike HIF-1α, HIF-2α is not thought to be involved in up-regulating glycolysis in hypoxia and appears more involved in the transactivation of genes that regulate redox state and cellular anti-oxidant capacity (*SOD2*), tumourigenesis and pro-survival factors (*cyclin D1*, *VEGF* and *TGF-α*) (Hu et al., 2003).

The HIF proteins are highly regulated, such that under ambient oxygen, HIF-1α protein levels remain low, with a half-life of less than five minutes (Berra et al., 2001). Despite tight regulation in normoxia limiting the transcriptional activity of the HIFs, HIF-dependent gene transcription, albeit low, occurs under ambient oxygen. Indeed, how the HIFs and their basal gene expression influence cell fate has previously been explored (Huang et al., 2004, Cai et al., 2008, Cramer and Johnson, 2003, Oktay et al., 2007). Interestingly, the basal gene expression of HIF-1α has been identified as vital for cardiac function (Huang et al., 2004), ischaemic preconditioning (Cai et al., 2008) and inflammation (Cramer et al., 2003). However, how the basal gene expression of the HIF proteins influences cellular homeostasis through regulation of mitochondrial function remains to be fully understood.

In comparison to HIF-1α, the role of HIF-2α in the regulation of mitochondrial function has been has been scarcely investigated. To date, there is one study in mice with global

*Epas1*/*Hif-2α* knockout and investigation into the chronic loss of *Epas1*/*Hif-2α* in liver mitochondria (Oktay et al., 2007). Oktay *et al* described livers of mice lacking *Epas1*/*Hif-2α* to exhibit a phenotype similar to that of the *Sod2*$^{-/-}$ mouse (Oktay et al., 2007). The *Epas1*/*Hif-2α*$^{-/-}$ mouse had previously allowed Scortegagna *et al* to identify the role for HIF-2α in the regulation of anti-oxidant homeostasis and the identification of *SOD2* as a HIF-2α target gene (Scortegagna et al., 2003). *SOD2* encodes manganese superoxide dismutase (MnSOD) which converts superoxide to hydrogen peroxide ($H_2O_2$). Investigation into the effects of *Epas1*/*Hif-2α* deficiency on mitochondrial homeostasis identified increased oxidative stress and superoxide levels, consistent with the loss of *Sod2* mRNA and protein expression which correlated with increased sensitivity to calcium induced mPTP opening (Oktay et al., 2007). *Epas1*/*Hif-2α*$^{-/-}$ mitochondria also demonstrated impaired respiratory coupling and as such, respiratory control ratio (RCR) was reduced by 25% for complex I-linked respiration. There was no impairment of ETC complex activities, consistent with TCA cycle dysfunction. The comparison of *Epas1*/*Hif-2α*$^{-/-}$ and *Sod2*$^{-/-}$ phenotypes was suggestive that there were distinct SOD2-independent mechanisms contributing to *Epas1*/*Hif-2α*$^{-/-}$ mitochondrial phenotype.

The activity of αKGDH and mitochondrial aconitase were both significantly decreased after *Epas1*/*Hif-2α* knockout, with no correlative decrease in protein levels. *Frataxin* was identified as a novel *Hif-2α* target gene, down-regulated in the *Epas1*/*Hif-2α* null liver mitochondria. Frataxin protects iron-sulphur clusters from disassembly or inactivation and dysfunction, in combination with increased oxidative stress lead to the observed mitochondrial dysfunction (Oktay et al., 2007).

In this chapter, we aimed to investigate the effects of transient *HIF-2α* silencing on mitochondrial homeostasis, explore the role of HIF-2α in the pVHL-mediated effects on mitochondrial function and morphology described in chapters 4 and 5, and delineate and/or propose a potential mechanism for the observed effects.

### 6.11.1 *Silencing of HIF-2α causes microtubule-dependent peri-nuclear mitochondrial clustering*

*HIF-2α* silencing clearly affected the subcellular localisation of mitochondria in 786O cells. Mitochondria appeared to be peri-nuclearly localised upon HIF-2α knockdown, a phenotype which could be reversed through de-polymerisation the microtubules. Peri-nuclear clustering of mitochondria has been observed in a number of studies (DeWitt et al.,

2006, Yu et al., 2010, Hashiatni et al., 2010, Al-Mehdi et al., 2012). Al-Mehdi *et al* demonstrated that under hypoxia, peri-nuclear mitochondria are observed in pulmonary artery endothelial cells (Al-Mehdi et al., 2012). Al-Mehdi *et al* also demonstrated that the retrograde mitochondrial movement observed was also dependent on the microtubules and the motor protein dynein. Peri-nuclear mitochondrial clustering was accompanied by an accumulation of ROS in the nucleus, promoting oxidative modifications on the *VEGF* promoter, increasing gene expression. *VEGF* gene transcription was reduced when mitochondrial clustering was disrupted, suggesting that ROS-dependent modifications are important for HIF-dependent gene transcription (Al-Mehdi et al., 2012). Additionally peri-nuclear mitochondria have been hypothesised to function as sensors of intracellular metabolites (Hashiatni et al., 2010), observed in the periods preceding apoptosis (DeWitt et al., 2006) and in oocyte maturation (Yu et al., 2010).

Interestingly, the peri-nuclear distribution of mitochondria observed upon HIF-2α knockdown was reversed with nocodazole. Nocodazole depolymerises the microtubules and prevents microtubule-dependent vesicular transport throughout the cell. The reversal of peri-nuclear mitochondrial clustering by nocodazole treatment, suggests that the microtubules play a role in this peri-nuclear localisation process. Microtubules are also important for movement of a number of organelles and whether distinct organelles alter their subcellular localisation in a HIF-2α-dependent manner is an interesting question. EM images suggest that this may be the case, particularly evident in the 786O-EV cells, which are devoid of functional pVHL. In cells transfected with siRNA targeted towards *HIF-2α*, large vacant areas of cytoplasm are evident, which are not as obvious in the 786O-VHL cells. Differences in global cell shape between the pVHL positive and negative cells make mitochondrial distribution within the cell difficult to interpret from the EM images. The pVHL positive (786O-VHL) cells are less elongated and more rounded than the pVHL negative (786O-EV) cells. Thus the distance from the nucleus to cell membrane in the 786O-VHL cells compared with the 786O-EV cells is not as great, and any peri-nuclear organelle localisation is therefore less obvious by EM. The gross peri-nuclear distribution of organelles observed by EM would need to be confirmed by immunostaining using markers for a number of organelles or using organelle-specific tracking dyes. In addition to nocodazole treatment, knockout of dynein would allow confirmation of the microtubule-dependence of the peri-nuclear mitochondrial localisation and it would be important to

establish a high-throughput imaging platform and analysis algorithms in order to get better quantification of organelle movement with respect to cell size and shape.

During mitophagy, mitochondria also become clustered around the nucleus (Okatsu, 2010). Peri-nuclear aggregation of mitochondria in response to FCCP-mediated mitochondrial depolarisation has been shown to be dependent on p62, however not essential for mitochondrial degradation (Okatsu, 2010). Interestingly, parkin mutations have been shown to affect the mitophagic process at distinct stages and "mitoaggresomes" identified that require dynein motors and microtubules for their peri-nuclear localisation (Lee et al., 2010b). Although all parkin mutants in the study by Lee *et al* were defective at clearing mitochondria, mutations in the ubiquitin E3-ligase domain of parkin, still associated with depolarised mitochondria after FCCP treatment and caused peri-nuclear aggregates of mitochondria. Peri-nuclear mitochondrial clustering was reversed by nocodazole-induced microtubule depolymerisation and loss of parkin-dependent ubiquitination failed to recruit p62 and histone deacetylase 6 (HDAC6) (Lee et al., 2010b). Our data however raises the intriguing possibility that HIF-2α is involved in the final clearance step of mitochondria between their nuclear transport and lysosomal degradation. Additionally, as demonstrated in the previous chapter (chapter 5;

Figure 5.9) there appear to be clear changes in the expression of parkin in the presence and absence of pVHL in the 786O cells, which has been discussed with respect to possible effects on mitochondrial morphology observed in the 786O cells (chapter 5). Based on these observations we decided to investigate the role of HIF-2α and pVHL in regulation of autophagy and mitophagy.

### 6.11.2 *The effects of HIF-2α on mitochondrial morphology and autophagy*

A number of interesting observations have emerged from the EM studies in relation to HIF-2α and pVHL status. As described and discussed in chapter 5, mitochondrial length was greater in 786O-EV cells compared to 786O-VHL cells, indicating a role for pVHL in regulating mitochondrial morphology. Smaller mitochondria may be more susceptible to removal through non-selective autophagy and more likely to be engulfed by an autophagosome, in a process based on proximity and size. Mitochondrial fusion and fission cycles may therefore be important in regulating mitochondria turnover by autophagy (Twig, 2008). Fission is required for mitophagy to occur and can be suppressed through introduction of a dominant negative form of DRP-1 (Twig, 2008, Youle and van der Bliek,

2012). Interestingly, silencing the constitutively stable and active HIF-2α in the 786O-EV cells in part reverses the increase in mitochondrial length observed in 786O-EV cells compared to the 786O-VHL. The change in mitochondrial length may suggest both pVHL and HIF-2α-dependent mechanisms function in parallel. One notable observation is the significant increase in mitochondrial length observed after *HIF-2α* silencing in the presence of pVHL, indicating that basal HIF-2α regulates mitochondrial length in the presence of pVHL.

As discussed in the chapter 5, pVHL status affects the number of autophagosomes observed within the cell and is associated with altered in mitochondrial length. In a similar observation, *HIF-2α* silencing in cells expressing functional pVHL increases the number of autophagosomes observed in the cell, therefore mitochondrial length may increase as a mechanism to avoid autophagic removal, as suggested elsewhere (Gomes et al., 2011, Rambold et al., 2011). It would be necessary to determine the effects *HIF-2α* silencing on the mitochondrial fusion and fission apparatus. Assessment of the fusion and fission machinery may reveal insights into the apparent pVHL-dependent effects on mitochondrial length. The phosphorylation status of DRP-1 would be of great interest, as would determination of the DRP-1 protein abundance localised at the mitochondria in the presence and absence of *HIF*-2α siRNA.

Behensky *et al* investigated the role of HIF-2α in autophagy in chondrocytes and observed that when *HIF-2α* was silenced there was an increase in LC3 punctae by immunofluorescence, evidence of autophagic induction (Bohensky et al., 2009). An increase in lysotracker activity and examination of electron micrographs suggested an increase number of autophagosomes present in the *HIF-2α* silenced cells compared to control (Bohensky et al., 2009). A reduced binding of beclin and BCL-2 was also observed, suggesting greater amounts of free beclin. The role of HIF-2α in autophagy has also been investigated in the context of hepatocellular carcinoma in a tumour spheroid model (Menrad et al., 2010). Menrad *et al* observed that after *HIF-2α* silencing there was a compensatory up-regulation of HIF-1α-dependent *BNIP3* expression, autophagy and an increase in pro-survival BCL-XL (Menrad et al., 2010).

To investigate the role of HIF-2α further and relate observations to pVHL status, independent of the influence of HIF-1α, autophagic flux assays were performed in 786O cells. Under basal conditions, loss of HIF-2α protein reduced LC3B-II protein levels. The

addition of chloroquine alone in the presence and absence of *HIF-2α* siRNA also caused an increase in LC3B-II in both the 786O-VHL and 786O-EV cells, suggesting LC3B-II is being synthesised effectively in the absence of *HIF-2α*. In the presence of FCCP, we observed an increase in LC3B-II protein in both HIF-2α knockdown and control cells, suggesting mitophagic induction is unaffected by *HIF-2α* silencing. To investigate LC3B-II turnover, cells were treated with both chloroquine, to inhibit the lysosome and FCCP to induce mitophagy. Analysis revealed a smaller increase in LC3B-II relative to FCCP alone, in cells with HIF-2α knocked down compared to NSC siRNA control, suggesting reduced turnover or degradation of LC3B-II. The failure to increase LC3B protein levels after mitophagic induction by FCCP in the context of lysosomal inhibition may suggest a block in autophagy/mitophagy at the terminal stages and decreased autophagosome degradation (Klionsky et al., 2012, Rubinsztein et al., 2009). These observations indicate that transient loss of *HIF-2α* in the presence of pVHL may affect autophagosome maturation or degradation. Therefore our observations suggest that silencing *HIF-2α* has little effect on autophagosome formation the 786O renal cells demonstrated through the increase in LC3B after chloroquine and FCCP in isolation. *HIF-2α* silencing may however affect autophagosome degradation (Rubinsztein et al., 2009). A schematic representation of our proposed hypothetical model is included below (Figure 6.12).

A follow-up experiment would involve using a second activator of autophagy and mitophagy. Rapamycin could be used to inhibit mTOR and combination of antimycin A and oligomycin to depolarise mitochondria promoting their removal. Use of these activators would allow interpretation of whether just mitochondrial removal is affected or the more encompassing process of macroautophagy. Rapamycin induces autophagy by removing the negative pressure of mTOR on autophagic axis.

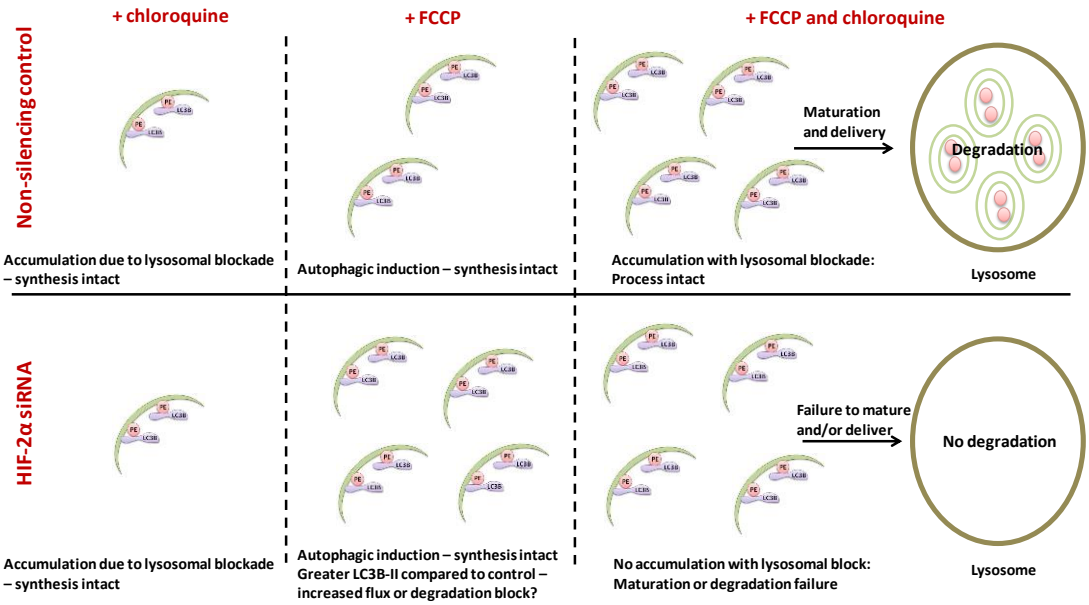


**Figure 6.12: Diagrammatic representation of the potential effects *HIF-2α* silencing on autophagy.**

**In the presence of chloroquine alone both control cells and cells treated with *HIF-2α* siRNA increase LC3B-II levels as degradation is blocked and basal synthesis remains functional. In the presence of FCCP, autophagic induction causes an increase in LC3B-II levels in both control and *HIF-2α* silenced cells. Treatment with chloroquine and FCCP reveals a functional system in the control cells, as there is a further increase in LC3B-II after FCCP induction and lysosomal inhibition by chloroquine. This suggests that the FCCP-mediated induction is going to completion. The lack of an increase in LC3B-II by FCCP in the presence of chloroquine in the *HIF-2α* silenced cells indicates a stalling in the pathway, resulting in the pathway not going to completion.**

EM revealed insights into the relationship of pVHL and HIF-2α in the regulation of autophagosome formation. Loss of *HIF-2α*, in the presence of pVHL increased the number of autophagosomes observed, suggesting that autophagosome formation is intact; however maturation and turnover cannot be assessed using this assay. The increase in autophagosomes in the 786O-VHL cells may however correlate with the data from the flux assay and suggest reduced autophagosome turnover. EM would need to be undertaken in the presence of inducers and inhibitors of the autophagic pathway, to confirm the autophagy is progressing to completion. Immunogold labelling of the autophagosomal structures and lysosomes would be required to confirm identify of these organelles. Although expert advice has been sought confirming their identification, this alternative approach remains necessary. Visualisation of lysosomal proteins, such as LAMP-2 would

allow identification of lysosomes and LC3B, the autophagosomes and allow confident identification of the two organelles. The EM phenotype observed is similar to that of the HDAC6 knockout (Lee et al., 2010a). The images from EM revealed an increase in the number of multilamellar bodes in the presence of *HIF-2α* siRNA compared to NSC siRNA control. Loss of HDAC6 causes failure of autophagosome fusion to the lysosome and results in accumulation of autophagosomes.

With respect to the data presented in this chapter, it is difficult to conclude if HIF-2α dependency for autophagosome maturation or degradation is limited to the removal of mitochondria or a more global macroautophagic dysfunction. To investigate this in 786O cells, an alternative to HBSS would need to be sought in order to induce macroautophagy and determine the effects in the presence and absence of HIF-2α protein. If this were to be a dysfunction in the terminal stages of autophagosome removal, one would hypothesise that the effects of HIF-2α is likely to affect global autophagy, as the two processes share a common terminal pathway of autophagosome turnover. Additionally, observations from EM reveal a global localisation of cytoplasmic components toward the nucleus after *HIF-2α* silencing. Nuclear organelle distribution again suggests that autophagy is affected on a macro scale. A number of assays could be performed to investigate whether this holds true and have been discussed in the previous chapter, including LC3-GFP, LC3-lysosome fusion assays and use of inhibitors and activators of the pathway. Experiments using rapamycin and FCCP individually and the addition of chloroquine, after *HIF-2α* silencing and imaging using EM may reveal the likely mechanism and would allow identification of precise part of the autophagic pathway that is disrupted after HIF-2α loss.

### 6.11.3 *Potential role for HIF-2α in mitophagy*

The selective degradation of mitochondria by autophagy is known as mitophagy. Autophagosome formation, elongation and degradation are performed by the same molecular players as for non-selective autophagy, described previously. Under physiological basal conditions mitochondria are cleared when damaged, dysfunctional or mature and a number of proteins orchestrate this selective turnover, including parkin, PINK1 and p62. Maintenance of a healthy mitochondrial population is essential for cell health and viability. Mitochondria are a significant source of ROS, therefore susceptible to oxidative damage and themselves mediators of apoptosis. Therefore, damage to mitochondria impacts on the global cellular health. Nutrient starvation can also stimulate mitophagy, which

experimentally can be visualised using GFP-LC3 and analysing mitochondrial co-localisation (Ravikumar et al., 2010). Finally, the mitochondrial permeability transition pore has also been implicated in mitophagy. This non-selective conductance pore allows solutes to transverse the mitochondrial membrane with a mass up to approximately 1500 Daltons and contributes to mitochondrial depolarisation (Lemasters et al., 2002, Kim et al., 2007).

*In vitro*, loss of mitochondrial inner membrane potential is used to trigger the mitophagic process. Constitutive expression of full length PINK1 protein is kept low by after import into the mitochondrial IMS and processing by the protease PARL (Deas et al., 2011a). Loss of mitochondrial inner membrane potential, through pharmacological uncoupling, prevents the processing of PINK1 and facilitates its accumulation on the outer mitochondrial membrane. The kinase activity of PINK1 recruits the E3-ligase parkin specifically to depolarised/damaged mitochondria. At mitochondria the E3-ligase activity of parkin increases (Matsuda, 2010) and parkin then ubiquitinates target proteins, predominantly Lys63-linked polyubiquitin on outer membrane proteins, tagging them for removal (Youle and Narendra, 2011, Youle and van der Bliek, 2012, Narendra, 2010, Vives-Bauza, 2010), through either autophagy or the ubiquitin proteasome system. Transient knockdown of HIF-2α has a small effect on parkin expression. We observed a small reproducible increase in protein and mRNA expression after *HIF-2α* silencing, the importance of which remains to be fully elucidated. The localisation of endogenous parkin and if and how its translocation to mitochondria is affected by *HIF-2α* silencing would be the next question to address.

To date, there are no reports of HIF-2α playing a role in the regulation of mitophagy. From the data presented in this chapter (Figure 6.7), it appears that in response to FCCP there is reduced mitophagic flux, likely due to decreased autophagosome clearance when *HIF-2α* is silenced. FCCP-meditated mitochondrial depolarisation is of course an extremely non-physiological model as doses required are in excess of those necessary to depolarise the membrane and induce maximum respiratory rate (Klionsky et al., 2012), but useful as a tool to determine a possible role for a protein in the pathway. A number of further experiments would need to be performed to understand the HIF-2α-mitophagy relationship.

Interestingly, reduction of HIF-2α protein has been observed to increase *BNIP3* expression (Raval et al., 2005), the homologue of NIX and over-expression of BNIP3 has been observed to induce autophagy and the co-localisation of mitochondria with autophagosomes. BNIP3 over-expression also increased parkin translocation and parkin-positive mitochondria

association with the autophagosomes, an effect reversed in the absence of BAK and BAX. BNIP3 has been also observed to interact directly with LC3B (Hanna et al., 2012). Interestingly, there appears to be an inverse relationship between HIF-2α status and BNIP3 expression. BNIP3 has been observed to be positively regulated by HIF-1α and responsible for increased mitophagy in hypoxia (Zhang et al., 2008). However stabilisation of HIF-2α in cells devoid of HIF-1α, or over-expression of HIF-2α causes decreased BNIP3 transcription (Raval et al., 2005). BNIP3 has been observed to augment autophagy through disruption of the beclin-BCL-2 complex, freeing beclin and accelerating the pathway. This process has also been observed to require DRP-1-mediated mitochondrial fission and parkin recruitment (Youngil et al., 2011). BNIP3 is involved in the recruitment of DRP-1 to mitochondria, and over-expression increases DRP-1 association with mitochondria, induces mitochondrial fragmentation and triggers parkin recruitment (Youngil et al., 2011). These observations suggest that in the absence of HIF-2α, BNIP3 levels may increase, recruiting DRP-1 to mitochondria and inducing mitochondrial fragmentation and turnover through parkin-mediated mitophagy. Mitochondrial isolation and immunoblotting for mitochondrially associated BNIP3, DRP-1 and parkin may reveal this mechanism. This mechanism could explain the smaller mitochondria observed after HIF-2α silencing in cells devoid of functional pVHL. It does not however explain the phenotype when HIF-2α is silenced in the presence of pVHL.

The accumulation of PINK1 on the mitochondrial outer membrane is necessary for parkin recruitment after pharmacological uncoupling (Matsuda, 2010, Narendra, 2010). Investigation into how loss of functional pVHL and *HIF-2α* silencing affects the association of stabilisation of PINK1 and recruitment process would be interesting to determine. Early indications suggest that in response to FCCP, PINK1 stabilisation is not affected by *HIF-2α* silencing. However further work is necessary to determine localisation and details in to the kinetics of PINK1 depolarisation-dependent stabilisation. Immunofluorescence of p62 in the presence and absence of pVHL and *HIF-2α* siRNA would allow identification of aggresomes of mitochondria and again give insight into the effect of the differential parkin expression between the 786O cells as parkin is required for the initial ubiquitination event that allows p62 targeting of mitochondria their clustering.

### 6.11.4 *HIF-2α silencing affects mitochondrial bioenergetics*

In response to *HIF-2α* silencing, in both HCT116 colon carcinoma and 786O renal carcinoma cells, basal respiration increased, demonstrated through an increase in OCR using the Oroboros O2K. There was also a significant increase in maximum respiratory rate after *HIF-2α* silencing in both cell lines. The increased OCR was both independent of pVHL status and any compensatory effects of *HIF-2α* silencing on HIF-1α activity. Increased OCR and maximum respiratory rate could be consequence of a number of factors. The increased OCR may suggest that there are more respiratory substrates feeding the electron transport chain; there is an increase in mitochondrial ETC components, greater amounts of mitochondria per cell or an increase in ATP demand. Bioenergetic flux ratios also suggest that minimal difference after HIF-2α loss on energetic status, including the degree of ETC uncoupling.

In contrast to the negative regulation on c-MYC activity by HIF-1α, HIF-2α promotes c-MYC transcriptional activity and cell cycle progression (Gordan et al., 2007, Gordan, 2008). HIF-1α-dependent transactivation of *MXI-1* and inhibition of c-MYC inhibits mitochondrial biogenesis (Zhang, 2007). Therefore one may predict that loss of *HIF-2α* in our system may negatively affect the transcriptional capacity of c-MYC, disrupting the MYC-MAX transcriptional complex (Gordan et al., 2007) and promote mitochondrial biogenesis. As discussed, activation of c-MYC has been shown to influence mitochondrial biogenesis through increasing mitochondria mass, mitochondrial DNA content and oxygen consumption rate (Li et al., 2005). These studies however do not correlate with what we observe, as transient *HIF-2α* silencing had little effect in mitochondrial mass (not shown), slightly increased mitochondrial DNA content and increased oxygen consumption rate. Therefore basal effects of HIF-2α on the regulation of c-MYC are either below the limits of detection or absent under ambient oxygen. Additionally, there was no effect on the transcription of PGC-1β, a c-MYC target involved in mitochondrial biogenesis, and notably in the absence of *HIF-2α* there are no changes observed in the expression of mitochondrial ETC proteins, contradictory to published observations (Hervouet et al., 2008).

Bertout *et al* demonstrated that HIF-2α negatively regulates p53 stabilisation and knockdown of HIF-2α promotes p53 stabilisation, phosphorylation and transcriptional activity on a select number of genes, through effects on ROS and alterations to the cellular redox state (Bertout, 2009). Shortly after this study was published, Roberts *et al* also

demonstrated in 786O-EV cells, the stabilisation and accumulation of HIF-2α, suppressed p53 activity through promoting the p53-HDM2 interaction. Loss of *HIF-2α* by RNA interference, or re-expression of pVHL, restores p53 activity by relieving this negative regulation (Roberts, 2009). p53 has also been observed to affect mitochondrial respiration through the transcriptional up-regulation of *SCO2*, an assembly factor for cytochrome c oxidase (Matoba et al., 2006). In light of this evidence, the role of p53 in the HIF-2α-dependent change in OCR was tested. In the presence of *HIF-2α* siRNA, OCR still increased in the absence of p53 compared to NSC control siRNA, suggesting the increase in OCR observed after *HIF-2α* silencing was independent of any HIF-2α-mediated effect on p53 (data not shown). Transcript levels of the p53 target gene, *SCO2* were also measured in these cells after silencing of *HIF-2α* and there was no significant difference (data not shown). The p53 independence of the HIF-2α-dependendent change in OCR suggests that, the silencing of *HIF-2α* and its effect on cellular OCR was independent of p53 stability and gene transcription, at least with respect to *SCO2*. p53 transcriptional targets have however been demonstrated to be cell type, context and post-translational modification dependent (Bertout, 2009).

Future experiments with respect to the role of HIF-2α in regulating mitochondrial respiration would be to silence *HIF-1β* in the 786O cells, which lack HIF-1α to determine if the role of HIF-2α is transcriptional and binding of the alpha and beta subunits is necessary. Alternatively, mitochondrial effects mediated by loss of HIF-2α may be due to the direct role of HIF-2α on a yet undefined process. Dissection of the ETC using ETC complex-linked substrates and respirometry in isolated mitochondria or permeabilised cells would allow determination of the direct role of HIF-2α on these processes. Spectrophotometric ETC complex assays or BN-PAGE and in-gel activity assays would confirm complex assembly and activity would continue to lay a foundation on which to build a conclusion as to the role of HIF-2α in mitochondrial bioenergetics.

### 6.11.5 *The role of HIF-2α in regulating mitochondrial DNA copy number*

Finally, mitochondrial DNA copy number has been shown to decrease with increased mitophagic flux (Klionsky et al., 2012). Interestingly, there is a slight, but reproducible increase in mitochondrial DNA copy number in all cell lines examined after *HIF-2α* silencing, however this does not reach significance, but may be suggestive of a decrease in mitophagic flux after *HIF-2α* silencing. An interesting series of experiment would be to

measure mitochondrial DNA copy number in cells treated with inhibitor(s) of autophagy, such as chloroquine and determine any change in the presence and absence of HIF-2α protein and the relationship with pVHL. Analysis of mitochondrial DNA content would also give a quantitative idea on mitophagic flux and could be combined with inducers of mitophagy to manipulate the process and determine how HIF-2α gene manipulation affects mitophagy under extreme conditions.

## 6.12 Summary

It is clear more work needs to be done to uncover the role of HIF-2α in the regulation of autophagy and cellular quality control. From the experiments presented here, HIF-2α appears necessary for the terminal maturation and/or clearance of autophagosomes, while autophagosome synthesis is maintained. HIF-2α also appears to differentially regulate mitochondrial length. Most importantly, pVHL-dependent regulation of mitochondrial length was found to be HIF-2α dependent.

Further experiments are necessary to determine whether the use of FCCP to induce mitophagic flux and the failure to increase LC3B-II in the presence of chloroquine, compared to FCCP treatment alone is specific to mitochondrial selective autophagy or extends to macroautophagy. Identification as to the role of HIF-2α in global autophagy can be achieved through use of alternative inducer(s) of autophagy. Alternatively, a distinct cell line could be starved in the presence of *HIF-2α* silencing and effects investigated after incubation with HBSS. The experiments outlined here are clearly among the most pressing to confirm or dismiss a role of basal HIF-2α in autophagy.

In this chapter, we have identified a potentially separable HIF-independent role for pVHL in mitochondrial function. Silencing of *HIF-2α* does not significantly affect the pVHL-dependent alterations in mitochondrial function, described in chapters 4 and 5, however does affect mitochondrial length.

The increase in basal OCR observed after *HIF-2α* silencing also remains unexplained. Whether the increase is related to the decreased in mitochondrial turnover or increased ATP demand after *HIF-2α* silencing remains unknown. However, increased OCR may be interpreted as a short-term adaptive response to decreased turnover of defective

mitochondria, whereby cells are respiring more to produce the same amount of energy, ATP.

From the work presented in this chapter a number of questions remain to be answered:

(i) What are the mechanisms underlying the change in autophagosome maturation and/or turnover after *HIF-2α* silencing?

(ii) Under basal conditions, how does the HIF-2α-dependent inhibition of terminal autophagosome clearance affect mitochondrial function?

(iii) How is the autophagic targeting of mitochondria regulated by HIF-2α?

(iv) Are HIF-2α-dependent mitochondrial morphology/localisation and bioenergetic changes associated with autophagy/mitophagy?

(v) What is the role of pVHL in regulating mitochondrial length and autophagy/mitophagy after transient loss of HIF-2α?

Data presented in this chapter are novel, and provide a platform on which to build further investigation with respect to both HIF-2α and pVHL in regulating autophagy/mitophagy and mitochondrial function. Significant work is necessary to confirm and further these observations, and ultimately to translate these findings as to their importance in disease.

# Chapter 7: Summary and conclusions

## 7.1 General background and summary

### 7.1.1 *HIF and the hypoxic response*

Cells are adapted to utilise oxygen to survive and it is necessary to maintain oxidative metabolism. Under oxygen limiting conditions, it is necessary for cells to sense and adapt to an environment of altered oxygenation. It is this role which the HIF/oxygen-sensing pathway plays. Oxygen, as a substrate for the PHD proteins keeps the HIF-α subunits tightly controlled under normal ambient conditions. When oxygen is limiting (hypoxia) PHDs are inhibited, limiting HIF-α turnover by pVHL and ultimately leading to HIF-α stabilisation, subsequent nuclear translocation and dimerisation with the HIF-1β subunit. HIF-dependent transactivation of target genes functions to maintain cellular homeostasis, allowing cell survival, demonstrating the physiological importance of this pathway.

Although physiologically necessary, the HIF/hypoxic response can become deregulated. The solid tumour micro-environment is a heterogeneous mass of cells that often becomes hypoxic towards its core. Under these conditions a robust hypoxic response is induced, promoting tumour growth and survival. Loss of the *VHL* tumour suppressor also promotes unopposed HIF-α stabilisation and associated pathology.

### 7.1.2 *The HIF-mitochondria relationship*

A well-established relationship between HIF and mitochondria exists. Metabolic adaptation to hypoxia involves HIF-dependent gene transactivation, regulating the balance of glycolytic and oxidative metabolism (Fukuda et al., 2007, Papandreou et al., 2006, Luo et al., 2011). Mitochondrial electron transport is also necessary for the hypoxic stabilisation of HIF-α. In this thesis, we investigated the relationship between the oxygen-sensing pathway and mitochondrial function, and have begun to delineate a more direct link between HIF-α and mitochondria. Additionally, we have begun to understand the HIF-2α/mitochondrial relationship and how HIF-2α specifically may act in cellular and mitochondrial quality control.

### 7.1.3 *Clinical significance of pVHL*

pVHL is the recognition component of the ECV E3-ligase responsible for the normoxic regulation of the HIF-α subunit, tags HIF-α for proteasomal degradation upon hydroxy-proline ubiquitination (Maxwell et al., 1999, Jaakkola et al., 2001). Study into the role of pVHL has contributed much towards our understanding of the cellular and physiological

response to hypoxia and mechanisms through which cells sense and react to altered oxygenation. Germline inactivation of *VHL* is a key event in the development of tumours characteristic of VHL disease and in the development of sporadic clear cell renal cell carcinomas. Here, we have established a novel role of pVHL distinct from that of HIF-α regulation. pVHL affects global mitochondrial properties after re-expression in renal cancer cells and positively modulates mitochondrial function.

## 7.2 Summary of key findings

In chapter 3, we first confirmed the HL-1 cell line as a suitable model for measuring and investigating the hypoxic response and HIF stabilisation *in vitro*. This validates previous observations (Nguyen and Claycomb, 1999) and identified a cardiomyocyte model for establishing a basis on which to further study the mitochondrial relationship with HIF-1α. We went on to identify several members of the oxygen-sensing machinery to be associated with mitochondria. We observed HIF-1α, HIF-1β, PHD2 and PHD3 in purified mitochondrial fractions from both cells and tissue. Interestingly, a hydroxylated HIF-1α species was also observed in mitochondrial preparations. Identification of HIF-1α protein at the mitochondria opens a number of exploratory avenues and the potential to uncover novel roles for HIF-1α protein outside that of nuclear transcriptional control.

Further to these observations, identification of the rapid accumulation of HIF-1α protein associated with mitochondria led to use of the PHD inhibitor DMOG, to investigate the early, transcriptional independent functions of HIF-1α. Investigations were extended to explore the HIF-1α independent roles of the PHD proteins. Although evidence suggests that the gene expression profile in MCF-7 cells after DMOG treatment correlates well with that of the hypoxic response (Elvidge et al., 2006), we have identified dissimilarities in the transcriptional independent, metabolic effects of DMOG compared with alternative PHD inhibitors suggesting off-target effects of DMOG.

A number of observations have identified a role for pVHL in the regulation of mitochondrial function in renal cells and in clear cell renal carcinoma (Shiao et al., 2000, Hervouet et al., 2005, Hervouet et al., 2008). In this thesis, we extended the studies of Hervouet *et al* to investigate the role of wild type and mutant pVHL re-expression in a defective pVHL renal carcinoma cell background. Interestingly, correlations can be made regarding pVHL

mutation and the mitochondrial phenotype observed. In this thesis, we have identified a role for pVHL in the regulation of mitochondrial protein expression, mitochondrial DNA maintenance and respiration, independent of HIF-α, but dependent on specific amino acid residues within the pVHL protein. We have also identified a role for pVHL in affecting mitochondrial mass or lipid content and pVHL-dependent effects on mitochondrial ribosomal protein expression. These data potentially link mitochondrial translation to the VHL-dependent mitochondrial ETC protein expression patterns observed in the 786O and RCC10 cells. Experiments using pVHL mutant protein expression suggest a phenotype dependent on pVHL protein stability and potentially a role for the ECV E3-ligase complex, linking pVHL-dependent mitochondrial phenotype toward a role for protein ubiquitination and potential turnover.

We have observed pVHL to affect mitochondrial morphology and mitochondrial length when re-expressed in 786O and RCC10 cells. Re-expression of pVHL decreases mitochondrial length by approximately 25% in 786O cells and produces a phenotype of less connected, rounder mitochondria compared with cells devoid of pVHL function. These observations were paralleled by pVHL-dependent expression of mitochondrial fusion and fission machinery. pVHL re-expression globally up-regulates MFN-1, MFN-2, OPA-1 and DRP-1. In the absence of pVHL an increase in phosphorylation of $Ser^{637}$ on DRP-1, inhibiting fission, without affecting the ratio of total DRP-1 to that phosphorylated at $Ser^{616}$, suggests a potential mechanism for the morphological change. pVHL re-expression is associated with an increased DRP-1: VDAC1 ratio present in mitochondrial fractions. Potentially, morphological alteration is a phenotype dependent on pVHL-mediated changes in macroautophagy, after an increased number of autophagosomes can be observed in the absence of pVHL in renal carcinoma cells and correlates with a mitochondrial sparing phenotype observed elsewhere (Rambold et al., 2011, Gomes et al., 2011).

Aiming to determine a relationship between the observed pVHL-dependent mitochondrial phenotype and HIF-2α, we identified these observations to being independent of HIF-2α status and in parallel identified a novel role for HIF-2α protein itself in mediating peri-nuclear organelle distribution, number of autophagosomes and FCCP-mediated mitophagy. An interesting HIF-2α-dependent effect on mitochondrial length was also observed in the 786O cells, a phenotype that appears to be determined by pVHL status.

## 7.3 Future studies

### 7.3.1 *Investigate the direct effect of the HIF-1 complex on mitochondria*

Data presented in this thesis suggests the potential for the localisation of the HIF-1 complex with mitochondria. Both HIF-1α and HIF-1β subunits have been identified in mitochondrial preparations from tissue and cells. Further work to investigate the sub-mitochondrial topology of HIF-1α and HIF-1β proteins and subsequently their function is necessary. In this thesis, mitochondrial localisation of the HIF proteins has been identified only through the isolation and preparation of purified mitochondria from cells and tissues. In order to expand these findings and to further understand the role of HIFs in directly regulating mitochondrial function, the subcellular localisation of the HIFs must be confirmed through additional, complementary approaches.

An increasing number of nuclear transcription factors have been identified in mitochondria (Gough et al., 2009, Marchenko et al., 2000, Psarra et al., 2005). Findings from this thesis suggest we may be able to add the HIF-1 complex to this select list of highly specialised proteins. Understanding the mitochondrial topology of the HIF-1 complex would aid in dissecting the role of the HIFs in directly regulating mitochondrial function. Identification of any potential mitochondrial nucleoid association of the HIF-1 complex, in line with its recognised role as a transcription factor, and investigations into the role of the HIFs in mitochondrial DNA maintenance and gene expression may be promising for further study. Investigations into the regulation of mitochondrial DNA, in the presence and absence of HIF-1α and the influence of hypoxia, may allow identification of novel mitochondrial gene regulation and mitochondrial adaptation to hypoxia.

Investigations into transcriptional independent roles of HIF-1α have identified the mitochondrial disulphide relay protein CHCHD4/MIA40 as a new regulator of the hypoxic response (Yang et al., 2012). Unpublished work from our laboratory indicate the possibility that HIF-1α binds CHCHD4 and regulates the electron transferring capacity of the DRS and consequently capacity of the mitochondrial ETC. This would suggest that HIF-1α may be present within the IMS, and/or affects CHCHD4/MIA40 import function.

Finally, having identified an association between HIF-1α and mitochondria, it is conceivable that the same relationship may exist between HIF-2α and mitochondria. Future work may concentrate on first identifying if HIF-2α protein can be detected with mitochondria and

follow-up with same confirmatory studies, including sub-mitochondrial topology and immunogold labelled protein, as detailed previously with relation to HIF-1α. Finally, targeting HIF-1α and/or HIF-2α to mitochondria may reveal a more subtle role for the complex.

### 7.3.2 *Identify a role for the PHD proteins in mitochondrial regulation of HIF-α or distinct mitochondrial hydroxylation targets*

Recently, the PHD proteins have emerged as an increasingly promiscuous class of enzymes. Initially, characterised in the negative regulation of the HIF-α subunit, the PHD proteins are ever more being recognised to bind, hydroxylate and mediate turnover of a large number of distinct proteins, involved in a diverse array of cellular functions (Xie et al., 2009, Hiwatashi et al., 2011, Kuznetsova et al., 2003).

As eluded to previously, with respect to mitochondrial localisation of HIF-1α, *in situ* confirmation of mitochondrial association/localisation of the PHD proteins is necessary. Having provided initial evidence supporting mitochondrial association of the PHD proteins and their emerging HIF-α independent function, proteomic analysis of PHD targets within mitochondria would provide a mechanism through which novel mitochondrial hydroxylation targets may be identified. Database search has already identified LXXLAP consensus hydroxylation sites in a number of mitochondrial proteins, including ATP5A and OPA-1.

### 7.3.3 *Further explore the relationship between pVHL and mitochondria in 786O cells*

There exists a multifaceted, as yet non-delineated relationship between pVHL and mitochondria. pVHL functions as the substrate recognition component of a multifunctional E3-ligase complex (Iwai et al., 1999, Kibel et al., 1995), best characterised for the normoxic proteasomal turnover of HIF-α subunits (Maxwell et al., 1999). However, pVHL is increasingly being recognised to have important HIF-α independent functions (Mukhopadhyay et al., 1997, Pal et al., 1997). How these HIF-α-independent roles of pVHL extend to regulating mitochondrial function and their importance in the tumour suppressor function of pVHL remains unknown. Investigation into the mitochondrial regulatory role of the ECV E3-ligase complex and the requirement for complex assembly and function is necessary to separate any potential independent roles of pVHL protein alone in controlling mitochondrial function. Mitochondrial effects of genetic manipulation of other ECV E3-

ligase complex components and determination of whether this would phenocopy the pVHL null phenotype would establish grounds on which to build a hypothesis.

Identification of mitochondrial substrates of pVHL or more likely cytoplasmic proteins that regulate mitochondrial function, whose fate is determined by the ECV E3-ligase complex would go somewhere to understanding the mitochondrial phenotype. Evidence suggests that pVHL may affect mitochondrial protein translation. We have identified a number of mitochondrial ribosomal protein subunits that are differentially expressed in the presence and absence of pVHL in 786O cells. Investigation into mitochondrial ribosome assembly and protein expression may begin to unravel a complex relationship and could be extended to understand any relationship between pVHL and mitochondrial translation using *in vitro* translation assays.

There is a clear relationship between pVHL status and mitochondrial DNA copy number established in this thesis. Further investigations into the mechanism behind this alteration may reveal novel targets for pVHL regulation. Understanding the cause versus effect relationship relating to mitochondrial morphology, bioenergetics and mitochondrial DNA maintenance is necessary to determine the focus for further mechanistic study.

To date, proteomic investigation of the pVHL interactome suggests few targets that may be responsible for mediating such a phenotype. Investigation into mitochondrial complex assembly in the presence and absence of pVHL may allow correlation to be established between the decrease in subunit protein expression and complex abundance and activity observed after loss of pVHL. These investigations could be extended to investigate mitochondrial super complex assembly and the impact of pVHL-dependent changes in mitochondrial lipid content.

### 7.3.4 *Investigate the cellular consequences of reversing mitochondrial morphology observed in the presence and absence of pVHL*

Prominent pVHL-dependent morphological alterations have been identified that are unable to be corrected after *HIF-2α* silencing in pVHL defective cells. Mitochondrial morphology has been observed to protect mitochondria from non-selective autophagic turnover, maintaining energy biosynthesis and cell survival (Gomes et al., 2011, Rambold et al., 2011). Understanding how reversal of the pVHL-dependent mitochondrial morphological phenotype affects cell viability and function would allow dissection of the significance of

this effect. Understanding the mechanism behind the pVHL-dependent morphological alterations would also be valuable. Investigation into the classical regulation of DRP-1 phosphorylation states would prove a starting point to begin to untangle the likely signalling involved. Investigation into how the dynamics of fusion and fission change after pVHL re-expression will be necessary to determine whether we are observing a phenotype of reduced fusion or increased fission.

### 7.3.5 *Investigate the pVHL-parkin relationship, understand the regulation and cellular consequence*

We have identified a strong correlation between pVHL status and parkin expression. Investigation is necessary to determine how the pVHL-parkin relationship observed in 786O cells extends across cell lines and once a positive correlation is established, investigation into the role of pVHL in parkin-mediated function could be investigated. In cells lacking pVHL there is a striking deficiency in parkin expression compared to those cells with pVHL re-expressed. Understanding the signalling involved in this transcriptional response would first be important to establish the likely scenarios under which these proteins and pathway cross-talk *in vivo*. Investigation into the cellular effects of parkin re-expression in a pVHL defective background may provide insight into the influence of this protein on the observed pVHL-dependent mitochondrial phenotype in 786O cells.

### 7.3.6 *Understand how the pVHL relationship with mitochondria extends across cell lines and tissues.*

Most importantly however, is to determine how the pVHL-dependent mitochondrial phenotype extends across cell lines. Characterisation of pVHL loss of function would be necessary to determine the extent to which pVHL controls mitochondrial function. Access to a conditional $VHL^{-/-}$ mouse, would allow identification of how a mitochondrial phenotype observed in *VHL* defective renal cell carcinoma, compared to that after stable re-expression extends *in vivo* and in different tissues. With respect to the role of pVHL in the apparent positive regulation of parkin expression and identification of parkin as a tumour suppressor protein, at least in hepatocellular carcinoma (Fujiwara et al., 2008) may indicate a role for pVHL in expression of this protein in tissues other than the kidney.

### 7.3.7 *Investigate the role of HIF-2α in renal cells and pVHL-dependent and independent regulation of autophagy and mitochondrial selective turnover*

The observations presented in this thesis regarding the role of HIF-2α in autophagy are clearly in their infancy and considerable amounts of further work are required to investigate this phenotype further. Studies of autophagic flux, the identification of autophagosome structures and investigation into any mechanism and impact on cellular function need to be established. The pVHL-HIF-2α dependent changes in mitochondrial length are also an interesting observation and further investigation into mitochondrial and protein turnover through autophagy may reveal some additional insights.

## 7.4 Limitations of the current study

As in any study, it is important to understand where limitations lie in data obtained and how these limitations impact on interpretation of results. Firstly, with respect to the hypothesis that DMOG has off-target affects that influence metabolism, although highly revealing, the metabolomic data is limited only to cell treatment with DMOG and no data has been obtained with the second PHD inhibitor. The lack of metabolomic analysis on PHD-I restricts comprehensive conclusions. Although a second PHD inhibitor does not phenocopy the effects of DMOG on mitochondrial function, it would be necessary to compare and contrast metabolite profiles to determine whether the TCA cycle interference hypothesis of DMOG remains valid.

As mentioned in chapter 3, there are inherent problems associated with subcellular fractionation and determining cellular topology of proteins. The chance of protein and organelle contamination through subcellular fractionation techniques need to be considered, and *in situ* localisation studies addressed in parallel, would add real value to the work presented in this thesis.

The pVHL positive and negative 786O cell model has been utilised throughout this thesis. The 786O cell model has many advantages, such as the defining expression of only HIF-2α and not HIF-1α. Additionally, the loss of pVHL and stable re-expression allows the genetic fault to be corrected and the role of this single protein change to be examined in matched cell lines. However stable re-expression of pVHL produces supra-physiological levels of the protein that one may associate with protein over-expression. In light of pVHL protein over-

expression, investigation into loss of pVHL, through silencing or knockout would useful in delineating a phenotype associated with over-expression to that of physiological function of pVHL. Finally, with respect to the observations involving HIF-2α, use of a second, validated siRNA is essential to confirm that we are observing a target-specific phenotype.

## 7.5 Final conclusions

### 7.5.1 *Chapter 3*

We have investigated a direct relationship between protein members of the oxygen-sensing pathway and mitochondria. We have identified a potential mitochondrial association between HIF and the PHD proteins and have begun to hypothesise novel routes through which the HIF-1 complex and the PHD proteins may directly regulate mitochondrial function and homeostasis.

In chapter 3, we have also established potential off-target effects of DMOG on metabolism, potentially through effects on the TCA cycle. As a well utilised method for pharmacological activation of the HIF/hypoxic response in normoxia, observations stemming from this thesis suggest that metabolic phenotypes identified using this compound in future, must be carefully interpreted before conclusions made. As analysis of metabolite profile in cells treated with DMOG suggests that it may affect several metabolic pathways and affect substrate supply to the ETC. Therefore, in any future studies, comparison must be made between DMOG and those with a more selective inhibitor and/or compound with alternative mechanism of action.

Therefore from chapter 3 we can conclude:

- HIF-1α and HIF-1β associate with mitochondria in cells and tissue
- PHD2 and PHD3 proteins associate with mitochondria
- DMOG treatment causes rapid mitochondrial and metabolic alterations, that cannot be reproduced with a second inhibitor of the PHD protein

### 7.5.2 *Chapter 4*

We have extended published observations (Hervouet et al., 2005, Hervouet et al., 2008) regarding the re-expression of pVHL in renal cell carcinoma and its effects on mitochondrial phenotype. In chapter 4, we have identified that this relationship is likely independent of

HIF-2α and potentially reliant on the capacity of the ECV E3-ligase complex. pVHL re-expression increases mitochondrial respiration, mitochondrial DNA content and has differential effects on the protein expression of a number of mitochondrially and nuclear encoded ETC subunits. Analysis of ETC subunit gene expression also suggests mitochondrial protein translational effects, potentially through pVHL-dependent regulation of mitochondrial ribosomal protein expression.

Therefore from chapter 4 we can conclude:

- pVHL status affects mitochondrial function in renal carcinoma cells
- The pVHL-dependent mitochondrial phenotype is primarily independent of HIF-α

### 7.5.3 *Chapter 5*

Here we have established a role in the regulation of mitochondrial morphology after re-expression of pVHL in renal cell carcinoma. Approaches to understand a mechanism behind these observations led to the identification of increased inhibitory phosphorylation events on DRP-1 in the 786O-EV cells. In the absence of pVHL a decrease in DRP-1, MFN-1 and MFN-2 and OPA-1 expression was also identified. A correlation between the re-expression of pVHL and presence of autophagosomes was also noted, confirming established links between pVHL and macroautophagy. A positive regulatory role of pVHL re-expression on parkin was also identified, potentially linking pVHL and/or renal cell carcinoma to alterations in mitochondrial turnover.

Therefore from chapter 5 we can conclude:

- pVHL status affect mitochondrial morphology and the expression and post-translational modification of mitochondrial fusion and fission proteins
- pVHL status affects markers of autophagy
- A relationship exists between pVHL status and parkin expression

### 7.5.4 *Chapter 6*

Here we have identified that loss of HIF-2α, is associated with peri-nuclear distribution of mitochondria. This nuclear re-distribution likely extends to distinct cytoplasmic organelles, a phenotype which may be associated with altered autophagic flux. Loss of HIF-2α also appears to affect mitochondrial respiration independently of pVHL status and has a small influence on mitochondrial DNA copy number, a phenotype evident across cell lines.

Interestingly, we have also identified a HIF-2α-dependent role in regulating mitochondrial length in 786O cells, a phenotype that is dependent on pVHL status.

Therefore from chapter 6 we can conclude:

- Loss of HIF-2α affects mitochondrial distribution and function
- Loss of HIF-2α may influence mitochondrial turnover and autophagy

## 7.6 Final thoughts

Throughout this thesis, we have aimed to identify novel regulatory mechanisms of the oxygen-sensing machinery on mitochondrial function. There is much still to learn and discover regarding the function of HIF and the PHD proteins, their coordination, regulation, localisation, relationship and mechanistic activity in influencing the mitochondrial phenotype. Additionally, we have established many pVHL-dependent effects on mitochondrial function using a wild type genetic gene re-expression in a renal carcinoma matched cell system. It is our hope that the findings presented in this thesis will lead to the identification of novel molecular mechanisms that regulate cellular health and homeostasis, and help us further understand specific disease pathologies that involve deregulation of the oxygen-sensing pathway.

# Bibliography

ACKER, T. 2005. Genetic evidence for a tumor suppressor role of HIF-2α. *Cancer Cell,* 8**,** 131-141.

ACTON, B. M., JURISICOVA, A., JURISICA, I. & CASPER, R. F. 2004. Alterations in mitochondrial membrane potential during preimplantation stages of mouse and human embryo development. *Molecular Human Reproduction,* 10**,** 23-32.

ADDABBO, F., MONTAGNANI, M. & GOLIGORSKY, M. S. 2009. Mitochondria and reactive oxygen species. *Hypertension,* 53**,** 885-92.

AGANI, F. H., PICHIULE, P., CARLOS CHAVEZ, J. & LAMANNA, J. C. 2002. Inhibitors of mitochondrial complex I attenuate the accumulation of hypoxia-inducible factor-1 during hypoxia in Hep3B cells. *Comp Biochem Physiol A Mol Integr Physiol,* 132**,** 107-9.

AGANI, F. H., PICHIULE, P., CHAVEZ, J. C. & LAMANNA, J. C. 2000. The role of mitochondria in the regulation of hypoxia-inducible factor 1 expression during hypoxia. *J Biol Chem,* 275**,** 35863-7.

AL-MEHDI, A.-B., PASTUKH, V. M., SWIGER, B. M., REED, D. J., PATEL, M. R., BARDWELL, G. C., PASTUKH, V. V., ALEXEYEV, M. F. & GILLESPIE, M. N. 2012. Perinuclear Mitochondrial Clustering Creates an Oxidant-Rich Nuclear Domain Required for Hypoxia-Induced Transcription. *Sci. Signal.,* 5**,** ra47-.

ALAM, H., WECK, J., MAIZELS, E., PARK, Y., LEE, E. J., ASHCROFT, M. & HUNZICKER-DUNN, M. 2009. Role of the phosphatidylinositol-3-kinase and extracellular regulated kinase pathways in the induction of hypoxia-inducible factor (HIF)-1 activity and the HIF-1 target vascular endothelial growth factor in ovarian granulosa cells in response to follicle-stimulating hormone. *Endocrinology,* 150**,** 915-928.

ALLEN, S., BALABANIDOU, V., SIDERIS, D. P., LISOWSKY, T. & TOKATLIDIS, K. 2005. Erv1 mediates the Mia40-dependent protein import pathway and provides a functional link to the respiratory chain by shuttling electrons to cytochrome c. *J.Mol.Biol.,* 353**,** 937-944.

ANDERSON, K., NORDQUIST, K. A., GAO, X., HICKS, K. C., ZHAI, B., GYGI, S. P. & PATEL, T. B. 2011. Regulation of Cellular Levels of Sprouty2 Protein by Prolyl Hydroxylase Domain and von Hippel-Lindau Proteins. *Journal of Biological Chemistry,* 286**,** 42027-42036.

APPELHOFF, R. J., TIAN, Y. M., RAVAL, R. R., TURLEY, H., HARRIS, A. L., PUGH, C. W., RATCLIFFE, P. J. & GLEADLE, J. M. 2004. Differential function of the prolyl hydroxylases PHD1, PHD2, and PHD3 in the regulation of hypoxia-inducible factor. *J Biol Chem,* 279**,** 38458-65.

APRELIKOVA, O., CHANDRAMOULI, G. V. R., WOOD, M., VASSELLI, J. R., RISS, J., MARANCHIE, J. K., LINEHAN, W. M. & BARRETT, J. C. 2004. Regulation of HIF prolyl hydroxylases by hypoxia-inducible factors. *Journal of Cellular Biochemistry,* 92**,** 491-501.

ARAGONES, J., FRAISL, P., BAES, M. & CARMELIET, P. 2009. Oxygen sensors at the crossroad of metabolism. *Cell Metab.,* 9**,** 11-22.

ARAGONES, J., SCHNEIDER, M., VAN GEYTE, K., FRAISL, P., DRESSELAERS, T., MAZZONE, M., DIRKX, R., ZACCHIGNA, S., LEMIEUX, H., JEOUNG, N. H., LAMBRECHTS, D., BISHOP, T., LAFUSTE, P., DIEZ-JUAN, A., HARTEN, S. K., VAN NOTEN, P., DE BOCK, K., WILLAM, C., TJWA, M., GROSFELD, A., NAVET, R., MOONS, L., VANDENDRIESSCHE, T., DEROOSE, C., WIJEYEKOON, B., NUYTS, J., JORDAN, B., SILASI-MANSAT, R., LUPU, F., DEWERCHIN, M., PUGH, C., SALMON, P., MORTELMANS, L., GALLEZ, B., GORUS, F., BUYSE, J., SLUSE, F., HARRIS, R. A., GNAIGER, E., HESPEL, P., VAN HECKE, P., SCHUIT, F., VAN VELDHOVEN, P., RATCLIFFE, P., BAES, M., MAXWELL, P. & CARMELIET, P. 2008. Deficiency or inhibition of oxygen sensor Phd1 induces hypoxia tolerance by reprogramming basal metabolism. *Nat Genet,* 40**,** 170-80.

ARANY, Z., HUANG, L. E., ECKNER, R., BHATTACHARYA, S., JIANG, C., GOLDBERG, M. A., BUNN, H. F. & LIVINGSTON, D. M. 1996. An essential role for p300/CBP in the cellular response to hypoxia. *Proc Natl Acad Sci U S A,* 93**,** 12969-73.

ARLT, H., STEGLICH, G., PERRYMAN, R., GUIARD, B., NEUPERT, W. & LANGER, T. 1998. The formation of respiratory chain complexes in mitochondria is under the proteolytic control of the m-AAA protease. *EMBO Journal,* 17**,** 4837-4847.

ARSTALL, M. A., ZHAO, Y. Z., HORNBERGER, L., KENNEDY, S. P., BUCHHOLZ, R. A., OSATHANONDH, R. & KELLY, R. A. 1998. Human ventricular myocytes in vitro exhibit both early and delayed preconditioning responses to simulated ischemia. *J Mol Cell Cardiol,* 30**,** 1019-25.

BAE, S. H., JEONG, J. W., PARK, J. A., KIM, S. H., BAE, M. K., CHOI, S. J. & KIM, K. W. 2004. Sumoylation increases HIF-1alpha stability and its transcriptional activity. *Biochem Biophys Res Commun,* 324**,** 394-400.

BALLINGER, S. W. 2005. Mitochondrial dysfunction in cardiovascular disease. *Free Radical Biology and Medicine,* 38**,** 1278-1295.

BANGIYEVA, V., ROSENBLOOM, A., ALEXANDER, A., ISANOVA, B., POPKO, T. & SCHOENFELD, A. 2009. Differences in regulation of tight junctions and cell morphology between VHL mutations from disease subtypes. *BMC Cancer,* 9**,** 229.

BARDOS, J. I. & ASHCROFT, M. 2005. Negative and positive regulation of HIF-1: a complex network. *Biochim Biophys Acta,* 1755**,** 107-20.

BARDOS, J. I., CHAU, N. M. & ASHCROFT, M. 2004. Growth factor-mediated induction of HDM2 positively regulates hypoxia-inducible factor 1alpha expression. *Mol Cell Biol,* 24**,** 2905-14.

BARRY, R. E. 2004. *Functional analysis of the von Hippel-Lindau tumour suppressor and its role in tumourigenesis.* DPhil, Universitat Basel.

BARTEL, D. P. 2004. MicroRNAs: Genomics, Biogenesis, Mechanism, and Function. *Cell,* 116**,** 281-297.

BARTH, S., EDLICH, F., BERCHNER-PFANNSCHMIDT, U., GNEUSS, S., JAHREIS, G., HASGALL, P. A., FANDREY, J., WENGER, R. H. & CAMENISCH, G. 2009. Hypoxia-inducible factor prolyl-4-hydroxylase PHD2 protein abundance depends on integral membrane anchoring of FKBP38. *J Biol Chem,* 284**,** 23046-58.

BARTH, S., GLICK, D. & MACLEOD, K. F. 2010. Autophagy: assays and artifacts. *The Journal of Pathology,* 221**,** 117-124.

BEESON, C. C., BEESON, G. C. & SCHNELLMANN, R. G. 2010. A high-throughput respirometric assay for mitochondrial biogenesis and toxicity. *Analytical Biochemistry,* 404**,** 75-81.

BELL, E. L., EMERLING, B. M. & CHANDEL, N. S. 2005. Mitochondrial regulation of oxygen sensing. *Mitochondrion,* 5**,** 322-332.

BELL, E. L., KLIMOVA, T. A., EISENBART, J., MORAES, C. T., MURPHY, M. P., BUDINGER, G. R. & CHANDEL, N. S. 2007. The Qo site of the mitochondrial complex III is required for the transduction of hypoxic signaling via reactive oxygen species production. *J Cell Biol,* 177**,** 1029-36.

BERRA, E., BENIZRI, E., GINOUVES, A., VOLMAT, V., ROUX, D. & POUYSSEGUR, J. 2003. HIF prolyl-hydroxylase 2 is the key oxygen sensor setting low steady-state levels of HIF-1alpha in normoxia. *Embo J,* 22**,** 4082-90.

BERRA, E., ROUX, D., RICHARD, D. E. & POUYSSEGUR, J. 2001. Hypoxia-inducible factor-1 alpha (HIF-1 alpha) escapes O(2)-driven proteasomal degradation irrespective of its subcellular localization: nucleus or cytoplasm. *EMBO Rep,* 2**,** 615-20.

BERTA, M. A., MAZURE, N., HATTAB, M., POUYSSEGUR, J. & BRAHIMI-HORN, M. C. 2007. SUMOylation of hypoxia-inducible factor-1alpha reduces its transcriptional activity. *Biochem Biophys Res Commun,* 360**,** 646-52.

BERTOUT, J. A. 2009. HIF2α inhibition promotes p53 pathway activity, tumor cell death, and radiation responses. *Proc. Natl Acad. Sci. USA,* 106**,** 14391-14396.

BHANDARY, B., MARAHATTA, A., KIM, H.-R. & CHAE, H.-J. 2012. Mitochondria in relation to cancer metastasis. *Journal of Bioenergetics and Biomembranes,* 44**,** 623-627.

BIEN, M., LONGEN, S., WAGENER, N., CHWALLA, I., HERRMANN, J. M. & RIEMER, J. 2010. Mitochondrial disulfide bond formation is driven by intersubunit electron transfer in Erv1 and proofread by glutathione. *Mol.Cell,* 37**,** 516-528.

BIHLMAIER, K., MESECKE, N., TERZIYSKA, N., BIEN, M., HELL, K. & HERRMANN, J. M. 2007. The disulfide relay system of mitochondria is connected to the respiratory chain. *J.Cell Biol.,* 179**,** 389-395.

BISWAS, S., TROY, H., LEEK, R., CHUNG, Y. L., LI, J. L., RAVAL, R. R., TURLEY, H., GATTER, K., PEZZELLA, F., GRIFFITHS, J. R., STUBBS, M. & HARRIS, A. L. 2010. Effects of HIF-1alpha and HIF2alpha on Growth and Metabolism of Clear-Cell Renal Cell Carcinoma 786-0 Xenografts. *J Oncol,* 2010**,** 757908.

BJØRKØY, G., LAMARK, T., BRECH, A., OUTZEN, H., PERANDER, M., ØVERVATN, A., STENMARK, H. & JOHANSEN, T. 2005. p62/SQSTM1 forms protein aggregates degraded by autophagy and has a protective effect on huntingtin-induced cell death. *The Journal of Cell Biology,* 171**,** 603-614.

BJØRKØY, G., LAMARK, T., PANKIV, S., ØVERVATN, A., BRECH, A. & JOHANSEN, T. 2009. Chapter 12 Monitoring Autophagic Degradation of p62/SQSTM1. *In:* DANIEL, J. K. (ed.) *Methods in Enzymology.* Academic Press.

BOGENHAGEN, D. F., ROUSSEAU, D. & BURKE, S. 2008. The Layered Structure of Human Mitochondrial DNA Nucleoids. *Journal of Biological Chemistry,* 283**,** 3665-3675.

BOHENSKY, J., TERKHORN, S. P., FREEMAN, T. A., ADAMS, C. S., GARCIA, J. A., SHAPIRO, I. M. & SRINIVAS, V. 2009. Regulation of autophagy in human and murine cartilage: Hypoxia-inducible factor 2 suppresses chondrocyte autophagy. *Arthritis & Rheumatism,* 60**,** 1406-1415.

BOLLI, R., SHINMURA, K., TANG, X. L., KODANI, E., XUAN, Y. T., GUO, Y. & DAWN, B. 2002. Discovery of a new function of cyclooxygenase (COX)-2: COX-2 is a cardioprotective protein that alleviates ischemia/reperfusion injury and mediates the late phase of preconditioning. *Cardiovasc Res,* 55**,** 506-19.

BOND, J., GALE, D. P., CONNOR, T., ADAMS, S., DE BOER, J., GASCOYNE, D. M., WILLIAMS, O., MAXWELL, P. H. & ANCLIFF, P. J. 2011. Dysregulation of the HIF pathway due to VHL mutation causing severe erythrocytosis and pulmonary arterial hypertension. *Blood,* 117**,** 3699-3701.

BOULAHBEL, H., DURAN, R. V. & GOTTLIEB, E. 2009. Prolyl hydroxylases as regulators of cell metabolism. *Biochem Soc Trans,* 37**,** 291-4.

BRAHIMI-HORN, C., MAZURE, N. & POUYSSEGUR, J. 2005. Signalling via the hypoxia-inducible factor-1alpha requires multiple posttranslational modifications. *Cell Signal,* 17**,** 1-9.

BRAND, M. D. & ESTEVES, T. C. 2005. Physiological functions of the mitochondrial uncoupling proteins UCP2 and UCP3. *Cell Metabolism,* 2**,** 85-93.

BRAND, M. D. & NICHOLLS, D. G. 2011. Assessing mitochondrial dysfunction in cells. *Biochem J,* 435**,** 297-312.

BRAUNWALD, E. & KLONER, R. A. 1985. Myocardial reperfusion: a double-edged sword? *J Clin Invest,* 76**,** 1713-9.

BRISTON, T., YANG, J. & ASHCROFT, M. 2011. HIF-1alpha localization with mitochondria: a new role for an old favorite? *Cell Cycle,* 10**,** 4170-1.

BROWN, S. T. & NURSE, C. A. 2008. Induction of HIF-2alpha is dependent on mitochondrial O2 consumption in an O2-sensitive adrenomedullary chromaffin cell line. *Am J Physiol Cell Physiol,* 294**,** C1305-12.

BRUCE ALBERTS, A. J., JULIAN LEWIS, MARTIN RAFF, KEITH ROBERTS, AND PETER WALTER 2002. *Molecular Biology of the Cell*, New York: Garland Science.

BRUNELLE, J. K., BELL, E. L., QUESADA, N. M., VERCAUTEREN, K., TIRANTI, V., ZEVIANI, M., SCARPULLA, R. C. & CHANDEL, N. S. 2005. Oxygen sensing requires mitochondrial ROS but not oxidative phosphorylation. *Cell Metab,* 1**,** 409-14.

BUNZ, F., DUTRIAUX, A., LENGAUER, C., WALDMAN, T., ZHOU, S., BROWN, J. P., SEDIVY, J. M., KINZLER, K. W. & VOGELSTEIN, B. 1998. Requirement for p53 and p21 to Sustain G2 Arrest After DNA Damage *Science* 282 1497-1501

CADENAS, S., ARAGONES, J. & LANDAZURI, M. O. 2010. Mitochondrial reprogramming through cardiac oxygen sensors in ischemic heart disease. *Cardiovasc Res,* 88**,** 219-28.

CAI, Z., ZHONG, H., BOSCH-MARCE, M., FOX-TALBOT, K., WANG, L., WEI, C., TRUSH, M. A. & SEMENZA, G. L. 2008. Complete loss of ischaemic preconditioning-induced cardioprotection in mice with partial deficiency of HIF-1 alpha. *Cardiovasc Res,* 77**,** 463-70.

CALDWELL, M. C., HOUGH, C., FURER, S., LINEHAN, W. M., MORIN, P. J. & GOROSPE, M. 2002. Serial analysis of gene expression in renal carcinoma cells reveals VHL-dependent sensitivity to TNFalpha cytotoxicity. *Oncogene,* 21**,** 929-36.

CAMPBELL, C. T., KOLESAR, J. E. & KAUFMAN, B. A. 2012. Mitochondrial transcription factor A regulates mitochondrial transcription initiation, DNA packaging, and genome copy number. *Biochimica et Biophysica Acta (BBA) - Gene Regulatory Mechanisms,* 1819**,** 921-929.

CAMPS, C., BUFFA, F. M., COLELLA, S., MOORE, J., SOTIRIOU, C., SHELDON, H., HARRIS, A. L., GLEADLE, J. M. & RAGOUSSIS, J. 2008. hsa-miR-210 Is Induced by Hypoxia and Is an Independent Prognostic Factor in Breast Cancer. *Clinical Cancer Research,* 14**,** 1340-1348.

CARDACI, S. & CIRIOLO, M. R. 2012. TCA Cycle Defects and Cancer: When Metabolism Tunes Redox State. *International Journal of Cell Biology,* 2012**,** 9.

CARROLL, V. A. & ASHCROFT, M. 2006. Role of hypoxia-inducible factor (HIF)-1alpha versus HIF-2alpha in the regulation of HIF target genes in response to hypoxia, insulin-like growth factor-I, or loss of von Hippel-Lindau function: implications for targeting the HIF pathway. *Cancer Res,* 66**,** 6264-70.

CARROLL, V. A. & ASHCROFT, M. 2008. Regulation of angiogenic factors by HDM2 in renal cell carcinoma. *Cancer Research.68(2):545-52,*.

CAVALLI, L., VARELLA-GARCIA, M. & LIANG, B. 1997. Diminished tumorigenic phenotype after depletion of mitochondrial DNA. *Cell Growth Differ,* 8**,** 1189-1198.

CEREGHETTI, G. M., STANGHERLIN, A., DE BRITO, O. M., CHANG, C. R., BLACKSTONE, C., BERNARDI, P. & SCORRANO, L. 2008. Dephosphorylation by calcineurin regulates translocation of Drp1 to mitochondria. *Proceedings of the National Academy of Sciences,* 105**,** 15803-15808.

CHACINSKA, A., PFANNSCHMIDT, S., WIEDEMANN, N., KOZJAK, V., SANJUAN SZKLARZ, L. K., SCHULZE-SPECKING, A., TRUSCOTT, K. N., GUIARD, B., MEISINGER, C. & PFANNER, N. 2004. Essential role of Mia40 in import and assembly of mitochondrial intermembrane space proteins. *Embo J,* 23**,** 3735-3746.

CHAMPAGNE, E., MARTINEZ, L. O., COLLET, X. & BARBARAS, R. 2006. Ecto-F1Fo ATP synthase/F1 ATPase: metabolic and immunological functions. *Curr Opin Lipidol,* 17**,** 279-84.

CHAN, D. C. 2012. Fusion and Fission: Interlinked Processes Critical for Mitochondrial Health. *Annu Rev Genet,* 46**,** 265-287.

CHAN, S. Y., ZHANG, Y.-Y., HEMANN, C., MAHONEY, C. E., ZWEIER, J. L. & LOSCALZO, J. 2009. MicroRNA-210 Controls Mitochondrial Metabolism during Hypoxia by Repressing the Iron-Sulfur Cluster Assembly Proteins ISCU1/2. *Cell Metabolism,* 10**,** 273-284.

CHANDEL, N. S., MALTEPE, E., GOLDWASSER, E., MATHIEU, C. E., SIMON, M. C. & SCHUMACKER, P. T. 1998. Mitochondrial reactive oxygen species trigger hypoxia-induced transcription. *Proc Natl Acad Sci U S A,* 95**,** 11715-20.

CHANDEL, N. S., MCCLINTOCK, D. S., FELICIANO, C. E., WOOD, T. M., MELENDEZ, J. A., RODRIGUEZ, A. M. & SCHUMACKER, P. T. 2000. Reactive oxygen species generated at mitochondrial complex III stabilize hypoxia-inducible factor-1alpha during hypoxia: a mechanism of O2 sensing. *J Biol Chem,* 275**,** 25130-8.

CHANDEL, N. S. & SCHUMACKER, P. T. 1999. Cells depleted of mitochondrial DNA (rho0) yield insight into physiological mechanisms. *FEBS Lett,* 454**,** 173-6.

CHANDRA, D. & SINGH, K. K. 2011. Genetic insights into OXPHOS defect and its role in cancer. *Biochimica et Biophysica Acta (BBA) - Bioenergetics,* 1807**,** 620-625.

CHANG, C.-R. & BLACKSTONE, C. 2007. Cyclic AMP-dependent Protein Kinase Phosphorylation of Drp1 Regulates Its GTPase Activity and Mitochondrial Morphology. *Journal of Biological Chemistry,* 282**,** 21583-21587.

CHAUGULE, V. K., BURCHELL, L., BARBER, K. R., SIDHU, A., LESLIE, S. J., SHAW, G. S. & WALDEN, H. 2011. Autoregulation of Parkin activity through its ubiquitin-like domain. *Embo J,* 30**,** 2853-2867.

CHEN, E. I., HEWEL, J., KRUEGER, J. S., TIRABY, C., WEBER, M. R., KRALLI, A., BECKER, K., YATES, J. R. & FELDING-HABERMANN, B. 2007. Adaptation of Energy Metabolism in Breast Cancer Brain Metastases. *Cancer Research,* 67**,** 1472-1486.

CHEN, H. & CHAN, D. C. 2004. Mitochondrial Dynamics in Mammals. *In:* GERALD, P. S. (ed.) *Current Topics in Developmental Biology.* Academic Press.

CHEN, H., CHOMYN, A. & CHAN, D. C. 2005. Disruption of fusion results in mitochondrial heterogeneity and dysfunction. *J Biol Chem,* 280**,** 26185-26192.

CHEN, H., VERMULST, M., WANG, Y. E., CHOMYN, A., PROLLA, T. A., MCCAFFERY, J. M. & CHAN, D. C. 2010. Mitochondrial Fusion Is Required for mtDNA Stability in Skeletal Muscle and Tolerance of mtDNA Mutations. *Cell,* 141**,** 280-289.

CHIANG, Y.-Y., CHEN, S.-L., HSIAO, Y.-T., HUANG, C.-H., LIN, T.-Y., CHIANG, I. P., HSU, W.-H. & CHOW, K.-C. 2009. Nuclear expression of dynamin-related protein 1 in lung adenocarcinomas. *Mod Pathol,* 22**,** 1139-1150.

CHICCO, A. J. & SPARAGNA, G. C. 2007. Role of cardiolipin alterations in mitochondrial dysfunction and disease. *American Journal of Physiology - Cell Physiology,* 292**,** C33-C44.

CHO, H., AHN, D. R., PARK, H. & YANG, E. G. 2007. Modulation of p300 binding by posttranslational modifications of the C-terminal activation domain of hypoxia-inducible factor-1alpha. *FEBS Lett,* 581**,** 1542-8.

CHOU, C.-H., LIN, C.-C., YANG, M.-C., WEI, C.-C., LIAO, H.-D., LIN, R.-C., TU, W.-Y., KAO, T.-C., HSU, C.-M., CHENG, J.-T., CHOU, A.-K., LEE, C.-I., LOH, J.-K., HOWNG, S.-L. & HONG, Y.-R. 2012. GSK3beta-Mediated Drp1 Phosphorylation Induced Elongated Mitochondrial Morphology against Oxidative Stress. *PLoS One,* 7**,** e49112.

CHRISTIAN, B. E. & SPREMULLI, L. L. 2012. Mechanism of protein biosynthesis in mammalian mitochondria. *Biochim Biophys Acta,* 1819**,** 1035-54.

CHUA, Y. L., DUFOUR, E., DASSA, E. P., RUSTIN, P., JACOBS, H. T., TAYLOR, C. T. & HAGEN, T. 2010. Stabilization of HIF-1alpha protein in hypoxia occurs independently of mitochondrial reactive oxygen species production. *J Biol Chem,* 285**,** 31277-84.

CHUN, Y. S., KIM, M. S. & PARK, J. W. 2002. Oxygen-dependent and -independent regulation of HIF-1alpha. *J Korean Med Sci,* 17**,** 581-8.

CLARK, I. E. 2006. Drosophila pink1 is required for mitochondrial function and interacts genetically with parkin. *Nature,* 441**,** 1162-1166.

CLAY MONTIER, L. L., DENG, J. J. & BAI, Y. 2009. Number matters: control of mammalian mitochondrial DNA copy number. *J Genet Genomics,* 36**,** 125-31.

CLAYCOMB, W. C., LANSON, N. A., JR., STALLWORTH, B. S., EGELAND, D. B., DELCARPIO, J. B., BAHINSKI, A. & IZZO, N. J., JR. 1998. HL-1 cells: a cardiac muscle cell line that contracts and retains phenotypic characteristics of the adult cardiomyocyte. *Proc Natl Acad Sci U S A,* 95**,** 2979-84.

COLLA, S., TAGLIAFERRI, S., MORANDI, F., LUNGHI, P., DONOFRIO, G., MARTORANA, D., MANCINI, C., LAZZARETTI, M., MAZZERA, L., RAVANETTI, L., BONOMINI, S., FERRARI, L., MIRANDA, C., LADETTO, M., NERI, T. M., NERI, A., GRECO, A., MANGONI, M., BONATI, A., RIZZOLI, V. & GIULIANI, N. 2007. The new tumor-suppressor gene inhibitor of growth family member 4 (ING4) regulates the production of proangiogenic molecules by myeloma cells and suppresses hypoxia-inducible factor-1 alpha (HIF-1alpha) activity: involvement in myeloma-induced angiogenesis. *Blood,* 110**,** 4464-75.

CONCHELLO, J.-A. & LICHTMAN, J. W. 2005. Optical sectioning microscopy. *Nat Meth,* 2**,** 920-931.

CORMIER-REGARD, S., NGUYEN, S. V. & CLAYCOMB, W. C. 1998. Adrenomedullin gene expression is developmentally regulated and induced by hypoxia in rat ventricular cardiac myocytes. *J Biol Chem,* 273**,** 17787-92.

CRAMER, T. & JOHNSON, R. S. 2003. A novel role for the hypoxia inducible transcription factor HIF-1alpha: critical regulation of inflammatory cell function. *Cell Cycle,* 2**,** 192-3.

CRAMER, T., YAMANISHI, Y., CLAUSEN, B. E., FÖRSTER, I., PAWLINSKI, R., MACKMAN, N., HAASE, V. H., JAENISCH, R., CORR, M., NIZET, V., FIRESTEIN, G. S., GERBER, H.-P., FERRARA, N. & JOHNSON, R. S. 2003. HIF-1α Is Essential for Myeloid Cell-Mediated Inflammation. *Cell,* 112**,** 645-657.

CRAVEN, R. A., HANRAHAN, S., TOTTY, N., HARNDEN, P., STANLEY, A. J., MAHER, E. R., HARRIS, A. L., TRIMBLE, W. S., SELBY, P. J. & BANKS, R. E. 2006. Proteomic identification of a role for the von Hippel Lindau tumour suppressor in changes in the expression of mitochondrial proteins and septin 2 in renal cell carcinoma. *PROTEOMICS,* 6**,** 3880-3893.

CRIBBS, J. T. & STRACK, S. 2007. Reversible phosphorylation of Drp1 by cyclic AMP-dependent protein kinase and calcineurin regulates mitochondrial fission and cell death. *EMBO Rep,* 8**,** 939-944.

CUMMINS, E. P., BERRA, E., COMERFORD, K. M., GINOUVES, A., FITZGERALD, K. T., SEEBALLUCK, F., GODSON, C., NIELSEN, J. E., MOYNAGH, P., POUYSSEGUR, J. & TAYLOR, C. T. 2006. Prolyl hydroxylase-1 negatively regulates IkappaB kinase-beta, giving insight into hypoxia-induced NFkappaB activity. *Proc Natl Acad Sci U S A,* 103**,** 18154-9.

DABIR, D. V., LEVERICH, E. P., KIM, S. K., TSAI, F. D., HIRASAWA, M., KNAFF, D. B. & KOEHLER, C. M. 2007. A role for cytochrome c and cytochrome c peroxidase in electron shuttling from Erv1. *Embo J,* 26**,** 4801-11.

DATE, T., MOCHIZUKI, S., BELANGER, A. J., YAMAKAWA, M., LUO, Z., VINCENT, K. A., CHENG, S. H., GREGORY, R. J. & JIANG, C. 2005. Expression of constitutively stable hybrid hypoxia-inducible factor-1alpha protects cultured rat cardiomyocytes against simulated ischemia-reperfusion injury. *Am J Physiol Cell Physiol,* 288**,** C314-20.

DAVIDOWITZ, E. J., SCHOENFELD, A. R. & BURK, R. D. 2001. VHL Induces Renal Cell Differentiation and Growth Arrest through Integration of Cell-Cell and Cell-Extracellular Matrix Signaling. *Molecular and Cellular Biology,* 21**,** 865-874.

DAVIS, M. A. 2002. *Apoptosis Methods in Pharmacology and Toxicology: Approaches to Measurement and Quantification*, Humana Press Incorporated.

DAWN, B. & BOLLI, R. 2005. HO-1 induction by HIF-1: a new mechanism for delayed cardioprotection? *Am J Physiol Heart Circ Physiol,* 289**,** H522-4.

DE VRIES, R. L. A. & PRZEDBORSKI, S. 2013. Mitophagy and Parkinson's disease: Be eaten to stay healthy. *Molecular and Cellular Neuroscience,* 55**,** 37-43.

DEAS, E., PLUN-FAVREAU, H., GANDHI, S., DESMOND, H., KJAER, S., LOH, S. H. Y., RENTON, A. E. M., HARVEY, R. J., WHITWORTH, A. J., MARTINS, L. M., ABRAMOV, A. Y. & WOOD, N. W. 2011a. PINK1 cleavage at position A103 by the mitochondrial protease PARL. *Human Molecular Genetics,* 20**,** 867-879.

DEAS, E., WOOD, N. W. & PLUN-FAVREAU, H. 2011b. Mitophagy and Parkinson's disease: The PINK1–parkin link. *Biochimica et Biophysica Acta (BBA) - Molecular Cell Research,* 1813**,** 623-633.

DEHAAN, C., HABIBI-NAZHAD, B., YAN, E., SALLOUM, N., PARLIAMENT, M. & ALLALUNIS-TURNER, J. 2004. Mutation in mitochondrial complex I ND6 subunit is associated with defective response to hypoxia in human glioma cells. *Mol Cancer,* 3**,** 19.

DELCARPIO, J. B., LANSON, N. A., JR., FIELD, L. J. & CLAYCOMB, W. C. 1991. Morphological characterization of cardiomyocytes isolated from a transplantable cardiac tumor derived from transgenic mouse atria (AT-1 cells). *Circ Res,* 69**,** 1591-600.

DENG, H., DODSON, M. W., HUANG, H. & GUO, M. 2008. The Parkinson's disease genes pink1 and parkin promote mitochondrial fission and/or inhibit fusion in Drosophila. *Proc. Natl Acad. Sci. USA,* 105**,** 14503-14508.

DEWITT, D. A., HURD, J. A., FOX, N., TOWNSEND, B. E., GRIFFIOEN, K. J. S., GHRIBI, O. & SAVORY, J. 2006. Peri-nuclear clustering of mitochondria is triggered during aluminum maltolate induced apoptosis. *Journal of Alzheimer's Disease,* 9**,** 195-205.

DI LISA, F. & BERNARDI, P. 2006. Mitochondria and ischemia-reperfusion injury of the heart: fixing a hole. *Cardiovasc Res,* 70**,** 191-9.

DING, W. X. 2010. Nix is critical to two distinct phases of mitophagy, reactive oxygen species-mediated autophagy induction and Parkin-ubiquitin-p62-mediated mitochondrial priming. *J. Biol. Chem.,* 285**,** 27879-27890.

DOEGE, K., HEINE, S., JENSEN, I., JELKMANN, W. & METZEN, E. 2005. Inhibition of mitochondrial respiration elevates oxygen concentration but leaves regulation of hypoxia-inducible factor (HIF) intact. *Blood,* 106**,** 2311-7.

DOWNEY, J. M., DAVIS, A. M. & COHEN, M. V. 2007. Signaling pathways in ischemic preconditioning. *Heart Fail Rev,* 12**,** 181-8.

DURANTEAU, J., CHANDEL, N. S., KULISZ, A., SHAO, Z. & SCHUMACKER, P. T. 1998. Intracellular signaling by reactive oxygen species during hypoxia in cardiomyocytes. *J Biol Chem,* 273**,** 11619-24.

EBERT, B. L., FIRTH, J. D. & RATCLIFFE, P. J. 1995. Hypoxia and mitochondrial inhibitors regulate expression of glucose transporter-1 via distinct Cis-acting sequences. *J Biol Chem,* 270**,** 29083-9.

ECKLE, T., KOHLER, D., LEHMANN, R., EL KASMI, K. & ELTZSCHIG, H. K. 2008. Hypoxia-inducible factor-1 is central to cardioprotection: a new paradigm for ischemic preconditioning. *Circulation,* 118**,** 166-75.

EIMRE, M., PAJU, K., PELLOUX, S., BERAUD, N., ROOSIMAA, M., KADAJA, L., GRUNO, M., PEET, N., ORLOVA, E., REMMELKOOR, R., PIIRSOO, A., SAKS, V. & SEPPET, E. 2008. Distinct organization of energy metabolism in HL-1 cardiac cell line and cardiomyocytes. *Biochimica et Biophysica Acta (BBA) - Bioenergetics,* 1777**,** 514-524.

EKSTRAND, M. I., FALKENBERG, M., RANTANEN, A., PARK, C. B., GASPARI, M., HULTENBY, K., RUSTIN, P., GUSTAFSSON, C. M. & LARSSON, N.-G. 2004. Mitochondrial transcription factor A regulates mtDNA copy number in mammals. *Human Molecular Genetics,* 13**,** 935-944.

ELVIDGE, G. P., GLENNY, L., APPELHOFF, R. J., RATCLIFFE, P. J., RAGOUSSIS, J. & GLEADLE, J. M. 2006. Concordant regulation of gene expression by hypoxia and 2-oxoglutarate-dependent dioxygenase inhibition: the role of HIF-1alpha, HIF-2alpha, and other pathways. *J Biol Chem,* 281**,** 15215-26.

EMA, M., TAYA, S., YOKOTANI, N., SOGAWA, K., MATSUDA, Y. & FUJII-KURIYAMA, Y. 1997. A novel bHLH-PAS factor with close sequence similarity to hypoxia-inducible factor 1alpha regulates the VEGF expression and is potentially involved in lung and vascular development. *Proc Natl Acad Sci U S A,* 94**,** 4273-8.

EMERLING, B. M., PLATANIAS, L. C., BLACK, E., NEBREDA, A. R., DAVIS, R. J. & CHANDEL, N. S. 2005. Mitochondrial reactive oxygen species activation of p38 mitogen-activated protein kinase is required for hypoxia signaling. *Mol Cell Biol,* 25**,** 4853-62.

ESKELINEN, E.-L. 2008. To be or not to be? Examples of incorrect identification of autophagic compartments in conventional transmission electron microscopy of mammalian cells. *Autophagy,* 4**,** 257-260.

FALKENBERG, M., LARSSON, N. G. & GUSTAFSSON, C. M. 2007. DNA replication and transcription in mammalian mitochondria. *Annu Rev Biochem,* 76**,** 679-99.

FELDSER, D., AGANI, F., IYER, N. V., PAK, B., FERREIRA, G. & SEMENZA, G. L. 1999. Reciprocal positive regulation of hypoxia-inducible factor 1alpha and insulin-like growth factor 2. *Cancer Res,* 59**,** 3915-8.

FERNANDEZ-MARCOS, P. J. & AUWERX, J. 2011. Regulation of PGC-1α, a nodal regulator of mitochondrial biogenesis. *The American Journal of Clinical Nutrition,* 93**,** 884S-890S.

FERNÁNDEZ-VIZARRA, E., TIRANTI, V. & ZEVIANI, M. 2009. Assembly of the oxidative phosphorylation system in humans: What we have learned by studying its defects. *Biochimica et Biophysica Acta (BBA) - Molecular Cell Research,* 1793**,** 200-211.

FERRICK, D. A., NEILSON, A. & BEESON, C. 2008. Advances in measuring cellular bioenergetics using extracellular flux. *Drug Discovery Today,* 13**,** 268-274.

FIRTH, J. D., EBERT, B. L. & RATCLIFFE, P. J. 1995. Hypoxic regulation of lactate dehydrogenase A. Interaction between hypoxia-inducible factor 1 and cAMP response elements. *J Biol Chem,* 270**,** 21021-7.

FORMAN, J. R., WORTH, C. L., BICKERTON, G. R. J., EISEN, T. G. & BLUNDELL, T. L. 2009. Structural bioinformatics mutation analysis reveals genotype–phenotype correlations in von Hippel-Lindau disease and suggests molecular mechanisms of tumorigenesis. *Proteins: Structure, Function, and Bioinformatics,* 77**,** 84-96.

FRANK, S., GAUME, B., BERGMANN-LEITNER, E. S., LEITNER, W. W., ROBERT, E. G., CATEZ, F., SMITH, C. L. & YOULE, R. J. 2001. The Role of Dynamin-Related Protein 1, a Mediator of Mitochondrial Fission, in Apoptosis. *Developmental Cell,* 1**,** 515-525.

FREY, P. A. 1996. The Leloir pathway: a mechanistic imperative for three enzymes to change the stereochemical configuration of a single carbon in galactose. *The FASEB Journal,* 10**,** 461-70.

FUJIWARA, M., MARUSAWA, H., WANG, H. Q., IWAI, A., IKEUCHI, K., IMAI, Y., KATAOKA, A., NUKINA, N., TAKAHASHI, R. & CHIBA, T. 2008. Parkin as a tumor suppressor gene for hepatocellular carcinoma. *Oncogene,* 27**,** 6002-6011.

FUKUDA, R., HIROTA, K., FAN, F., JUNG, Y. D., ELLIS, L. M. & SEMENZA, G. L. 2002. Insulin-like growth factor 1 induces hypoxia-inducible factor 1-mediated vascular endothelial growth factor expression, which is dependent on MAP kinase and phosphatidylinositol 3-kinase signaling in colon cancer cells. *J Biol Chem,* 277**,** 38205-11.

FUKUDA, R., ZHANG, H., KIM, J.-W., SHIMODA, L., DANG, C. V. & SEMENZA, G. L. 2007. HIF-1 regulates cytochrome oxidase subunits to optimize efficiency of respiration in hypoxic cells. *Cell,* 129**,** 111-122.

GALLOWAY, C. A., LEE, H. & YOON, Y. 2012. Mitochondrial morphology—emerging role in bioenergetics. *Free Radical Biology and Medicine,* 53**,** 2218-2228.

GALMICHE, L., SERRE, V., BEINAT, M., ASSOULINE, Z., LEBRE, A.-S., CHRETIEN, D., NIETSCHKE, P., BENES, V., BODDAERT, N., SIDI, D., BRUNELLE, F., RIO, M., MUNNICH, A. & RÖTIG, A. 2011. Exome sequencing identifies MRPL3 mutation in mitochondrial cardiomyopathy. *Human Mutation,* 32**,** 1225-1231.

GAO, C., CAO, W., BAO, L., ZUO, W., XIE, G., CAI, T., FU, W., ZHANG, J., WU, W., ZHANG, X. & CHEN, Y.-G. 2010. Autophagy negatively regulates Wnt signalling by promoting Dishevelled degradation. *Nat Cell Biol,* 12**,** 781-790.

GARCIA FERNANDEZ, M. I., CECCARELLI, D. & MUSCATELLO, U. 2004. Use of the fluorescent dye 10-N-nonyl acridine orange in quantitative and location assays of cardiolipin: a study on different experimental models. *Analytical Biochemistry,* 328**,** 174-180.

GEGG, M. E. 2010. Mitofusin 1 and mitofusin 2 are ubiquitinated in a PINK1/parkin-dependent manner upon induction of mitophagy. *Hum. Mol. Genet.,* 19**,** 4861-4870.

GEISLER, S. 2010. PINK1/Parkin-mediated mitophagy is dependent on VDAC1 and p62/SQSTM1. *Nature Cell Biol.,* 12**,** 119-131.

GERALD, D., BERRA, E., FRAPART, Y. M., CHAN, D. A., GIACCIA, A. J., MANSUY, D., POUYSSEGUR, J., YANIV, M. & MECHTA-GRIGORIOU, F. 2004. JunD reduces tumor angiogenesis by protecting cells from oxidative stress. *Cell,* 118**,** 781-94.

GNARRA, J. R., TORY, K., WENG, Y., SCHMIDT, L., WEI, M. H., LI, H., LATIF, F., LIU, S., CHEN, F., DUH, F. M. & ET AL. 1994. Mutations of the VHL tumour suppressor gene in renal carcinoma. *Nat Genet,* 7**,** 85-90.

GOH, J., ENNS, L., FATEMIE, S., HOPKINS, H., MORTON, J., PETTAN-BREWER, C. & LADIGES, W. 2011. Mitochondrial targeted catalase suppresses invasive breast cancer in mice. *BMC Cancer,* 11**,** 191.

GOHIL, V. M., SHETH, S. A., NILSSON, R., WOJTOVICH, A. P., LEE, J. H., PEROCCHI, F., CHEN, W., CLISH, C. B., AYATA, C., BROOKES, P. S. & MOOTHA, V. K. 2010. Nutrient-sensitized screening for drugs that shift energy metabolism from mitochondrial respiration to glycolysis. *Nat Biotech,* 28**,** 249-255.

GOMES, L. C., BENEDETTO, G. D. & SCORRANO, L. 2011. During autophagy mitochondria elongate, are spared from degradation and sustain cell viability. *Nat Cell Biol,* 13**,** 589-598.

GONG, Y. & AGANI, F. H. 2005. Oligomycin inhibits HIF-1alpha expression in hypoxic tumor cells. *Am J Physiol Cell Physiol,* 288**,** 1023-1029.

GONZALVEZ, F., D'AURELIO, M., BOUTANT, M., MOUSTAPHA, A., PUECH, J.-P., LANDES, T., ARNAUNÉ-PELLOQUIN, L., VIAL, G., TALEUX, N., SLOMIANNY, C., WANDERS, R. J., HOUTKOOPER, R. H., BELLENGUER, P., MØLLER, I. M., GOTTLIEB, E., VAZ, F. M., MANFREDI, G. & PETIT, P. X. 2013. Barth syndrome: Cellular compensation of mitochondrial dysfunction and apoptosis inhibition due to changes in cardiolipin remodeling linked to tafazzin (TAZ) gene mutation. *Biochimica et Biophysica Acta (BBA) - Molecular Basis of Disease,* 1832**,** 1194-1206.

GORDAN, J. D. 2008. HIF-α effects on c-Myc distinguish two subtypes of sporadic VHL-deficient clear cell renal carcinoma. *Cancer Cell,* 14**,** 435-446.

GORDAN, J. D., BERTOUT, J. A., HU, C.-J., DIEHL, J. A. & SIMON, M. C. 2007. HIF-2α Promotes Hypoxic Cell Proliferation by Enhancing c-Myc Transcriptional Activity. *Cancer Cell,* 11**,** 335-347.

GOSWAMI, S. K., MAULIK, N. & DAS, D. K. 2007. Ischemia-reperfusion and cardioprotection: a delicate balance between reactive oxygen species generation and redox homeostasis. *Ann Med,* 39**,** 275-89.

GOUGH, D. J., CORLETT, A., SCHLESSINGER, K., WEGRZYN, J., LARNER, A. C. & LEVY, D. E. 2009. Mitochondrial STAT3 supports Ras-dependent oncogenic transformation. *Science,* 324**,** 1713-6.

GU, Y. Z., MORAN, S. M., HOGENESCH, J. B., WARTMAN, L. & BRADFIELD, C. A. 1998. Molecular characterization and chromosomal localization of a third alpha-class hypoxia inducible factor subunit, HIF3alpha. *Gene Expr,* 7**,** 205-13.

GUO, S., OLM-SHIPMAN, A., WALTERS, A., URCIUOLI, W. R., DEVITO, S., NADTOCHIY, S. M., WOJTOVICH, A. P. & BROOKES, P. S. 2012. A Cell-Based Phenotypic Assay to Identify Cardioprotective Agents. *Circulation Research,* 110**,** 948-957.

GUO, Y., JONES, W. K., XUAN, Y. T., TANG, X. L., BAO, W., WU, W. J., HAN, H., LAUBACH, V. E., PING, P., YANG, Z., QIU, Y. & BOLLI, R. 1999. The late phase of ischemic preconditioning is abrogated by targeted disruption of the inducible NO synthase gene. *Proc Natl Acad Sci U S A,* 96**,** 11507-12.

GUZY, R. D., HOYOS, B., ROBIN, E., CHEN, H., LIU, L., MANSFIELD, K. D., SIMON, M. C., HAMMERLING, U. & SCHUMACKER, P. T. 2005. Mitochondrial complex III is required for hypoxia-induced ROS production and cellular oxygen sensing. *Cell Metab.,* 1**,** 401-408.

GUZY, R. D. & SCHUMACKER, P. T. 2006. Oxygen sensing by mitochondria at complex III: the paradox of increased reactive oxygen species during hypoxia. *Exp.Physiol,* 91**,** 807-819.

HACKER, K. E., LEE, C. M. & RATHMELL, W. K. 2008. VHL Type 2B Mutations Retain VBC Complex Form and Function. *PLoS One,* 3**,** e3801.

HAGEN, T., TAYLOR, C. T., LAM, F. & MONCADA, S. 2003. Redistribution of intracellular oxygen in hypoxia by nitric oxide: effect on HIF1alpha. *Science,* 302**,** 1975-8.

HALESTRAP, A. P., CLARKE, S. J. & KHALIULIN, I. 2007. The role of mitochondria in protection of the heart by preconditioning. *Biochim Biophys Acta,* 1767**,** 1007-31.

HAN, X.-J., LU, Y.-F., LI, S.-A., KAITSUKA, T., SATO, Y., TOMIZAWA, K., NAIRN, A. C., TAKEI, K., MATSUI, H. & MATSUSHITA, M. 2008. CaM kinase Iα–induced phosphorylation of Drp1 regulates mitochondrial morphology. *The Journal of Cell Biology,* 182**,** 573-585.

HANNA, R. A., QUINSAY, M. N., OROGO, A. M., GIANG, K., RIKKA, S. & GUSTAFSSON, A. B. 2012. Microtubule-Associated Protein 1 Light Chain 3 (LC3) Interacts with Bnip3 to Selectively Remove Endoplasmic Reticulum and Mitochondria via Autophagy. *Journal of Biological Chemistry*.

HARA, S., HAMADA, J., KOBAYASHI, C., KONDO, Y. & IMURA, N. 2001. Expression and characterization of hypoxia-inducible factor (HIF)-3alpha in human kidney: suppression of HIF-mediated gene expression by HIF-3alpha. *Biochem Biophys Res Commun,* 287**,** 808-13.

HARTEN, S. K., ASHCROFT, M. & MAXWELL, P. H. 2010. Prolyl hydroxylase domain inhibitors: a route to HIF activation and neuroprotection. *Antioxid Redox Signal,* 12**,** 459-80.

HARTEN, S. K., ESTEBAN, M. A. & MAXWELL, P. H. 2009. Identification of novel VHL regulated genes by transcriptomic analysis of RCC10 renal carcinoma cells. *Adv Enzyme Regul,* 49**,** 43-52.

HASHIATNI, H., LANG, R. J. & SUZUKI, H. 2010. Role of perinuclear mitochondria in the spatiotemporal dynamics of spontaneous Ca2+ waves in interstitial cells of Cajal-like cells of the rabbit urethra. *British Journal of Pharmacology,* 161**,** 680-694.

HATCH, G. M. 2004. Cell biology of cardiac mitochondrial phospholipids. *Biochemistry and Cell Biology,* 82**,** 99-112.

HAUSENLOY, D. J. & YELLON, D. M. 2007. Preconditioning and postconditioning: united at reperfusion. *Pharmacol Ther,* 116**,** 173-91.

HE, C. & KLIONSKY, D. J. 2009. Regulation Mechanisms and Signaling Pathways of Autophagy. *Annu Rev Genet,* 43**,** 67-93.

HEGGENESS, M. H., SIMON, M. & SINGER, S. J. 1978. Association of mitochondria with microtubules in cultured cells. *Proceedings of the National Academy of Sciences,* 75**,** 3863-3866.

HEINEMAN, F. W. & BALABAN, R. S. 1990. Control of mitochondrial respiration in the heart in vivo. *Annu Rev Physiol,* 52**,** 523-42.

HELTON, R., CUI, J., SCHEEL, J. R., ELLISON, J. A., AMES, C., GIBSON, C., BLOUW, B., OUYANG, L., DRAGATSIS, I., ZEITLIN, S., JOHNSON, R. S., LIPTON, S. A. & BARLOW, C. 2005. Brain-specific knock-out of hypoxia-inducible factor-1alpha reduces rather than increases hypoxic-ischemic damage. *J Neurosci,* 25**,** 4099-107.

HERVOUET, E., CIZKOVA, A., DEMONT, J., VOJTISKOVA, A., PECINA, P., FRANSSEN-VAN HAL, N. L., KEIJER, J., SIMONNET, H., IVANEK, R., KMOCH, S., GODINOT, C. & HOUSTEK, J. 2008. HIF and reactive oxygen species regulate oxidative phosphorylation in cancer. *Carcinogenesis,* 29**,** 1528-37.

HERVOUET, E., DEMONT, J., PECINA, P., VOJTISKOVA, A., HOUSTEK, J., SIMONNET, H. & GODINOT, C. 2005. A new role for the von Hippel-Lindau tumor suppressor protein: stimulation of mitochondrial oxidative phosphorylation complex biogenesis. *Carcinogenesis,* 26**,** 531-9.

HICKEY, M. M., LAM, J. C., BEZMAN, N. A., RATHMELL, W. K. & SIMON, M. C. 2007. von Hippel–Lindau mutation in mice recapitulates Chuvash polycythemia via hypoxia-inducible factor-2α signaling and splenic erythropoiesis. *The Journal of Clinical Investigation,* 117**,** 3879-3889.

HIWATASHI, Y., KANNO, K., TAKASAKI, C., GORYO, K., SATO, T., TORII, S., SOGAWA, K. & YASUMOTO, K.-I. 2011. PHD1 interacts with ATF4 and negatively regulates its transcriptional activity without prolyl hydroxylation. *Experimental Cell Research,* 317**,** 2789-2799.

HOFMANN, S., ROTHBAUER, U., MUHLENBEIN, N., BAIKER, K., HELL, K. & BAUER, M. F. 2005. Functional and mutational characterization of human MIA40 acting during import into the mitochondrial intermembrane space. *J.Mol.Biol.,* 353**,** 517-528.

HOLMES, J. L. & POLLENZ, R. S. 1997. Determination of Aryl Hydrocarbon Receptor Nuclear Translocator Protein Concentration and Subcellular Localization in Hepatic and Nonhepatic Cell Culture Lines: Development of Quantitative Western Blotting Protocols for Calculation of Aryl Hydrocarbon Receptor and Aryl Hydrocarbon Receptor Nuclear Translocator Protein in Total Cell Lysates. *Molecular Pharmacology,* 52**,** 202-211.

HOLMQUIST-MENGELBIER, L. 2006. Recruitment of HIF-1α and HIF-2α to common target genes is differentially regulated in neuroblastoma: HIF-2α promotes an aggressive phenotype. *Cancer Cell,* 10**,** 413-423.

HOPFER, U., HOPFER, H., JABLONSKI, K., STAHL, R. A. & WOLF, G. 2006. The novel WD-repeat protein Morg1 acts as a molecular scaffold for hypoxia-inducible factor prolyl hydroxylase 3 (PHD3). *J Biol Chem,* 281**,** 8645-55.

HOPPINS, S., LACKNER, L. & NUNNARI, J. 2007. The machines that divide and fuse mitochondria. *Annu Rev Biochem,* 76**,** 751-780.

HU, C. J., SATAUR, A., WANG, L., CHEN, H. & SIMON, M. C. 2007. The N-terminal transactivation domain confers target gene specificity of hypoxia-inducible factors HIF-1α and HIF-2α. *Mol. Biol. Cell,* 18**,** 4528-4542.

HU, C. J., WANG, L. Y., CHODOSH, L. A., KEITH, B. & SIMON, M. C. 2003. Differential roles of hypoxia-inducible factor 1alpha (HIF-1alpha) and HIF-2alpha in hypoxic gene regulation. *Mol Cell Biol,* 23**,** 9361-74.

HUANG, L. E., WILLMORE, W. G., GU, J., GOLDBERG, M. A. & BUNN, H. F. 1999. Inhibition of hypoxia-inducible factor 1 activation by carbon monoxide and nitric oxide. Implications for oxygen sensing and signaling. *J Biol Chem,* 274**,** 9038-44.

HUANG, M., CHAN, D. A., JIA, F., XIE, X., LI, Z., HOYT, G., ROBBINS, R. C., CHEN, X., GIACCIA, A. J. & WU, J. C. 2008. Short hairpin RNA interference therapy for ischemic heart disease. *Circulation,* 118**,** S226-33.

HUANG, Y., HICKEY, R. P., YEH, J. L., LIU, D., DADAK, A., YOUNG, L. H., JOHNSON, R. S. & GIORDANO, F. J. 2004. Cardiac myocyte-specific HIF-1alpha deletion alters vascularization, energy availability, calcium flux, and contractility in the normoxic heart. *Faseb J,* 18**,** 1138-40.

HUDSON, C. C., LIU, M., CHIANG, G. G., OTTERNESS, D. M., LOOMIS, D. C., KAPER, F., GIACCIA, A. J. & ABRAHAM, R. T. 2002. Regulation of hypoxia-inducible factor 1alpha expression and function by the mammalian target of rapamycin. *Mol Cell Biol,* 22**,** 7004-14.

HUGHES, M., KAPLLANI, E., ALEXANDER, A., BURK, R. & SCHOENFELD, A. 2007. HIF-2alpha downregulation in the absence of functional VHL is not sufficient for renal cell differentiation. *Cancer Cell International,* 7**,** 13.

HYVARINEN, J., HASSINEN, I. E., SORMUNEN, R., MAKI, J. M., KIVIRIKKO, K. I., KOIVUNEN, P. & MYLLYHARJU, J. 2010. Hearts of hypoxia-inducible factor prolyl 4-hydroxylase-2 hypomorphic mice show protection against acute ischemia-reperfusion injury. *J.Biol.Chem.,* 285**,** 13646-13657.

ICHISHITA, R., TANAKA, K., SUGIURA, Y., SAYANO, T., MIHARA, K. & OKA, T. 2008. An RNAi Screen for Mitochondrial Proteins Required to Maintain the Morphology of the Organelle in Caenorhabditis elegans. *Journal of Biochemistry,* 143**,** 449-454.

ILIOPOULOS, O., KIBEL, A., GRAY, S. & KAELIN, W. G. 1995. Tumour suppression by the human von Hippel-Lindau gene product. *Nat Med,* 1**,** 822-826.

IMAI, Y. 2012. Mitochondrial Regulation by PINK1-Parkin Signaling. *ISRN Cell Biology,* 2012**,** 15.

ISHIHARA, N., NOMURA, M., JOFUKU, A., KATO, H., SUZUKI, S. O., MASUDA, K., OTERA, H., NAKANISHI, Y., NONAKA, I., GOTO, Y.-I., TAGUCHI, N., MORINAGA, H., MAEDA, M., TAKAYANAGI, R., YOKOTA, S. & MIHARA, K. 2009. Mitochondrial fission factor Drp1 is essential for embryonic development and synapse formation in mice. *Nat Cell Biol,* 11**,** 958-966.

ISHIKAWA, K., TAKENAGA, K., AKIMOTO, M., KOSHIKAWA, N., YAMAGUCHI, A., IMANISHI, H., NAKADA, K., HONMA, Y. & HAYASHI, J. 2008. ROS-generating mitochondrial DNA mutations can regulate tumor cell metastasis. *Science,* 320**,** 661-4.

IWAI, K., YAMANAKA, K., KAMURA, T., MINATO, N., CONAWAY, R. C., CONAWAY, J. W., KLAUSNER, R. D. & PAUSE, A. 1999. Identification of the von Hippel–Lindau tumor-suppressor protein as part of an active E3 ubiquitin ligase complex. *Proceedings of the National Academy of Sciences,* 96**,** 12436-12441.

IYER, N. V., KOTCH, L. E., AGANI, F., LEUNG, S. W., LAUGHNER, E., WENGER, R. H., GASSMANN, M., GEARHART, J. D., LAWLER, A. M., YU, A. Y. & SEMENZA, G. L. 1998. Cellular and developmental control of O2 homeostasis by hypoxia-inducible factor 1 alpha. *Genes Dev,* 12**,** 149-62.

JAAKKOLA, P., MOLE, D. R., TIAN, Y. M., WILSON, M. I., GIELBERT, J., GASKELL, S. J., KRIEGSHEIM, A., HEBESTREIT, H. F., MUKHERJI, M., SCHOFIELD, C. J., MAXWELL, P. H., PUGH, C. W. & RATCLIFFE, P. J. 2001. Targeting of HIF-alpha to the von Hippel-Lindau ubiquitylation complex by O2-regulated prolyl hydroxylation. *Science,* 292**,** 468-72.

JACOBSON, J., DUCHEN, M. R. & HEALES, S. J. R. 2002. Intracellular distribution of the fluorescent dye nonyl acridine orange responds to the mitochondrial membrane potential: implications for assays of cardiolipin and mitochondrial mass. *Journal of Neurochemistry,* 82**,** 224-233.

JAFRI, M. S., DUDYCHA, S. J. & O'ROURKE, B. 2001. Cardiac energy metabolism: models of cellular respiration. *Annu Rev Biomed Eng,* 3**,** 57-81.

JEREMY M BERG, J. L. T. A. L. S. 2002. *Biochemistry,* New York, WH Freeman.

JIANG, B. H., RUE, E., WANG, G. L., ROE, R. & SEMENZA, G. L. 1996a. Dimerization, DNA binding, and transactivation properties of hypoxia-inducible factor 1. *J Biol Chem,* 271**,** 17771-8.

JIANG, B. H., SEMENZA, G. L., BAUER, C. & MARTI, H. H. 1996b. Hypoxia-inducible factor 1 levels vary exponentially over a physiologically relevant range of O2 tension. *Am J Physiol,* 271**,** C1172-80.

JIANG, Y., ZHANG, W., KONDO, K., KLCO, J. M., ST. MARTIN, T. B., DUFAULT, M. R., MADDEN, S. L., KAELIN, W. G. & NACHT, M. 2003. Gene Expression Profiling in a Renal Cell Carcinoma Cell Line: Dissecting VHL and Hypoxia-Dependent Pathways. *Molecular Cancer Research,* 1**,** 453-462.

JIN, F., BROCKMEIER, U., OTTERBACH, F. & METZEN, E. 2012. New Insight into the SDF-1/CXCR4 Axis in a Breast Carcinoma Model: Hypoxia-Induced Endothelial SDF-1 and Tumor Cell CXCR4 Are Required for Tumor Cell Intravasation. *Molecular Cancer Research,* 10**,** 1021-1031.

JOUAVILLE, L. S., PINTON, P., BASTIANUTTO, C., RUTTER, G. A. & RIZZUTO, R. 1999. Regulation of mitochondrial ATP synthesis by calcium: Evidence for a long-

term metabolic priming. *Proceedings of the National Academy of Sciences,* 96**,** 13807-13812.

KAELIN, W. G. 2002. Molecular basis of the VHL hereditary cancer syndrome. *Nat Rev Cancer,* 2**,** 673-682.

KAELIN, W. G. 2008. The von Hippel-Lindau tumour suppressor protein: O2 sensing and cancer. *Nature Rev. Cancer,* 8**,** 865-873.

KAGEYAMA, Y., KOSHIJI, M., TO, K. K., TIAN, Y. M., RATCLIFFE, P. J. & HUANG, L. E. 2004. Leu-574 of human HIF-1alpha is a molecular determinant of prolyl hydroxylation. *Faseb J,* 18**,** 1028-30.

KALLIO, P. J., PONGRATZ, I., GRADIN, K., MCGUIRE, J. & POELLINGER, L. 1997. Activation of hypoxia-inducible factor 1alpha: posttranscriptional regulation and conformational change by recruitment of the Arnt transcription factor. *Proc Natl Acad Sci U S A,* 94**,** 5667-72.

KARBOWSKI, M., NEUTZNER, A. & YOULE, R. J. 2007. The mitochondrial E3 ubiquitin ligase MARCH5 is required for Drp1 dependent mitochondrial division. *The Journal of Cell Biology,* 178**,** 71-84.

KAWAJIRI, S. 2010. PINK1 is recruited to mitochondria with parkin and associates with LC3 in mitophagy. *FEBS Lett.,* 584**,** 1073-1079.

KEITH, B., JOHNSON, R. S. & SIMON, M. C. 2012. HIF1α and HIF2α: sibling rivalry in hypoxic tumour growth and progression. *Nat Rev Cancer,* 12**,** 9-22.

KHAN, M. N., BHATTACHARYYA, T., ANDRIKOPOULOS, P., ESTEBAN, M. A., BAROD, R., CONNOR, T., ASHCROFT, M., MAXWELL, P. H. & KIRIAKIDIS, S. 2011. Factor inhibiting HIF (FIH-1) promotes renal cancer cell survival by protecting cells from HIF-1alpha-mediated apoptosis. *Br J Cancer,* 104**,** 1151-9.

KHAN, Z., MICHALOPOULOS, G. K. & STOLZ, D. B. 2006. Peroxisomal localization of hypoxia-inducible factors and hypoxia-inducible factor regulatory hydroxylases in primary rat hepatocytes exposed to hypoxia-reoxygenation. *Am J Pathol,* 169**,** 1251-69.

KIBEL, A., ILIOPOULOS, O., DECAPRIO, J. A. & KAELIN, W. G., JR. 1995. Binding of the von Hippel-Lindau tumor suppressor protein to Elongin B and C. *Science,* 269**,** 1444-6.

KIDO, M., DU, L., SULLIVAN, C. C., LI, X., DEUTSCH, R., JAMIESON, S. W. & THISTLETHWAITE, P. A. 2005. Hypoxia-inducible factor 1-alpha reduces infarction and attenuates progression of cardiac dysfunction after myocardial infarction in the mouse. *J Am Coll Cardiol,* 46**,** 2116-24.

KIM, I., RODRIGUEZ-ENRIQUEZ, S. & LEMASTERS, J. J. 2007. Selective degradation of mitochondria by mitophagy. *Arch. Biochem. Biophys.,* 462**,** 245-253.

KIM, J.-H., KONONENKO, A., ERLIANDRI, I., KIM, T.-A., NAKANO, M., IIDA, Y., BARRETT, J. C., OSHIMURA, M., MASUMOTO, H., EARNSHAW, W. C., LARIONOV, V. & KOUPRINA, N. 2011. Human artificial chromosome (HAC)

vector with a conditional centromere for correction of genetic deficiencies in human cells. *Proceedings of the National Academy of Sciences,* 108**,** 20048-20053.

KIM, J.-W., TCHERNYSHYOV, I., SEMENZA, G. L. & DANG, C. V. 2006. HIF-1-mediated expression of pyruvate dehydrogenase kinase: a metabolic switch required for cellular adaptation to hypoxia. *Cell Metab,* 3**,** 177-185.

KIRKIN, V., MCEWAN, D. G., NOVAK, I. & DIKIC, I. 2009. A Role for Ubiquitin in Selective Autophagy. *Mol Cell,* 34**,** 259-269.

KLIONSKY, D. J. 2010. A comprehensive glossary of autophagy-related molecules and processes. *Autophagy,* 6**,** 438-448.

KLIONSKY, D. J., ABDALLA, F. C., ABELIOVICH, H., ABRAHAM, R. T., ACEVEDO-AROZENA, A., ADELI, K., AGHOLME, L., AGNELLO, M., AGOSTINIS, P., AGUIRRE-GHISO, J. A., AHN, H. J., AIT-MOHAMED, O., AIT-SI-ALI, S., AKEMATSU, T., AKIRA, S., AL-YOUNES, H. M., AL-ZEER, M. A., ALBERT, M. L., ALBIN, R. L., ALEGRE-ABARRATEGUI, J., ALEO, M. F., ALIREZAEI, M., ALMASAN, A., ALMONTE-BECERRIL, M., AMANO, A., AMARAVADI, R. K., AMARNATH, S., AMER, A. O., ANDRIEU-ABADIE, N., ANANTHARAM, V., ANN, D. K., ANOOPKUMAR-DUKIE, S., AOKI, H., APOSTOLOVA, N., ARANCIA, G., ARIS, J. P., ASANUMA, K., ASARE, N. Y. O., ASHIDA, H., ASKANAS, V., ASKEW, D. S., AUBERGER, P., BABA, M., BACKUES, S. K., BAEHRECKE, E. H., BAHR, B. A., BAI, X.-Y., BAILLY, Y., BAIOCCHI, R., BALDINI, G., BALDUINI, W., BALLABIO, A., BAMBER, B. A., BAMPTON, E. T. W., JUHÁSZ, G., BARTHOLOMEW, C. R., BASSHAM, D. C., BAST, R. C., BATOKO, H., BAY, B.-H., BEAU, I., BÉCHET, D. M., BEGLEY, T. J., BEHL, C., BEHRENDS, C., BEKRI, S., BELLAIRE, B., BENDALL, L. J., BENETTI, L., BERLIOCCHI, L., BERNARDI, H., BERNASSOLA, F., BESTEIRO, S., BHATIA-KIŠŠOVÁ, I., BI, X., BIARD-PIECHACZYK, M., BLUM, J. S., BOISE, L. H., BONALDO, P., BOONE, D. L., BORNHAUSER, B. C., BORTOLUCI, K. R., BOSSIS, I., BOST, F., BOURQUIN, J.-P., BOYA, P., BOYER-GUITTAUT, M., BOZHKOV, P. V., BRADY, N. R., BRANCOLINI, C., BRECH, A., BRENMAN, J. E., BRENNAND, A., BRESNICK, E. H., BREST, P., BRIDGES, D., BRISTOL, M. L., BROOKES, P. S., BROWN, E. J., BRUMELL, J. H., et al. 2012. Guidelines for the use and interpretation of assays for monitoring autophagy. *Autophagy,* 8**,** 445-544.

KLUZA, J., CORAZAO-ROZAS, P., TOUIL, Y., JENDOUBI, M., MAIRE, C., GUERRESCHI, P., JONNEAUX, A., BALLOT, C., BALAYSSAC, S., VALABLE, S., CORROYER-DULMONT, A., BERNAUDIN, M., MALET-MARTINO, M., DE LASSALLE, E. M., MABOUDOU, P., FORMSTECHER, P., POLAKOWSKA, R., MORTIER, L. & MARCHETTI, P. 2012. Inactivation of the HIF-1α/PDK3 Signaling Axis Drives Melanoma toward Mitochondrial Oxidative Metabolism and Potentiates the Therapeutic Activity of Pro-Oxidants. *Cancer Research,* 72**,** 5035-5047.

KOC, E. C., RANASINGHE, A., BURKHART, W., BLACKBURN, K., KOC, H., MOSELEY, A. & SPREMULLI, L. L. 2001. A new face on apoptosis: death-associated protein

3 and PDCD9 are mitochondrial ribosomal proteins. *FEBS Letters,* 492**,** 166-170.

KODITZ, J., NESPER, J., WOTTAWA, M., STIEHL, D. P., CAMENISCH, G., FRANKE, C., MYLLYHARJU, J., WENGER, R. H. & KATSCHINSKI, D. M. 2007. Oxygen-dependent ATF-4 stability is mediated by the PHD3 oxygen sensor. *Blood,* 110**,** 3610-7.

KOEHLER, C. M. & TIENSON, H. L. 2009. Redox regulation of protein folding in the mitochondrial intermembrane space. *Biochim.Biophys.Acta,* 1793**,** 139-145.

KOH, M. Y. & POWIS, G. 2009. HAF : the new player in oxygen-independent HIF-1alpha degradation. *Cell Cycle,* 8**,** 1359-66.

KOIVUNEN, P., HIRSILA, M., REMES, A. M., HASSINEN, I. E., KIVIRIKKO, K. I. & MYLLYHARJU, J. 2007a. Inhibition of hypoxia-inducible factor (HIF) hydroxylases by citric acid cycle intermediates: possible links between cell metabolism and stabilization of HIF. *J Biol Chem,* 282**,** 4524-4532.

KOIVUNEN, P., TIAINEN, P., HYVARINEN, J., WILLIAMS, K. E., SORMUNEN, R., KLAUS, S. J., KIVIRIKKO, K. I. & MYLLYHARJU, J. 2007b. An endoplasmic reticulum transmembrane prolyl 4-hydroxylase is induced by hypoxia and acts on hypoxia-inducible factor alpha. *J Biol Chem,* 282**,** 30544-52.

KONDO, K., KIM, W. Y., LECHPAMMER, M. & KAELIN, W. G. 2003. Inhibition of HIF2α is sufficient to suppress pVHL-defective tumor growth. *PLoS Biol.,* 1**,** e83.

KULAWIEC, M., OWENS, K. M. & SINGH, K. K. 2009. Cancer cell mitochondria confer apoptosis resistance and promote metastasis. *Cancer Biology & Therapy,* 8**,** 1378-1385.

KULSHRESHTHA, R., FERRACIN, M., WOJCIK, S. E., GARZON, R., ALDER, H., AGOSTO-PEREZ, F. J., DAVULURI, R., LIU, C.-G., CROCE, C. M., NEGRINI, M., CALIN, G. A. & IVAN, M. 2007. A MicroRNA Signature of Hypoxia. *Molecular and Cellular Biology,* 27**,** 1859-1867.

KUZNETSOVA, A. V., MELLER, J., SCHNELL, P. O., NASH, J. A., IGNACAK, M. L., SANCHEZ, Y., CONAWAY, J. W., CONAWAY, R. C. & CZYZYK-KRZESKA, M. F. 2003. von Hippel-Lindau protein binds hyperphosphorylated large subunit of RNA polymerase II through a proline hydroxylation motif and targets it for ubiquitination. *Proc Natl Acad Sci U S A,* 100**,** 2706-11.

LAI, Y., SONG, M., HAKALA, K., WEINTRAUB, S. T. & SHIIO, Y. 2011. Proteomic Dissection of the von Hippel–Lindau (VHL) Interactome. *Journal of Proteome Research,* 10**,** 5175-5182.

LANCASTER, D. E., MCDONOUGH, M. A. & SCHOFIELD, C. J. 2004a. Factor inhibiting hypoxia-inducible factor (FIH) and other asparaginyl hydroxylases. *Biochem Soc Trans,* 32**,** 943-5.

LANCASTER, D. E., MCNEILL, L. A., MCDONOUGH, M. A., APLIN, R. T., HEWITSON, K. S., PUGH, C. W., RATCLIFFE, P. J. & SCHOFIELD, C. J. 2004b. Disruption of

dimerization and substrate phosphorylation inhibit factor inhibiting hypoxia-inducible factor (FIH) activity. *Biochem J,* 383**,** 429-37.

LANDO, D., PEET, D. J., WHELAN, D. A., GORMAN, J. J. & WHITELAW, M. L. 2002. Asparagine hydroxylation of the HIF transactivation domain a hypoxic switch. *Science,* 295**,** 858-61.

LAUGHNER, E., TAGHAVI, P., CHILES, K., MAHON, P. C. & SEMENZA, G. L. 2001. HER2 (neu) signaling increases the rate of hypoxia-inducible factor 1alpha (HIF-1alpha) synthesis: novel mechanism for HIF-1-mediated vascular endothelial growth factor expression. *Mol Cell Biol,* 21**,** 3995-4004.

LEE, J.-Y., KOGA, H., KAWAGUCHI, Y., TANG, W., WONG, E., GAO, Y.-S., PANDEY, U. B., KAUSHIK, S., TRESSE, E., LU, J., TAYLOR, J. P., CUERVO, A. M. & YAO, T.-P. 2010a. HDAC6 controls autophagosome maturation essential for ubiquitin-selective quality-control autophagy. *Embo J,* 29**,** 969-980.

LEE, J. W., BAE, S. H., JEONG, J. W., KIM, S. H. & KIM, K. W. 2004. Hypoxia-inducible factor (HIF-1)alpha: its protein stability and biological functions. *Exp Mol Med,* 36**,** 1-12.

LEE, J. Y., NAGANO, Y., TAYLOR, J. P., LIM, K. L. & YAO, T. P. 2010b. Disease-causing mutations in Parkin impair mitochondrial ubiquitination, aggregation, and HDAC6-dependent mitophagy. *J. Cell Biol.,* 189**,** 671-679.

LEE, S., CHEN, D. Y., HUMPHREY, J. S., GNARRA, J. R., LINEHAN, W. M. & KLAUSNER, R. D. 1996. Nuclear/cytoplasmic localization of the von Hippel-Lindau tumor suppressor gene product is determined by cell density. *Proceedings of the National Academy of Sciences,* 93**,** 1770-1775.

LEE, S., NAKAMURA, E., YANG, H., WEI, W., LINGGI, M. S., SAJAN, M. P., FARESE, R. V., FREEMAN, R. S., CARTER, B. D., KAELIN, W. G., JR. & SCHLISIO, S. 2005. Neuronal apoptosis linked to EglN3 prolyl hydroxylase and familial pheochromocytoma genes: developmental culling and cancer. *Cancer Cell,* 8**,** 155-67.

LEE, S. H., WOLF, P. L., ESCUDERO, R., DEUTSCH, R., JAMIESON, S. W. & THISTLETHWAITE, P. A. 2000. Early expression of angiogenesis factors in acute myocardial ischemia and infarction. *N Engl J Med,* 342**,** 626-33.

LEGROS, F., LOMBÈS, A., FRACHON, P. & ROJO, M. 2002. Mitochondrial fusion in human cells is efficient, requires the inner membrane potential, and is mediated by mitofusins. *Molecular Biology of the Cell,* 13**,** 4343-4354.

LEIGH-BROWN, S., ENRIQUEZ, J. & ODOM, D. 2010. Nuclear transcription factors in mammalian mitochondria. *Genome Biology,* 11**,** 215.

LEMASTERS, J., CALDWELL-KENKEL, J., GAO, W., NIEMINEN, A., HERMAN, B. & THURMAN, R. 1992. Hypoxic, ischemic and reperfusion injury in the liver. *Pathophysiology of Reperfusion Injury* Boca Raton, FL: CRC.

LEMASTERS, J. J. 2005. Selective mitochondrial autophagy, or mitophagy, as a targeted defense against oxidative stress, mitochondrial dysfunction, and aging. *Rejuvenation Res,* 8**,** 3-5.

LEMASTERS, J. J., QIAN, T., HE, L., KIM, J. S., ELMORE, S. P., CASCIO, W. E. & BRENNER, D. A. 2002. Role of mitochondrial inner membrane permeabilization in necrotic cell death, apoptosis, and autophagy. *Antioxid Redox Signal,* 4**,** 769-81.

LEVRAUT, J., IWASE, H., SHAO, Z.-H., VANDEN HOEK, T. L. & SCHUMACKER, P. T. 2003a. Cell death during ischemia: relationship to mitochondrial depolarization and ROS generation. *Am J Physiol Heart Circ Physiol,* 284**,** 549-558.

LEVRAUT, J., IWASE, H., SHAO, Z. H., VANDEN HOEK, T. L. & SCHUMACKER, P. T. 2003b. Cell death during ischemia: relationship to mitochondrial depolarization and ROS generation. *Am J Physiol Heart Circ Physiol,* 284**,** H549-58.

LEWIS, M. D. & ROBERTS, B. J. 2003. Role of the C-terminal [alpha]-helical domain of the von Hippel-Lindau protein in its E3 ubiquitin ligase activity. *Oncogene,* 23**,** 2315-2323.

LEYSSENS, A., NOWICKY, A. V., PATTERSON, L., CROMPTON, M. & DUCHEN, M. R. 1996. The relationship between mitochondrial state, ATP hydrolysis, [Mg2+]i and [Ca2+]i studied in isolated rat cardiomyocytes. *The Journal of Physiology,* 496**,** 111-128.

LI, C. & JACKSON, R. M. 2002. Reactive species mechanisms of cellular hypoxia-reoxygenation injury. *Am J Physiol Cell Physiol,* 282**,** C227-41.

LI, F., WANG, Y., ZELLER, K. I., POTTER, J. J., WONSEY, D. R., O'DONNELL, K. A., KIM, J.-W., YUSTEIN, J. T., LEE, L. A. & DANG, C. V. 2005. Myc Stimulates Nuclearly Encoded Mitochondrial Genes and Mitochondrial Biogenesis. *Molecular and Cellular Biology,* 25**,** 6225-6234.

LI, K., LI, Y., SHELTON, J. M., RICHARDSON, J. A., SPENCER, E., CHEN, Z. J., WANG, X. & WILLIAMS, R. S. 2000. Cytochrome c deficiency causes embryonic lethality and attenuates stress-induced apoptosis. *Cell,* 101**,** 389-99.

LI, M. & KIM, W. Y. 2011. Two sides to every story: the HIF-dependent and HIF-independent functions of pVHL. *J Cell Mol Med,* 15**,** 187-195.

LICHTMAN, J. W. & CONCHELLO, J.-A. 2005. Fluorescence microscopy. *Nat Meth,* 2**,** 910-919.

LIEB, M. E., MENZIES, K., MOSCHELLA, M. C., NI, R. & TAUBMAN, M. B. 2002. Mammalian EGLN genes have distinct patterns of mRNA expression and regulation. *Biochem Cell Biol,* 80**,** 421-6.

LIESA, M., PALACÍN, M. & ZORZANO, A. 2009. Mitochondrial Dynamics in Mammalian Health and Disease. *Physiological Reviews,* 89**,** 799-845.

LIN, C.-S., LEE, H.-T., LEE, S.-Y., SHEN, Y.-A., WANG, L.-S., CHEN, Y.-J. & WEI, Y.-H. 2012. High Mitochondrial DNA Copy Number and Bioenergetic Function Are Associated with Tumor Invasion of Esophageal Squamous Cell Carcinoma Cell Lines. *International Journal of Molecular Sciences,* 13**,** 11228-11246.

LIN, X., DAVID, C. A., DONNELLY, J. B., MICHAELIDES, M., CHANDEL, N. S., HUANG, X., WARRIOR, U., WEINBERG, F., TORMOS, K. V., FESIK, S. W. & SHEN, Y. 2008. A chemical genomics screen highlights the essential role of mitochondria in HIF-1 regulation. *Proc Natl Acad Sci U S A,* 105**,** 174-179.

LIPSCOMB, E. A., SARMIERE, P. D. & FREEMAN, R. S. 2001. SM-20 is a novel mitochondrial protein that causes caspase-dependent cell death in nerve growth factor-dependent neurons. *J Biol Chem,* 276**,** 5085-92.

LIU, W., XIN, H., ECKERT, D. T., BROWN, J. A. & GNARRA, J. R. 2011. Hypoxia and cell cycle regulation of the von Hippel-Lindau tumor suppressor. *Oncogene,* 30**,** 21-31.

LIU, Y., HUO, Z., YAN, B., LIN, X., ZHOU, Z.-N., LIANG, X., ZHU, W., LIANG, D., LI, L., LIU, Y., ZHAO, H., SUN, Y. & CHEN, Y.-H. 2010. Prolyl hydroxylase 3 interacts with Bcl-2 to regulate doxorubicin-induced apoptosis in H9c2 cells. *Biochemical and Biophysical Research Communications,* 401**,** 231-237.

LOOR, G. & SCHUMACKER, P. T. 2008. Role of hypoxia-inducible factor in cell survival during myocardial ischemia-reperfusion. *Cell Death.Differ.,* 15**,** 686-690.

LOSÓN, O. C., SONG, Z., CHEN, H. & CHAN, D. C. 2013. Fis1, Mff, MiD49, and MiD51 mediate Drp1 recruitment in mitochondrial fission. *Molecular Biology of the Cell,* 24**,** 659-667.

LUO, W., HU, H., CHANG, R., ZHONG, J., KNABEL, M., O'MEALLY, R., COLE, ROBERT N., PANDEY, A. & SEMENZA, GREGG L. 2011. Pyruvate Kinase M2 Is a PHD3-Stimulated Coactivator for Hypoxia-Inducible Factor 1. *Cell,* 145**,** 732-744.

LUO, W. & SEMENZA, G. L. 2011. Pyruvate kinase M2 regulates glucose metabolism by functioning as a coactivator for hypoxia-inducible factor 1 in cancer cells. *Oncotarget,* 2**,** 551-6.

MAHON, P. C., HIROTA, K. & SEMENZA, G. L. 2001. FIH-1: a novel protein that interacts with HIF-1alpha and VHL to mediate repression of HIF-1 transcriptional activity. *Genes Dev,* 15**,** 2675-86.

MAIURI, M. C., LE TOUMELIN, G., CRIOLLO, A., RAIN, J.-C., GAUTIER, F., JUIN, P., TASDEMIR, E., PIERRON, G., TROULINAKI, K., TAVERNARAKIS, N., HICKMAN, J. A., GENESTE, O. & KROEMER, G. 2007. Functional and physical interaction between Bcl-XL and a BH3-like domain in Beclin-1. *Embo J,* 26**,** 2527-2539.

MAKINO, Y., CAO, R., SVENSSON, K., BERTILSSON, G., ASMAN, M., TANAKA, H., CAO, Y., BERKENSTAM, A. & POELLINGER, L. 2001. Inhibitory PAS domain protein

is a negative regulator of hypoxia-inducible gene expression. *Nature,* 414**,** 550-4.

MAKINO, Y., KANOPKA, A., WILSON, W. J., TANAKA, H. & POELLINGER, L. 2002. Inhibitory PAS domain protein (IPAS) is a hypoxia-inducible splicing variant of the hypoxia-inducible factor-3alpha locus. *J Biol Chem,* 277**,** 32405-8.

MAMBO, E., CHATTERJEE, A., XING, M., TALLINI, G., HAUGEN, B. R., YEUNG, S.-C. J., SUKUMAR, S. & SIDRANSKY, D. 2005. Tumor-specific changes in mtDNA content in human cancer. *International Journal of Cancer,* 116**,** 920-924.

MANSFIELD, K. D., GUZY, R. D., PAN, Y., YOUNG, R. M., CASH, T. P., SCHUMACKER, P. T. & SIMON, M. C. 2005. Mitochondrial dysfunction resulting from loss of cytochrome c impairs cellular oxygen sensing and hypoxic HIF-alpha activation. *Cell Metab.,* 1**,** 393-399.

MARCHENKO, N. D., ZAIKA, A. & MOLL, U. M. 2000. Death signal-induced localization of p53 protein to mitochondria. A potential role in apoptotic signaling. *J Biol Chem,* 275**,** 16202-12.

MARGINEANTU, D. H., GREGORY COX, W., SUNDELL, L., SHERWOOD, S. W., BEECHEM, J. M. & CAPALDI, R. A. 2002. Cell cycle dependent morphology changes and associated mitochondrial DNA redistribution in mitochondria of human cell lines. *Mitochondrion,* 1**,** 425-35.

MARTINEZ-OUTSCHOORN, U. E., BALLIET, R. M., RIVADENEIRA, D., CHIAVARINA, B., PAVLIDES, S., WANG, C., WHITAKER-MENEZES, D., DAUMER, K., LIN, Z., WITKIEWICZ, A., FLOMENBERG, N., HOWELL, A., PESTELL, R., KNUDSEN, E., SOTGIA, F. & LISANTI, M. P. 2010a. Oxidative stress in cancer associated fibroblasts drives tumor-stroma co-evolution: A new paradigm for understanding tumor metabolism, the field effect and genomic instability in cancer cells. *Cell Cycle,* 9**,** 3276-3296.

MARTINEZ-OUTSCHOORN, U. E., TRIMMER, C., LIN, Z., WHITAKER-MENEZES, D., CHIAVARINA, B., ZHOU, J., WANG, C., PAVLIDES, S., MARTINEZ-CANTARIN, M. P., CAPOZZA, F., WITKIEWICZ, A. K., FLOMENBERG, N., HOWELL, A., PESTELL, R. G., CARO, J., LISANTI, M. P. & SOTGIA, F. 2010b. Autophagy in cancer associated fibroblasts promotes tumor cell survival: Role of hypoxia, HIF1 induction and NFκB activation in the tumor stromal microenvironment. *Cell Cycle,* 9**,** 3515-3533.

MASSON, N., WILLAM, C., MAXWELL, P. H., PUGH, C. W. & RATCLIFFE, P. J. 2001. Independent function of two destruction domains in hypoxia-inducible factor-alpha chains activated by prolyl hydroxylation. *Embo J,* 20**,** 5197-206.

MATEO, J., GARCIA-LECEA, M., CADENAS, S., HERNANDEZ, C. & MONCADA, S. 2003. Regulation of hypoxia-inducible factor-1alpha by nitric oxide through mitochondria-dependent and -independent pathways. *Biochem J,* 376**,** 537-44.

MATOBA, S., KANG, J.-G., PATINO, W. D., WRAGG, A., BOEHM, M., GAVRILOVA, O., HURLEY, P. J., BUNZ, F. & HWANG, P. M. 2006. p53 Regulates Mitochondrial Respiration. *Science,* 312**,** 1650-1653.

MATSUDA, N. 2010. PINK1 stabilized by mitochondrial depolarization recruits Parkin to damaged mitochondria and activates latent Parkin for mitophagy. *J. Cell Biol.,* 189**,** 211-221.

MAXWELL, P. H. 2005. Hypoxia-inducible factor as a physiological regulator. *Exp Physiol,* 90**,** 791-7.

MAXWELL, P. H., PUGH, C. W. & RATCLIFFE, P. J. 1993. Inducible operation of the erythropoietin 3' enhancer in multiple cell lines: evidence for a widespread oxygen-sensing mechanism. *Proc Natl Acad Sci U S A,* 90**,** 2423-7.

MAXWELL, P. H., WIESENER, M. S., CHANG, G. W., CLIFFORD, S. C., VAUX, E. C., COCKMAN, M. E., WYKOFF, C. C., PUGH, C. W., MAHER, E. R. & RATCLIFFE, P. J. 1999. The tumour suppressor protein VHL targets hypoxia-inducible factors for oxygen-dependent proteolysis. *Nature,* 399**,** 271-5.

MCNEILL, L. A., HEWITSON, K. S., CLARIDGE, T. D., SEIBEL, J. F., HORSFALL, L. E. & SCHOFIELD, C. J. 2002. Hypoxia-inducible factor asparaginyl hydroxylase (FIH-1) catalyses hydroxylation at the beta-carbon of asparagine-803. *Biochem J,* 367**,** 571-5.

MEEUSEN, S., DEVAY, R., BLOCK, J., CASSIDY-STONE, A., WAYSON, S., MCCAFFERY, J. M. & NUNNARI, J. 2006. Mitochondrial Inner-Membrane Fusion and Crista Maintenance Requires the Dynamin-Related GTPase Mgm1. *Cell,* 127**,** 383-395.

MELÉNDEZ, A. & NEUFELD, T. P. 2008. The cell biology of autophagy in metazoans: a developing story. *Development,* 135**,** 2347-2360.

MENRAD, H., WERNO, C., SCHMID, T., COPANAKI, E., DELLER, T., DEHNE, N. & BRÜNE, B. 2010. Roles of hypoxia-inducible factor-1α (HIF-1α) versus HIF-2α in the survival of hepatocellular tumor spheroids. *Hepatology,* 51**,** 2183-2192.

MESECKE, N., TERZIYSKA, N., KOZANY, C., BAUMANN, F., NEUPERT, W., HELL, K. & HERRMANN, J. M. 2005. A disulfide relay system in the intermembrane space of mitochondria that mediates protein import. *Cell,* 121**,** 1059-1069.

METZEN, E., BERCHNER-PFANNSCHMIDT, U., STENGEL, P., MARXSEN, J. H., STOLZE, I., KLINGER, M., HUANG, W. Q., WOTZLAW, C., HELLWIG-BURGEL, T., JELKMANN, W., ACKER, H. & FANDREY, J. 2003. Intracellular localisation of human HIF-1 alpha hydroxylases: implications for oxygen sensing. *J Cell Sci,* 116**,** 1319-26.

METZEN, E., STIEHL, D. P., DOEGE, K., MARXSEN, J. H., HELLWIG-BURGEL, T. & JELKMANN, W. 2005. Regulation of the prolyl hydroxylase domain protein 2 (phd2/egln-1) gene: identification of a functional hypoxia-responsive element. *Biochem J,* 387**,** 711-7.

MIKHAYLOVA, O., IGNACAK, M. L., BARANKIEWICZ, T. J., HARBAUGH, S. V., YI, Y., MAXWELL, P. H., SCHNEIDER, M., VAN GEYTE, K., CARMELIET, P., REVELO, M. P., WYDER, M., GREIS, K. D., MELLER, J. & CZYZYK-KRZESKA, M. F. 2008. The von Hippel-Lindau tumor suppressor protein and Egl-9-Type proline hydroxylases regulate the large subunit of RNA polymerase II in response to oxidative stress. *Mol Cell Biol,* 28**,** 2701-17.

MIKHAYLOVA, O., STRATTON, Y., HALL, D., KELLNER, E., EHMER, B., DREW, ANGELA F., GALLO, CATHERINE A., PLAS, DAVID R., BIESIADA, J., MELLER, J. & CZYZYK-KRZESKA, MARIA F. 2012. VHL-Regulated MiR-204 Suppresses Tumor Growth through Inhibition of LC3B-Mediated Autophagy in Renal Clear Cell Carcinoma. *Cancer Cell,* 21**,** 532-546.

MINAMISHIMA, Y. A., MOSLEHI, J., BARDEESY, N., CULLEN, D., BRONSON, R. T. & KAELIN, W. G., JR. 2008. Somatic inactivation of the PHD2 prolyl hydroxylase causes polycythemia and congestive heart failure. *Blood,* 111**,** 3236-44.

MINET, E., MOTTET, D., MICHEL, G., ROLAND, I., RAES, M., REMACLE, J. & MICHIELS, C. 1999. Hypoxia-induced activation of HIF-1: role of HIF-1alpha-Hsp90 interaction. *FEBS Lett,* 460**,** 251-6.

MISRA, M. K., SARWAT, M., BHAKUNI, P., TUTEJA, R. & TUTEJA, N. 2009. Oxidative stress and ischemic myocardial syndromes. *Med Sci Monit,* 15**,** RA209-219.

MITRA, K., WUNDER, C., ROYSAM, B., LIN, G. & LIPPINCOTT-SCHWARTZ, J. 2009. A hyperfused mitochondrial state achieved at G1–S regulates cyclin E buildup and entry into S phase. *Proceedings of the National Academy of Sciences,* 106**,** 11960-11965.

MIZUSHIMA, N. 2005. The pleiotropic role of autophagy: from protein metabolism to bactericide. *Cell Death Differ,* 12**,** 1535-1541.

MIZUSHIMA, N. 2007. Autophagy: process and function. *Genes & Development,* 21**,** 2861-2873.

MIZUSHIMA, N., YOSHIMORI, T. & LEVINE, B. 2010. Methods in Mammalian Autophagy Research. *Cell,* 140**,** 313-326.

MOLE, D. R., BLANCHER, C., COPLEY, R. R., POLLARD, P. J., GLEADLE, J. M., RAGOUSSIS, J. & RATCLIFFE, P. J. 2009. Genome-wide association of hypoxia-inducible factor (HIF)-1alpha and HIF-2alpha DNA binding with expression profiling of hypoxia-inducible transcripts. *J Biol Chem,* 284**,** 16767-75.

MOLE, D. R., SCHLEMMINGER, I., MCNEILL, L. A., HEWITSON, K. S., PUGH, C. W., RATCLIFFE, P. J. & SCHOFIELD, C. J. 2003. 2-oxoglutarate analogue inhibitors of HIF prolyl hydroxylase. *Bioorg Med Chem Lett,* 13**,** 2677-80.

MONGE, C., BERAUD, N., TEPP, K., PELLOUX, S., CHAHBOUN, S., KAAMBRE, T., KADAJA, L., ROOSIMAA, M., PIIRSOO, A., TOURNEUR, Y., KUZNETSOV, A. V., SAKS, V. & SEPPET, E. 2009. Comparative analysis of the bioenergetics of adult cardiomyocytes and nonbeating HL-1 cells: respiratory chain activities, glycolytic enzyme profiles, and metabolic fluxesThis article is one of a

selection of papers from the NATO Advanced Research Workshop on Translational Knowledge for Heart Health (published in part 2 of a 2-part Special Issue). *Canadian Journal of Physiology and Pharmacology,* 87**,** 318-326.

MÖPERT, K., HAJEK, P., FRANK, S., CHEN, C., KAUFMANN, J. & SANTEL, A. 2009. Loss of Drp1 function alters OPA1 processing and changes mitochondrial membrane organization. *Experimental Cell Research,* 315**,** 2165-2180.

MORTIBOYS, H., THOMAS, K. J., KOOPMAN, W. J., KLAFFKE, S., ABOU-SLEIMAN, P., OLPIN, S., WOOD, N. W., WILLEMS, P. H., SMEITINK, J. A., COOKSON, M. R. & BANDMANN, O. 2008. Mitochondrial function and morphology are impaired in parkin-mutant fibroblasts. *Ann Neurol,* 64**,** 555-65.

MUKHOPADHYAY, D., KNEBELMANN, B., COHEN, H. T., ANANTH, S. & SUKHATME, V. P. 1997. The von Hippel-Lindau tumor suppressor gene product interacts with Sp1 to repress vascular endothelial growth factor promoter activity. *Molecular and Cellular Biology,* 17**,** 5629-39.

MULLER, F. L., LIU, Y. & VAN REMMEN, H. 2004. Complex III releases superoxide to both sides of the inner mitochondrial membrane. *J Biol Chem,* 279**,** 49064-73.

MURRY, C. E., JENNINGS, R. B. & REIMER, K. A. 1986. Preconditioning with ischemia: a delay of lethal cell injury in ischemic myocardium. *Circulation,* 74**,** 1124-36.

MYLONIS, I., CHACHAMI, G., SAMIOTAKI, M., PANAYOTOU, G., PARASKEVA, E., KALOUSI, A., GEORGATSOU, E., BONANOU, S. & SIMOS, G. 2006. Identification of MAPK phosphorylation sites and their role in the localization and activity of hypoxia-inducible factor-1alpha. *J Biol Chem,* 281**,** 33095-106.

NADANACIVA, S., RANA, P., BEESON, G., CHEN, D., FERRICK, D., BEESON, C. & WILL, Y. 2012. Assessment of drug-induced mitochondrial dysfunction via altered cellular respiration and acidification measured in a 96-well platform. *Journal of Bioenergetics and Biomembranes,* 44**,** 421-437.

NAKAYAMA, K., FREW, I. J., HAGENSEN, M., SKALS, M., HABELHAH, H., BHOUMIK, A., KADOYA, T., ERDJUMENT-BROMAGE, H., TEMPST, P., FRAPPELL, P. B., BOWTELL, D. D. & RONAI, Z. E. 2004. Siah2 Regulates Stability of Prolyl-Hydroxylases, Controls HIF1α Abundance, and Modulates Physiological Responses to Hypoxia. *Cell,* 117**,** 941-952.

NAOE, M., OHWA, Y., ISHIKAWA, D., OHSHIMA, C., NISHIKAWA, S., YAMAMOTO, H. & ENDO, T. 2004. Identification of Tim40 that mediates protein sorting to the mitochondrial intermembrane space. *J Biol Chem,* 279**,** 47815-21.

NARENDRA, D., KANE, L., HAUSER, D., FEARNLEY, I. & YOULE, R. 2010. p62/SQSTM1 is required for Parkin-induced mitochondrial clustering but not mitophagy; VDAC1 is dispensible for both. *Autophagy,* 6**,** 1090-1106.

NARENDRA, D., TANAKA, A., SUEN, D. F. & YOULE, R. J. 2008. Parkin is recruited selectively to impaired mitochondria and promotes their autophagy. *J. Cell Biol.,* 183**,** 795-803.

NARENDRA, D. P. 2010. PINK1 is selectively stabilized on impaired mitochondria to activate Parkin. *PLoS Biol.,* 8**,** e1000298.

NEELY, J. R. & MORGAN, H. E. 1974. Relationship between carbohydrate and lipid metabolism and the energy balance of heart muscle. *Annu Rev Physiol,* 36**,** 413-59.

NEELY, J. R., ROVETTO, M. J. & ORAM, J. F. 1972. Myocardial utilization of carbohydrate and lipids. *Prog Cardiovasc Dis,* 15**,** 289-329.

NEUSPIEL, M., ZUNINO, R., GANGARAJU, S., RIPPSTEIN, P. & MCBRIDE, H. 2005. Activated Mitofusin 2 Signals Mitochondrial Fusion, Interferes with Bax Activation, and Reduces Susceptibility to Radical Induced Depolarization. *Journal of Biological Chemistry,* 280**,** 25060-25070.

NGUYEN, S. V. & CLAYCOMB, W. C. 1999. Hypoxia regulates the expression of the adrenomedullin and HIF-1 genes in cultured HL-1 cardiomyocytes. *Biochem Biophys Res Commun,* 265**,** 382-6.

NOLDEN, M., EHSES, S., KOPPEN, M., BERNACCHIA, A., RUGARLI, E. I. & LANGER, T. 2005. The m-AAA Protease Defective in Hereditary Spastic Paraplegia Controls Ribosome Assembly in Mitochondria. *Cell,* 123**,** 277-289.

O'BRIEN, T. W. 2003. Properties of Human Mitochondrial Ribosomes. *IUBMB Life,* 55**,** 505-513.

OCKAILI, R., NATARAJAN, R., SALLOUM, F., FISHER, B. J., JONES, D., FOWLER, A. A., 3RD & KUKREJA, R. C. 2005. HIF-1 activation attenuates postischemic myocardial injury: role for heme oxygenase-1 in modulating microvascular chemokine generation. *Am J Physiol Heart Circ Physiol,* 289**,** H542-8.

OEHME, F., ELLINGHAUS, P., KOLKHOF, P., SMITH, T. J., RAMAKRISHNAN, S., HUTTER, J., SCHRAMM, M. & FLAMME, I. 2002. Overexpression of PH-4, a novel putative proline 4-hydroxylase, modulates activity of hypoxia-inducible transcription factors. *Biochem Biophys Res Commun,* 296**,** 343-9.

OHH, M., PARK, C. W., IVAN, M., HOFFMAN, M. A., KIM, T. Y., HUANG, L. E., PAVLETICH, N., CHAU, V. & KAELIN, W. G. 2000. Ubiquitination of hypoxia-inducible factor requires direct binding to the beta-domain of the von Hippel-Lindau protein. *Nat Cell Biol,* 2**,** 423-7.

OHTSUKA, T., NISHIJIMA, M., SUZUKI, K. & AKAMATSU, Y. 1993. Mitochondrial dysfunction of a cultured Chinese hamster ovary cell mutant deficient in cardiolipin. *Journal of Biological Chemistry,* 268**,** 22914-9.

OKATSU, K. 2010. p62/SQSTM1 cooperates with Parkin for perinuclear clustering of depolarized mitochondria. *Genes Cells,* 15**,** 887-900.

OKTAY, Y., DIOUM, E., MATSUZAKI, S., DING, K., YAN, L. J., HALLER, R. G., SZWEDA, L. I. & GARCIA, J. A. 2007. Hypoxia-inducible factor 2alpha regulates expression of the mitochondrial aconitase chaperone protein frataxin. *J Biol Chem,* 282**,** 11750-6.

OSTRANDER, D. B., ZHANG, M., MILEYKOVSKAYA, E., RHO, M. & DOWHAN, W. 2001. Lack of Mitochondrial Anionic Phospholipids Causes an Inhibition of Translation of Protein Components of the Electron Transport Chain: A YEAST GENETIC MODEL SYSTEM FOR THE STUDY OF ANIONIC PHOSPHOLIPID FUNCTION IN MITOCHONDRIA. *Journal of Biological Chemistry,* 276**,** 25262-25272.

OTERA, H., ISHIHARA, N. & MIHARA, K. 2013. New insights into the function and regulation of mitochondrial fission. *Biochim Biophys Acta,* 1833**,** 1256-68.

OTERA, H., WANG, C., CLELAND, M. M., SETOGUCHI, K., YOKOTA, S., YOULE, R. J. & MIHARA, K. 2010. Mff is an essential factor for mitochondrial recruitment of Drp1 during mitochondrial fission in mammalian cells. *The Journal of Cell Biology,* 191**,** 1141-1158.

PADDOCK, S. W. 2005. Microscopy. *In:* KEITH WILSON, J. W. (ed.) *Principles and Techniques of Biochemistry and Molecular Biology.* 6 ed. New York, USA: Cambridge University Press.

PAGLIARINI, D. J., CALVO, S. E., CHANG, B., SHETH, S. A., VAFAI, S. B., ONG, S.-E., WALFORD, G. A., SUGIANA, C., BONEH, A., CHEN, W. K., HILL, D. E., VIDAL, M., EVANS, J. G., THORBURN, D. R., CARR, S. A. & MOOTHA, V. K. 2008. A Mitochondrial Protein Compendium Elucidates Complex I Disease Biology. *Cell,* 134**,** 112-123.

PAL, S., CLAFFEY, K. P., DVORAK, H. F. & MUKHOPADHYAY, D. 1997. The von Hippel-Lindau gene product inhibits vascular permeability factor/vascular endothelial growth factor expression in renal cell carcinoma by blocking protein kinase C pathways. *J Biol Chem,* 272**,** 27509-12.

PAN, Y., MANSFIELD, K. D., BERTOZZI, C. C., RUDENKO, V., CHAN, D. A., GIACCIA, A. J. & SIMON, M. C. 2007. Multiple factors affecting cellular redox status and energy metabolism modulate hypoxia-inducible factor prolyl hydroxylase activity in vivo and in vitro. *Mol Cell Biol,* 27**,** 912-925.

PANKIV, S. 2007. p62/SQSTM1 binds directly to Atg8/LC3 to facilitate degradation of ubiquitinated protein aggregates by autophagy. *J. Biol. Chem.,* 282**,** 24131-24145.

PAPANDREOU, I., CAIRNS, R. A., FONTANA, L., LIM, A. L. & DENKO, N. C. 2006. HIF-1 mediates adaptation to hypoxia by actively downregulating mitochondrial oxygen consumption. *Cell Metab.,* 3**,** 187-197.

PARK, J. 2006. Mitochondrial dysfunction in Drosophila PINK1 mutants is complemented by parkin. *Nature,* 441**,** 1157-1161.

PARK, S. K., DADAK, A. M., HAASE, V. H., FONTANA, L., GIACCIA, A. J. & JOHNSON, R. S. 2003. Hypoxia-induced gene expression occurs solely through the action of hypoxia-inducible factor 1alpha (HIF-1alpha): role of cytoplasmic trapping of HIF-2alpha. *Mol Cell Biol,* 23**,** 4959-71.

PARONE, P. A., DA CRUZ, S., TONDERA, D., MATTENBERGER, Y., JAMES, D. I., MAECHLER, P., BARJA, F. & MARTINOU, J.-C. 2008. Preventing mitochondrial fission impairs mitochondrial function and leads to loss of mitochondrial DNA. *PLoS One,* 3.

PATTEN, D. A., LAFLEUR, V. N., ROBITAILLE, G. A., CHAN, D. A., GIACCIA, A. J. & RICHARD, D. E. 2010. Hypoxia-inducible Factor-1 Activation in Nonhypoxic Conditions: The Essential Role of Mitochondrial-derived Reactive Oxygen Species. *Mol Biol Cell,* 21**,** 3247-57.

PATTINGRE, S., TASSA, A., QU, X., GARUTI, R., LIANG, X. H., MIZUSHIMA, N., PACKER, M., SCHNEIDER, M. D. & LEVINE, B. 2005. Bcl-2 Antiapoptotic Proteins Inhibit Beclin 1-Dependent Autophagy. *Cell,* 122**,** 927-939.

PENG, J., ZHANG, L., DRYSDALE, L. & FONG, G. H. 2000. The transcription factor EPAS-1/hypoxia-inducible factor 2alpha plays an important role in vascular remodeling. *Proc Natl Acad Sci U S A,* 97**,** 8386-91.

PESCADOR, N., CUEVAS, Y., NARANJO, S., ALCAIDE, M., VILLAR, D., LANDAZURI, M. O. & DEL PESO, L. 2005. Identification of a functional hypoxia-responsive element that regulates the expression of the egl nine homologue 3 (egln3/phd3) gene. *Biochem J,* 390**,** 189-97.

PESTA, D. & GNAIGER, E. 2012. High-Resolution Respirometry: OXPHOS Protocols for Human Cells and Permeabilized Fibers from Small Biopsies of Human Muscle. *In:* PALMEIRA, C. M. & MORENO, A. J. (eds.) *Mitochondrial Bioenergetics.* Humana Press.

PI, Y., GOLDENTHAL, M. J. & MARIN-GARCIA, J. 2007. Mitochondrial involvement in IGF-1 induced protection of cardiomyocytes against hypoxia/reoxygenation injury. *Mol Cell Biochem,* 301**,** 181-9.

POLLENZ, R. S., SATTLER, C. A. & POLAND, A. 1994. The aryl hydrocarbon receptor and aryl hydrocarbon receptor nuclear translocator protein show distinct subcellular localizations in Hepa 1c1c7 cells by immunofluorescence microscopy. *Molecular Pharmacology,* 45**,** 428-438.

POOLE, A. C. 2008. The PINK1/Parkin pathway regulates mitochondrial morphology. *Proc. Natl Acad. Sci. USA,* 105**,** 1638-1643.

POON, E., HARRIS, A. L. & ASHCROFT, M. 2009. Targeting the hypoxia-inducible factor (HIF) pathway in cancer. *Expert Rev Mol Med,* 11**,** e26.

POYTON, R. O., CASTELLO, P. R., BALL, K. A., WOO, D. K. & PAN, N. 2009. Mitochondria and hypoxic signaling: a new view. *Ann N Y Acad Sci,* 1177**,** 48-56.

PSARRA, A. M. & SEKERIS, C. E. 2009. Glucocorticoid receptors and other nuclear transcription factors in mitochondria and possible functions. *Biochim Biophys Acta,* 1787**,** 431-6.

PSARRA, A. M., SOLAKIDI, S., TROUGAKOS, I. P., MARGARITIS, L. H., SPYROU, G. & SEKERIS, C. E. 2005. Glucocorticoid receptor isoforms in human hepatocarcinoma HepG2 and SaOS-2 osteosarcoma cells: presence of glucocorticoid receptor alpha in mitochondria and of glucocorticoid receptor beta in nucleoli. *Int J Biochem Cell Biol,* 37**,** 2544-58.

PUISSANT, A., FENOUILLE, N. & AUBERGER, P. 2012. When autophagy meets cancer through p62/SQSTM1. *Am J Cancer Res,* 2**,** 397-413.

QI, X., DISATNIK, M. H., SHEN, N., SOBEL, R. A. & MOCHLY-ROSEN, D. 2011. Aberrant mitochondrial fission in neurons induced by protein kinase C{delta} under oxidative stress conditions in vivo. *Mol Biol Cell,* 22**,** 256-65.

RAMBOLD, A. S., KOSTELECKY, B., ELIA, N. & LIPPINCOTT-SCHWARTZ, J. 2011. Tubular network formation protects mitochondria from autophagosomal degradation during nutrient starvation. *Proc Natl Acad Sci U S A,* 108**,** 10190-5.

RANE, S., HE, M., SAYED, D., VASHISTHA, H., MALHOTRA, A., SADOSHIMA, J., VATNER, D. E., VATNER, S. F. & ABDELLATIF, M. 2009. Downregulation of miR-199a derepresses hypoxia-inducible factor-1alpha and Sirtuin 1 and recapitulates hypoxia preconditioning in cardiac myocytes. *Circ.Res.,* 104**,** 879-886.

RANTANEN, K., PURSIHEIMO, J.-P., HÖGEL, H., MIIKKULAINEN, P., SUNDSTRÖM, J. & JAAKKOLA, P. M. 2013. p62/SQSTM1 regulates cellular oxygen sensing by attenuating PHD3 activity through aggregate sequestration and enhanced degradation. *Journal of Cell Science,* 126**,** 1144-1154.

RAVAL, R. R., LAU, K. W., TRAN, M. G. B., SOWTER, H. M., MANDRIOTA, S. J., LI, J.-L., PUGH, C. W., MAXWELL, P. H., HARRIS, A. L. & RATCLIFFE, P. J. 2005. Contrasting Properties of Hypoxia-Inducible Factor 1 (HIF-1) and HIF-2 in von Hippel-Lindau-Associated Renal Cell Carcinoma. *Molecular and Cellular Biology,* 25**,** 5675-5686.

RAVIKUMAR, B., SARKAR, S., DAVIES, J. E., FUTTER, M., GARCIA-ARENCIBIA, M., GREEN-THOMPSON, Z. W., JIMENEZ-SANCHEZ, M., KOROLCHUK, V. I., LICHTENBERG, M., LUO, S., MASSEY, D. C. O., MENZIES, F. M., MOREAU, K., NARAYANAN, U., RENNA, M., SIDDIQI, F. H., UNDERWOOD, B. R., WINSLOW, A. R. & RUBINSZTEIN, D. C. 2010. Regulation of Mammalian Autophagy in Physiology and Pathophysiology. *Physiological Reviews,* 90**,** 1383-1435.

RECHSTEINER, M. P., VON TEICHMAN, A., NOWICKA, A., SULSER, T., SCHRAML, P. & MOCH, H. 2011. VHL Gene Mutations and Their Effects on Hypoxia Inducible Factor HIFα: Identification of Potential Driver and Passenger Mutations. *Cancer Research,* 71**,** 5500-5511.

REDDY, P. H., REDDY, T. P., MANCZAK, M., CALKINS, M. J., SHIRENDEB, U. & MAO, P. 2011. Dynamin-related protein 1 and mitochondrial fragmentation in neurodegenerative diseases. *Brain Res Rev,* 67**,** 103-18.

RICHARD, D. E., BERRA, E. & POUYSSEGUR, J. 2000. Nonhypoxic pathway mediates the induction of hypoxia-inducible factor 1alpha in vascular smooth muscle cells. *J Biol Chem,* 275**,** 26765-71.

ROBERTS, A. M. 2009. Suppression of hypoxia-inducible factor 2α restores p53 activity via Hdm2 and reverses chemoresistance of renal carcinoma cells. *Cancer Res.,* 69**,** 9056-9064.

ROBIN, E., GUZY, R. D., LOOR, G., IWASE, H., WAYPA, G. B., MARKS, J. D., HOEK, T. L. & SCHUMACKER, P. T. 2007. Oxidant stress during simulated ischemia primes cardiomyocytes for cell death during reperfusion. *J Biol Chem,* 282**,** 19133-43.

ROHRBACH, S., SIMM, A., PREGLA, R., FRANKE, C. & KATSCHINSKI, D. R. M. 2005. Age-dependent increase of prolyl-4-hydroxylase domain (PHD) 3 expression in human and mouse heart. *Biogerontology.* Springer Netherlands.

ROSE, N. R., MCDONOUGH, M. A., KING, O. N., KAWAMURA, A. & SCHOFIELD, C. J. 2011. Inhibition of 2-oxoglutarate dependent oxygenases. *Chem Soc Rev,* 40**,** 4364-97.

RÖTIG, A. 2011. Human diseases with impaired mitochondrial protein synthesis. *Biochimica et Biophysica Acta (BBA) - Bioenergetics,* 1807**,** 1198-1205.

ROUSCHOP, K. M. A., VAN DEN BEUCKEN, T., DUBOIS, L., NIESSEN, H., BUSSINK, J., SAVELKOULS, K., KEULERS, T., MUJCIC, H., LANDUYT, W., VONCKEN, J. W., LAMBIN, P., VAN DER KOGEL, A. J., KORITZINSKY, M. & WOUTERS, B. G. 2010. The unfolded protein response protects human tumor cells during hypoxia through regulation of the autophagy genes MAP1LC3B and ATG5. *The Journal of Clinical Investigation,* 120**,** 127-141.

RUBINSZTEIN, D. C., CUERVO, A. M., RAVIKUMAR, B., SARKAR, S., KOROLCHUK, V. I., KAUSHIK, S. & KLIONSKY, D. J. 2009. In search of an “autophagomometer”. *Autophagy,* 5**,** 585-589.

SALCEDA, S. & CARO, J. 1997. Hypoxia-inducible factor 1alpha (HIF-1alpha) protein is rapidly degraded by the ubiquitin-proteasome system under normoxic conditions. Its stabilization by hypoxia depends on redox-induced changes. *J Biol Chem,* 272**,** 22642-7.

SARRAF, S. A., RAMAN, M., GUARANI-PEREIRA, V., SOWA, M. E., HUTTLIN, E. L., GYGI, S. P. & HARPER, J. W. 2013. Landscape of the PARKIN-dependent ubiquitylome in response to mitochondrial depolarization. *Nature,* 496**,** 372-376.

SARTO, C., MAROCCHI, A., SANCHEZ, J. C., GIANNONE, D., FRUTIGER, S., GOLAZ, O., WILKINS, M. R., DORO, G., CAPPELLANO, F., HUGHES, G., HOCHSTRASSER, D.

F. & MOCARELLI, P. 1997. Renal cell carcinoma and normal kidney protein expression. *Electrophoresis,* 18**,** 599-604.

SATO, M., SAKOTA, M. & NAKAYAMA, K. 2010. Human PRP19 interacts with prolyl-hydroxylase PHD3 and inhibits cell death in hypoxia. *Experimental Cell Research,* 316**,** 2871-2882.

SCARPULLA, R. C. 2008. Nuclear control of respiratory chain expression by nuclear respiratory factors and PGC-1-related coactivator. *Ann N Y Acad Sci,* 1147**,** 321-34.

SCHMITTGEN, T. D. & LIVAK, K. J. 2008. Analyzing real-time PCR data by the comparative CT method. *Nat. Protocols,* 3**,** 1101-1108.

SCHOENFELD, A. R., DAVIDOWITZ, E. J. & BURK, R. D. 2000a. Elongin BC complex prevents degradation of von Hippel-Lindau tumor suppressor gene products. *Proceedings of the National Academy of Sciences,* 97**,** 8507-8512.

SCHOENFELD, A. R., PARRIS, T., EISENBERGER, A., DAVIDOWITZ, E. J., DE LEON, M., TALASAZAN, F., DEVARAJAN, P. & BURK, R. D. 2000b. The von Hippel-Lindau tumor suppressor gene protects cells from UV-mediated apoptosis. *Oncogene,* 19**,** 5851-7.

SCHROEDL, C., MCCLINTOCK, D. S., BUDINGER, G. R. & CHANDEL, N. S. 2002. Hypoxic but not anoxic stabilization of HIF-1alpha requires mitochondrial reactive oxygen species. *Am J Physiol Lung Cell Mol Physiol,* 283**,** L922-31.

SCORTEGAGNA, M., DING, K., OKTAY, Y., GAUR, A., THURMOND, F., YAN, L. J., MARCK, B. T., MATSUMOTO, A. M., SHELTON, J. M., RICHARDSON, J. A., BENNETT, M. J. & GARCIA, J. A. 2003. Multiple organ pathology, metabolic abnormalities and impaired homeostasis of reactive oxygen species in Epas1-/- mice. *Nat Genet,* 35**,** 331-40.

SELVANAYAGAM, P. & RAJARAMAN, S. 1996. Detection of mitochondrial genome depletion by a novel cDNA in renal cell carcinoma. *Laboratory investigation; a journal of technical methods and pathology,* 74**,** 592-599.

SEMENZA, G. 2007a. HIF-1 mediates the Warburg effect in clear cell renal carcinoma. *Journal of Bioenergetics and Biomembranes,* 39**,** 231-234.

SEMENZA, G. L. 2003. Targeting HIF-1 for cancer therapy. *Nat Rev Cancer,* 3**,** 721-32.

SEMENZA, G. L. 2004. Hydroxylation of HIF-1: oxygen sensing at the molecular level. *Physiology (Bethesda),* 19**,** 176-82.

SEMENZA, G. L. 2007b. Oxygen-dependent regulation of mitochondrial respiration by hypoxia-inducible factor 1. *Biochem.J.,* 405**,** 1-9.

SEMENZA, G. L., AGANI, F., BOOTH, G., FORSYTHE, J., IYER, N., JIANG, B. H., LEUNG, S., ROE, R., WIENER, C. & YU, A. 1997. Structural and functional analysis of hypoxia-inducible factor 1. *Kidney Int,* 51**,** 553-5.

SEMENZA, G. L., NEJFELT, M. K., CHI, S. M. & ANTONARAKIS, S. E. 1991 Hypoxia-inducible nuclear factors bind to an enhancer element located 3' to the

human erythropoietin gene *Proceedings of the National Academy of Sciences of the United States of America* 88 5680-5684

SEMENZA, G. L. & WANG, G. L. 1992. A nuclear factor induced by hypoxia via de novo protein synthesis binds to the human erythropoietin gene enhancer at a site required for transcriptional activation. *Mol. Cell. Biol.,* 12**,** 5447-5454.

SEN BANERJEE, S., THIRUNAVUKKARASU, M., TIPU RISHI, M., SANCHEZ, J. A., MAULIK, N. & MAULIK, G. 2012. HIF-prolyl hydroxylases and cardiovascular diseases. *Toxicol Mech Methods,* 22**,** 347-58.

SHEN, C. & KAELIN JR, W. G. 2013. The VHL/HIF axis in clear cell renal carcinoma. *Seminars in Cancer Biology,* 23**,** 18-25.

SHIAO, Y. H., RESAU, J. H., NAGASHIMA, K., ANDERSON, L. M. & RAMAKRISHNA, G. 2000. The von Hippel-Lindau tumor suppressor targets to mitochondria. *Cancer Res,* 60**,** 2816-9.

SHIMODA, L. A., FALLON, M., PISARCIK, S., WANG, J. & SEMENZA, G. L. 2006. HIF-1 regulates hypoxic induction of NHE1 expression and alkalinization of intracellular pH in pulmonary arterial myocytes. *American Journal of Physiology - Lung Cellular and Molecular Physiology,* 291**,** L941-L949.

SHMUELI, M. D., SCHNAIDER, L., ROSENBLUM, D., HERZOG, G., GAZIT, E. & SEGAL, D. 2013. Structural Insights into the Folding Defects of Oncogenic pVHL Lead to Correction of Its Function In Vitro. *PLoS One,* 8**,** e66333.

SHOHET, R. V. & GARCIA, J. A. 2007. Keeping the engine primed: HIF factors as key regulators of cardiac metabolism and angiogenesis during ischemia. *J.Mol.Med.,* 85**,** 1309-1315.

SHUTT, T., GEOFFRION, M., MILNE, R. & MCBRIDE, H. M. 2012. The intracellular redox state is a core determinant of mitochondrial fusion. *EMBO Rep,* 13**,** 909-915.

SIMONNET, H., ALAZARD, N., PFEIFFER, K., GALLOU, C., BÉROUD, C., DEMONT, J., BOUVIER, R., SCHÄGGER, H. & GODINOT, C. 2002. Low mitochondrial respiratory chain content correlates with tumor aggressiveness in renal cell carcinoma. *Carcinogenesis,* 23**,** 759-768.

SMIRNOVA, E., GRIPARIC, L., SHURLAND, D.-L. & VAN DER BLIEK, A. M. 2001. Dynamin-related Protein Drp1 Is Required for Mitochondrial Division in Mammalian Cells. *Molecular Biology of the Cell,* 12**,** 2245-2256.

SMIRNOVA, N. A., RAKHMAN, I., MOROZ, N., BASSO, M., PAYAPPILLY, J., KAZAKOV, S., HERNANDEZ-GUZMAN, F., GAISINA, I. N., KOZIKOWSKI, A. P., RATAN, R. R. & GAZARYAN, I. G. 2010. Utilization of an in vivo reporter for high throughput identification of branched small molecule regulators of hypoxic adaptation. *Chem Biol,* 17**,** 380-91.

SMITS, P., SMEITINK, J. & VAN DEN HEUVEL, L. 2010. Mitochondrial translation and beyond: processes implicated in combined oxidative phosphorylation deficiencies. *J Biomed Biotechnol,* 2010**,** 737385.

SOLAINI, G., BARACCA, A., LENAZ, G. & SGARBI, G. 2010. Hypoxia and mitochondrial oxidative metabolism. *Biochim.Biophys.Acta,* 1797**,** 1171-1177.

SOLAINI, G. & HARRIS, D. A. 2005. Biochemical dysfunction in heart mitochondria exposed to ischaemia and reperfusion. *Biochem J,* 390**,** 377-394.

SOTGIA, F., WHITAKER-MENEZES, D., MARTINEZ-OUTSCHOORN, U. E., FLOMENBERG, N., BIRBE, R., WITKIEWICZ, A. K., HOWELL, A., PHILP, N. J., PESTELL, R. G. & LISANTI, M. P. 2012. Mitochondrial metabolism in cancer metastasis: Visualizing tumor cell mitochondria and the "reverse Warburg effect" in positive lymph node tissue. *Cell Cycle,* 11**,** 1445-1454.

SRIDHARAN, V., GUICHARD, J., BAILEY, R. M., KASIGANESAN, H., BEESON, C. & WRIGHT, G. L. 2007. The prolyl hydroxylase oxygen-sensing pathway is cytoprotective and allows maintenance of mitochondrial membrane potential during metabolic inhibition. *Am J Physiol Cell Physiol,* 292**,** C719-28.

SRIDHARAN, V., GUICHARD, J., LI, C. Y., MUISE-HELMERICKS, R., BEESON, C. C. & WRIGHT, G. L. 2008. O(2)-sensing signal cascade: clamping of O(2) respiration, reduced ATP utilization, and inducible fumarate respiration. *Am J Physiol Cell Physiol,* 295**,** C29-37.

SRINIVAS, V., LESHCHINSKY, I., SANG, N., KING, M. P., MINCHENKO, A. & CARO, J. 2001. Oxygen sensing and HIF-1 activation does not require an active mitochondrial respiratory chain electron-transfer pathway. *J Biol Chem,* 276**,** 21995-21998.

ST-PIERRE, J., BUCKINGHAM, J. A., ROEBUCK, S. J. & BRAND, M. D. 2002. Topology of superoxide production from different sites in the mitochondrial electron transport chain. *J Biol Chem,* 277**,** 44784-90.

STEBBINS, C. E., KAELIN, W. G. & PAVLETICH, N. P. 1999. Structure of the VHL-ElonginC-ElonginB Complex: Implications for VHL Tumor Suppressor Function. *Science,* 284**,** 455-461.

STOJANOVSKI, D., KOUTSOPOULOS, O. S., OKAMOTO, K. & RYAN, M. T. 2004. Levels of human Fis1 at the mitochondrial outer membrane regulate mitochondrial morphology. *Journal of Cell Science,* 117**,** 1201-1210.

SU, X. & DOWHAN, W. 2006. Translational Regulation of Nuclear Gene COX4 Expression by Mitochondrial Content of Phosphatidylglycerol and Cardiolipin in Saccharomyces cerevisiae. *Molecular and Cellular Biology,* 26**,** 743-753.

SULEIMAN, M. S., SINGH, R. J. & STEWART, C. E. 2007. Apoptosis and the cardiac action of insulin-like growth factor I. *Pharmacol Ther,* 114**,** 278-94.

SUN, J. & TRUMPOWER, B. L. 2003. Superoxide anion generation by the cytochrome bc1 complex. *Arch Biochem Biophys,* 419**,** 198-206.

SYNNESTVEDT, K., FURUTA, G. T., COMERFORD, K. M., LOUIS, N., KARHAUSEN, J., ELTZSCHIG, H. K., HANSEN, K. R., THOMPSON, L. F. & COLGAN, S. P. 2002. Ecto-5'-nucleotidase (CD73) regulation by hypoxia-inducible factor-1

mediates permeability changes in intestinal epithelia. *J Clin Invest,* 110**,** 993-1002.

TAGUCHI, N., ISHIHARA, N., JOFUKU, A., OKA, T. & MIHARA, K. 2007. Mitotic phosphorylation of dynamin-related GTPase Drp1 participates in mitochondrial fission. *J Biol Chem,* 282**,** 11521-11529.

TAKAMURA, H., KOYAMA, Y., MATSUZAKI, S., YAMADA, K., HATTORI, T., MIYATA, S., TAKEMOTO, K., TOHYAMA, M. & KATAYAMA, T. 2012. TRAP1 Controls Mitochondrial Fusion/Fission Balance through Drp1 and Mff Expression. *PLoS One,* 7**,** e51912.

TAKEDA, K., HO, V. C., TAKEDA, H., DUAN, L. J., NAGY, A. & FONG, G. H. 2006. Placental but not heart defects are associated with elevated hypoxia-inducible factor alpha levels in mice lacking prolyl hydroxylase domain protein 2. *Mol Cell Biol,* 26**,** 8336-46.

TANAKA, A., CLELAND, M. M., XU, S., NARENDRA, D. P., SUEN, D.-F., KARBOWSKI, M. & YOULE, R. J. 2010. Proteasome and p97 mediate mitophagy and degradation of mitofusins induced by Parkin. *The Journal of Cell Biology,* 191**,** 1367-1380.

TAYLOR, C. T. 2008. Mitochondria and cellular oxygen sensing in the HIF pathway. *Biochem.J.,* 409**,** 19-26.

TAYLOR, C. T. & POUYSSEGUR, J. 2007. Oxygen, hypoxia, and stress. *Ann N Y Acad Sci,* 1113**,** 87-94.

TAZUKE, S. I., MAZURE, N. M., SUGAWARA, J., CARLAND, G., FAESSEN, G. H., SUEN, L. F., IRWIN, J. C., POWELL, D. R., GIACCIA, A. J. & GIUDICE, L. C. 1998. Hypoxia stimulates insulin-like growth factor binding protein 1 (IGFBP-1) gene expression in HepG2 cells: a possible model for IGFBP-1 expression in fetal hypoxia. *Proc Natl Acad Sci U S A,* 95**,** 10188-93.

TELLO, D., BALSA, E., ACOSTA-IBORRA, B., FUERTES-YEBRA, E., ELORZA, A., ORDÓÑEZ, Á., CORRAL-ESCARIZ, M., SORO, I., LÓPEZ-BERNARDO, E., PERALES-CLEMENTE, E., MARTÍNEZ-RUIZ, A., ENRÍQUEZ, JOSÉ A., ARAGONÉS, J., CADENAS, S. & LANDÁZURI, MANUEL O. 2011. Induction of the Mitochondrial NDUFA4L2 Protein by HIF-1α Decreases Oxygen Consumption by Inhibiting Complex I Activity. *Cell Metabolism,* 14**,** 768-779.

TIAN, H., HAMMER, R. E., MATSUMOTO, A. M., RUSSELL, D. W. & MCKNIGHT, S. L. 1998. The hypoxia-responsive transcription factor EPAS1 is essential for catecholamine homeostasis and protection against heart failure during embryonic development. *Genes Dev.,* 12**,** 3320-3324.

TIAN, H., MCKNIGHT, S. L. & RUSSELL, D. W. 1997. Endothelial PAS domain protein 1 (EPAS1), a transcription factor selectively expressed in endothelial cells. *Genes Dev,* 11**,** 72-82.

TOKATLIDIS, K. 2005. A disulfide relay system in mitochondria. *Cell,* 121**,** 965-967.

TORMOS, K. V. & CHANDEL, N. S. 2010. Inter-connection between mitochondria and HIFs. *J Cell Mol Med,* 14**,** 795-804.

TREMPE, J.-F., SAUVÉ, V., GRENIER, K., SEIRAFI, M., TANG, M. Y., MÉNADE, M., AL-ABDUL-WAHID, S., KRETT, J., WONG, K., KOZLOV, G., NAGAR, B., FON, E. A. & GEHRING, K. 2013. Structure of Parkin Reveals Mechanisms for Ubiquitin Ligase Activation. *Science,* 340**,** 1451-1455.

TWIG, G. 2008. Fission and selective fusion govern mitochondrial segregation and elimination by autophagy. *EMBO J.,* 27**,** 433-446.

ULLAH, M. S., DAVIES, A. J. & HALESTRAP, A. P. 2006. The Plasma Membrane Lactate Transporter MCT4, but Not MCT1, Is Up-regulated by Hypoxia through a HIF-1α-dependent Mechanism. *Journal of Biological Chemistry,* 281**,** 9030-9037.

VAN DER BLIEK, A. M., SHEN, Q. & KAWAJIRI, S. 2013. Mechanisms of Mitochondrial Fission and Fusion. *Cold Spring Harbor Perspectives in Biology,* 5.

VARDATSIKOS, G., SAHU, A. & SRIVASTAVA, A. K. 2009. The insulin-like growth factor family: molecular mechanisms, redox regulation, and clinical implications. *Antioxid Redox Signal,* 11**,** 1165-90.

VAUX, E. C., METZEN, E., YEATES, K. M. & RATCLIFFE, P. J. 2001. Regulation of hypoxia-inducible factor is preserved in the absence of a functioning mitochondrial respiratory chain. *Blood,* 98**,** 296-302.

VEERIAH, S., TAYLOR, B. S., MENG, S., FANG, F., YILMAZ, E., VIVANCO, I., JANAKIRAMAN, M., SCHULTZ, N., HANRAHAN, A. J., PAO, W., LADANYI, M., SANDER, C., HEGUY, A., HOLLAND, E. C., PATY, P. B., MISCHEL, P. S., LIAU, L., CLOUGHESY, T. F., MELLINGHOFF, I. K., SOLIT, D. B. & CHAN, T. A. 2010. Somatic mutations of the Parkinson's disease-associated gene PARK2 in glioblastoma and other human malignancies. *Nat Genet,* 42**,** 77-82.

VENEGAS, V. & HALBERG, M. 2012. Measurement of Mitochondrial DNA Copy Number. *In:* WONG, P. D. L.-J. C. (ed.) *Mitochondrial Disorders.* Humana Press.

VENTURA-CLAPIER, R., GARNIER, A. & VEKSLER, V. 2008. Transcriptional control of mitochondrial biogenesis: the central role of PGC-1α. *Cardiovascular Research*.

VIDONI, S., ZANNA, C., RUGOLO, M., SARZI, E. & LENAERS, G. 2013. Why mitochondria must fuse to maintain their genome integrity. *Antioxid Redox Signal,* 19**,** 379-88.

VINCOW, E. S., MERRIHEW, G., THOMAS, R. E., SHULMAN, N. J., BEYER, R. P., MACCOSS, M. J. & PALLANCK, L. J. 2013. The PINK1-Parkin pathway promotes both mitophagy and selective respiratory chain turnover in vivo. *Proc Natl Acad Sci U S A,* 110**,** 6400-5.

VIVES-BAUZA, C. 2010. PINK1-dependent recruitment of Parkin to mitochondria in mitophagy. *Proc. Natl Acad. Sci. USA,* 107**,** 378-383.

VIVES-BAUZA, C. & PRZEDBORSKI, S. 2011. Mitophagy: the latest problem for Parkinson's disease. *Trends in Molecular Medicine,* 17**,** 158-165.

VON BALLMOOS, C., WIEDENMANN, A. & DIMROTH, P. 2009. Essentials for ATP synthesis by F1F0 ATP synthases. *Annu Rev Biochem,* 78**,** 649-72.

WALLACE, D. C. 2012. Mitochondria and cancer. *Nat Rev Cancer,* 12**,** 685-698.

WANG, G. L., JIANG, B. H., RUE, E. A. & SEMENZA, G. L. 1995. Hypoxia-inducible factor 1 is a basic-helix-loop-helix-PAS heterodimer regulated by cellular O2 tension. *Proceedings of the National Academy of Sciences of the United States of America,* 92**,** 5510-5514.

WANG, G. L. & SEMENZA, G. L. 1993. Characterization of hypoxia-inducible factor 1 and regulation of DNA binding activity by hypoxia. *J Biol Chem,* 268**,** 21513-8.

WANG, G. L. & SEMENZA, G. L. 1995. Purification and characterization of hypoxia-inducible factor 1. *J Biol Chem,* 270**,** 1230-7.

WANG, H., SONG, P., DU, L., TIAN, W., YUE, W., LIU, M., LI, D., WANG, B., ZHU, Y., CAO, C., ZHOU, J. & CHEN, Q. 2011. Parkin Ubiquitinates Drp1 for Proteasome-dependent Degradation: IMPLICATION OF DYSREGULATED MITOCHONDRIAL DYNAMICS IN PARKINSON DISEASE. *Journal of Biological Chemistry,* 286**,** 11649-11658.

WARBURG, O. 1956. On the origin of cancer cells. *Science,* 123**,** 309-14.

WARD, J. B. J., LAWLER, K., AMU, S., TAYLOR, C. T., FALLON, P. G. & KEELY, S. J. 2011. Hydroxylase inhibition attenuates colonic epithelial secretory function and ameliorates experimental diarrhea. *The FASEB Journal,* 25**,** 535-543.

WEBB, J. D., COLEMAN, M. L. & PUGH, C. W. 2009. Hypoxia, hypoxia-inducible factors (HIF), HIF hydroxylases and oxygen sensing. *Cell Mol Life Sci,* 66**,** 3539-54.

WEIDEMANN, A. & JOHNSON, R. S. 2008. Biology of HIF-1alpha. *Cell Death Differ,* 15**,** 621-7.

WEINBERG, F., HAMANAKA, R., WHEATON, W. W., WEINBERG, S., JOSEPH, J., LOPEZ, M., KALYANARAMAN, B., MUTLU, G. M., BUDINGER, G. R. S. & CHANDEL, N. S. 2010. Mitochondrial metabolism and ROS generation are essential for Kras-mediated tumorigenicity. *Proceedings of the National Academy of Sciences*.

WENGER, R. H. 2002. Cellular adaptation to hypoxia: O2-sensing protein hydroxylases, hypoxia-inducible transcription factors, and O2-regulated gene expression. *Faseb J,* 16**,** 1151-62.

WHEATON, W. W. & CHANDEL, N. S. 2011. Hypoxia. 2. Hypoxia regulates cellular metabolism. *Am J Physiol Cell Physiol,* 300**,** C385-93.

WHITE, S. M., CONSTANTIN, P. E. & CLAYCOMB, W. C. 2004. Cardiac physiology at the cellular level: use of cultured HL-1 cardiomyocytes for studies of cardiac

muscle cell structure and function. *Am J Physiol Heart Circ Physiol,* 286**,** H823-9.

WITTIG, I. & SCHÄGGER, H. 2009. Supramolecular organization of ATP synthase and respiratory chain in mitochondrial membranes. *Biochimica et Biophysica Acta (BBA) - Bioenergetics,* 1787**,** 672-680.

WU, S., ZHOU, F., ZHANG, Z. & XING, D. 2011. Mitochondrial oxidative stress causes mitochondrial fragmentation via differential modulation of mitochondrial fission-fusion proteins. *FEBS J,* 278**,** 941-54.

XIE, L., PI, X., MISHRA, A., FONG, G., PENG, J. & PATTERSON, C. 2012. PHD3-dependent hydroxylation of HCLK2 promotes the DNA damage response. *The Journal of Clinical Investigation,* 122**,** 2827-2836.

XIE, L., XIAO, K., WHALEN, E. J., FORRESTER, M. T., FREEMAN, R. S., FONG, G., GYGI, S. P., LEFKOWITZ, R. J. & STAMLER, J. S. 2009. Oxygen-regulated beta(2)-adrenergic receptor hydroxylation by EGLN3 and ubiquitylation by pVHL. *Sci Signal,* 2**,** ra33.

YAN, B., JIAO, S., ZHANG, H.-S., LV, D.-D., XUE, J., FAN, L., WU, G.-H. & FANG, J. 2011. Prolyl hydroxylase domain protein 3 targets Pax2 for destruction. *Biochemical and Biophysical Research Communications,* 409**,** 315-320.

YANG, J., STAPLES, O., THOMAS, L. W., BRISTON, T., ROBSON, M., POON, E., SIMOES, M. L., EL-EMIR, E., BUFFA, F. M., AHMED, A., ANNEAR, N. P., SHUKLA, D., PEDLEY, B. R., MAXWELL, P. H., HARRIS, A. L. & ASHCROFT, M. 2012. Human CHCHD4 mitochondrial proteins regulate cellular oxygen consumption rate and metabolism and provide a critical role in hypoxia signaling and tumor progression. *J Clin Invest,* 122**,** 600-11.

YAO, Z., JONES, A. W. E., FASSONE, E., SWEENEY, M. G., LEBIEDZINSKA, M., SUSKI, J. M., WIECKOWSKI, M. R., TAJEDDINE, N., HARGREAVES, I. P., YASUKAWA, T., TUFO, G., BRENNER, C., KROEMER, G., RAHMAN, S. & SZABADKAI, G. 2013. PGC-1[beta] mediates adaptive chemoresistance associated with mitochondrial DNA mutations. *Oncogene,* 32**,** 2592-2600.

YASINSKA, I. M. & SUMBAYEV, V. V. 2003. S-nitrosation of Cys-800 of HIF-1alpha protein activates its interaction with p300 and stimulates its transcriptional activity. *FEBS Lett,* 549**,** 105-9.

YOON, Y., PITTS, K. R. & MCNIVEN, M. A. 2001. Mammalian Dynamin-like Protein DLP1 Tubulates Membranes. *Molecular Biology of the Cell,* 12**,** 2894-2905.

YOULE, R. J. & NARENDRA, D. P. 2011. Mechanisms of mitophagy. *Nat Rev Mol Cell Biol,* 12**,** 9-14.

YOULE, R. J. & VAN DER BLIEK, A. M. 2012. Mitochondrial Fission, Fusion, and Stress. *Science,* 337**,** 1062-1065.

YOUNGIL, L., HWA-YOUN, L., RITA, A. H. & ÅSA, B. G. 2011. Mitochondrial autophagy by Bnip3 involves Drp1-mediated mitochondrial fission and

recruitment of Parkin in cardiac myocytes. *American Journal of Physiology - Heart and Circulatory Physiology,* 301**,** H1924-H1931.

YU, W., SUN, Y., GUO, S. & LU, B. 2011. The PINK1/Parkin pathway regulates mitochondrial dynamics and function in mammalian hippocampal and dopaminergic neurons. *Human Molecular Genetics,* 20**,** 3227-3240.

YU, Y., DUMOLLARD, R., ROSSBACH, A., LAI, F. A. & SWANN, K. 2010. Redistribution of mitochondria leads to bursts of ATP production during spontaneous mouse oocyte maturation. *Journal of Cellular Physiology,* 224**,** 672-680.

ZELZER, E., LEVY, Y., KAHANA, C., SHILO, B. Z., RUBINSTEIN, M. & COHEN, B. 1998. Insulin induces transcription of target genes through the hypoxia-inducible factor HIF-1alpha/ARNT. *Embo J,* 17**,** 5085-94.

ZHANG, H. 2007. HIF-1 inhibits mitochondrial biogenesis and cellular respiration in VHL-deficient renal cell carcinoma by repression of C-MYC activity. *Cancer Cell,* 11**,** 407-420.

ZHANG, H., BOSCH-MARCE, M., SHIMODA, L. A., TAN, Y. S., BAEK, J. H., WESLEY, J. B., GONZALEZ, F. J. & SEMENZA, G. L. 2008. Mitochondrial autophagy is an HIF-1-dependent adaptive metabolic response to hypoxia. *J Biol Chem,* 283**,** 10892-10903.

ZHAO, J., ZHANG, J., YU, M., XIE, Y., HUANG, Y., WOLFF, D. W., ABEL, P. W. & TU, Y. 2012. Mitochondrial dynamics regulates migration and invasion of breast cancer cells. *Oncogene,* 32**,** 4814-24.

ZIELLO, J. E., JOVIN, I. S. & HUANG, Y. 2007. Hypoxia-Inducible Factor (HIF)-1 regulatory pathway and its potential for therapeutic intervention in malignancy and ischemia. *Yale J Biol Med,* 80**,** 51-60.

ZIVIANI, E. & WHITWORTH, A. J. 2010. How could Parkin-mediated ubiquitination of mitofusin promote mitophagy? *Autophagy,* 6**,** 660-662.

# Appendix

## *Chapter 3: Full analysis of cellular metabolites*

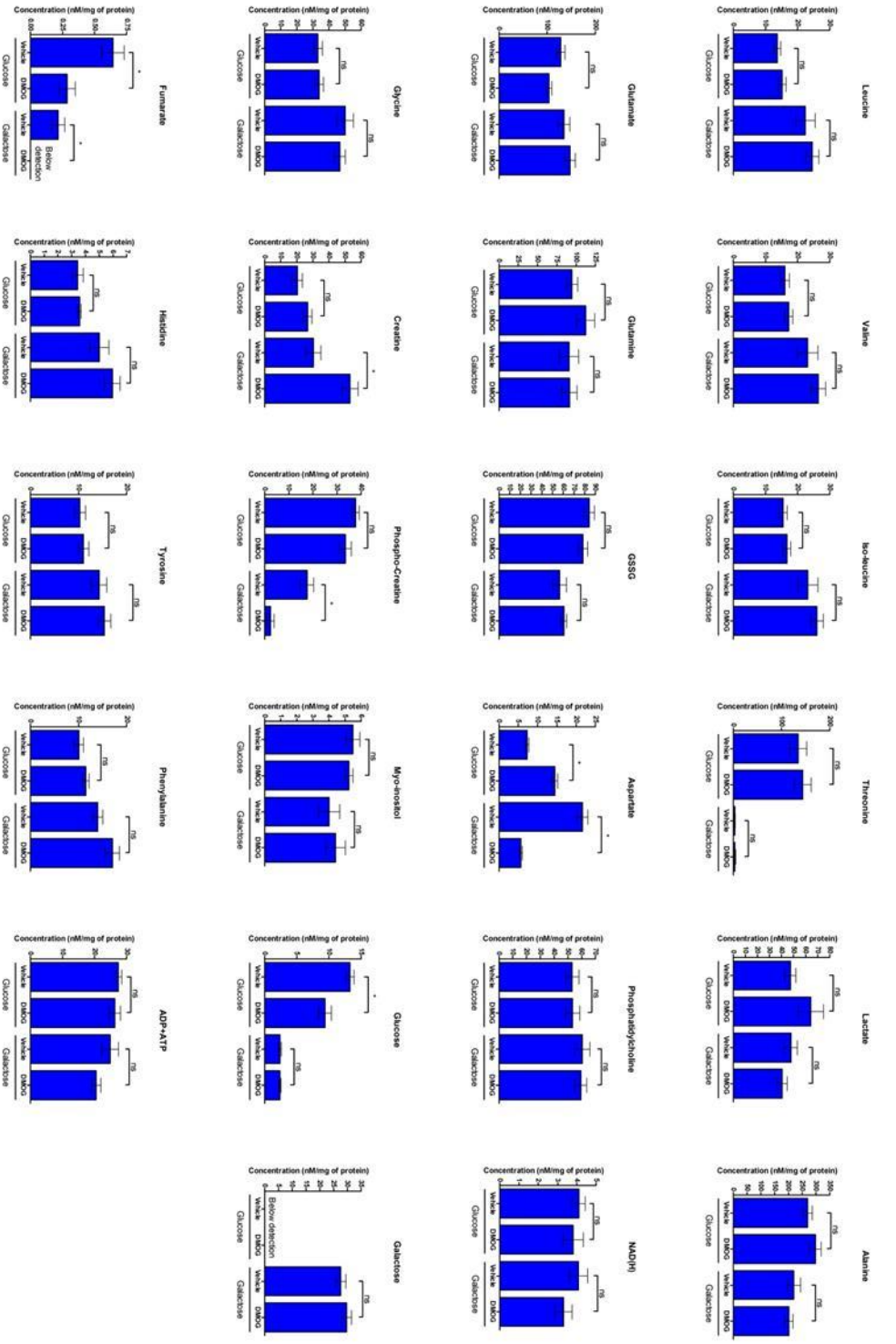

## *Chapter 3: Full analysis of media metabolites*